https://ntrs.nasa.gov/search.jsp?R=19780014548 2020-03-22T04:50:48+00:00Z

NI

NASA Contractor Report 141433

Laser Doppler Velocimeter Aerial Spray Measurements

Andrew D Zalay, William R. Eberle, Robert E Howle,
and Kenneth R Shrider

(NASA-CR-141433) LASER DOPPLER VELOCIMETER AERIAL SPRAY MEASUREMENTS (Lockheed Missiles and Space Co.) 223 p HC A10/MF A09 CSCL 13B

N78-22491

Unclas
G3/45 16614

April 1978

National Aeronautics and
Space Administration

Wallops Flight Center
Wallops Island, Virginia 23337
AC 804 824-3411

NASA Contractor Report 141433

Laser Doppler Velocimeter Aerial Spray Measurements

Andrew D Zalay, William R Eberle, Robert E Howle,
and Kenneth R Shrider

Lockheed Missiles & Space Company, Inc
Huntsville Research & Engineering Center
Huntsville, Alabama 35807

Prepared Under Contract No NAS6-2825

National Aeronautics and
Space Administration

Wallops Flight Center
Wallops Island Virginia 23337
AC 804 824-3411

SUMMARY

Swath patterns generated by an agricultural aircraft were scanned with a mobile laser Doppler velocimeter to remotely measure their location, spatial extent, and relative concentration, thereby providing a new tool for aerial spray studies. The aerial spray tests consisted of 25 low-level passes by a Piper Pawnee agricultural aircraft over a test site instrumented with ground sampling plates and filter type air samplers. The 25 low-level passes included variations in aircraft height above the ground, composition of the spray material, and spray rate. The laser system scanned the cross section of the aerial spray pattern continuously up to 13 minutes after the spray release. The measurements showed the location and relative concentration of the swath cross section up to two hundred meters downwind from the release point. Initially (within 10 sec of the release), the remote sensing measurements showed high relative particulate concentrations of an order of magnitude above the ambient level confined to an elongated region above the release point. Later (10 to 30 sec after the release) the region of high relative concentration moved downwind, closer to the ground, and increased in cross-sectional area and decreased in intensity. Within 60 sec after release, the particulate concentration near the release point returned to ambient levels.

The results of the test program demonstrated that the mobile laser Doppler velocimeter is capable of identifying, monitoring, and providing quantitative measurements of aerial spray parameters from agricultural aircraft. The laser Doppler velocimeter may be used in the future to provide assessment of the effectiveness of various aerial spray techniques.

TABLE OF CONTENTS

		Page
SECTION 1.	INTRODUCTION	1
SECTION 2.	INSTRUMENTATION	3
	2.1 Laser Doppler Velocimeter System	3
	2.2 Data Processing	18
SECTION 3.	DESCRIPTION OF EXPERIMENTAL TESTS	39
	3.1 Flight Test Program	39
	3.2 Operation of Laser Doppler Velocimeter	39
SECTION 4.	RESULTS OF LASER DOPPLER VELOCIMETER MEASUREMENTS	43
	4.1 Typical Measurements of Airborne Spray Characteristics	43
	4.2 Relative Concentration of Spray Cloud	60
	4.3 Fallout of Particulates from the Spray Cloud	68
	4.4 Spray Transport	68
	4.5 Wind Measurement	77
SECTION 5.	CONCLUSIONS AND RECOMMENDATIONS	84
	REFERENCES	85
APPENDIX A	Spray Applications and Conventional Drift Measurements	A-1
APPENDIX B	Aerial Spray Cross-Section Plots Measured by Laser Doppler Velocimeter System	B-1

LIST OF ILLUSTRATIONS

Figure	Title	Page
1.	Optical Component Configuration of the Lockheed LDV	5
2.	Schematic of LDV Optic Scanning System	7
3.	Multimode Scanner	8
4.	Scan Capabilities of LDV	9
5.	Range Resolution of LDV Measured by Backscattered Intensity	10
6.	Signal Characteristics for Identification of Spray Cloud Boundary by Range Scanning	12

Figure	Title	Page
7.	System Configuration	16
8.	Typical LDV Output Signal Displayed by the Spectrum Analyzer	17
9.	Lockheed LDV System Used for Tracking of Effluent from Agricultural Aircraft	19
10.	View Through Side Window of Laser Doppler Velocimeter Depicting Scanning Optics	20
11.	Interior View of Laser Doppler Velocimeter Van Looking Forward	21
12.	Interior View of Laser Doppler Velocimeter Van Depicting Display and Scanner Controls in First Rack, Computer in Second Rack, Digital Tape Unit Aft and Optics Package on Right	22
13.	General Elements of LDV Data Acquisition and Data Processing System	23
14.	Typical Spectrum Analyzer Output	25
15.	Full Spectrum Data Logger Macro Flow Chart	26
16.	Data Processing Sequence Carried Out for the Bryan Aerial Spray Measurements	27
17.	Output from Aerial Spray Program — Full Spectrum Plot, Test 23, Time 41 sec Before Release, y = 73 (m), z = 2.4 (m)	29
18.	Output from Aerial Program — Full Spectrum Plot, Test 23, Time 17 sec After Release, y = 107.2 (m), z = 3.2 (m) (Airplane Located at y = 61 (m), z = 10 (m))	30
19.	Output from Aerial Spray Program — Intensity Sum Plot	32
20.	Principle of VAD Operation	33
21.	Azimuth Angle Dependence of Measured Velocity Component	35
22.	Sample Output Plot from the VAD and Vortex Track Program Operating in the VAD Mode	36
23.	Derectified Line-of-Sight Velocity for VAD Mode	37
24.	Diagram of Bryan, Texas, Test Site	41
25.	Typical Scan Configuration for LDV Aerial Spray Measurements	42
26.	Particulate Concentration Regions for Aerial Spray Measured with Laser Doppler Velocimeter	44
27.	Cumulative Relative Frequency Distribution for ISUM Near Release Point (z = 2 to 5 m, y = 50 to 100 m)	45
28.	Typical Aerial Spray Cross-Section Plot	47
29.	Typical Aerial Spray Cross-Section Plot Showing Details of the Relative Concentration Distribution	56

Figure	Title	Page
30.	Typical Aerial Spray Cross-Section Plot Showing Details of the Line-of-Sight Velocity Distributions	58
31.	Typical Relative Concentration Profile Measured During Range Scan of the Spray Cloud at Approximately the Spray Release Altitude (z = 3.2 m)	61
32.	Relative Aerial Spray Concentration as a Function of Range Downwind from Release Point at Approximately the Spray Release Altitude (z = 3.2 m)	62
33.	Relative Aerial Spray Concentration as a Function of Altitude at the Release Line (y = 0 m)	63
34.	Relative Aerial Spray Concentration as a Function of Altitude and Downwind Distance	65
35.	Comparison of Vertical Relative Concentration Profile Measured by the LDV and Measured by Tower Mounted Cascade Impactors	66
36.	Comparison of Horizontal Relative Concentration Distribution at 3.2 m Altitude Observed for Different Spray Rates and Airplane Heights	67
37.	Calculation of Total Mass of Airborne Particulates	69
38.	Variation in Particulate Mass Above Release Point	70
39.	Lateral Displacement of Spray Cloud High Concentration Region for Test 23	72
40.	Observed Lateral Motion of Spray Cloud Cross Section	73
41.	Trailing Vortex Streamlines Computed for an Agricultural Aircraft Flying at 6 m Altitude in a 4.5 m/sec Crosswind	75
42.	Selected Crosswind Profile for Trailing Vortex Streamline Calculation	76
43.	Wind Speed as a Function of Altitude	78
44.	Wind Direction as a Function of Altitude	79
45.	Down Runway Velocity as a Function of Altitude	80
46.	Cross Runway Wind Velocity as a Function of Altitude	81

1. INTRODUCTION

Drift and dispersion of pesticides and herbicides away from the target area is a serious problem for the agricultural aviation industry. Spray drift is estimated to waste approximately 50% of the chemicals applied aerially in the field (Ref. 1). This loss is significant in terms of the: (1) dollar value of the chemicals involved; (2) damage to surrounding crops due to herbicide drift; and (3) health hazards posed by unintentional pesticide and herbicide fallout. Spray drift and dispersion involve several factors including ambient weather conditions, composition and volume of spray applied, type of spray equipment used and the manner (e.g., aircraft altitude) in which the spray application is made. An understanding of the effects of the various factors which influence spray drift and dispersion can lead to more effective and more efficient techniques for achieving crop coverage with aerial sprays. Development of a methodology for measuring spray transport is important for the evaluation of different spray equipment, aircraft, and applicator techniques.

Currently, there is no available technique to identify; monitor and to provide detailed measurements of the physical characteristics of airborne spray releases from agricultural aircraft. As a result, progress to improve aerial spray technology has been slow. Evaluation of existing spray techniques is based on dye and tracer fallout measurements which do not provide information regarding the airborne spray cloud. An experimental tool for identifying, monitoring, and measuring aerial spray cloud parameters is needed. Spray application technology improvements which are based on the accurate measurement of the location, velocity, and droplet size distribution of airborne clouds as a function of wind, spray, aircraft and flight parameters can be developed.

In order to assist the agricultural aviation industry, NASA is spearheading an applied technology program in conjunction with USDA, EPA, and FAA. The present study is a part of the long-range NASA effort to determine the physical characteristics of aerial spray releases, to establish baseline spray recovery rates, and to develop improved agricultural spray equipment and techniques. The purpose of the study was to investigate the feasibility of utilizing a laser Doppler velocimeter system for measuring aerial spray cloud characteristics.

A remote sensing laser Doppler velocimeter (LDV) which measures the frequency and intensity of the coherent laser backscatter from particulates in the atmosphere has the potential for measuring the details of aerial spray patterns. The LDV has successfully measured the velocity of particulates in exhaust plumes (Ref. 2), tracked the motion of particulate matter

contained in aircraft wake vortices (Ref. 3), and measured the line-of-sight velocity and relative concentration of ground fog (Ref. 4). To investigate the feasibility of using an LDV for the study of spray transport and dispersion, a research program was conducted at the USDA Agricultural Research Service facility located at the Texas A&M Research and Extension Center, Bryan, Texas. The swath patterns generated by an agricultural aircraft were scanned with a ground based mobile LDV system to determine their location, spatial extent, and relative concentration. In conjunction with the LDV surveys, ground fallout measurements and wind and temperature measurements were conducted by the USDA Agricultural Research Service. These measurements are summarized in a paper by L. F. Bouse, J. B. Carlton, and H. R. Crookshank entitled "Spray Applications and Conventional Drift Measurements" which has been included as Appendix A.

The overall objective of the tests was to demonstrate the feasibility of measuring the transport and dispersion characteristics of airborne spray for different spray rates, compositions, and aircraft altitudes with a remote sensing LDV system. The results of the aerial spray measurements are presented in this report which includes a discussion of the experimental tests, instrumentation, and the location, spatial extent, and relative concentration of airborne spray clouds observed with the LDV. The technique described herein is a systematic measurement process which allows quantification of aerial spray characteristics.

2. INSTRUMENTATION

The aerial spray and atmospheric wind measurements were carried out by means of a scanning LDV system contained in a mobile van. Laser Doppler velocimetry is a proven concept for accurate remote measurement of air movement and has also been used for previous measurements of the relative concentration of particulate matter in the atmosphere. This section describes the principle of operation and the general characteristics of the LDV system used for the aerial spray measurements.

2.1 Laser Doppler Velocimeter System

The LDV system developed and fabricated at Lockheed-Huntsville was used to obtain the aerial spray and wind measurements during the Bryan tests. A description of the LDV system is given including the principle of operation, the basic optical system, the optical scanning system, the measurement of relative particle concentration, the signal processing system and the data recording and display.

2.1.1 Principle of Operation

An analogy can be drawn between an LDV and a conventional microwave Doppler radar. The microwave Doppler radar employs relatively long wavelengths of electromagnetic energy which are backscattered by large objects such as aircraft, thunderheads, etc. The LDV transmits much shorter wavelength (10.6 μm) radiation and receives energy backscattered from small objects such as aerosols, water droplets, salt spray, etc. In both cases the velocities of the backscattering targets are determined from the Doppler shift of the returned radiation. In the case of the microwave radar, the range to the target is typically determined by round trip time of a pulse of energy from the transmitter to the target and back to the receiver. With the Lockheed LDV depicted herein, the range to the target is determined by focusing the system optics to selectively view radiation backscattered from specified ranges.

An LDV system senses air movement by measurement of the Doppler frequency shift of laser radiation backscattered by the atmospheric aerosol. An instrument must incorporate means to transmit the laser radiation to the region of interest, collect the radiation scattered from the atmospheric aerosol and to photomix the scattered radiation and a portion of the transmitted beam on a photodetector. The difference between the transmitted frequency and the returned frequency is the Doppler shift frequency. The Doppler frequency shift signal is generated at the photodetector and is translatable into an along-optic axis wind velocity component using appropriate electronics. The magnitude of the Doppler shift, Δf, is given by the equation shown on the following page.

$$\Delta f = \frac{2}{\lambda} |\bar{V}| \cos\theta \qquad (1)$$

where

$\bar{V}$ = the velocity vector in the region being sensed

λ = the laser radiation wavelength, and

θ = the angle subtended by the velocity vector and the optic system line of sight.

A Doppler shift of 188 KHz results per m/sec of line-of-sight velocity component. Thus, measurement of the Doppler shift frequency, Δf, yields directly the line-of-sight velocity component $|\bar{V}| \cos\theta$. Some typical advantages of the laser Doppler method are: (1) the Doppler shift is a direct absolute measure of the velocity (for example, the hot wire yields velocity via a cooling effect on the wire), (2) the ease with which the position of the sensing volume can be varied (optics pointing and focusing operations only being involved); (3) the ambient aerosol provides sufficient scattering, thus enabling operation in "clear air" conditions; (4) the ambient aerosol tracer has a small inertia and responds quickly to variations in airspeed and is thus a good turbulence indicator; and (5) from the intensity of the backscattered laser radiation the relative particulate concentration can be determined.

2.1.2 Basic Optical System

The basic optical system is shown in Fig. 1. The system depends on focusing the transmitter telescope at the location of interest to control the range at which the measurements are taken.

A horizontally polarized, 20-watt, continuous wave CO_2 laser beam (10.6 micron wavelength) emerges from the laser (1) and is deflected 90 degrees by a mirror (3). The approximately 6 mm diameter beam then passes through a Brewster window (4) and a CdS quarter waveplate (5) which converts it to circular polarization. The beam impinges on the secondary mirror (6) and is expanded and reflected into the primary mirror (30 cm diameter) (7) and then focused out into the atmosphere. A small portion of the original laser beam is reflected by the secondary mirror and the Brewster window (4) and is used as a reference frequency on the photodetector (10). Energy scattered by aerosols, at the focal volume (8) is collected by the primary mirror (7), collimated by the secondary (6), and passes through the quarter waveplate (5). The quarter waveplate changes

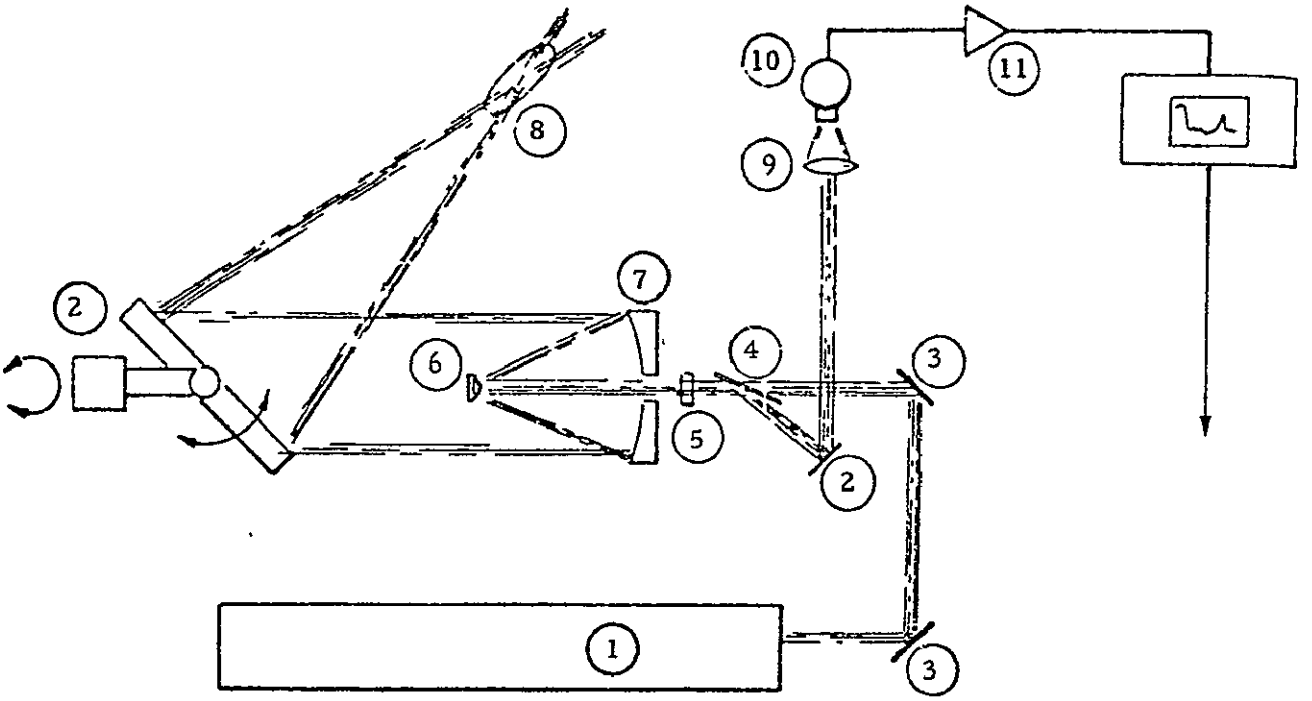

1. CO_2 Laser
2. Mirror
3. Mirror
4. Brewster Window
5. Quarter Wave Plate
6. Secondary Mirror
7. Primary Mirror
8. Focal Volume
9. Lens
10. Photodetector
11. Preamplifier
12. Spectrum Analyzer

Fig. 1 - Optical Component Configuration of the Lockheed LDV

the polarization of the aerosol backscattered radiation from circular to vertical linear polarization. The vertically polarized beam is approximately 78% reflected off the Brewster window (4). After passing through the collecting lens (9) the two beams (i.e., a small portion of the original beam and the beam backscattered from the focal volume) are photomixed on the detector (10) in a heterodyne configuration. The electrical output of the detector (10) is amplified (1) with a 5 MHz bandwidth, 20 dB gain low noise type preamplifier and fed into a spectrum analyzer (12) which gives an output of laser beam intensity as a function of Doppler frequency shift.

2.1.3 Optic Scanning System

In order to provide the flexibility required to operate the various required modes, a scanning arrangement as shown in Fig. 2 is utilized. The required modes of operation include coordinated range and elevation scanning for tracking airborne aerosols and velocity azimuth display (VAD) for measurement of atmospheric wind. The mirror assembly, AB, can be rotated about the vertical axis for scanning in azimuth necessary for the VAD (also called conical scan mode of operation) and discussed in more detail in Section 2.2.3. Mirror A is adjusted to control the elevation angle of the beam, thus controlling the cone angle of the conical scan. The scanning hardware as deployed on the mobile van is shown in Fig. 3. The system's scan capabilities are shown in Fig. 4.

Range scanning of the system's focal volume is accomplished by varying the distance between the telescope secondary mirror, E, and the primary mirror, D. This is effected by varying the position of the secondary mirror, E, in a controlled manner by an electric motor/optical encoder combination.

The limits of the focal volume in the range direction are defined as the points at which the intensity of the backscattered radiation per unit depth of the focal volume is half of the maximum backscattered intensity per unit depth. For the theoretical distribution of intensity along the focal axis, the sensing volume length, ΔR (i.e., the distance between the two half maximum intensity points) is

$$\Delta R = 4.4 \lambda R^2/\pi a^2 \qquad (2)$$

where λ is the laser wavelength (10.6 μ), R is the range to focus, and a is the radius of the telescope primary mirror (15 cm). The theoretical and measured range resolution of the LDV is shown in Fig. 5. The measured values were obtained by focusing the beam at a hard target for maximum returned intensity and then increasing or decreasing the range until the half maximum intensity points were reached.

The nominal focal volume in the plane normal to the optic line-of-sight axis is defined as the area which contains half of the total laser intensity. The laser intensity in the plane normal to the optic line-of-sight axis is normally

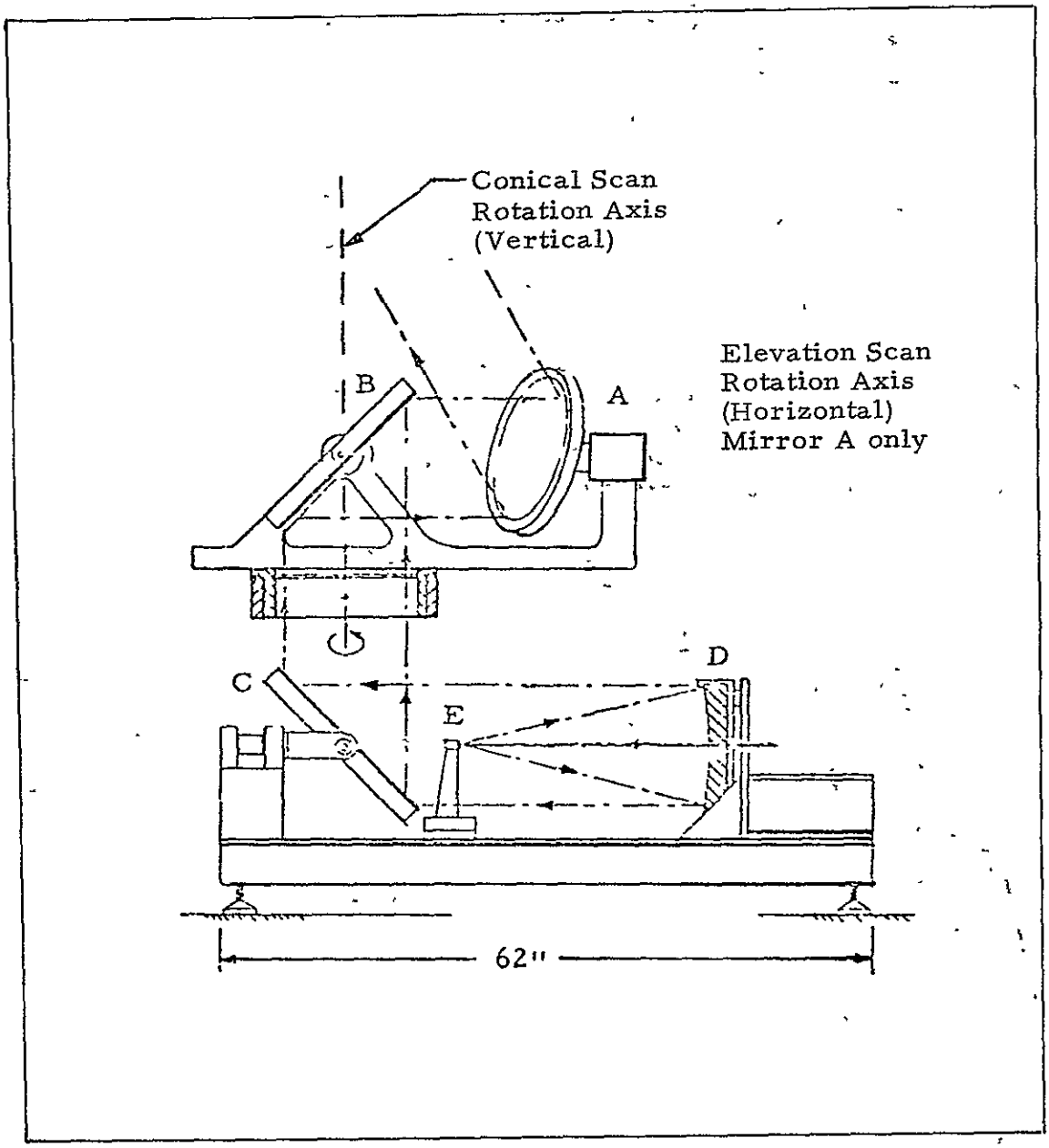

Fig. 2 - Schematic of LDV Optic Scanning System

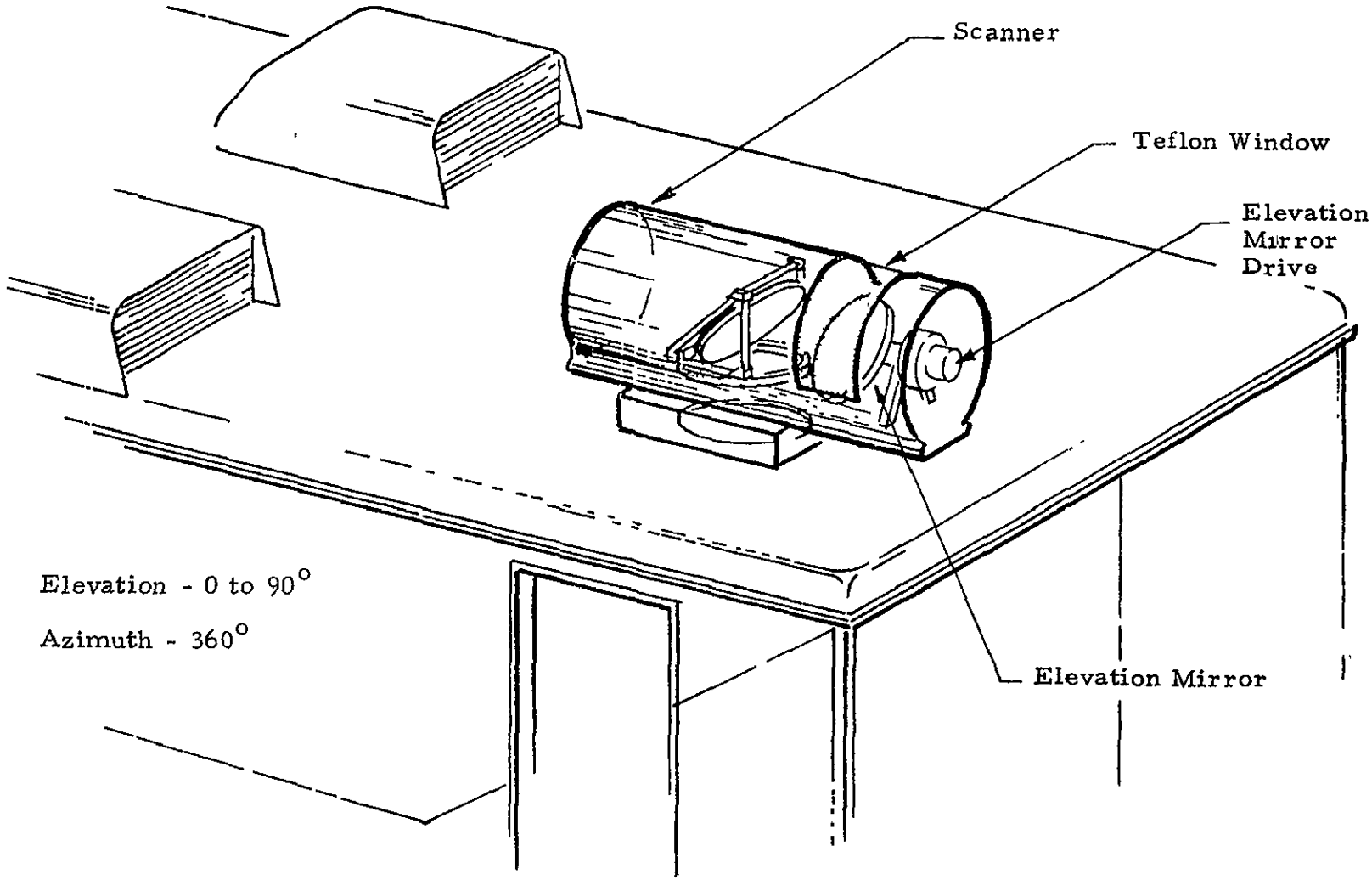

Fig. 3 - Multimode Scanner

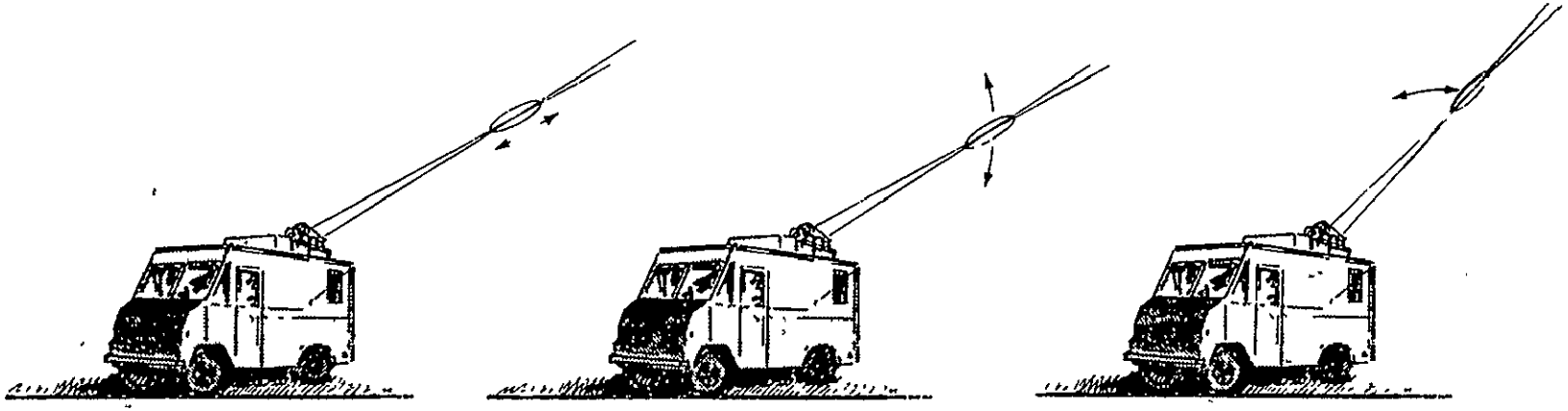

RANGE SCAN

Limits		Rates
Max	Min	
100 to 999 m	16 to 969 m	0 1 to 6 9 Hz
One meter increment		0 1 Hz increm

Also can be stepped between 8 pre-selectable ranges

ELEVATION SCAN

Limits		Rates
Max	Min	
10 to 90°	0 to 90°	0 1 to 0 5 Hz
1 deg increment		0 1 Hz increm

AZIMUTH SCAN

Currently 360° open loop operation
Can be modified for closed loop pointing and scanning

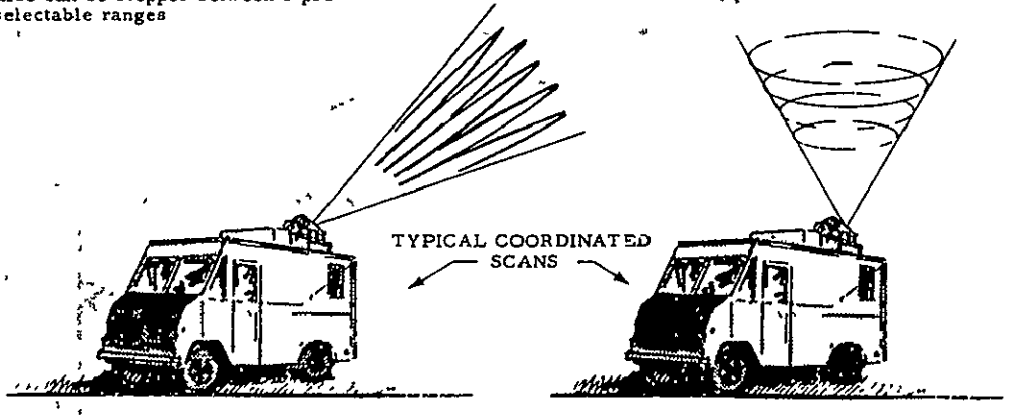

Range - Elevation

(scan used for agricultrual aerial spray measurements)

Range - Azimuth

(for wind measurement)

Notes

- Maximum Sampling Rate.
  - Current Technique – 70 Hz
  - Advanced Technique – 1 kHz
- Focal Volume Varies with Square of Range and Output Optics Size i e ,

Range \ Optics Size	30 cm
30 m	30 cm
300 m	30 m

Fig. 4 - Scan Capabilities of LDV

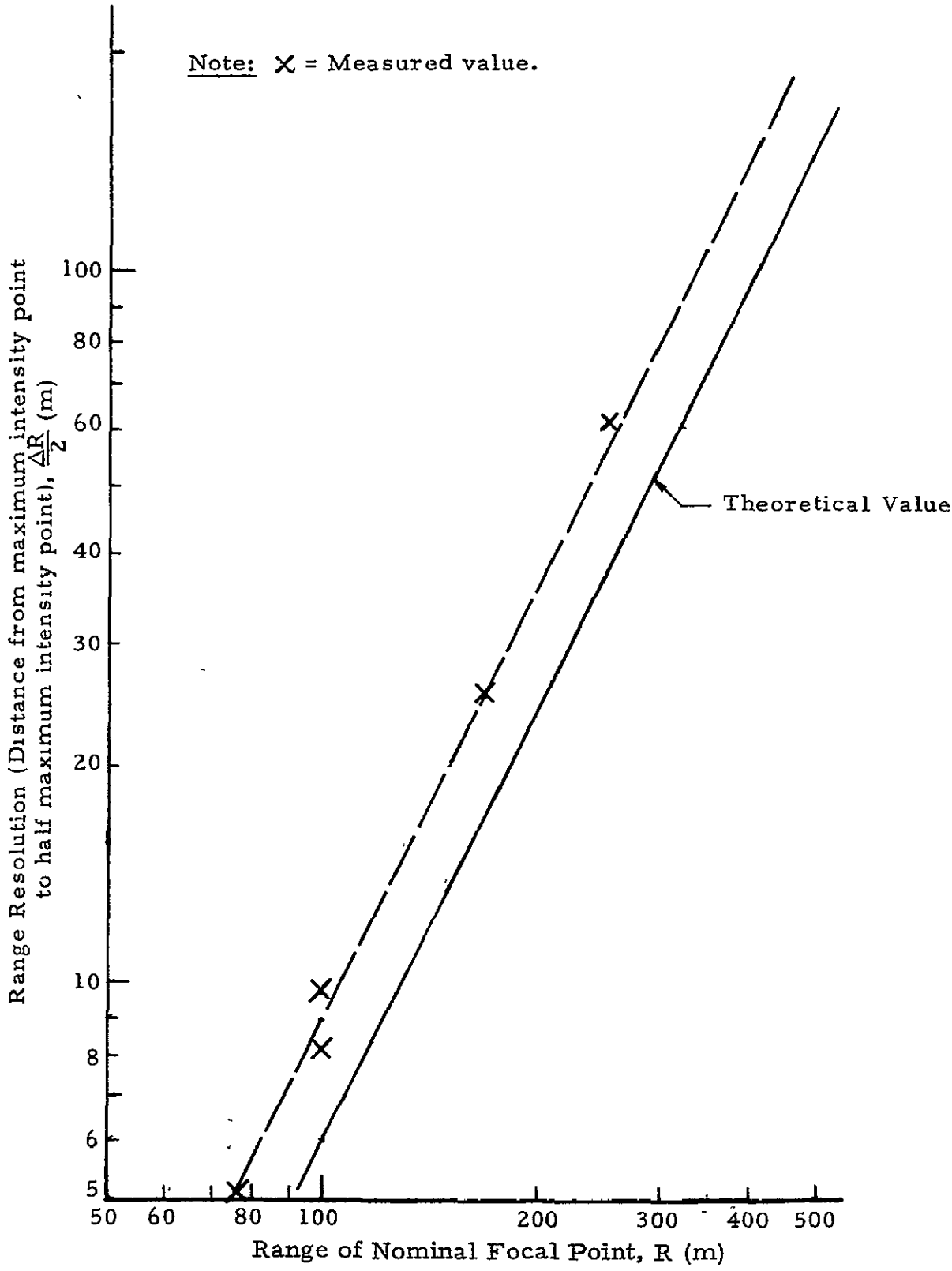

Fig. 5 - Range Resolution of LDV Measured by Backscattered Intensity

distributed with respect to the transverse direction. The relationship for the lateral limits of the focal volume is

$$\Delta Y = \lambda R/a \tag{3}$$

The theoretical and measured transverse spatial resolution of the LDV is tabulated below.

Range to Focus R (m)	Sensing Volume Width ΔY (m)	
	Measured	Eq. (3)
50	3.3×10^{-3}	1.8×10^{-3}
100	6.6×10^{-3}	3.5×10^{-3}
200	1.3×10^{-2}	7.0×10^{-3}
600	3.9×10^{-2}	2.1×10^{-2}

The measured value was obtained from a power meter with a pinhole attachment and is the lateral position at which the power meter reading was e^{-2} of the maximum power meter reading.

The sampling volume of the LDV is a narrow elongated region whose width is small in comparison to the dimensions of the aerial spray cloud but whose length can approach the dimension of the spray cloud at large ranges. For example, if the LDV system is tracking the swath pattern at a range of 60 m, the half-power level signal is confined to a region 6.4 m in length and 4 cm in diameter. At extended ranges, i.e., 300 m, the length of the focal volume affects the ability of the LDV to locate the spray cloud.

In the measurement of the boundary of the aerial spray the backscatter from outside the nominal focal volume can affect the returned signal when the cloud boundary intersects the focal axis. However, the cloud boundary can be clearly identified. Figure 6 shows the relative returned intensity (total returned intensity — not merely that the nominal focal volume) as a function of nondimensionalized displacement of the nominal focal point from a discontinuity in particulate concentration. For the example, the dense particulate concentration is ten times that of the "clear air" concentration. The plume boundary is clearly defined as the point at which the returned intensity is midway between the return in clear air and that in the plume. The location of the spray cloud can always be identified within 1 focal volume length.

If the particulate concentration is uniform in the focal volume, the returned laser intensity is independent of range and is directly proportional to the particulate density in the focal volume. However, when the length of the focal volume is large in comparison to the spray cloud, the signal level is no longer independent of range since the number of particles is not uniform in the focal volume. For example, the amplitude of the return signal from the spray is insufficient for detection at 300 m range if the spray cloud is present only over a small extent of the 160 m long region from which the half-power signal level can emanate.

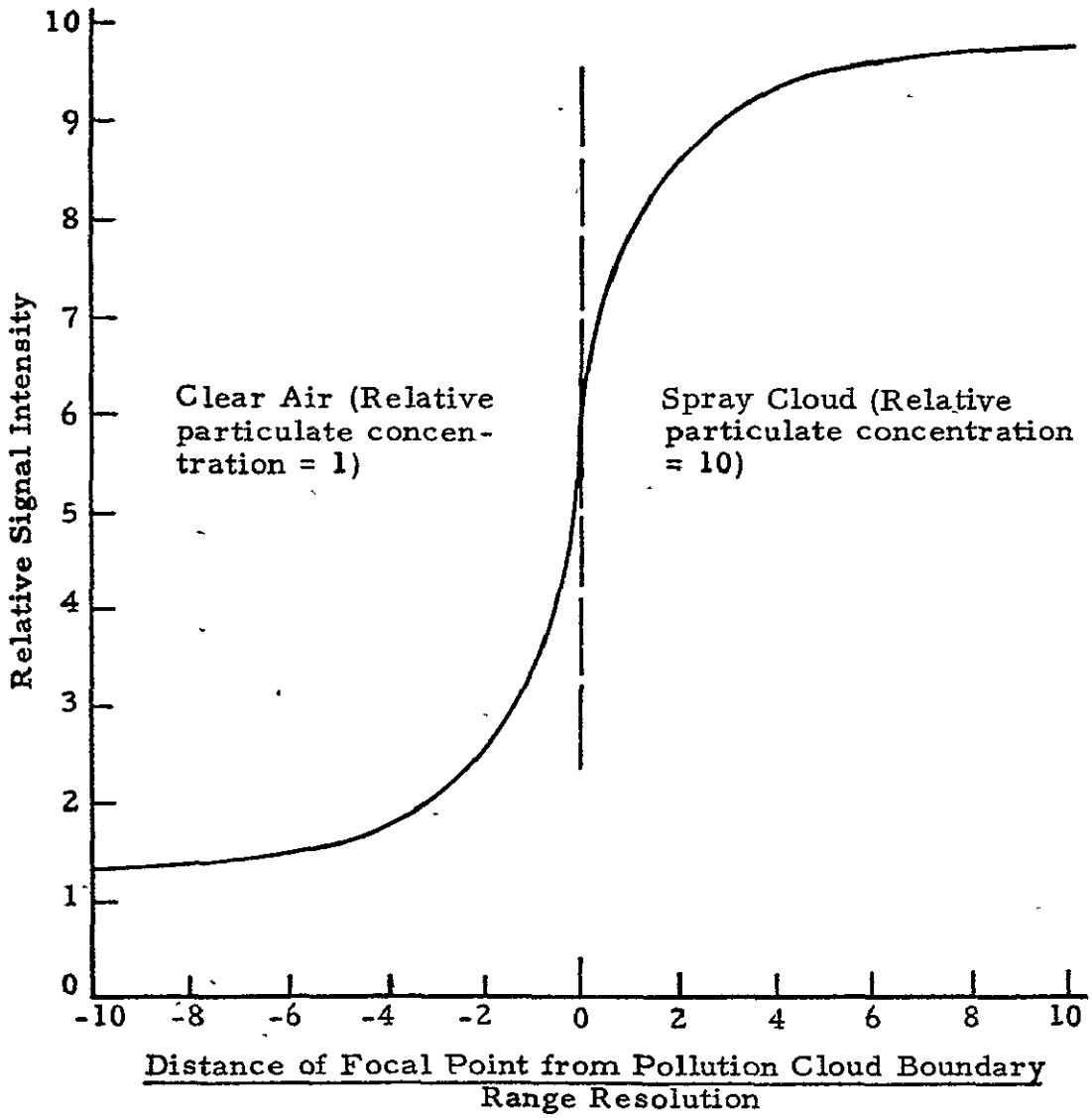

Fig. 6 - Signal Characteristics for Identification of Spray Cloud Boundary by Range Scanning

The pertinent operating characteristics of the Lockheed LDV system used in the Bryan aerial spray measurement tests are summarized as follows:

Performance

1. Velocity Measurement Threshold: 1.06 m/sec
2. Velocity Range: 1.06 to 10.60 m/sec
3. Velocity Resolution: 0.16 m/sec

Sample Rate

1. 70 Hz

Spatial Resolution

1. Range Accuracy: $\pm$3.2 m at 60 m, $\pm$80 m at 300 m
2. Elevation Angle Accuracy: $\pm$0.25 deg

Scan Modes

1. Coordinated Range and Elevation Scan (Finger Scan)
2. VAD Scan
3. Range Scan at Fixed Elevation Angles
4. Arc Scan at Fixed Ranges

2.1.4 Measurement of Relative Particle Concentration

The amplitude of the LDV signal is proportional to the collected optical power which consists of the total laser energy backscattered by the particulates. For a system (such as the Lockheed LDV) which determines range to the sensing volume by optics focusing, the intensity of the laser signal received by the receiver optics is

$$I \propto I_o \beta e^{-2\int_o^R \gamma(R)\, dR} \tag{4}$$

where

I_o = incident laser intensity (output of LDV optics)

β = laser backscatter coefficient of aerosol

γ = laser attenuation coefficient of atmosphere

R = range to focus

Physically, the backscatter coefficient is the ratio of backscattered laser intensity to incident laser intensity per unit depth (i.e., range direction) of the focal volume. It is a function of particle size and particle

number density and can be expressed as

$$\beta = \pi \sum_{j=1}^{n} r_j^2 \bar{n}_j K_j \tag{5}$$

where

r_j = radius of j^{th} particle size class

$\bar{n}_j$ = number of particles in j^{th} particle size class

K_j = scattering area coefficient of j^{th} particle size class

The scattering coefficient, K_j, is a function of the particle size class, index of refraction, and the wavelength of light illuminating the particle. For spherical particles whose radii are smaller than about one-tenth the wavelength of the scattered radiation, the scattering coefficient K_j is a simple function of the number of scatterers, their diameter, and index of refraction according to the Rayleigh scattering theory. Where the Rayleigh condition on the wavelength-to-radius ratio is not satisfied, recourse must be made to the more complex Mie theory of scattering to compute the backscatter coefficient. However, for a constant particle size and index of refraction and a given wavelength of illumination, the backscatter coefficient of the aerosol is directly proportional to the number density of particles in the focal volume. In Eq. (4) the attenuation coefficient (physically, the fraction of laser intensity lost to attenuation per unit of range) is proportional to the backscatter coefficient. The 2 in the above equation is to account for attenuation for both incident and backscattered radiation. A more detailed discussion of the observed laser backscatter phenomenon is given in Ref. 5.

For the test described herein, the natural aerosol density of the atmosphere was much less than that of the aerial spray. Also, the depth of the spray cloud (in the range direction) was assumed to be sufficiently small so that significant attenuation of the laser beam did not occur in the aerial spray cloud. Therefore, the returned laser intensity is proportional to the backscatter coefficient which is directly proportional to the number density of particles in the focal volume. In the absence of attenuation, the signal intensity is independent of range to focus, R, and also of the optic diameter, a. The physical reason is that the sensed volume varies as $(R/a)^4$. (Recall that the radius of the focal volume varies as (R/a) and the length varies as $(R/a)^2$.) The number of targets is therefore proportional to R^4 which cancels the R^{-4} dependence of the return from a single target. (The intensity of the outgoing and returning signal each vary as R^{-2} so that the returned signal varies as R^{-4}.) By virtue of these factors, the absolute LDV signal strength can be directly related to the relative particular mass concentration. While such a calibration was not carried out in the present study, Ref. 6 has reported a linear relationship between signal strength from an LDV monitoring smoke stack effluents and attenuation coefficient measured in the visible spectrum by a transmissometer, suggesting that the calibration is possible.

In addition to measuring the frequency and amplitude of the backscattered laser energy, the LDV system incorporates means of scanning the sensing volume and processing and recording the output signals.

The hardware implementation of the field laser Doppler unit utilized during this investigation is discussed in the following subsections. The overall configuration is summarized in Fig. 7.

2.1.5 Signal Processing System

The Doppler frequency shift of the photodetector output is processed by a spectrum analyzer which provides frequency spectra (intensity of returned signal as a function of Doppler shift) at a rate of 70 signatures per second. The resolution and range of the velocities (frequencies) measured with the LDV is determined largely by the spectrum analyzer settings. During the Bryan tests, the spectrum analyzer was set at 0 to 2 MHz corresponding to a velocity range of 0 to 10.60 m/sec. Sample runs indicated that the observed velocities of the aerial spray cloud were well within this range. The bandwidth of the spectrum analyzer, defined as the frequency span where the signal decreased 2 dB, was set at 30 kHz. This provided approximately a 0.15 m/sec resolution in velocity.

The typical output signal displayed by the spectrum analyzer is illustrated in Fig. 8. The intensity versus frequency spectrum from the ambient crosswind before spray release and approximately 5 sec after spray release is illustrated in Fig. 8. The sample spectrum analyzer output signal shows that the magnitude of the mean line-of-sight velocity is approximately 5.3 m/sec (~1 MHz) for the ambient crosswind and approximately 6.4 m/sec (~1.2 MHz) for the spray cloud. The amplitude of the signal, a measure of the aerosol backscatter coefficient, is nearly an order of magnitude higher during the spray release than the ambient level. The spectrum velocities (frequencies) found in the spray cloud is also considerably broader than the range of velocities associated with the ambient wind. This may be due to the enhanced sensitivity of the LDV resulting from the elevated signal levels backscattered from the high relative concentration regions of the spray cloud.

2.1.6 Data Recording and Display

Primary: The primary data gathering function is performed by an SEL 810A general purpose minicomputer. Data gathering by the Mobile Atmospheric Unit is formatted by the computer software and stored on magnetic tape for subsequent processing on the Univac 1108. The SEL 7-track tape control and magnetic tape units allow digital recording of data at 800 bpi at 45 ips, which recording density is common to the Univac 1108 I/O system. The data logged by the computer includes:

- All scan volume location parameters
- "Mode of operation" identifier
- The instantaneous line-of-sight velocity information

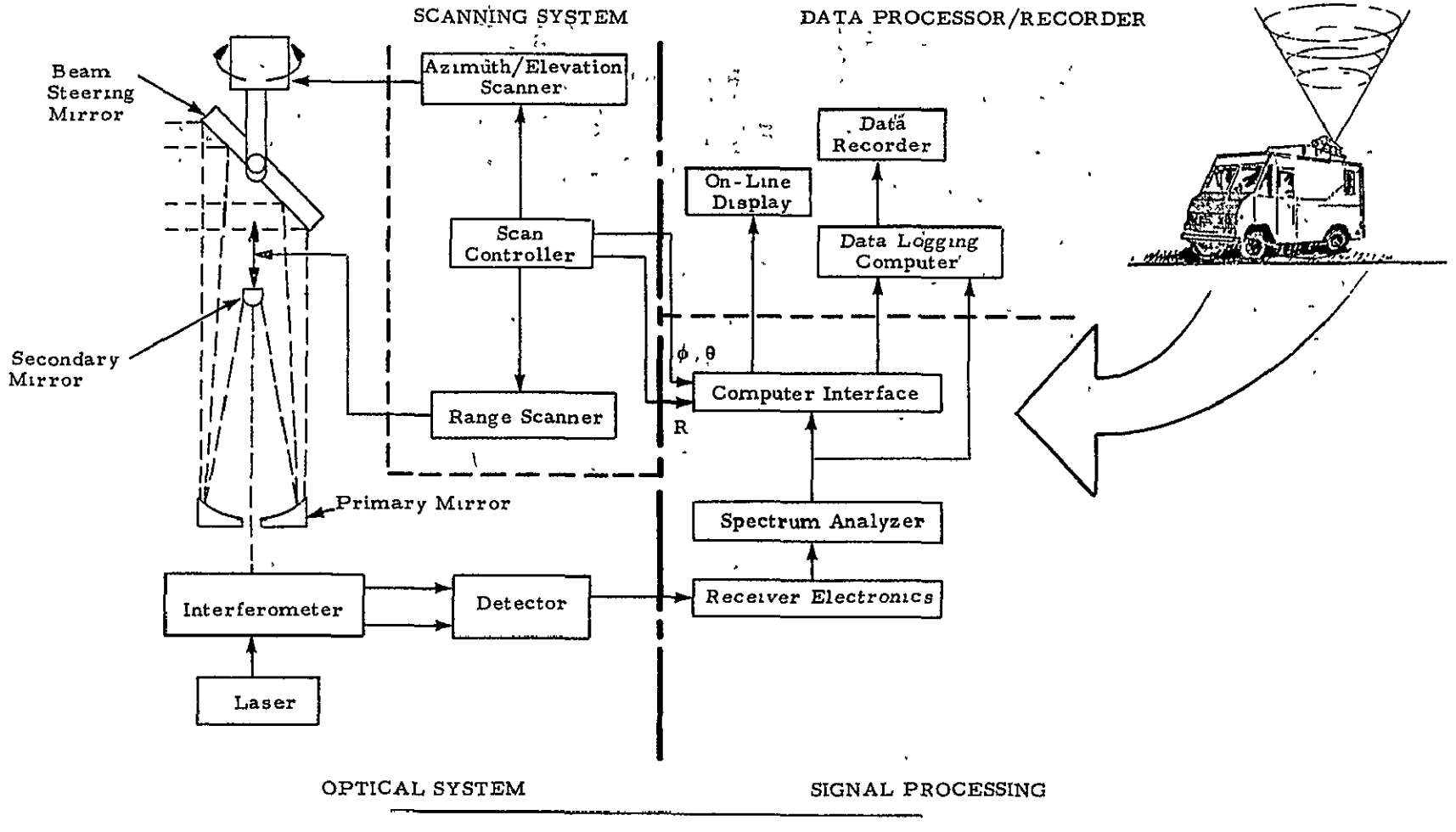

Fig. 7 - System Configuration

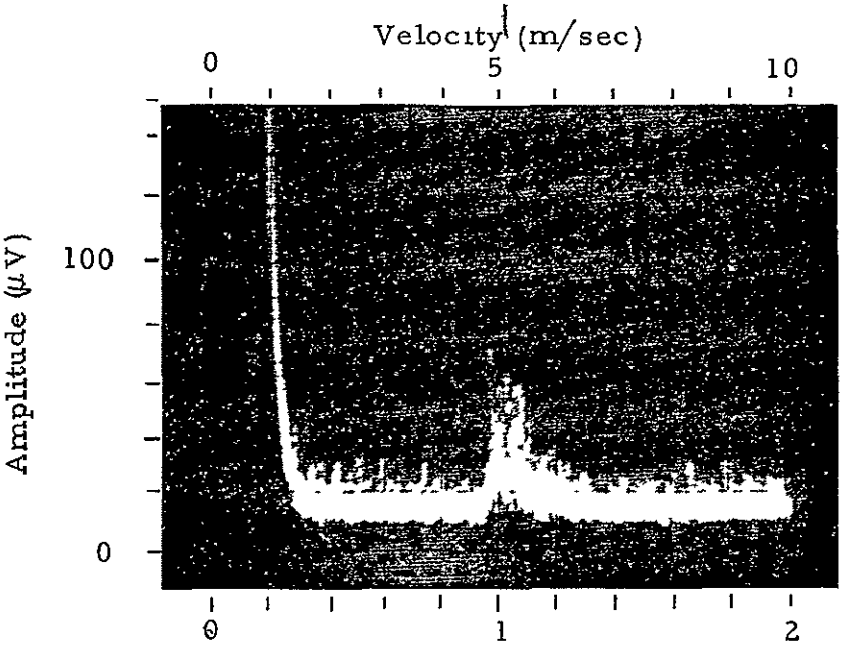

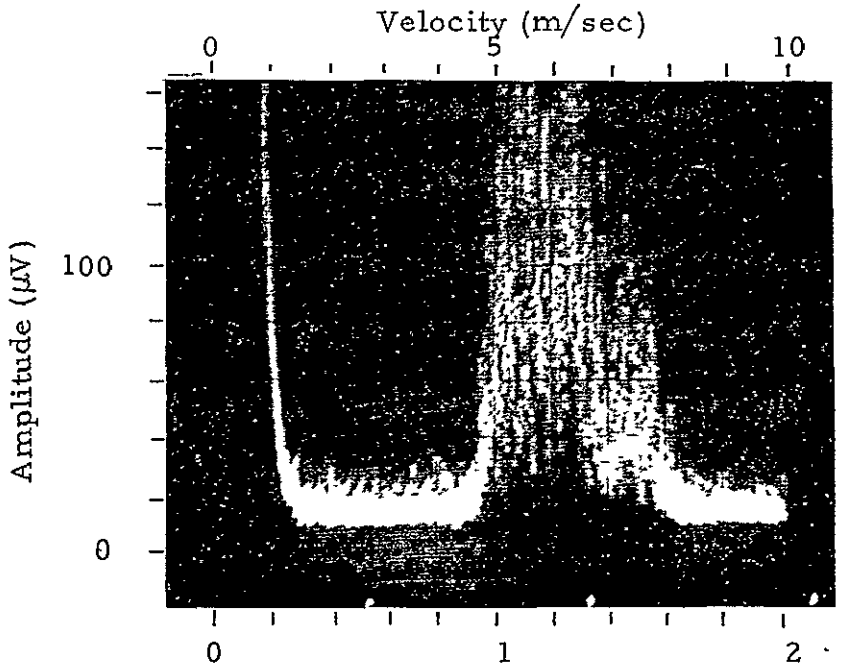

Fig. 8 - Typical LDV Output Signal Displayed by the Spectrum Analyzer

- The Doppler spectrum peak strength
- Full spectrum intensity and frequency information (optical)
- A data quality identifier.

Properties of the Doppler spectrum, namely, the amplitude and frequency corresponding to the spectral peak are obtained as a result of on-line computer processing.

Secondary: The velocity processor output estimate of the instantaneous line-of-sight velocity, updated at a 70 Hz rate, is available in analog format which can be recorded directly on a strip chart recorder, an option which is extremely useful during the VAD mode of operation for monitoring the characteristic profile.

Some overall views of the mobile unit hardware as utilized during this program are shown in Figs. 9 through 12.

2.2 Data Processing

The output from the LDV system, consisting of the coherent backscatter intensity versus frequency from the focal volume as well as the location of the focal volume in space, was processed to yield the location, velocity, and relative concentration of the spray release from agricultural aircraft and the ambient wind velocity field. A description of the LDV data processing system and the data processing algorithms for aerial spray and wind measurements are discussed in the following sections.

2.2.1 Description of LDV Data Processing System

Acquisition and processing of the LDV signature is accomplished by means of a compact data handling system developed specifically for the Lockheed-Huntsville mobile LDV. The general elements of the data acquisition and data processing system are shown in Fig. 13. The digitized LDV intensity versus frequency signal along with its coordinates in space is fed into the SEL 810 minicomputer. Preprocessing of the LDV signal is carried out on the minicomputer utilizing on-line computer programs written in SEL machine language. Information from the SEL 810 is stored on magnetic tape and is used as an input to the off-line processing algorithms. Off-line processing of the LDV signal is carried out on a Univac 1108 computer with programs written in FORTRAN language using card inputs. The information from the data logs recorded by the operators at the time the measurements are taken are used as a guide in the data processing. On-line manipulation of the data is carried out by the SEL Data Logger program. The off-line processing of the spray parameters and the wind parameters was carried out by the Aerial Spray program and the VAD and Vortex Track programs, respectively.

Data acquisition in the LDV is carried out by the SEL Data Logger program. A sweeping spectrum analyzer is used to detect the Doppler shift

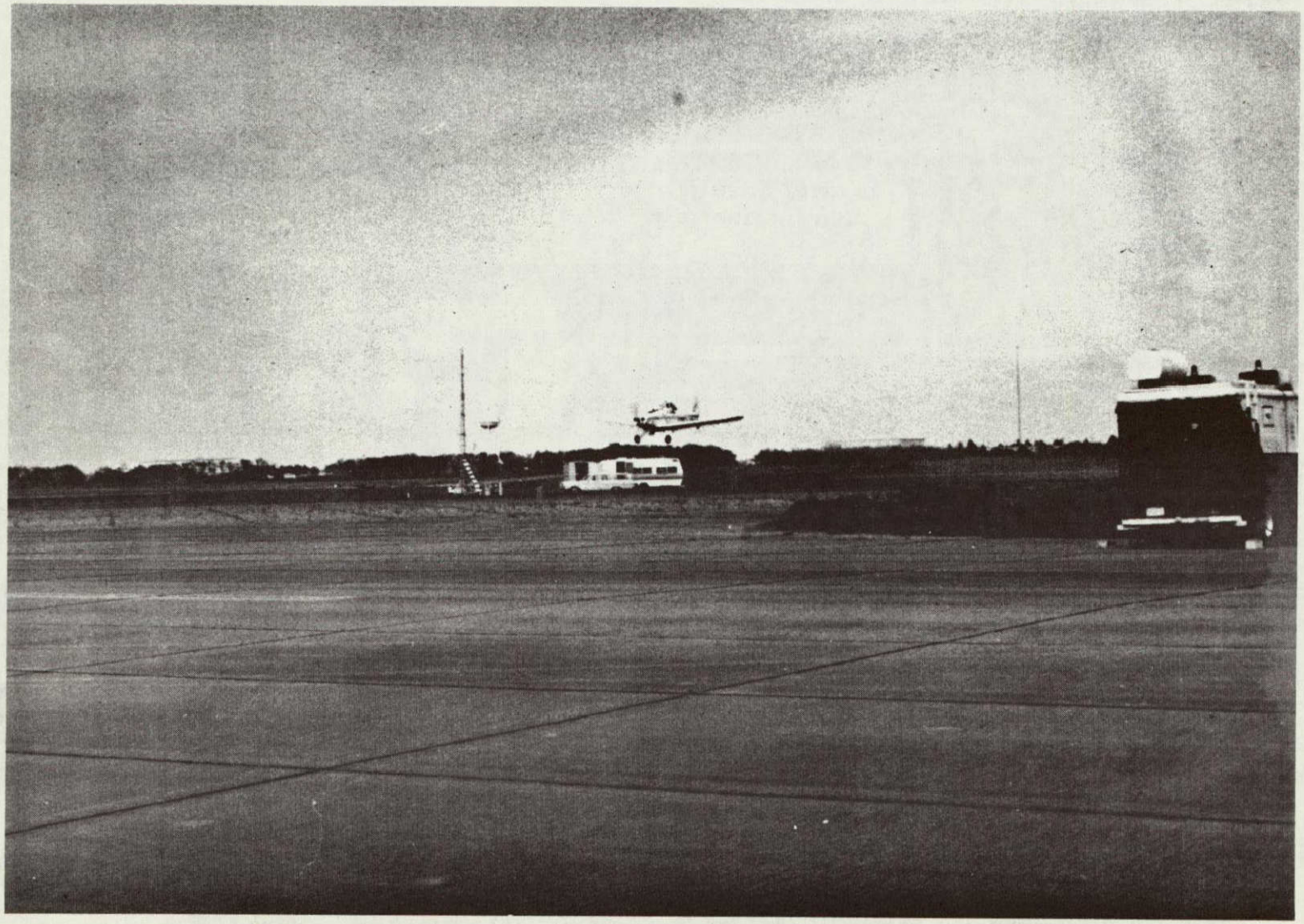

Fig. 9 - Lockheed LDV System Used for Tracking of Effluent from Agricultural Aircraft

REPRODUCIBILITY OF THE
ORIGINAL PAGE IS POOR

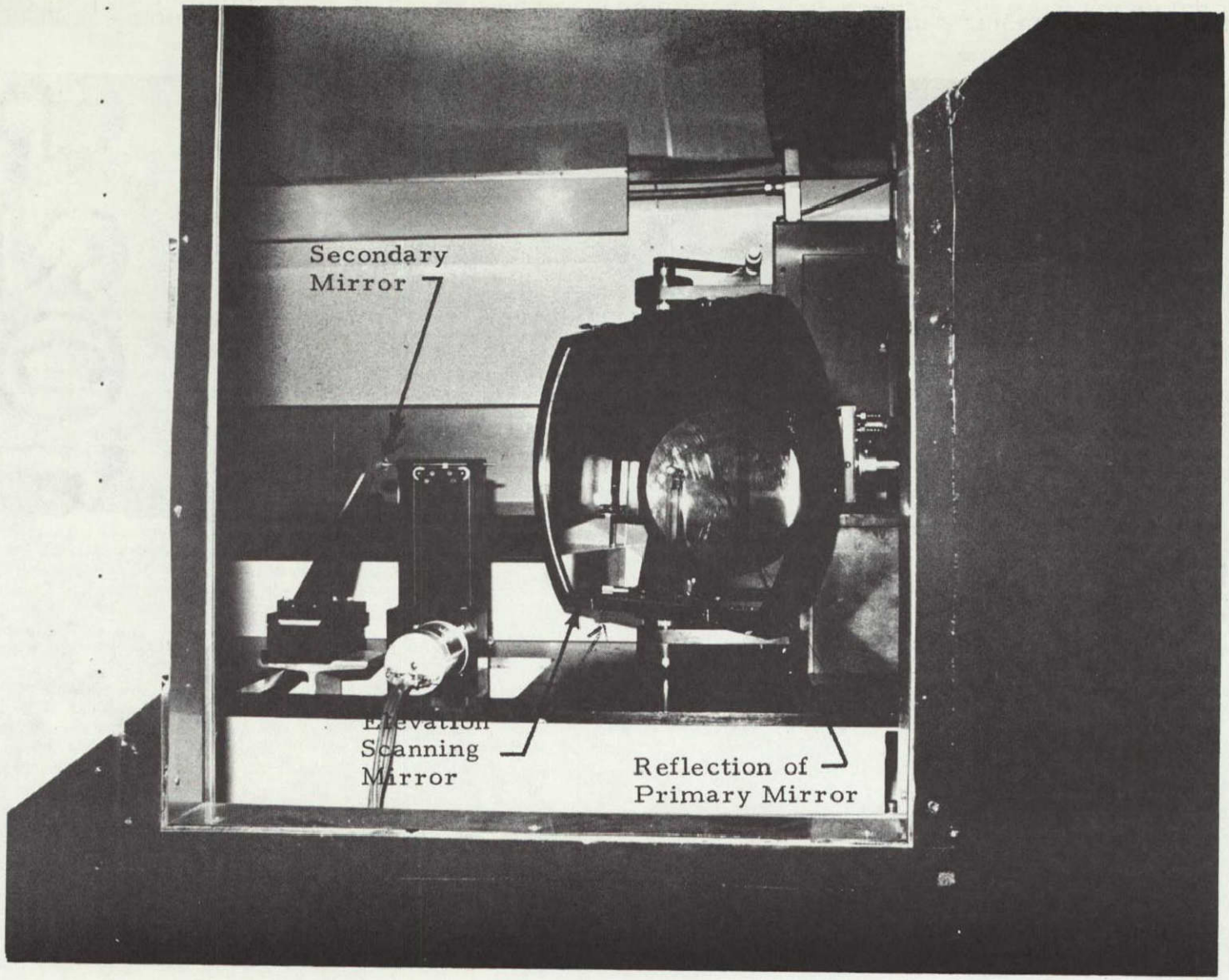

Fig. 10 - View Through Side Window of Laser Doppler Velocimeter Depicting Scanning Optics
(Note reflection of telescope primary mirror in elevation scanning mirror)

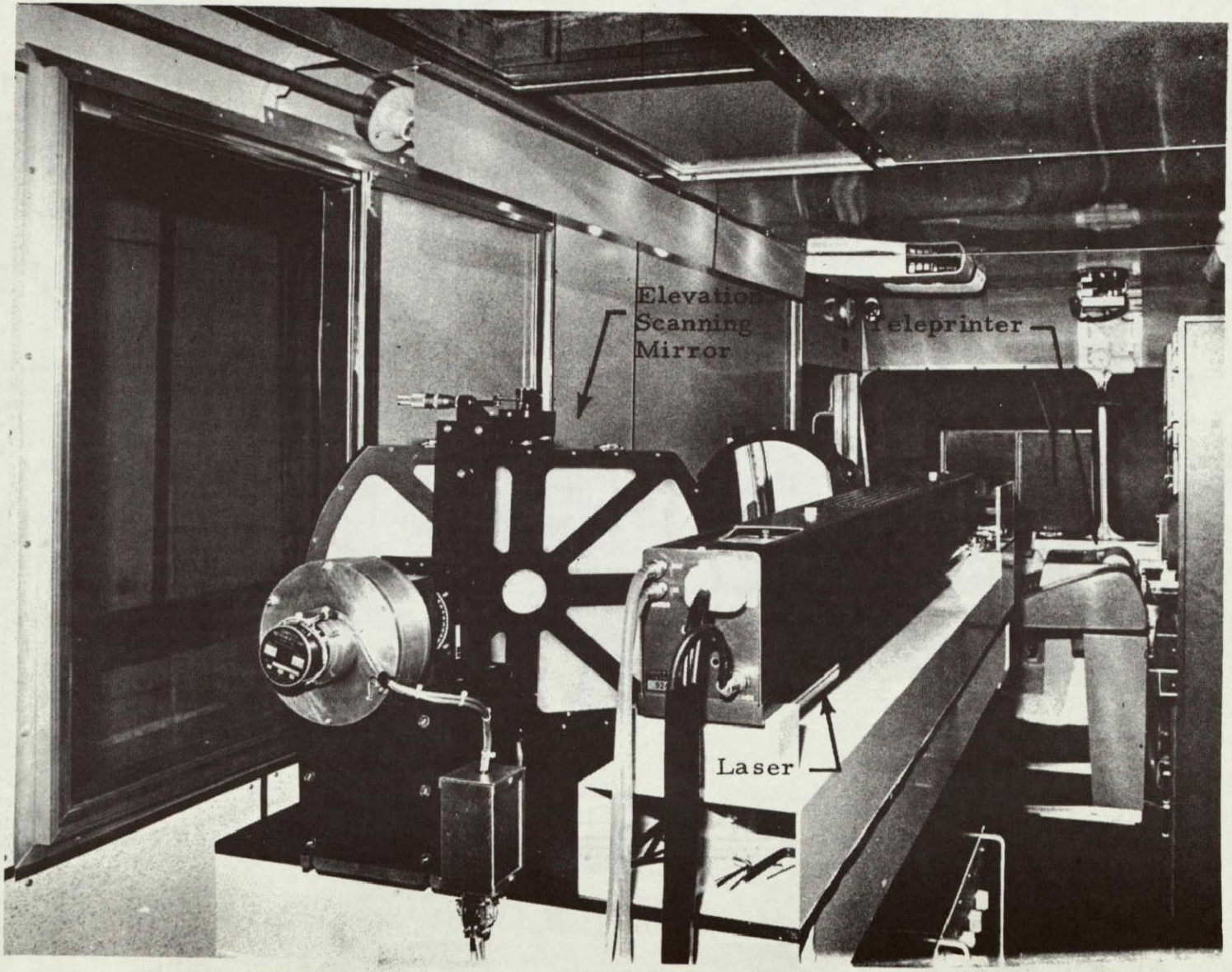

Fig. 11 - Interior View of Laser Doppler Velocimeter Van Looking Forward (Depicted in foreground is elevation scanning mirror on left and laser on right. Teleprinter in right rear.)

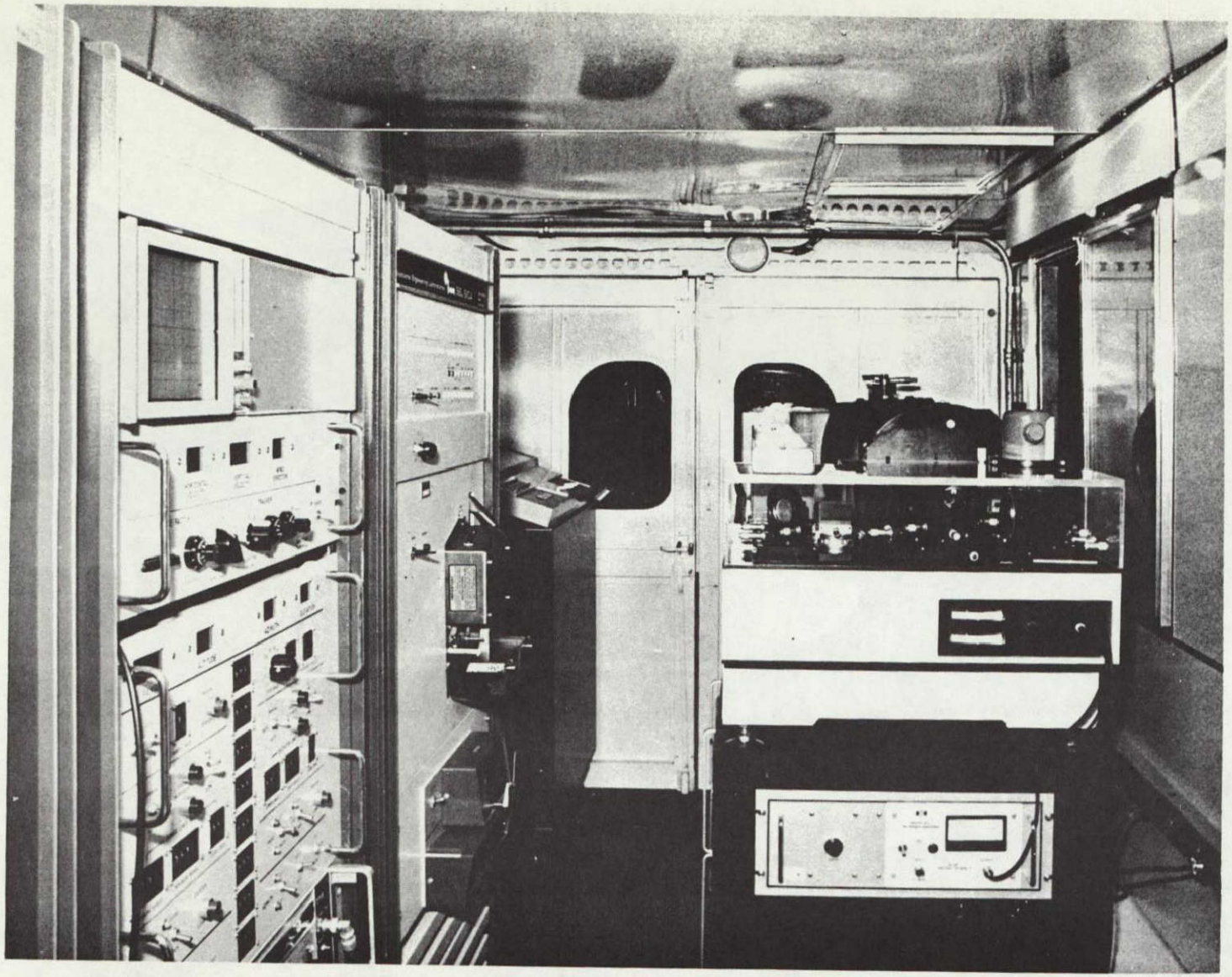

Fig. 12 · Interior View of Laser Doppler Velocimeter Van Depicting Display and Scanner Controls in First Rack, Computer in Second Rack, Digital Tape Unit Aft and Optics Package on Right

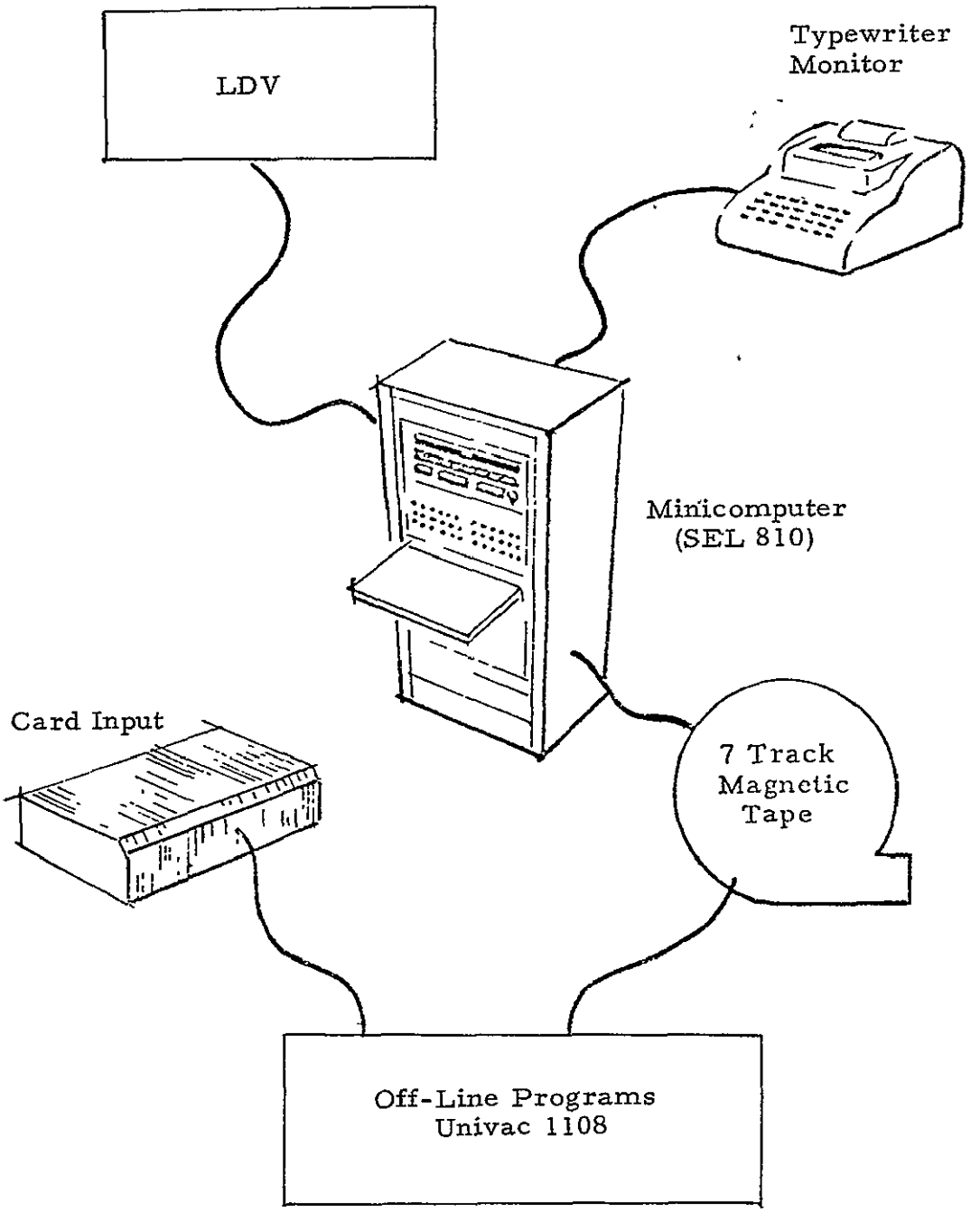

Fig. 13 - General Elements of LDV Data Acquisition and Data Processing System

frequency. A diagram of the output of the spectrum analyzer is shown in Fig. 14. The output of the spectrum analyzer is the value of signal intensity for each of one hundred frequency bands spanning the entire frequency scale. The data logger on the SEL computer records the signal intensity for each frequency band for which the Doppler frequency shift exceeds the velocity threshold and the signal intensity exceeds the amplitude threshold. These data were stored on magnetic tape for off-line processing. A flow diagram of the data logger is shown in Fig. 15.

2.2.2 Processing of Aerial Spray Measurements

The manner in which the aerial spray measurements were processed is summarized as follows: (1) the LDV signal was processed by the spectrum analyzer to yield the frequency and intensity spectrum of the laser return; (2) the output from the spectrum analyzer and the optical scanner was recorded by the SEL Data Logger program; and (3) the aerial spray and wind parameters were computed by the Aerial Spray program. A flow chart of the data processing sequence used for the Bryan aerial spray study is shown in Fig. 16.

The Aerial Spray program was developed for this study to decode the 7-track digital tape containing the full spectrum files and to compute the location, relative intensity, and line-of-sight velocity of the aerial spray cloud and the ambient wind velocities. The line-of-sight velocity was computed from Eq. (1). The relative spray concentration was computed from the intensity of the LDV signal. Previous measurements by Lockheed-Huntsville of particulates entrained in aircraft wake vortices have shown that the relative aerosol concentration can be obtained from the integration of the backscatter intensity versus frequency signal. The total area under the intensity versus frequency curve is a measure of the scattering cross section in the system's field of view. The parameter ISUM was used in the Aerial Spray program as a measure of the relative spray concentration, defined as

$$\text{ISUM} = \sum_{N=A}^{100} [I(N) - I(0)] \tag{6}$$

where I(N) is the intensity of the N^{th} frequency bin, I(0) is the amplitude threshold or the lowest acceptable intensity (typically 64 out of 1028), and A is the frequency threshold or the lowest acceptable frequency bin (typically 17 out of 100). Based on the results shown earlier in Fig. 6, the edge of the spray cloud is defined as the location where the integrated intensity, ISUM(e), falls midway between the maximum observed value, ISUM(m), and the background value, ISUM(b),

$$\text{ISUM(e)} = \frac{\text{ISUM(m)} - \text{ISUM(b)}}{2} \tag{7}$$

Sample outputs from the Aerial Spray program are shown in Table 1 and Figs. 17 and 18. The program lists the time from the start of the file, relative total intensity (ISUM), intensity of the frequency channel having the maximum intensity (I), line-of-sight velocity associated with the frequency

V_{pk} = Highest velocity (frequency) detectable above amplitude threshold

V_{ms} = Velocity (frequency) corresponding to maximum signal intensity

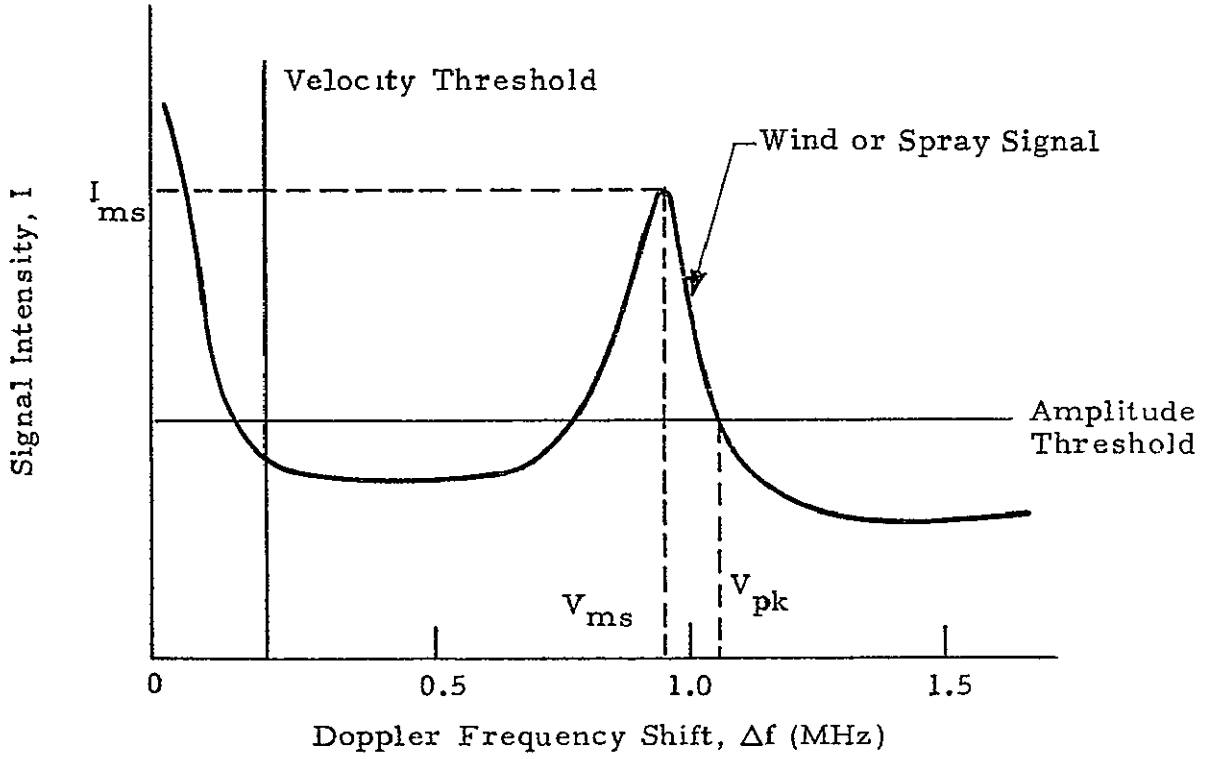

Fig. 14 - Typical Spectrum Analyzer Output

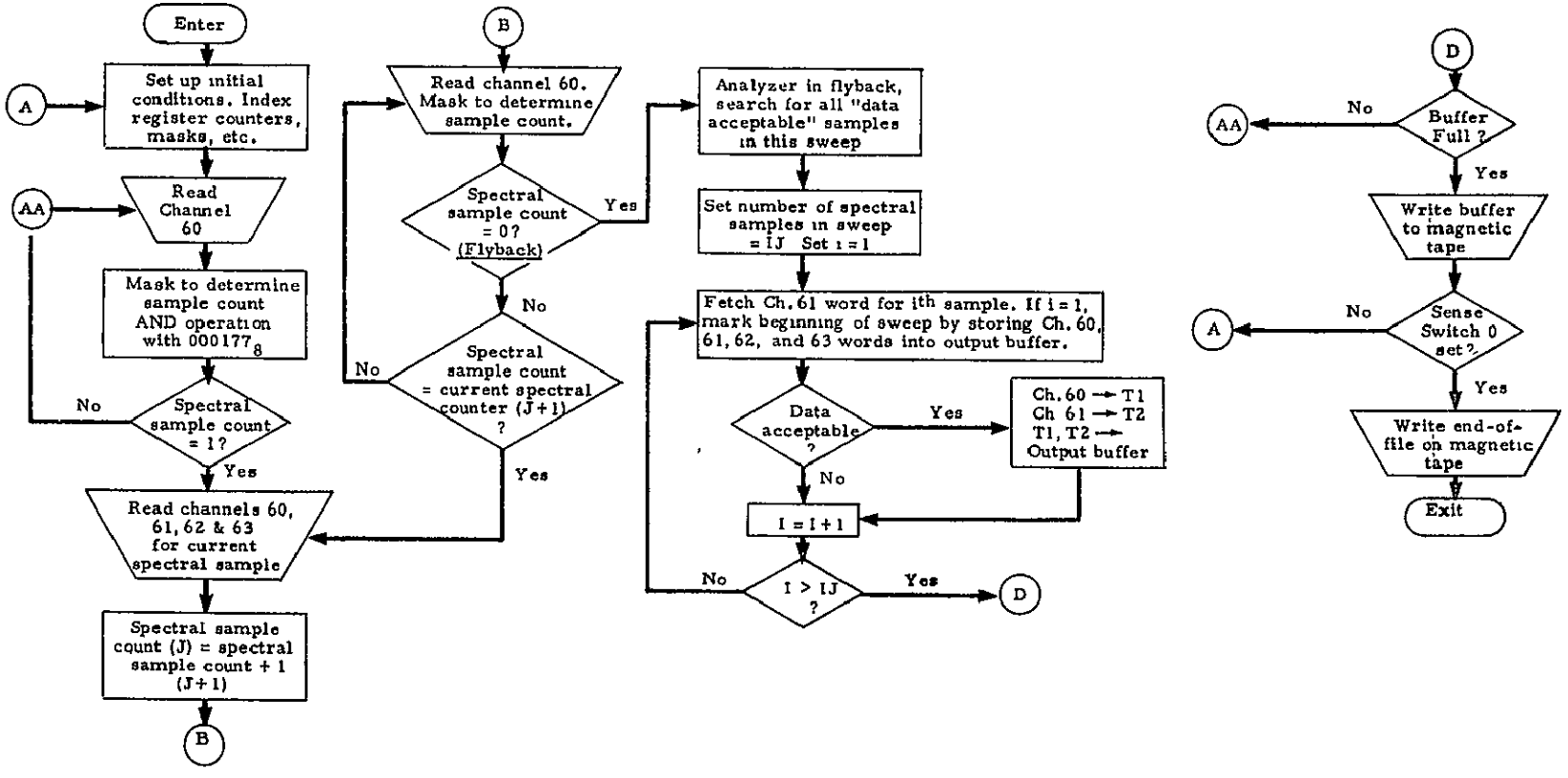

Fig. 15 - Full Spectrum Data Logger Macro Flow Chart

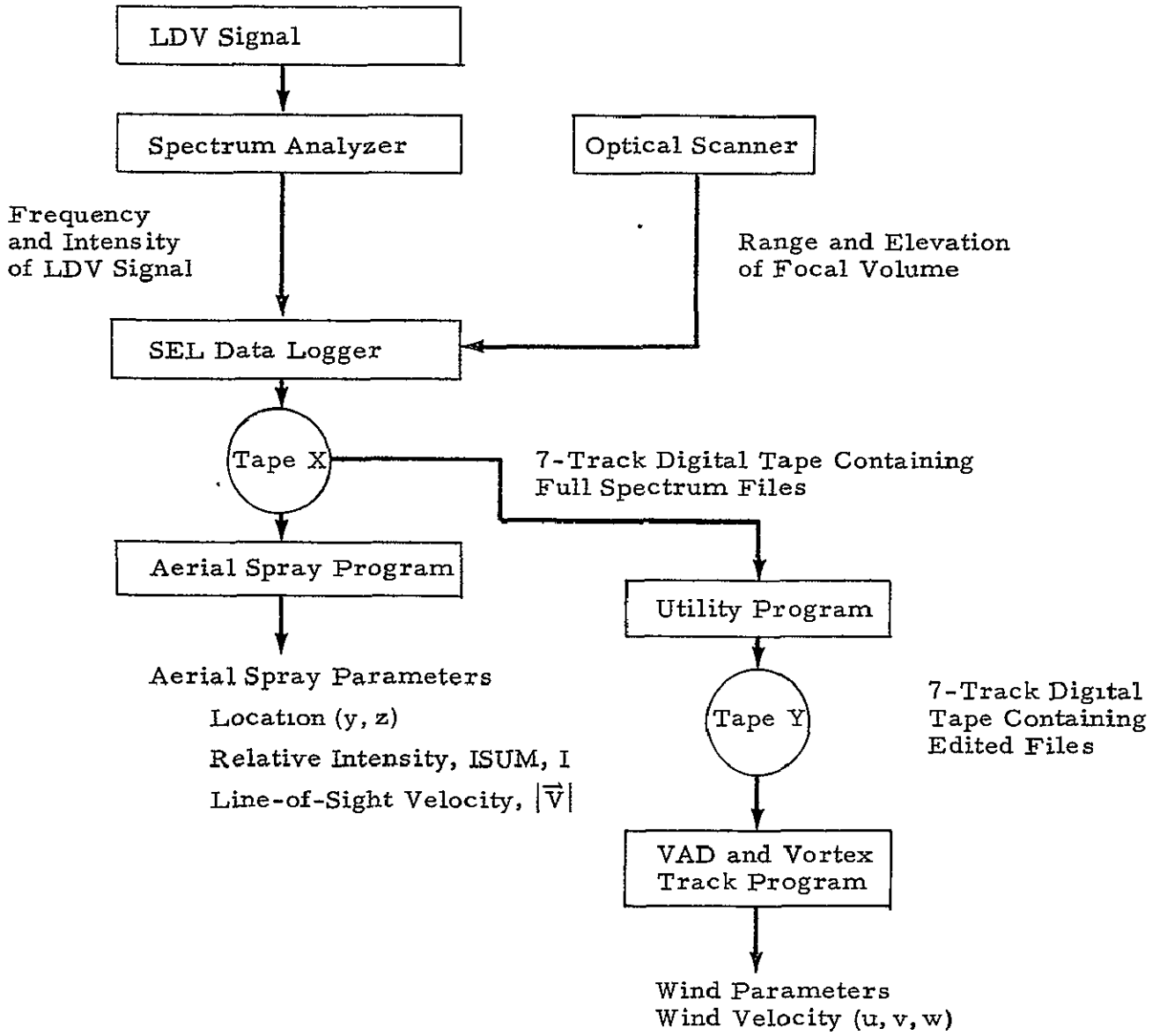

Fig. 16 - Data Processing Sequence Carried Out for the Bryan Aerial Spray Measurements

Table 1

OUTPUT FROM AERIAL SPRAY PROGRAM – PRINTOUT OF LDV SAMPLE POINTS FROM TEST 23

RECORD 6 OF FILE 1

Time (sec)	ISUM	I	VMS (m/sec)	VPK (m/sec)	R (m)	Theta (deg)	Y (m)	Z (m)
46.443	847.000	222	4.452	4.028	107.800	3.000	107.800	3.200
46.457	504.000	158	5.618	5.300	141.300	3.000	141.300	3.200
46.471	445.000	128	5.936	4.982	136.200	3.000	136.200	3.200
46.486	907.000	228	6.042	4.982	130.600	3.000	130.600	3.200
46.500	778.000	264	6.360	4.982	125.500	3.000	125.500	3.200
46.514	1205.000	254	5.936	4.770	119.200	3.000	119.200	3.200
46.529	886.000	150	6.254	3.498	113.500	3.000	113.500	3.200
46.543	1601.000	254	5.724	4.876	108.400	3.000	108.400	3.200
46.557	1743.000	240	5.724	3.180	102.500	3.000	102.500	3.200
46.571	1476.000	256	5.830	4.558	96.800	3.000	96.800	3.200
46.586	1447.000	208	5.512	4.240	91.700	3.000	91.700	3.200
46.600	919.000	174	5.406	4.134	85.900	3.000	85.900	3.200
46.614	724.000	256	5.618	3.604	80.800	3.000	80.800	3.200
46.629	404.000	122	5.088	3.604	75.700	3.000	75.700	3.200
46.643	348.000	160	4.982	3.604	70.100	3.000	70.100	3.200
46.657	210.000	128	5.088	3.710	64.900	3.000	64.900	3.200
46.671	28.000	80	4.876	4.876	59.600	3.000	59.600	3.200
46.686	6.000	68	4.558	4.558	54.300	3.000	54.300	3.200
46.700	29.000	76	4.346	4.346	53.000	3.000	53.000	3.200
46.714	28.000	80	4.028	4.028	57.800	3.000	57.800	3.200
46.729	122.000	92	5.088	4.134	63.000	3.000	63.000	3.200
46.743	283.000	126	5.088	3.604	68.400	3.000	68.400	3.200
46.757	315.000	128	5.194	4.028	73.600	3.000	73.600	3.200
46.771	707.000	224	5.724	3.922	79.100	3.000	79.100	3.200
46.786	835.000	230	6.572	4.770	84.400	3.000	84.400	3.200
46.800	1298.000	202	5.724	3.498	89.500	3.000	89.500	3.200
46.814	1359.000	256	6.148	3.498	95.400	3.000	95.400	3.200
46.829	1032.000	154	7.208	3.922	99.900	3.000	99.900	3.200
46.843	1350.000	192	6.360	2.650	106.000	3.000	106.000	3.200
46.857	1292.000	254	6.784	4.982	110.900	3.000	110.900	3.200
46.871	1530.000	254	6.784	5.194	116.300	3.000	116.300	3.200
46.886	1133.000	216	6.572	4.982	121.500	3.000	121.500	3.200
46.900	913.000	202	6.360	5.194	127.200	3.000	127.200	3.200
46.914	1156.000	318	6.254	4.876	132.500	3.000	132.500	3.200

REPRODUCIBILITY OF THE ORIGINAL PAGE IS POOR

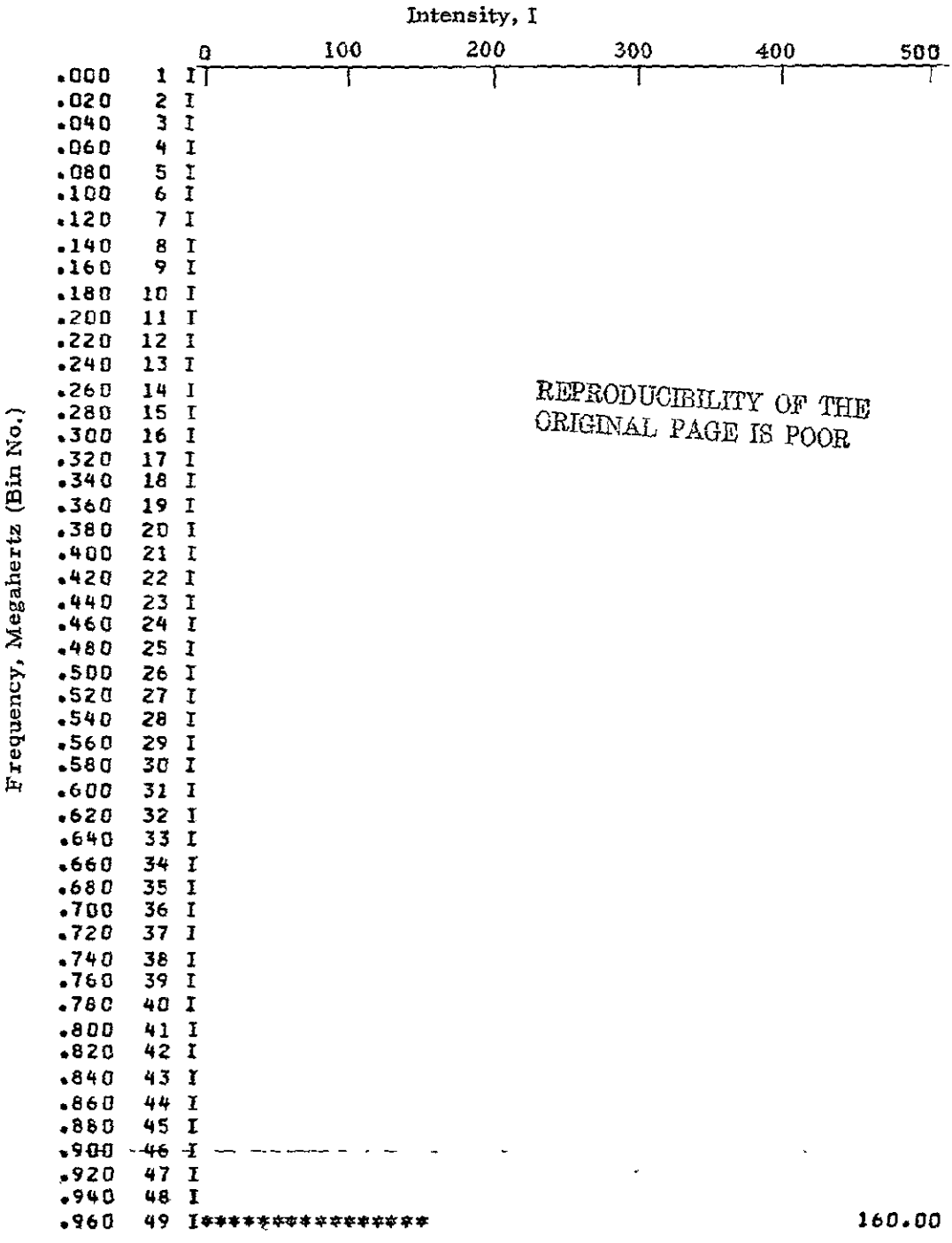

REPRODUCIBILITY OF THE
ORIGINAL PAGE IS POOR

Fig. 17 - Output from Aerial Spray Program – Full Spectrum Plot, Test 23
Time 41 sec Before Release, y = 73 (m), z = 2.4 (m)

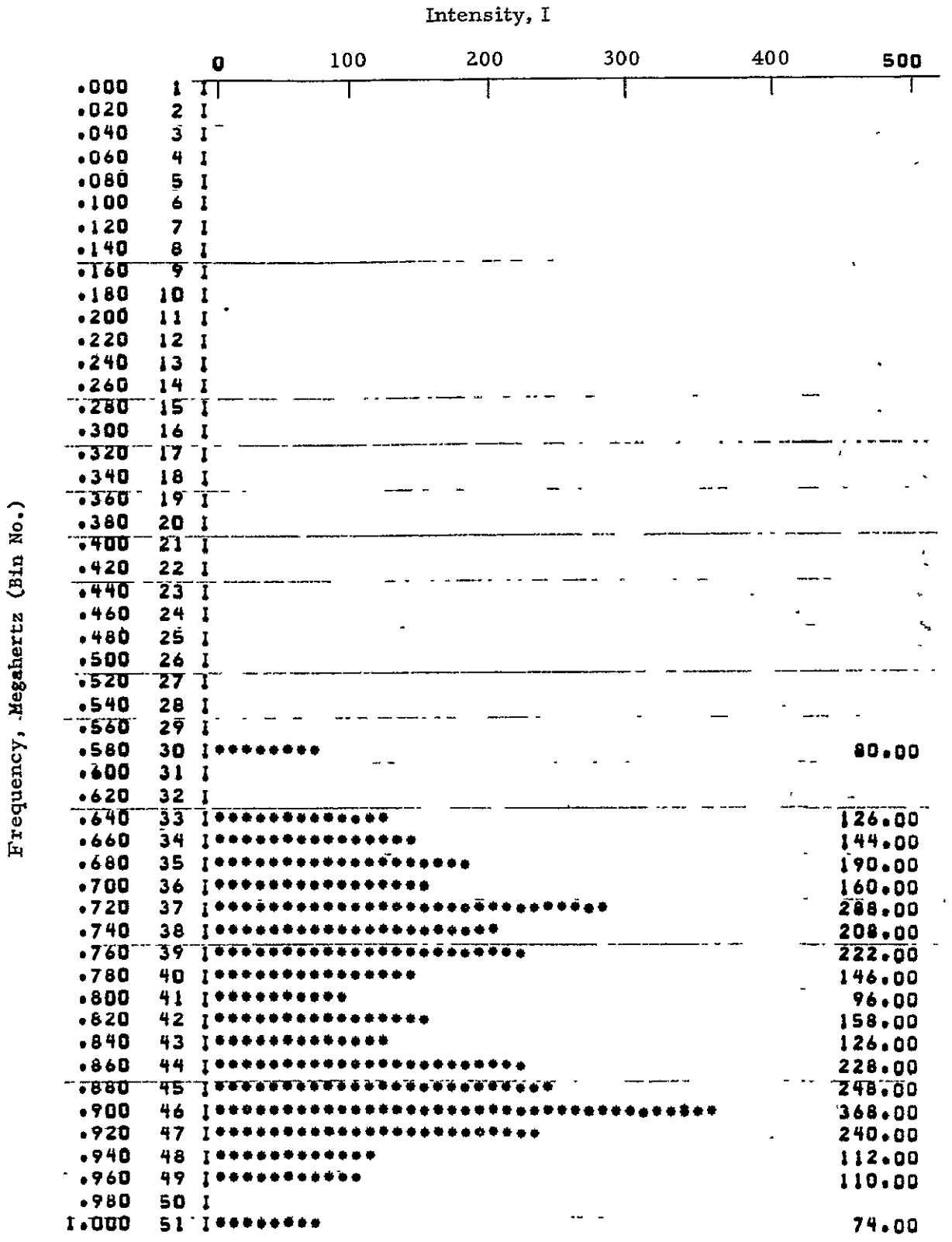

Fig. 18 - Output from Aerial Program — Full Spectrum Plot Test 23, Time 17 sec After Release, y = 107.2 (m), z = 3.2 (m) (Airplane Located at y = 61 (m), z = 10 (m))

channel having the maximum intensity (BMS), peak line-of-sight velocity (VPK), range (R), elevation angle (θ), and the Y and Z coordinates of each sample point as illustrated in Table 1. For the sample case shown, the presence of the aerial spray is noted by the high ISUM values for Y ranging from 90 to 130 m. The complete intensity versus frequency spectrum of selected sample points is plotted on a line printer as shown in Fig. 17. The vertical scale is the signal intensity and the horizontal scale is the signal frequency in megahertz (or bin number). The intensity of the signal in each frequency bin is plotted by a bar graph using star symbols where each star represents an intensity value of 10 or fraction thereof on a scale of 0 to 1028. The full spectrum plots illustrated in Figs. 17 and 18 show the typical signal level before spray release and during the release, respectively. Prior to the spray release, a low intensity signal, I = 160, is noted at 0.960 MHz corresponding to a line-of-sight velocity of 5.1 m/sec and associated with the ambient wind. After the spray release, a broad spectrum of high intensity signals is observed ranging from 0.580 to 1.000 MHz corresponding to a line-of-sight velocity range of 3 to 5.3 m/sec. The highest intensity signal, I = 368, measured earlier. The presence of the aerial spray increases the backscatter intensity and the range of velocities observed by the LDV system. Note that the integral of the intensity/frequency spectrum, ISUM, is 20 times higher in the spray cloud than the ambient level (ISUM = 3324 and 160, respectively). The total area under the intensity/frequency curve, ISUM, is a measure of the scattering cross section in the systems field of view and is used as a discriminant for locating the spray cloud.

Additional plots generated by the Aerial Spray program show the magnitude and location of the high backscatter intensity regions measured by the LDV system. A sample plot of the integrated spectrum, ISUM, is illustrated in Fig. 19. The plot shows the location of low, medium, and high ISUM values given by the dot, M, and square symbols, respectively, 0 to 10 sec after spray release. From the shaded areas indicating the square symbols, the center of the aerial cloud is estimated to be at 3 m altitude 25 m downwind of the release. The output from the Aerial Spray program is illustrated in more detail in Section 4.1.

2.2.3 Processing of Wind Measurements

The line-of-sight velocity measurements obtained in the VAD scan mode were processed to yield the three component wind field at altitudes between 20 and 600 m. The VAD mode for wind measurements was originally proposed by Lhermitte and Atlas and is discussed in Ref. 7. In the VAD mode the telescope is focused at the altitude of interest, the beam being directed at a zenith angle, β. The beam is then scanned in azimuth, thus tracing out a circle at the selected altitude (Fig. 20).

The instantaneous line-of-sight component of velocity within the sensing volume as measured by the LDV, v_r, is given by

$$v_r = v_h \sin\beta \cos(\theta - \theta_o) + w \cos\beta \qquad (8)$$

v_h and θ_o, respectively, being the speed and direction of the horizontal wind motion and w the vertical motion at the height being sampled. The azimuthal dependence of v_r is sufficient to yield the horizontal speed and direction and vertical component of velocity, respectively.

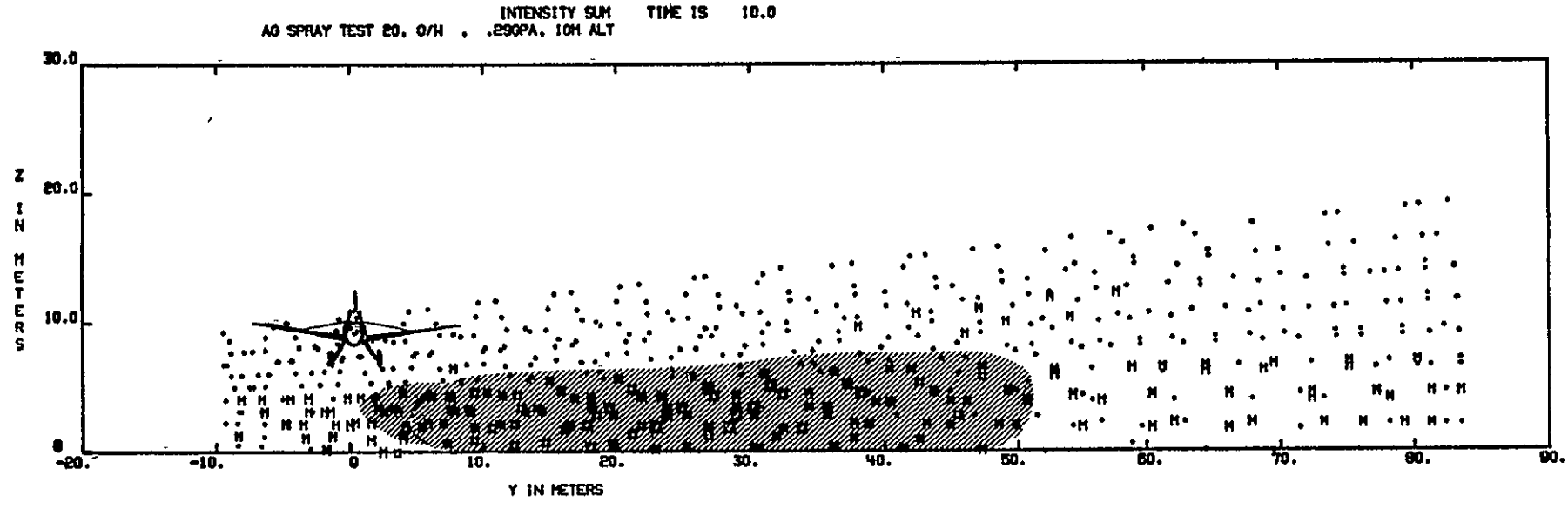

Fig. 19 - Output from Aerial Spray Program – Intensity Sum Plot

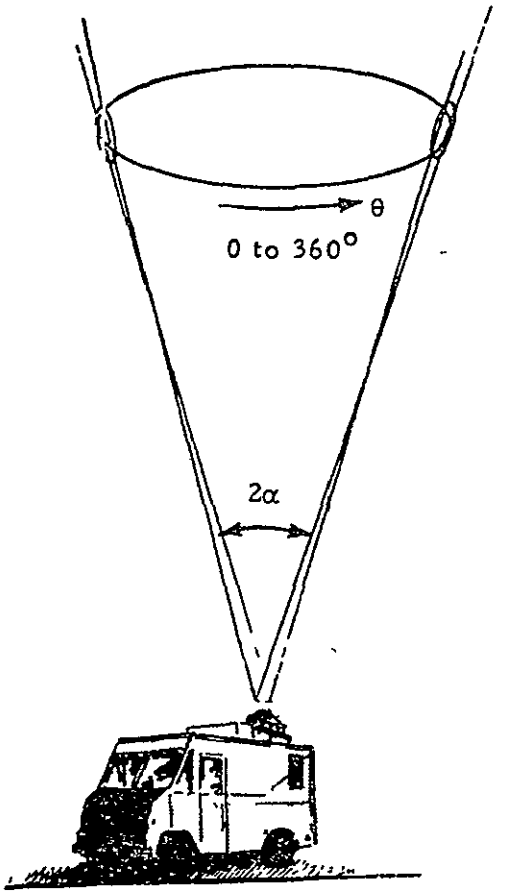

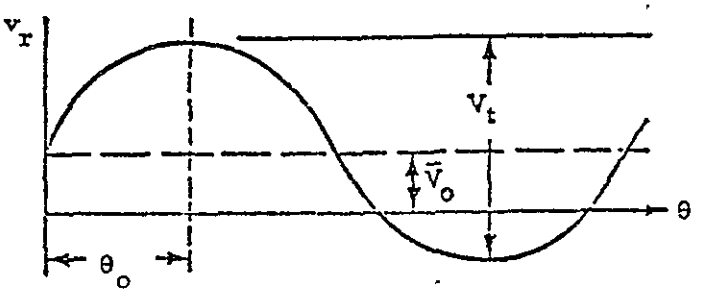

w = vertical wind component
= $\bar{V}_o/\cos\alpha$

v_h = horizontal wind component
= $V_t/(2\sin\alpha)$

θ_o = direction of horizontal wind component

Fig. 20 - Principle of VAD Operation

In the present mode of operation, the system is unable to distinuish between positive and negative values of v_r. Therefore, it is the absolute value of v_r ($|v_r|$) that is sensed. This results in a signal as shown in Fig. 21 instead of the sinusoidal signal as shown in Fig. 20. This results in an ambiguity of 180 deg in the wind direction since it is uncertain which peak in Fig. 21 represents looking into the wind. In practice, no problem occurs because the operator records approximate wind direction, and the data processing technique can then calculate exact wind direction. This resolves all wind direction ambiguities if the operator's input estimate is within ± 89 deg of the true wind direction.

A sample wind signature is shown in Fig. 22. The signal is derectified according to the line-of-sight velocity maximum which is closest to the operator estimated wind direction. A sample derectified signature is shown in Fig. 23. The wind is calculated by curve-fitting the points shown in Fig. 22 to a sine wave in a least squares sense. This is accomplished by determining the coefficients A, B, and C which minimize

$$\sum (V_i - C - A\cos\theta_i - B\sin\theta_i)^2 \tag{9}$$

where V_i is the line-of-sight velocity (derectified) at point i, θ_i is azimuth at point i. Thus we obtain A, B, and C by

$$\left[\sum_i \cos^2\theta_i\right]A + \left[\sum_i \cos\theta_i \sin\theta_i\right]B + \left[\sum_i \cos\theta_i\right]C = \sum_i V_i \cos\theta_i \tag{10}$$

$$\left[\sum_i \cos\theta_i \sin\theta_i\right]A + \left[\sum_i \sin^2\theta_i\right]B + \left[\sum_i \sin\theta_i\right]C = \sum_i V_i \sin\theta_i \tag{11}$$

$$\left[\sum_i \cos\theta_i\right]A + \left[\sum_i \sin\theta_i\right]B + nC = \sum_i V_i \tag{12}$$

The steps for calculating wind using the least squares algorithm are:

1. Find least squares curve fit for a sine wave to the data according to Eqs. (10) through (12).
2. Compute horizontal velocity

$$V_h = \frac{\sqrt{A^2 + B^2}}{\sin(\text{cone angle}/2)} \tag{13}$$

$$V_h = (V_1 + V_2)/2 \sin\theta$$
$$w = (V_1 - V_2)/2 \cos\theta$$

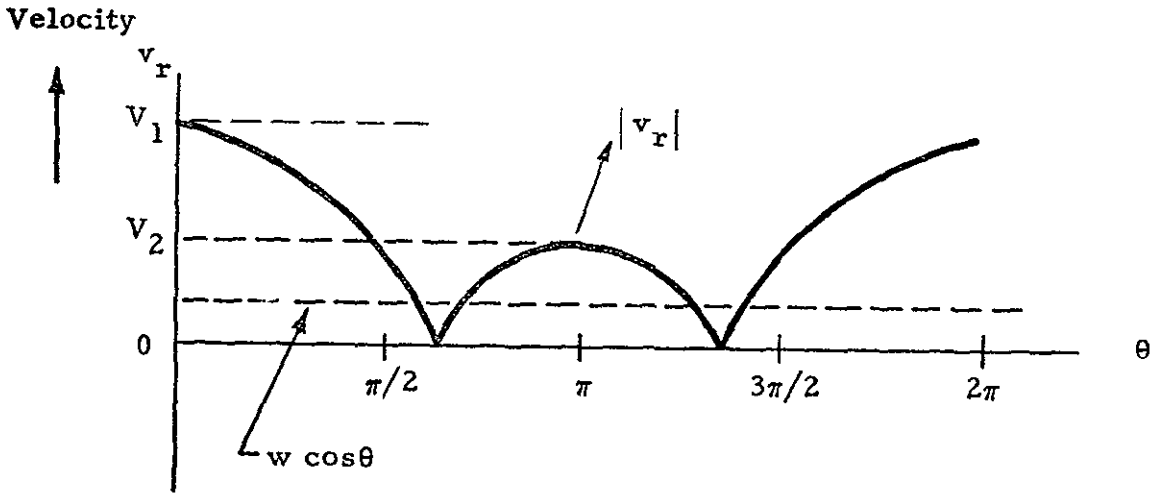

Fig. 21 - Azimuth Angle Dependence of Measured Velocity Component

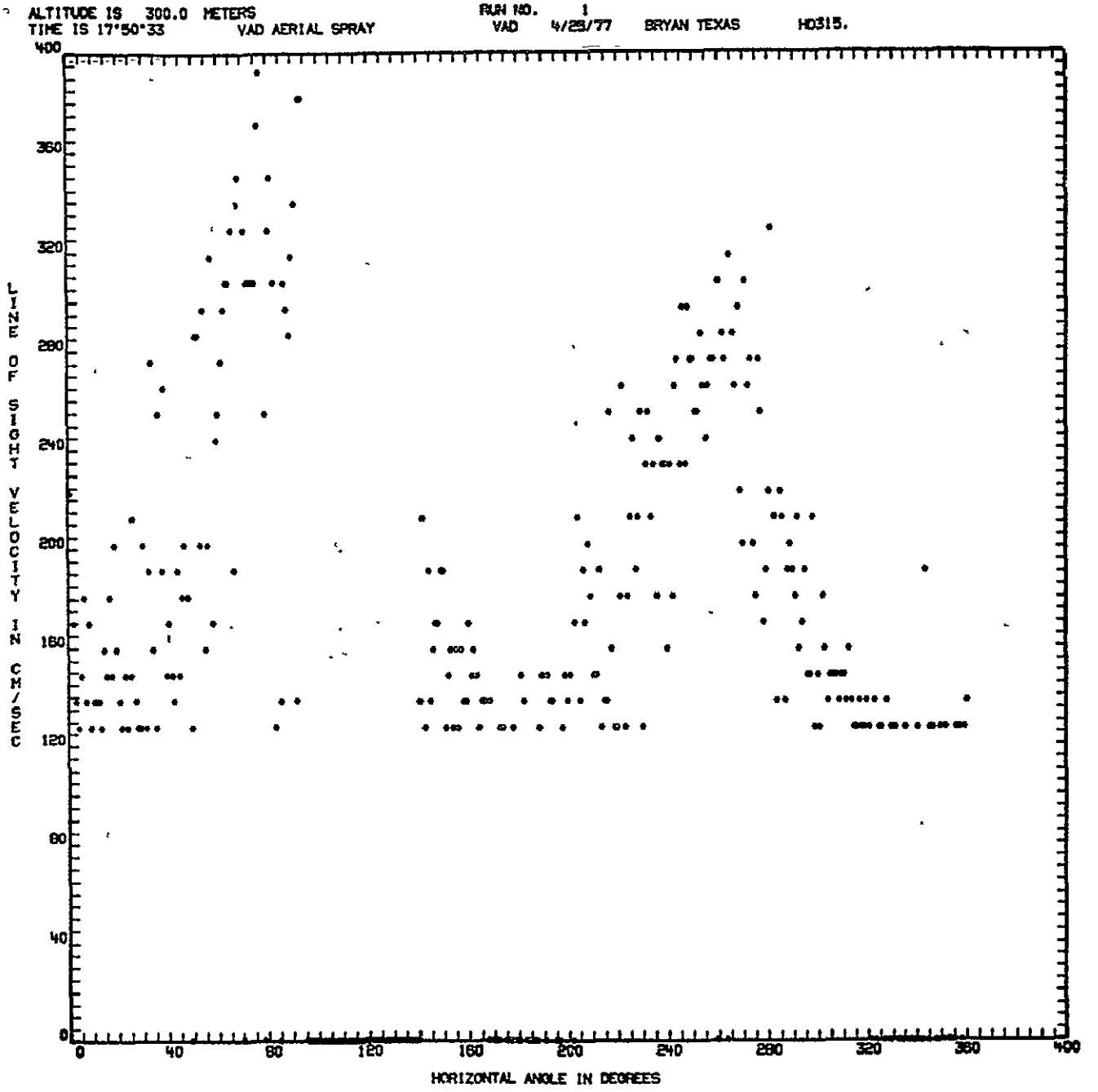

Fig. 22 - Sample Output Plot from the VAD and Vortex Track Program Operating in the VAD Mode

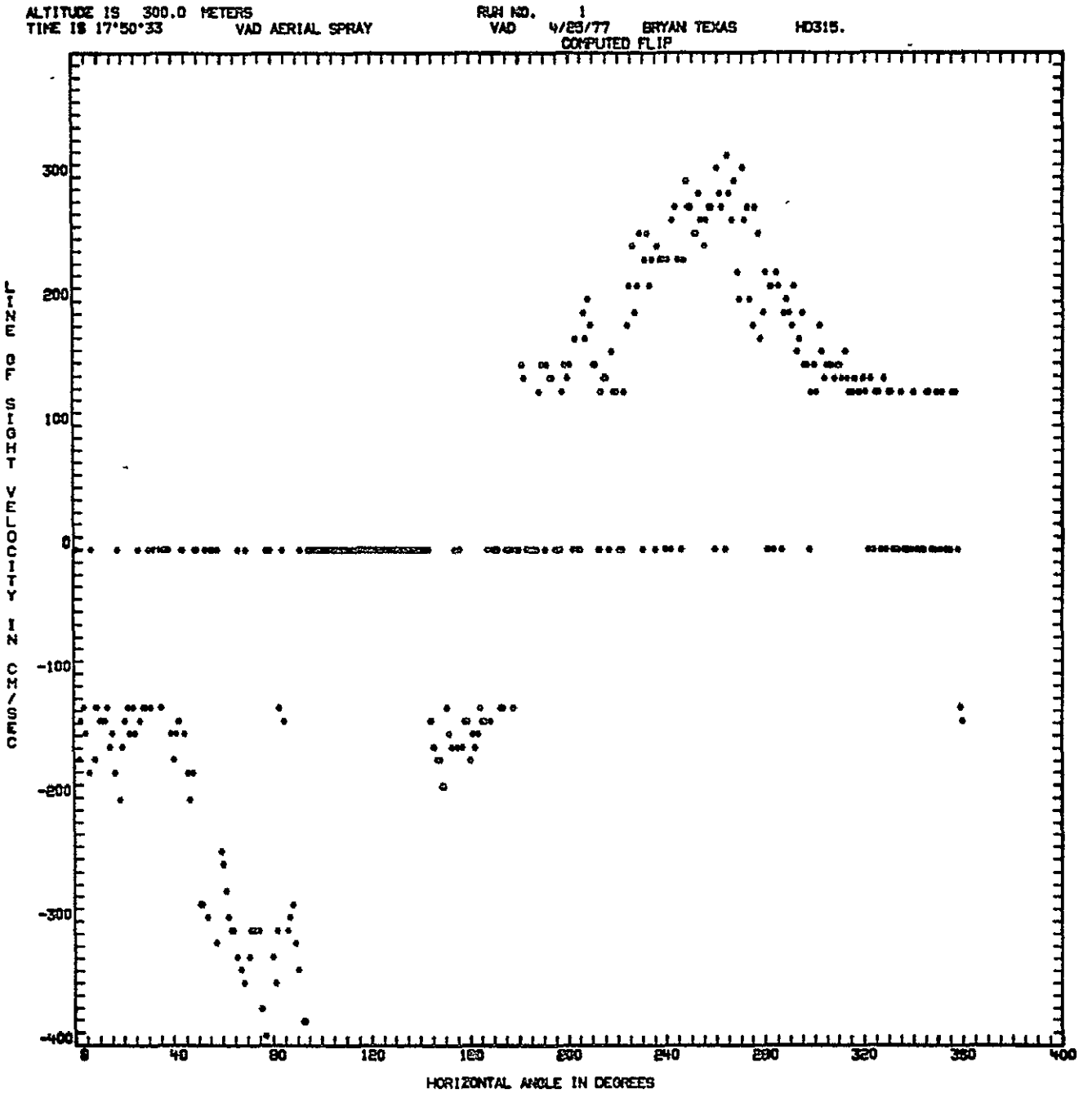

Fig. 23 - Derectified Line-of-Sight Velocity for VAD Mode

3. Compute horizontal angle

$$\text{Angle}_h = \text{Atan}(B/A) \tag{14}$$

4. Compute vertical wind velocity

$$w = \frac{-C}{\cos(\text{cone angle}/2)} \tag{15}$$

A more detailed discussion of the LDV wind processing technique is given in Refs. 3 and 4.

REPRODUCIBILITY OF THE
ORIGINAL PAGE IS POOR

3. DESCRIPTION OF EXPERIMENTAL TESTS

3.1 Flight Test Program

The aerial spray tests consisted of 25 low-level passes by a Piper Pawnee agricultural aircraft over an instrumented test site located at the Texas A&M Research and Extension Center at Bryan, Texas. A summary of the test conditions including aircraft height above ground, composition of spray material, and spray rate is shown in Table 2. The type of nozzles used and the associated flow rates and pressures are also listed in Table 2. The staff at the Agricultural Research Service at Texas A&M University conducted the flight tests and generated the controlled swath patterns and carried out ground fallout measurements discussed in more detail in Appendix A. A diagram of the Bryan test site is shown in Fig. 24. The LDV van was located at the intersection of runway 17R and 28. Two sample lines for fallout collection were set up along runway 17R and 28, and a 5 m meteorological tower was located approximately 100 m east of the N-S sample line. The flight path was oriented approximately perpendicular to the wind direction with sampling stations at selected downwind distances. The optic line-of-sight of the LDV was aligned along the sampling line.

3.2 Operation of Laser Doppler Velocimeter

To obtain measurement of the airborne spray, the LDV system was located adjacent to the flight path ($\sim$ 600 m for Tests 1 through 8 and 60 m for the remaining cases) and the laser focal volume was scanned in a plane normal to the flight path as illustrated in Fig. 25. With the laser scanning in range and elevation, the cross-section of the aerial spray pattern was interrogated continuously in time up to 13 minutes after the release. The test configuration was arranged so that the swath pattern drifted, away from the LDV, for Tests 9 through 24 and toward the LDV for Tests 1 through 8.

The three-dimensional wind velocity profile was obtained before and after each series of flybys with the LDV operating in the VAD mode.

Table 2

LOG FOR LDV AERIAL SPRAY DRIFT MEASUREMENT FEASIBILITY TEST

Test No.	Date/Time April (day/hr.)	(min)	(sec)	Spray Material*	Aircraft Height (m)	Nozzle Type/Size	Spraybar Pressure (kg/cm^2)	Material Flow Rate (liter/sec)	Application Rate** (liter/hectare)
1	24 19	08	04	water	3	D10-45	2.81	2.12	37.0
2	24 19	44	00	water	10	D10-45	2.81	2.12	37.0
3	25 13	45	45	water	3	TX4	3.51	0.15	2.6
4	25 14	27	33	water	10	TX4	3.51	0.15	2.6
5	25 18	05	00	o/w	3	TX4	3.51	0.15	2.7
6	25 18	42	52	o/w	10	TX4	3.51	0.15	2.7
7	25 19	22	56	o/w	3	D10-45	2.81	2.35	41.0
8	25 19	56	24	o/w	10	D10-45	2.81	2.35	41.0
9	26 14	58	26	o/w+n	3	D10-45	2.81	2.29	40.0
10	26 15	40	24	o/w+n	10	D10-45	2.81	2.29	40.0
11	26 17	39	59	o/w+n	3	TX4	3.51	0.19	3.3
12	26 18	21	45	o/w+n	10	TX4	3.51	0.19	3.3
13	27 09	25	59	water	3	TX4	3.51	0.15	2.6
14	27 09	58	50	water	10	TX4	3.51	0.15	2.6
15	27 11	31	21	water	3	D10-45	2.81	2.12	37.0
16	27 12	11	08	water	10	D10-45	2.81	2.12	37.0
17	28 07	17	46	o/w	3	D10-45	2.81	2.35	41.0
18	28 07	50	33	o/w	10	D10-45	2.81	2.35	41.0
19	28 08	34	26	o/w	3	TX4	3.51	0.15	2.7
20	28 09	59	16	o/w	10	TX4	3.51	0.15	2.7
21	28 17	41	56	o/w+n	3	D10-45	2.81	2.29	40.0
22	28 18	16	15	o/w+n	10	D10-45	2.81	2.29	40.0
23	28 18	56	32	o/w+n	3	TX4	3.51	0.19	3.3
24	28 19	22	54	o/w+n	10	TX4	3.51	0.19	3.3
D***	28 09	39	17	—	10	—	—	—	—

*Water— Contained 1.2% manganese sulfate and .0375% methylene blue dye; o/w — Oil/water emulsion containing 1/3 ratio of diesel oil to water. Also contained Triton X-100 emulsifier (1.56% of diesel volume), manganese sulfate (1.2% of water by weight), and methylene blue dye (.0375% of water by weight), and, o/w+n — same as o/w except Nalco-trol (polyvinyl polymer) was added at the rate of 62.4cc per 100 liters of water.

**Application rate in liters per hectare assuming a 12.2 m wide effective spray swath and based on an aircraft speed of 169 km/hr. This is equivalent to 3.44 hectare/Min. (8.48 Acres/Min.

***Dummy run — no spray.

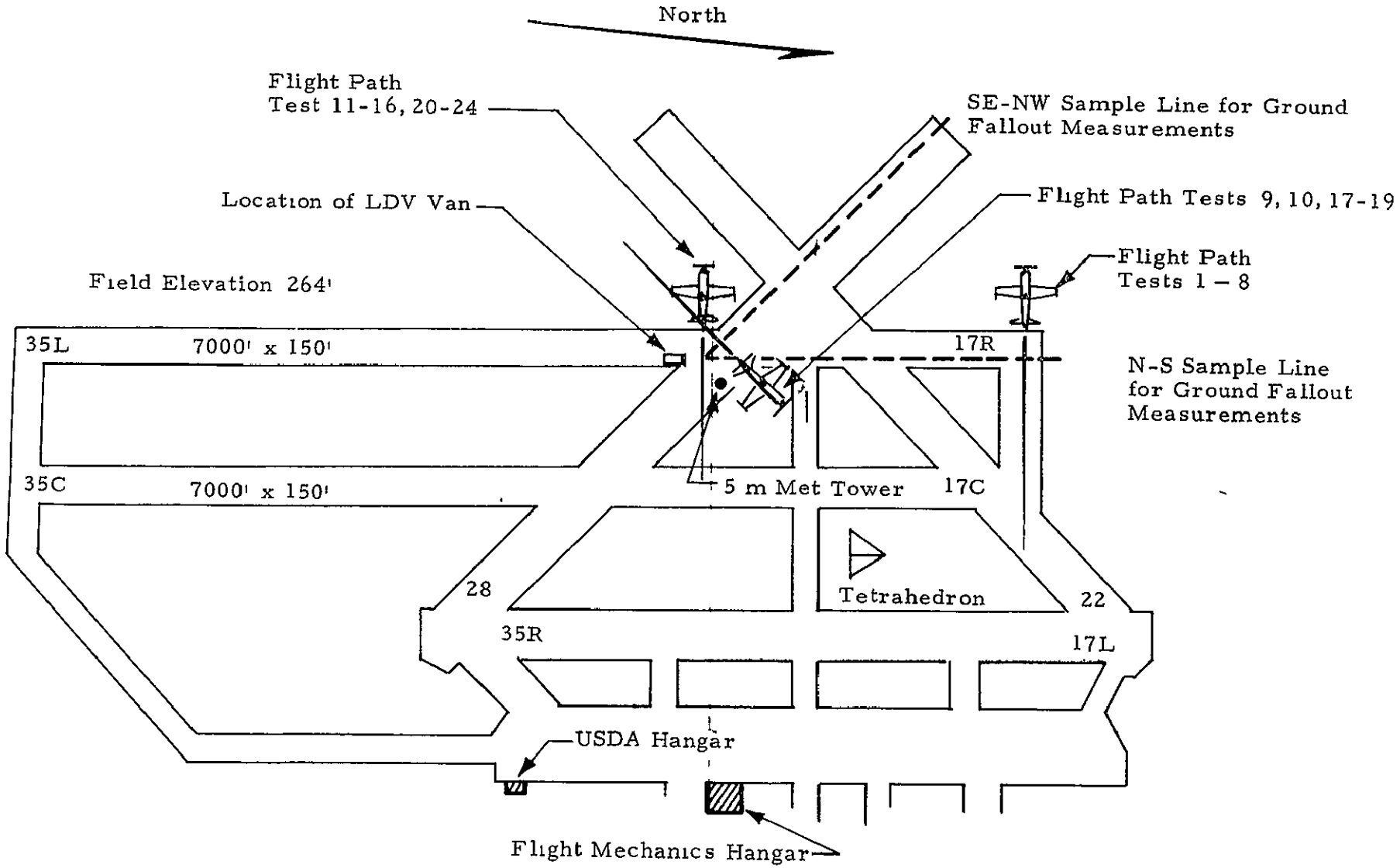

Fig. 24 - Diagram of Bryan, Texas, Test Site

LDV Scan Parameters

Scan Mode	Coordinated Range and Elevation
Elevation Angle	Max 45 deg Min -3 deg
Range	Max 600 m Min 50 m
Scan Rate	Elevation 0.1 to 0.4 Hz Range 1 to 2 Hz

Aircraft Parameters

Altitude	3 – 10 m
Lateral Distance from LDV	60 – 600 m

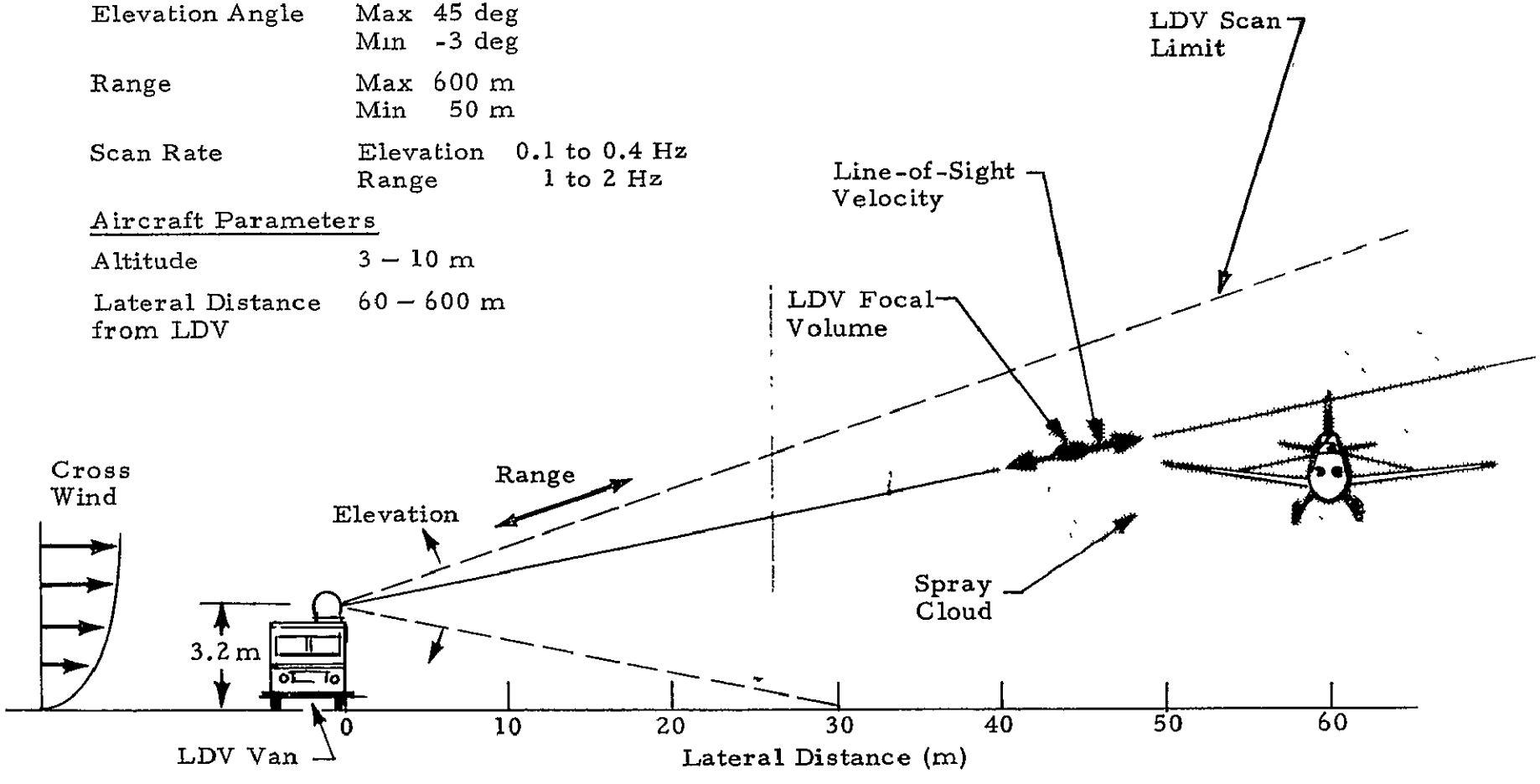

Fig. 25 - Typical Scan Configuration for LDV Aerial Spray Measurements

4. RESULTS OF LASER DOPPLER VELOCIMETER MEASUREMENTS

The LDV measurements obtained during the tests have been analyzed to determine the location, spatial extent, and relative concentration of the airborne spray releases and the ambient wind velocity profiles. In the following section, a discussion of the typical airborne spray measurements, the observed airborne spray transport and dispersion characteristics, and the observed wind velocities is given.

4.1 Typical Measurements of Airborne Spray Characteristics

The airborne spray release from the agricultural aircraft was detected by the LDV as a high backscatter intensity region. The cross section of the high intensity region was a quasi-elliptical region extending downwind from the release point as illustrated in Fig. 26. The extreme limits of the spray cloud, shown in Fig. 26, are indicative of the LDV scan limits. The regions of low, moderate, and high relative particulate concentration were defined based on the integrated backscatter intensity, ISUM, observed at each sample point. The integrated backscatter intensity from the spray cloud was an order of magnitude above the backscatter intensity from the ambient atmospheric aerosol which was illustrated earlier in Figs. 17 and 18.

The typical cumulative relative frequency distribution observed during the tests for ISUM near the release point is given in Fig. 27. Prior to the release, the probability that ISUM exceeds 300 is 0. During the spray release, the probability for ISUM to exceed 300 is 0.93. A few minutes after the release, the ISUM distribution has essentially returned to the background levels. The difference in ISUM between ambient and spray conditions, shown in Fig. 27, indicates that the airborne spray cloud can be discriminated from the background aerosol based on an ISUM criterion.

The criteria for determining the relative aerosol concentrations from the ISUM values and the corresponding symbols are given in Table 3. To show the detailed relative aerosol concentration, the ISUM values were divided into 27 divisions (26 equal divisions and a 27th catch-all class) and are labeled separately. For showing the coarse relative concentrations, the ISUM values were grouped into three general classes including background (ISUM = 0 to 299), moderate (ISUM = 300 to 999), and high (ISUM $\geq$ 1000). The symbols for each division and class were increased in size from the low to high values to further accentuate the gradations in relative concentration.

A typical aerial spray cross-section plot showing coarse gradations in relative particulate concentration is given in Fig. 28. From the shaded area around the square or M symbols, indicative of high ISUM values, the location

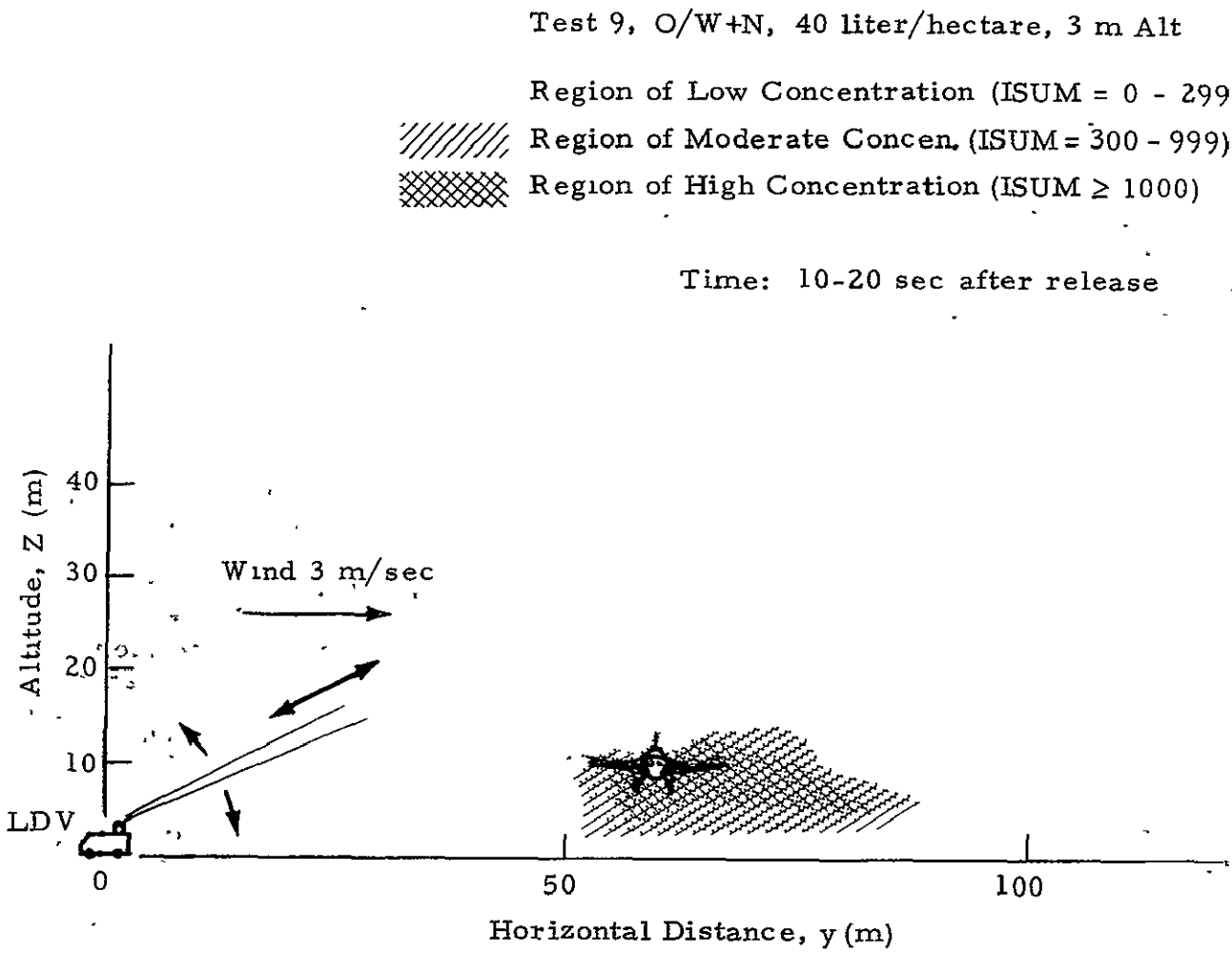

Fig. 26 - Particulate Concentration Regions for Aerial Spray Measured with Laser Doppler Velocimeter

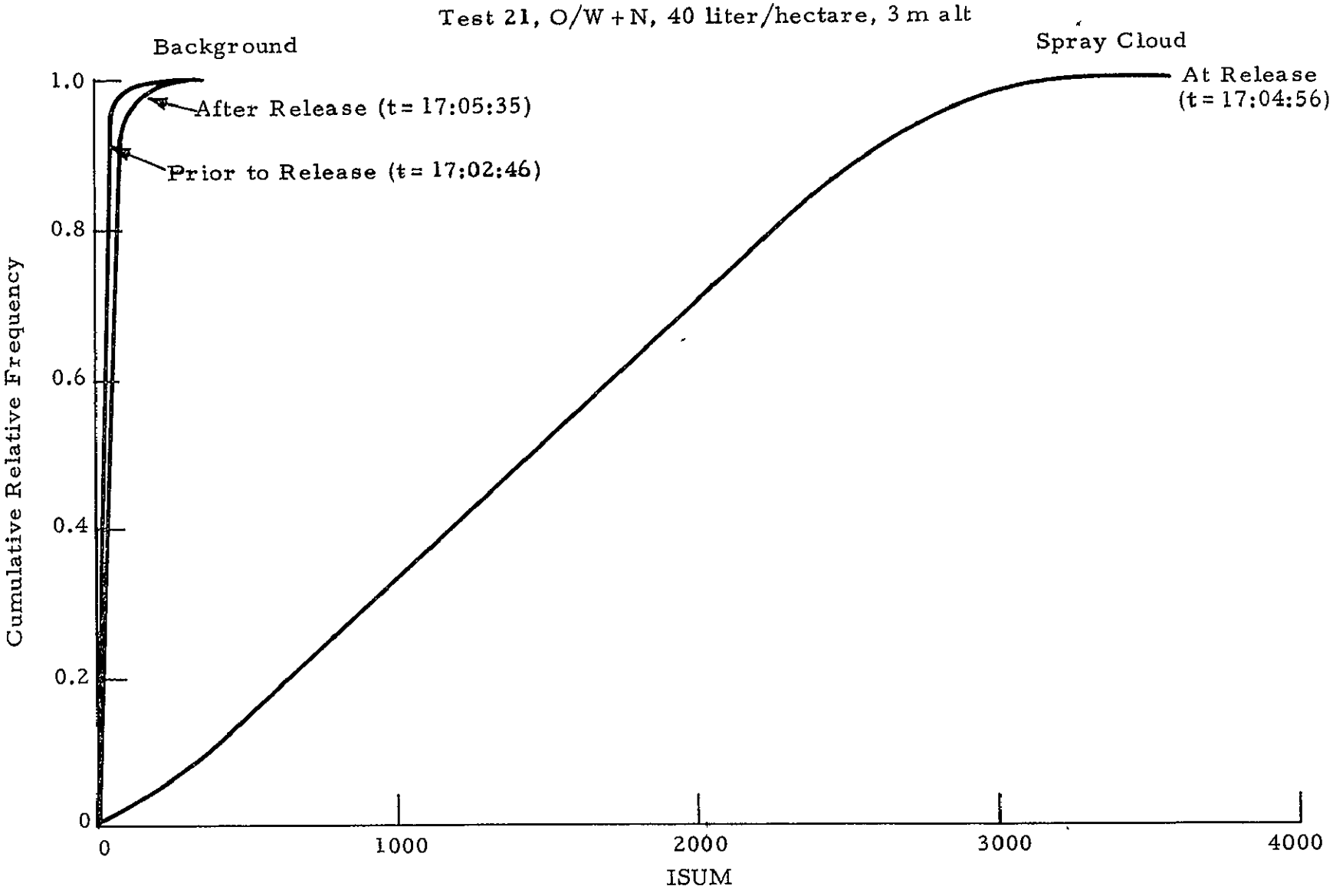

Fig. 27 - Cumulative Relative Frequency Distribution for ISUM Near Release Point (z = 2 to 5 m, y = 50 to 100 m)

Table 3

RELATIVE AEROSOL CONCENTRATION ISUM CRITERIA

Symbol		ISUM	Aerosol Concentration
Fine	Coarse		
•		0 - 99	Low (Background)
B	•	100 - 199	
C		200 - 299	
D		300 - 399	
E		400 - 499	
F		500 - 699	
G	M	600 - 699	Moderate
H		700 - 799	
I		800 - 899	
J		900 - 999	
K		1000 - 1099	
L		1100 - 1199	
M		1200 - 1299	
N		1300 - 1399	High
O		1400 - 1499	
P		1500 - 1599	
Q		1600 - 1699	
R		1700 - 1799	
S		1800 - 1899	
T	□	1900 - 1999	
U		2000 - 2099	
V		2100 - 2199	
W		2200 - 2299	
X		2300 - 2399	
Y		2400 - 2499	
Z		2500 - 2599	
□		Over 2599	

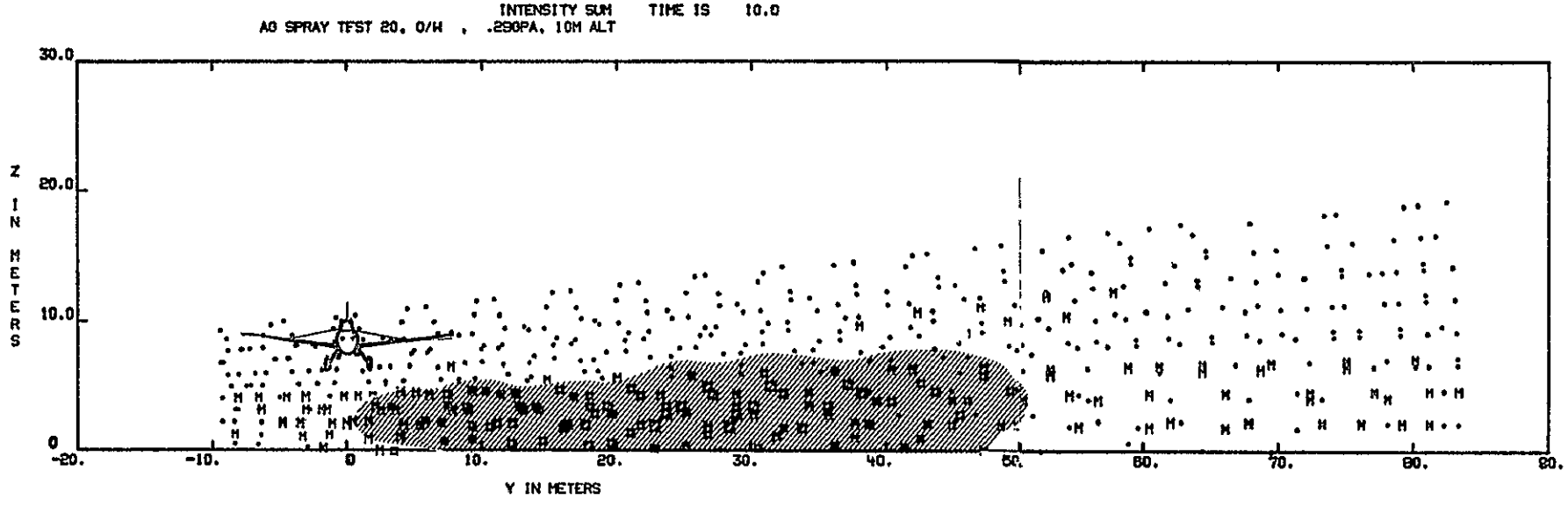

Fig. 28 - Typical Aerial Spray Cross-Section Plot

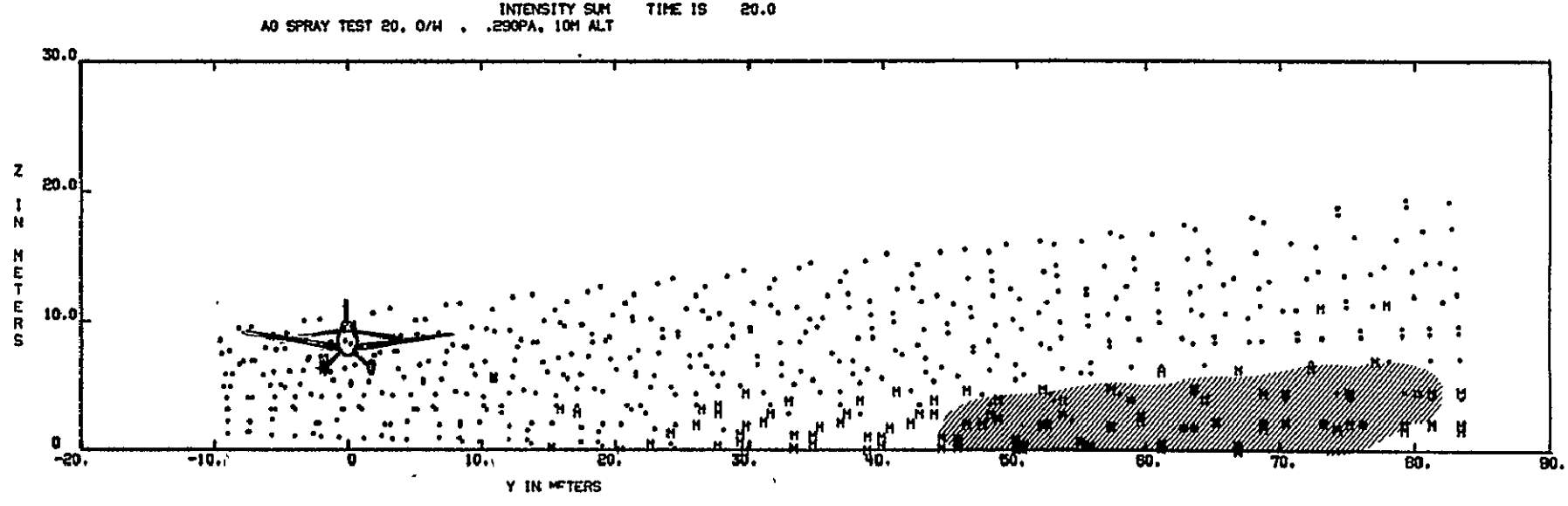

Fig. 28 (Continued)

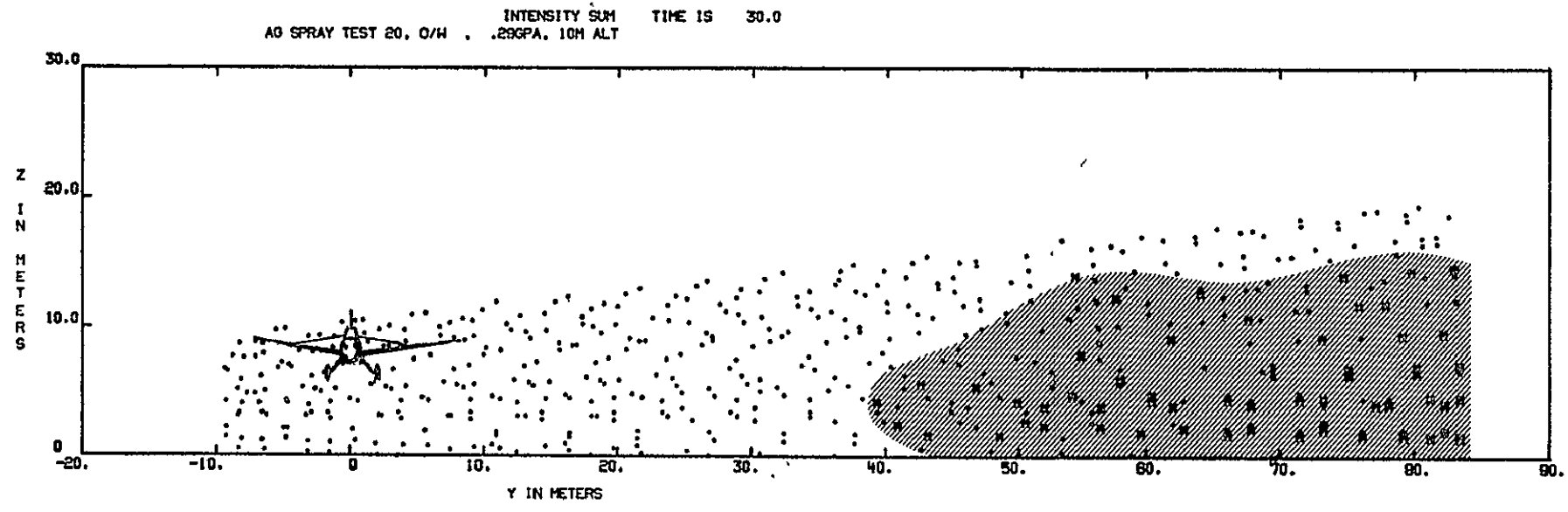

Fig. 28 (Continued)

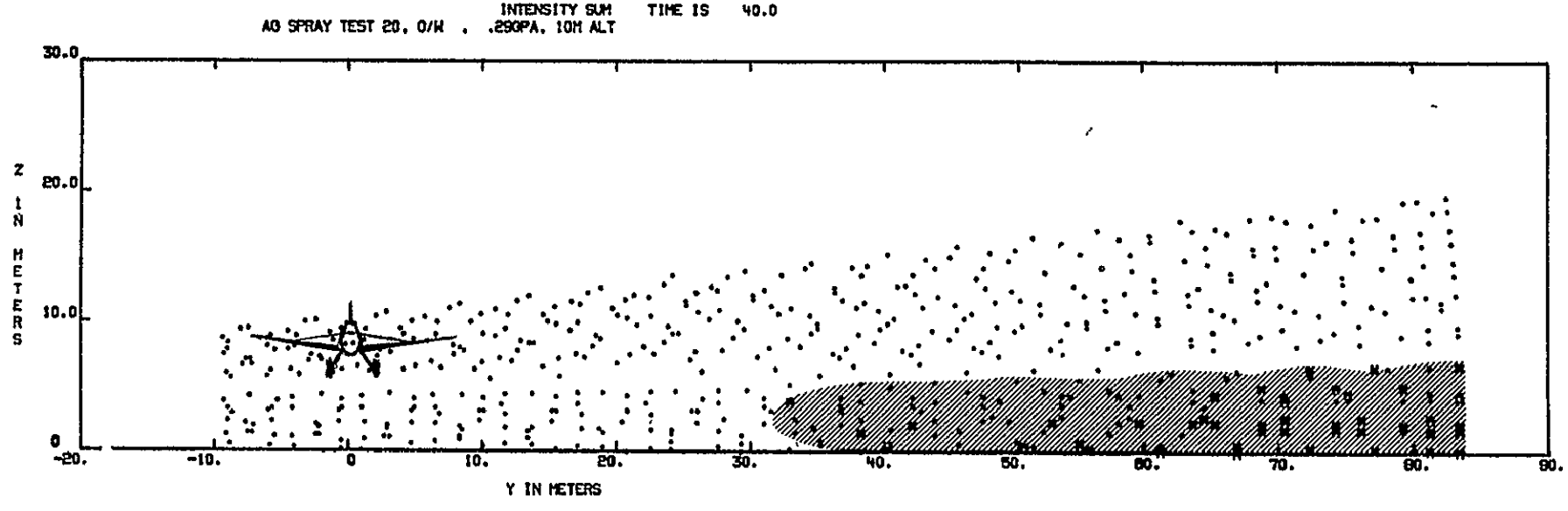

Fig. 28 (Continued)

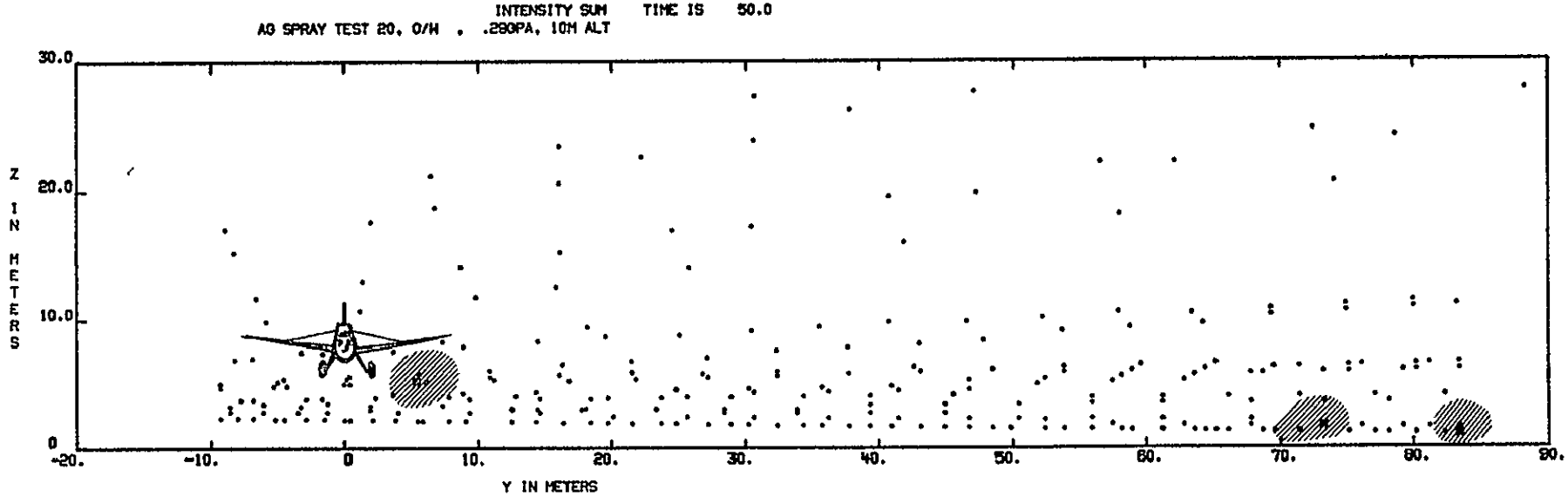

Fig. 28 (Continued)

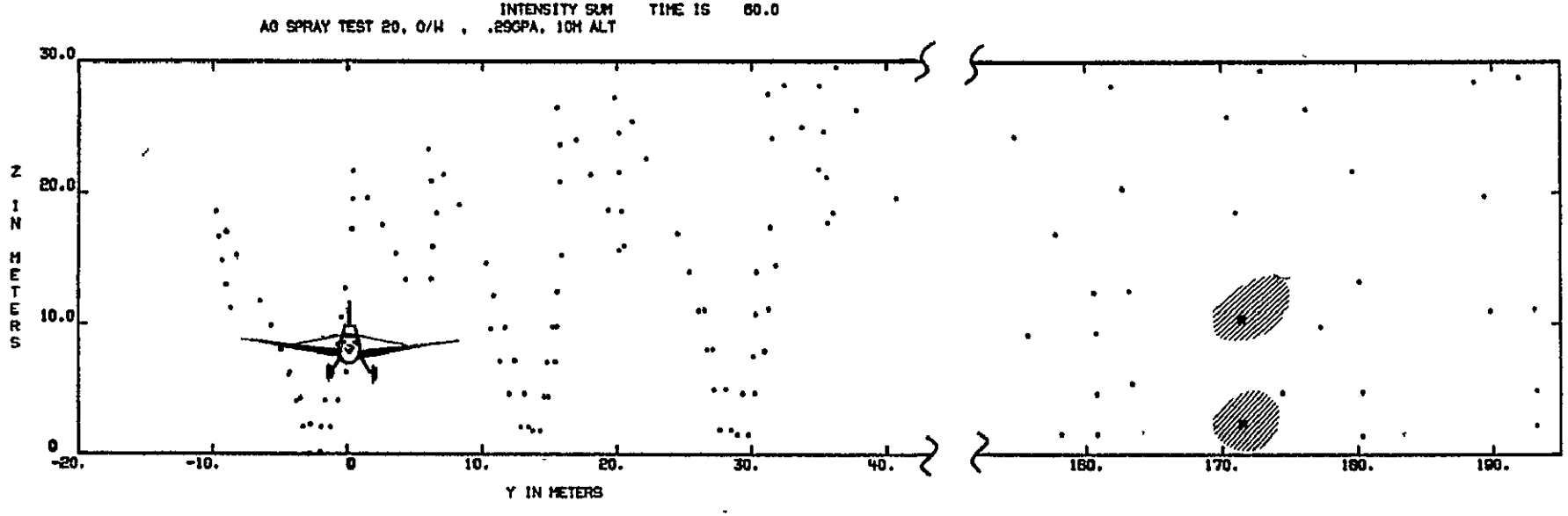

Fig. 28 (Continued)

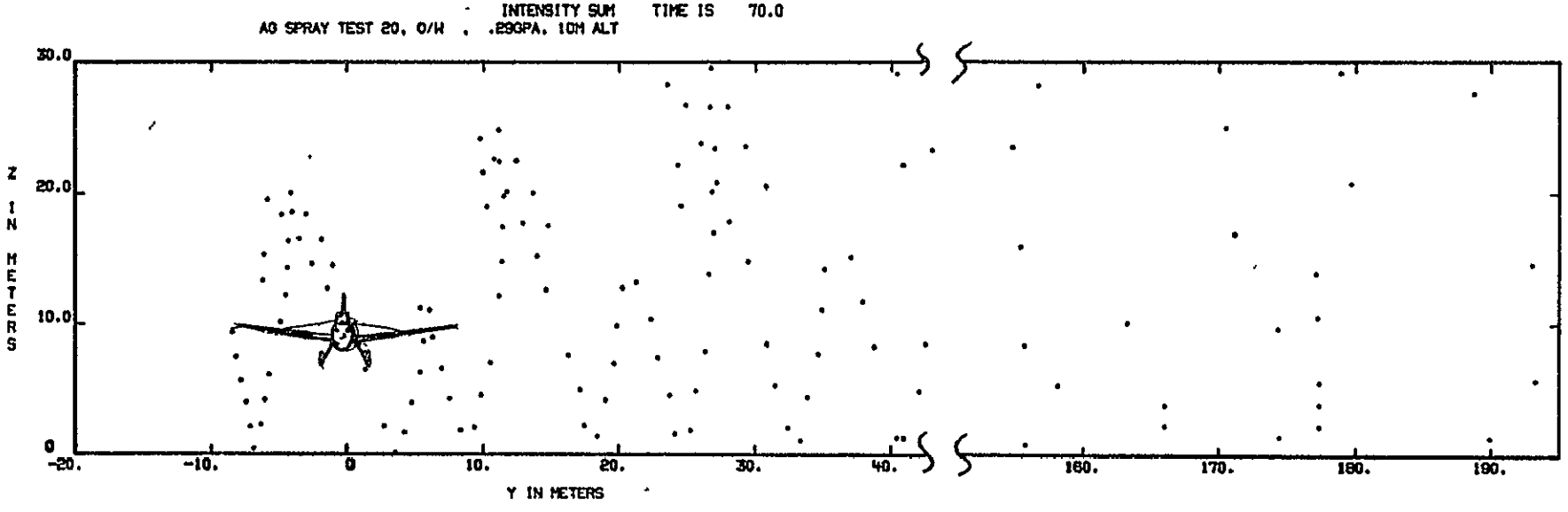

Fig. 28 (Concluded)

and spatial extent of the spray cloud can be noted. For example, at 0 to 10 sec after the release, the center of the cloud is approximately 25 on downwind and 7 m below the release point. The cloud has a quasi-elliptical cross-sectional area with horizontal and vertical dimensions of 40 and 5 m, respectively. Non-uniformities in the spray cloud concentration can be noted in the overlapping of the high and low ISUM symbols, particularly at the edges of the spray cloud. The extreme limits of the spray cloud, shown by the distribution of the M symbols, extends 8 m upwind, 80 m downwind, and 2 m above the spray release point. Due to the elongated focal volume of the LDV, discussed earlier in Section 2.1.3, it is possible that some of these weaker intensity signals may have resulted from the detection of high intensity regions far away from the focus. Thus, the extreme downwind and upwind limits of the airborne spray cloud may be slightly exaggerated by the LDV system.

At 20 to 30 sec, the plots in Fig. 28 show the cloud center to be approximately 60 m downwind and 8 m below the release point. The extreme limits of the spray cloud extend horizontally from 10 to 85 m downwind and vertically from the ground up to the release altitude. A reduction in the high particulate concentration is evidenced by the smaller size symbols.

At 20 to 30 sec, the relative concentration of the airborne spray is diminished considerably and the cloud is drifting downwind out of the scan limits and expanding vertically to 13 m above the ground as shown by the shaded M symbols in Fig. 28.

At 30 to 40 sec, the upwind edge of the cloud remains 30 to 40 m downwind of the release but the vertical dimension of the cloud is reduced to 5 m from the ground.

At 40 to 50 sec, the concentration of the cloud is diminished considerably. The well-defined cross section of the cloud is replaced by three solitary patches of medium intensity circled in Fig. 28. The patches are located at 5, 75, and 85 m downwind of the release point.

At 50 to 60 sec, two medium intensity regions are present at 170 m downwind of the release point as shown by the circles in Fig. 28.

At 60 to 70 sec, no high or medium intensity regions are present within 200 m downwind of the release point. Indications are that the spray cloud has drifted out of the scan area and has dispersed.

The typical cross-section plots shown in Fig. 28 illustrates the capability of the LDV to determine the location, spatial extent, and relative concentration of the airborne spray cloud. From these cross-section plots, the vertical and downwind motion and the trajectory of the swath pattern has been estimated which is discussed in more detail in Section 4.4.

Additional detail regarding the relative aerosol concentration is provided by plots with finer gradations for the value of ISUM. A series of

typical cross-section plots, given in Fig. 29, shows the details of the spray cloud relative concentration. The results in Fig. 29 indicate: (1) the background aerosol concentration 212 sec prior to release; (2) a high concentration downwind of the release point 10 sec after release; (3) continued downwind transport of the spray 20 sec after release; and (4) transport of the spray out of the near field of view 40 sec after release. The general cloud transport and dispersion trends illustrated in Fig. 29 are similar to the results shown earlier in Fig. 28. However, Fig. 29 also shows the distribution of the relative concentration by the large variations in symbols horizontally and vertically across the cloud. The highest ISUM values occur near the ground plane, possibly indicative of large particulates settling out of the spray cloud. Within the spray cloud, patches of high and medium high ISUM values are evident, suggestive of active turbulent mixing and dispersion. Alternate high and low value regions are noted at the edges of the cloud, showing that the spray cloud is a dynamic phenomenon. Its spatial boundaries are not sharply defined and vary as a function of time. The typical cross-section plots illustrated in Fig. 29 depict details of the spatial and temporal relative concentration distribution of the airborne spray cloud which is discussed in more detail in Section 4.2.

In conjunction with the measurements of the spray cloud relative concentration, the line-of-sight velocity distribution of the spray cloud was also measured. Since the LDV was oriented so that the cross section of the spray cloud drifted horizontally along the optic line of sight, the line-of-sight velocity distribution observed with the LDV was a measure of the lateral transport velocity of the particulates within the spray cloud. The typical line-of-sight velocity distributions illustrated in Fig. 30 show the spatial and temporal variations in the parameter VMS, the velocity corresponding to the maximum signal intensity. At 212 sec prior to the spray release, the mean crosswind velocity is in the range 4.49 to 5.49 m/sec as shown by the J and K symbols in Fig. 30. At 10 to 20 sec after the spray release, two high velocity "hits" (over 12.499 m/sec) are seen at 40 to 50 m downwind of the spray release point at 0 and 12 m altitude, respectively, as indicated by the two square symbols in Fig. 30. These localized high velocity regions may be identified with the aircraft trailing vortex pair. However, the mean crosswind velocity in the spray region remains in the 4.49 to 5.59 m/sec regime. At 20 to 30 sec after spray release, the high velocity "hits" noted earlier are absent and the line-of-sight velocity is essentially the same level as the background recorded prior to the spray release. At 40 to 50 sec after the spray release, an increase in the crosswind is noted. The M and N symbols indicate that the line-of-sight velocity is in the range 5.99 to 6.49 m/sec. This increase in the overall velocity level is attributed to the ambient winds. The typical line-of-sight velocity distribution illustrated in Fig. 30 indicates that the aircraft spray release does not significantly perturb the ambient crosswinds. However, variability in the crosswind velocity is noted for time scales less than the life span of the spray cloud. Thus, the spray cloud appears to be transported laterally at the crosswind velocity which can fluctuate rapidly in magnitude during the transport of the cloud.

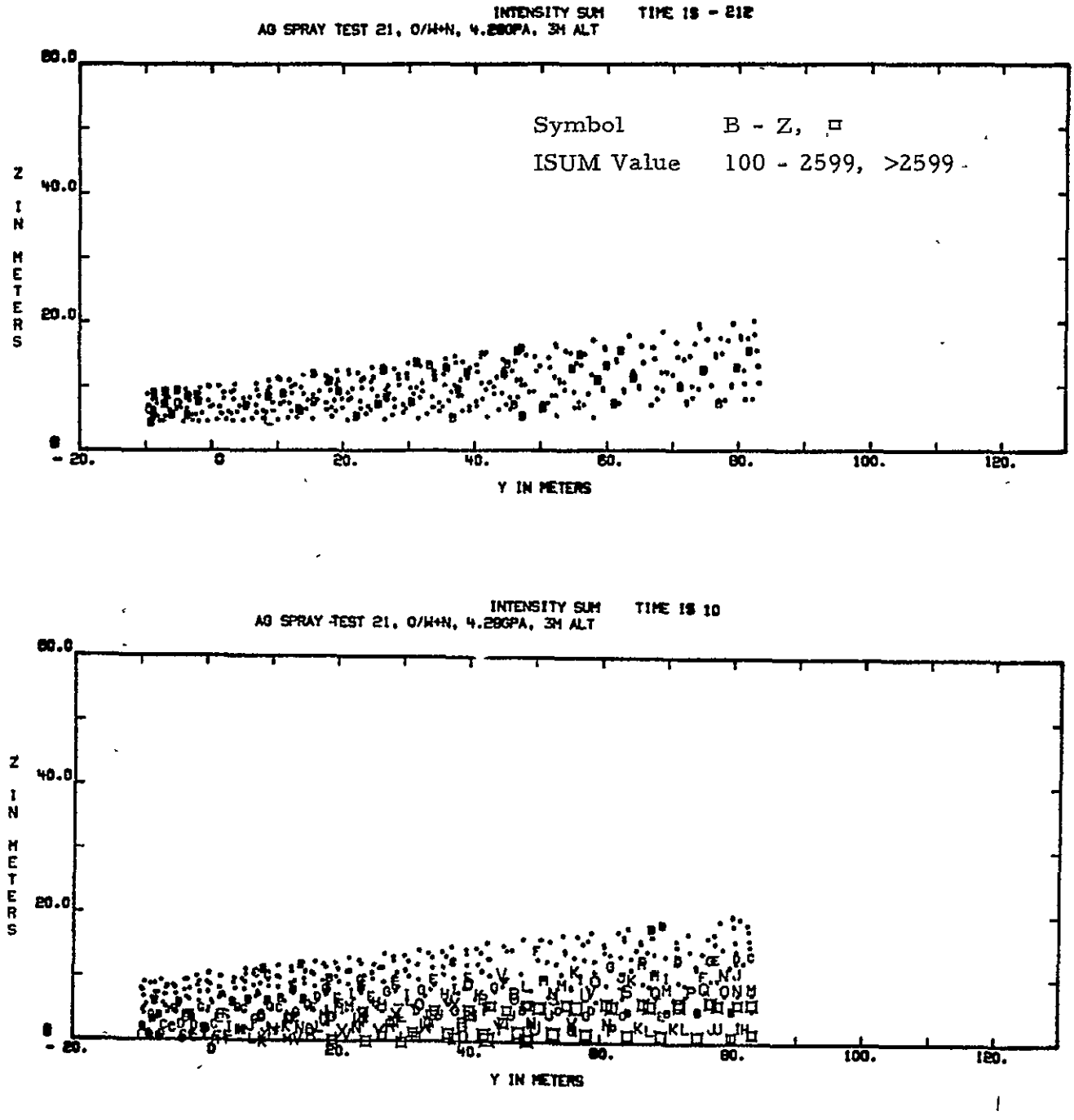

Fig. 29 - Typical Aerial Spray Cross-Section Plot Showing Details of the Relative Concentration Distribution

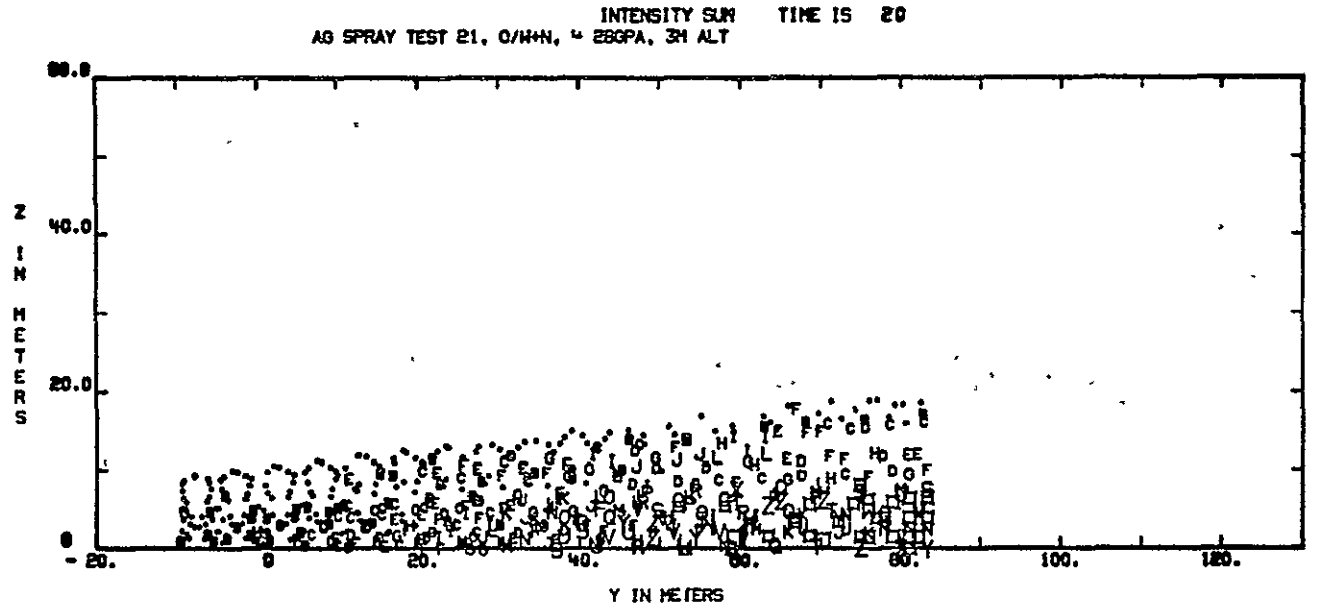

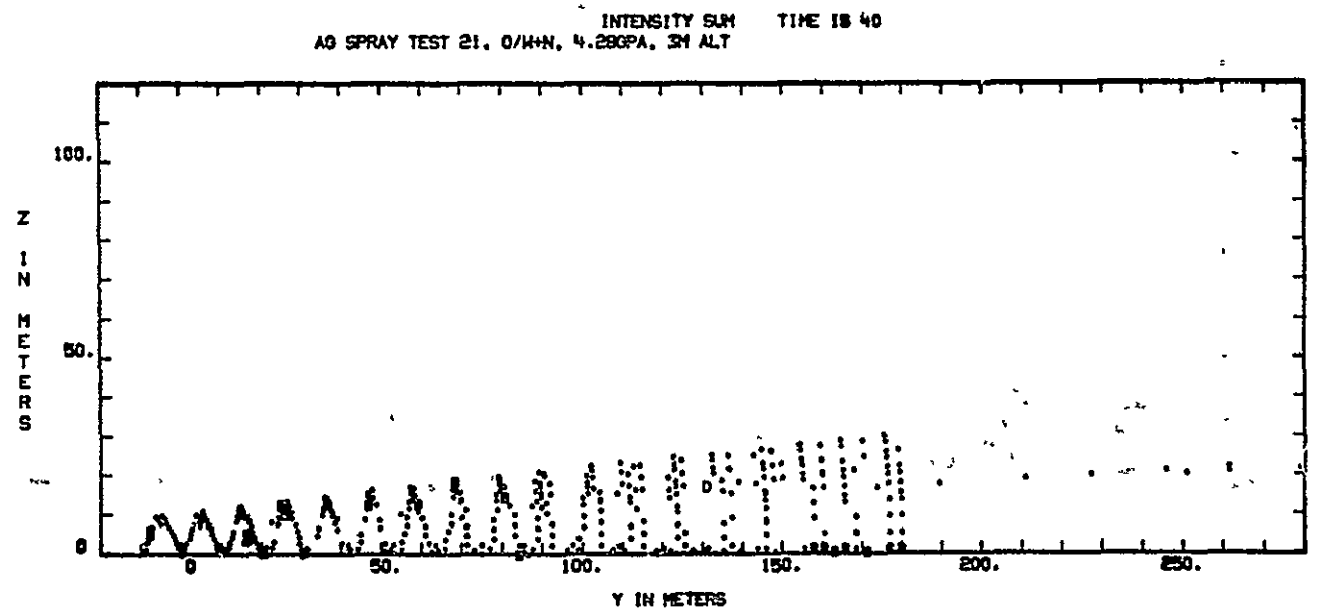

Fig. 29 (Concluded)

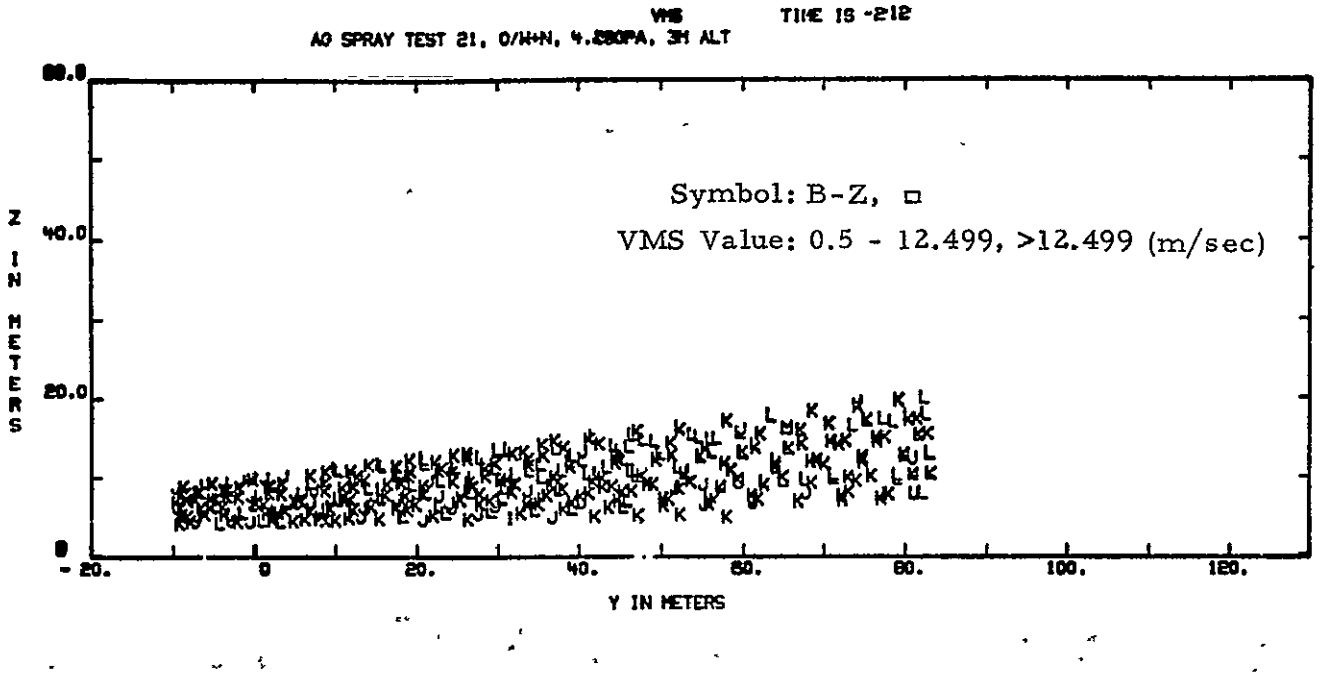

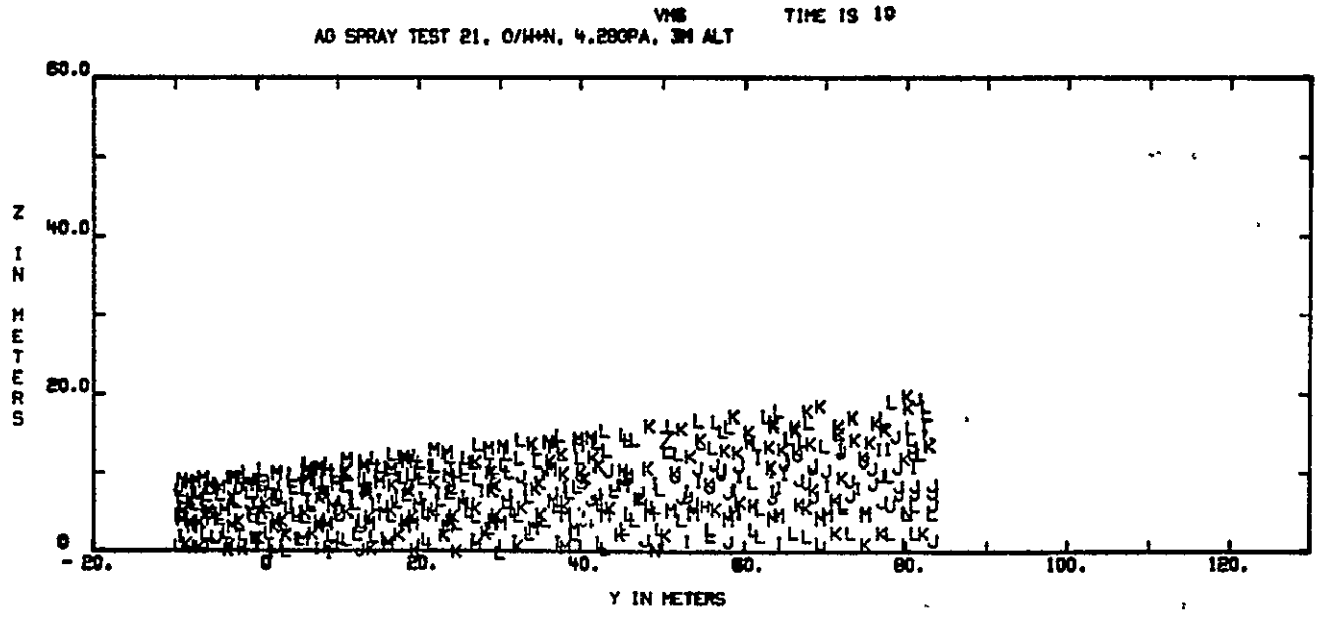

Fig. 30 - Typical Aerial Spray Cross-Section Plot Showing Details of the Line-of-Sight Velocity Distributions

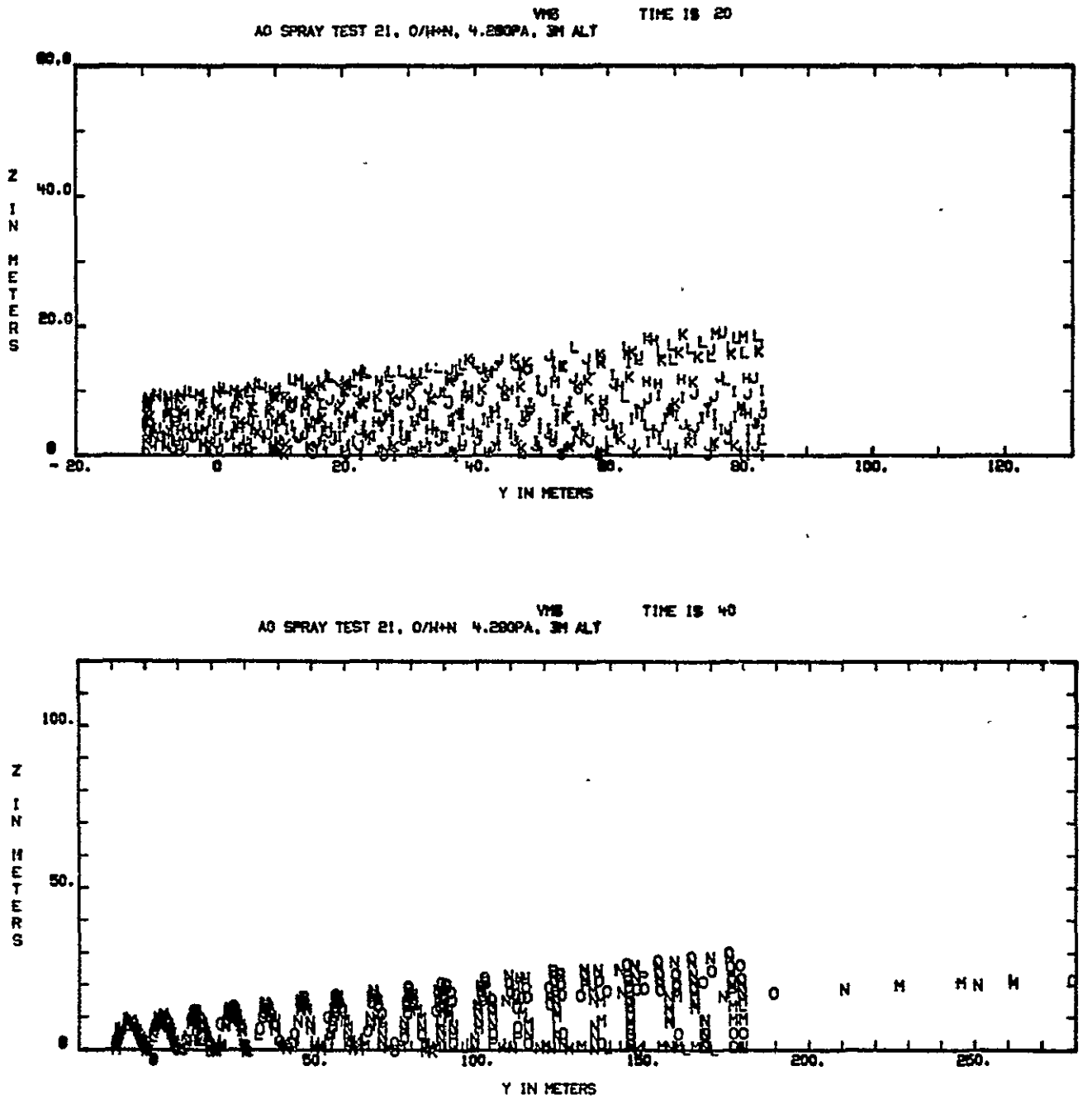

Fig. 30 (Concluded)

4.2 Relative Concentration of Spray Cloud

The relative concentration of the spray cloud was monitored with the LDV to determine the location, spatial extent, and transport characteristics of the swath pattern. The observed horizontal and vertical relative concentration profiles of the spray cloud are discussed in this section.

The typical relative concentration profile observed during a range scan of the spray cloud at approximately the spray release altitude ($z = 3.2$ m) is shown in Fig. 31. The circle and square symbols indicate the relative concentrations sampled during a horizontal range scan in the positive and negative y directions through the cloud cross section, respectively. The observed relative concentrations show some scatter which may be attributed to nonuniformities in the spray cloud concentration. Since the data were sampled at a rapid rate (70 Hz), the graph represents a snapshot of the instantaneous relative concentrations rather than smooth a time-averaged picture. A smooth curve was drawn through the maximum points, indicative of the peak concentration levels, to obtain a profile of the relative concentrations. The relative aerosol concentration is above the ambient level 20 to 85 m downwind of the release point. The lateral extent of the spray cloud is from 43 to 82 m based on the ISUM(e) criteria given in Eq. (7). The maximum relative concentration occurs at 64 m which is presumably the centroid of the cloud.

From LDV measurements similar to the results presented in Fig. 31, the time-averaged maximum relative aerial spray concentrations as a function of range and attitude have been computed. The relative aerial spray concentration as a function of downwind location at approximately the spray release altitude ($z = 3.2$ m) is shown in Fig. 32. Initially, at $t = 1$ sec, the high concentration region is approximately 20 m in breadth. Later, at 10 to 15 sec after spray release, the lateral extent of the spray cloud has grown by a factor of 2 and the maximum relative concentration levels have increased by 50%. The increase in the spray cloud lateral extent and relative concentration indicates a net increase in mass along the scan line. The area under the relative concentration versus range curve is a measure of total subtended mass. The initial increase in mass may be due to the redistribution of the spray material (i.e., the spray material originally carried downward by the wake vortices is transported upward across the scan line due to vertical dispersion or due to wake vortex bouncing). At later times, 30 sec and beyond, a decrease in total mass along the scan line, a decrease in the relative concentration, and an increase in the lateral extent of the spray cloud is noted. Within 60 sec after the release, the relative concentration has returned to the same ambient level noted 10 sec prior to the release.

The relative concentration profile of the spray in the vertical direction at the release point is shown in Fig. 33. The measurements were obtained with the LDV operating in the arc scan mode. From 1 to 5 sec after release, the altitude of the maximum relative concentration decreases from 4 to 1 m and the magnitude of the maximum relative concentration decreases by 36%. The decrease in altitude is attributed to the fallout of the particulates due to gravity. The decrease in peak concentration levels may be due to dispersion or, more likely, to the lateral transport of the spray cloud away from the

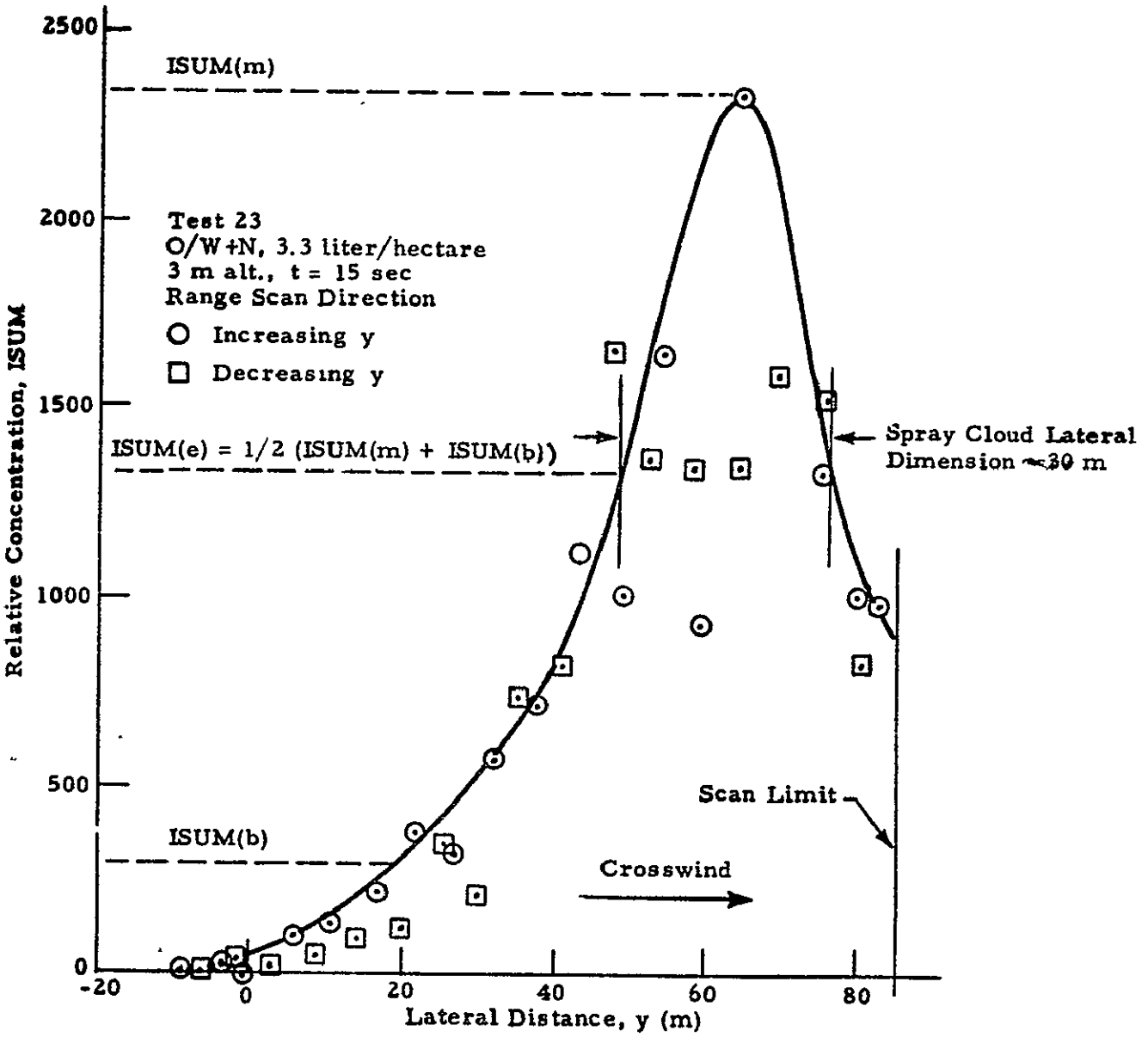

Fig. 31 - Typical Relative Concentration Profile Measured During Range Scan of the Spray Cloud at Approximately the Spray Release Altitude (z = 3.2 cm)

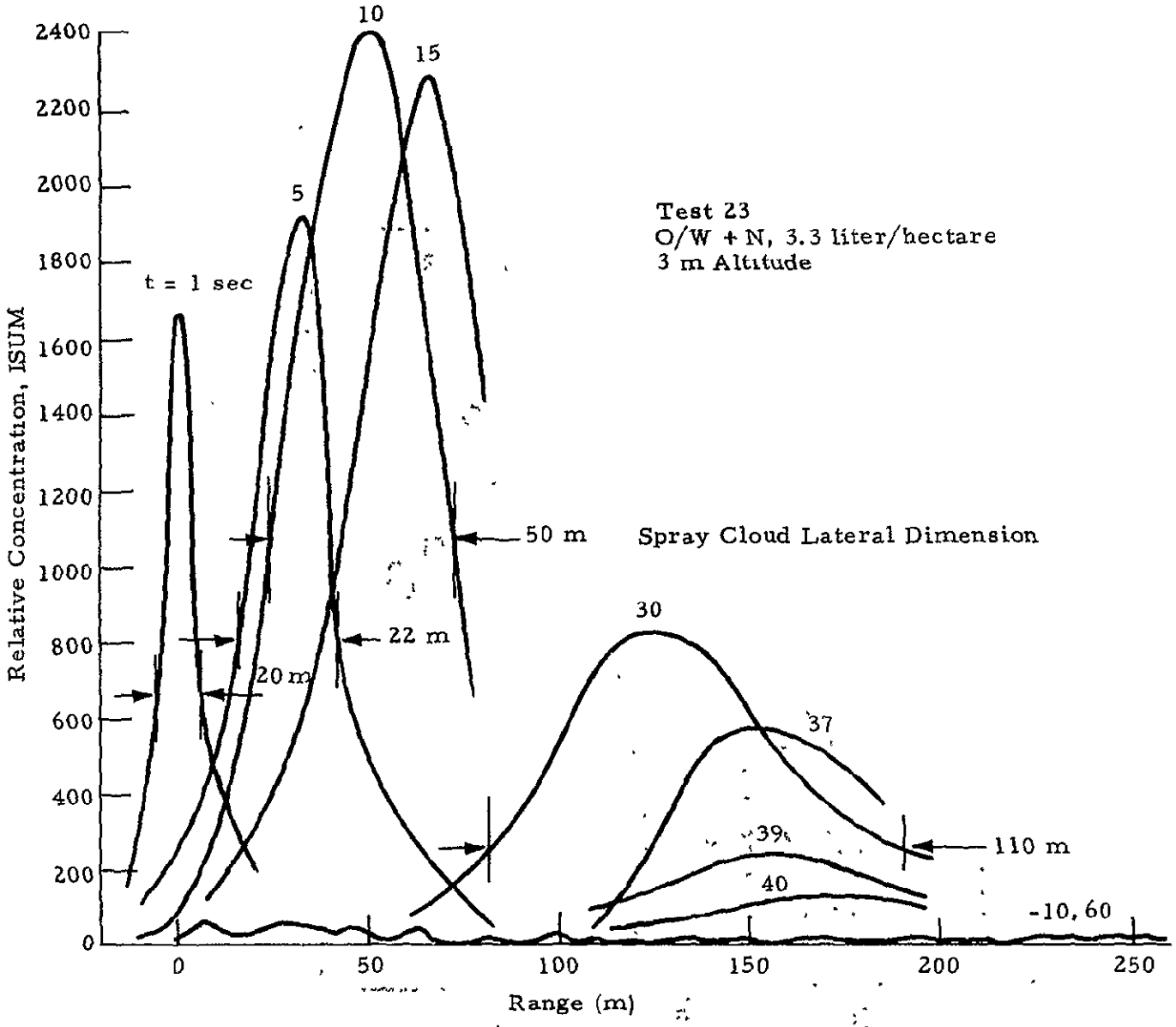

Fig. 32 - Relative Aerial Spray Concentration as a Function of Range Downwind from Release Point at Approximately the Spray Release Altitude (z_r = 3.2 m)

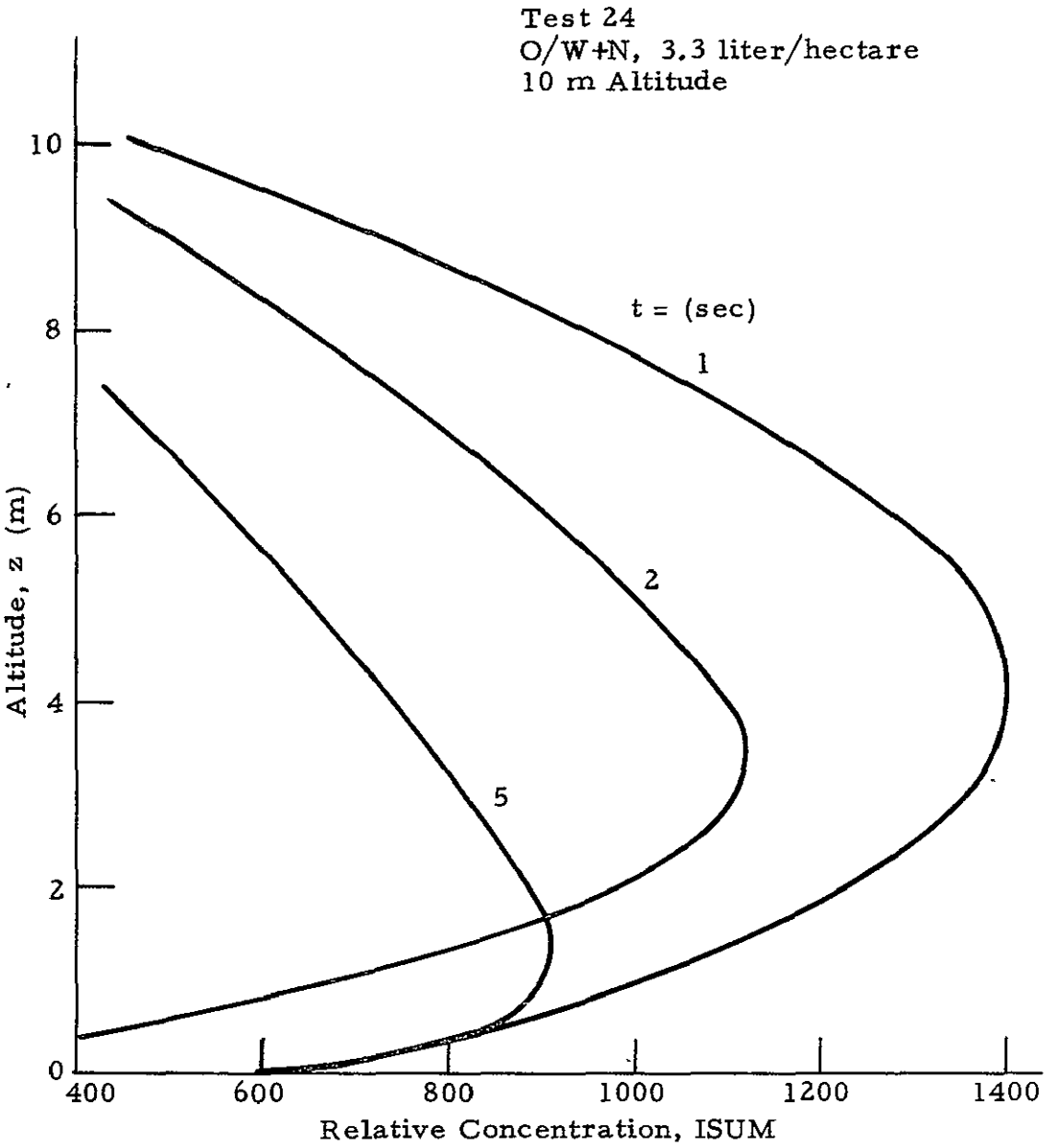

Fig. 33 - Relative Aerial Spray Concentration as a Function of Altitude at the Release Line (y = 0 m)

release. The area under the relative concentration versus altitude curve in Fig. 33 decreases as a function of time. This indicates a decrease in mass above the release point due to lateral transport and fallout.

The relative aerial spray concentration as a function of both altitude and range is shown in Fig. 34. The measurements were obtained by scanning the LDV in elevation at fixed downwind positions, or ranges. The downwind positions were selected near the centroid of the spray cloud based on the on-line spectrum analyzer display. Initially, at t = 1 sec after release, the maximum relative concentration occurs between 3 and 4 m altitude. A decrease in the maximum relative concentration and a decrease in the altitude at which the maximum concentration is noted 16 to 21 sec later. At 49 sec after the release, the maximum relative concentration level occurs at approximately 2 m altitude. The decrease in the magnitude and the altitude of the maximum relative concentration curves shown in Fig. 34 indicate a dilution of the spray cloud and a settling of the particulates.

The vertical relative concentration profile illustrated in Fig. 34 can be compared with measurements made with cascade impactors described in Ref. 8. Whereas the LDV provides a nearby instantaneous measurement of the relative concentrations, a filter-type impactor provides a time averaged concentration measurement with a sampling time on the order of several minutes to hours. The relative concentration, defined as the local concentration divided by the peak observed spray concentration, is shown as a function of altitude in Fig. 35 from both the tower mounted cascade impactors and the LDV. The aircraft height, spray composition, spray rate, crosswind velocity, and other spray release parameters were different for the two tests as shown in Fig. 35. The cascade impactor measurements indicate that the peak concentration occurs at 3 to 4 m altitude and extends as high as 15 m. The LDV measurements show that the peak concentration occurs at 2 to 3 m altitude and extends above 10 m. Since the cascade impactor and LDV measurements represent a time-averaged versus instantaneous sampling of the spray and since the two measurements were made under different test conditions, a direct comparison between the two measurements is not meaningful. However, quantitatively, the two relative concentration profiles are very similar. The LDV measurements shown in Fig. 35 indicate that the centroid of the spray cloud (the location of peak concentration) is 1 or 2 m below the centroid observed with the cascade impactors. This good agreement may be fortiutous and further tests are necessary to evaluate the LDV and the air sampler for aerial spray measurements.

In the LDV relative concentration measurements, differences were noted in spray cloud relative concentration as a function of spray application rate and aircraft altitude. A comparison between a high volume high altitude release (Test 22) and a low volume low altitude release (Test 23) is shown in Fig. 36. The maximum relative concentration and the spray cloud lateral dimension at the 3.2 m altitude is approximately double for the high volume high altitude application compared to the low volume low altitude application. The maximum relative concentration for the high volume high altitude release diminishes rapidly as shown by a 45% decrease in the peak ISUM value between 2 and 6 sec after release. This is attributed to fallout and vertical transport. For the low volume low altitude release, the maximum relative concentration

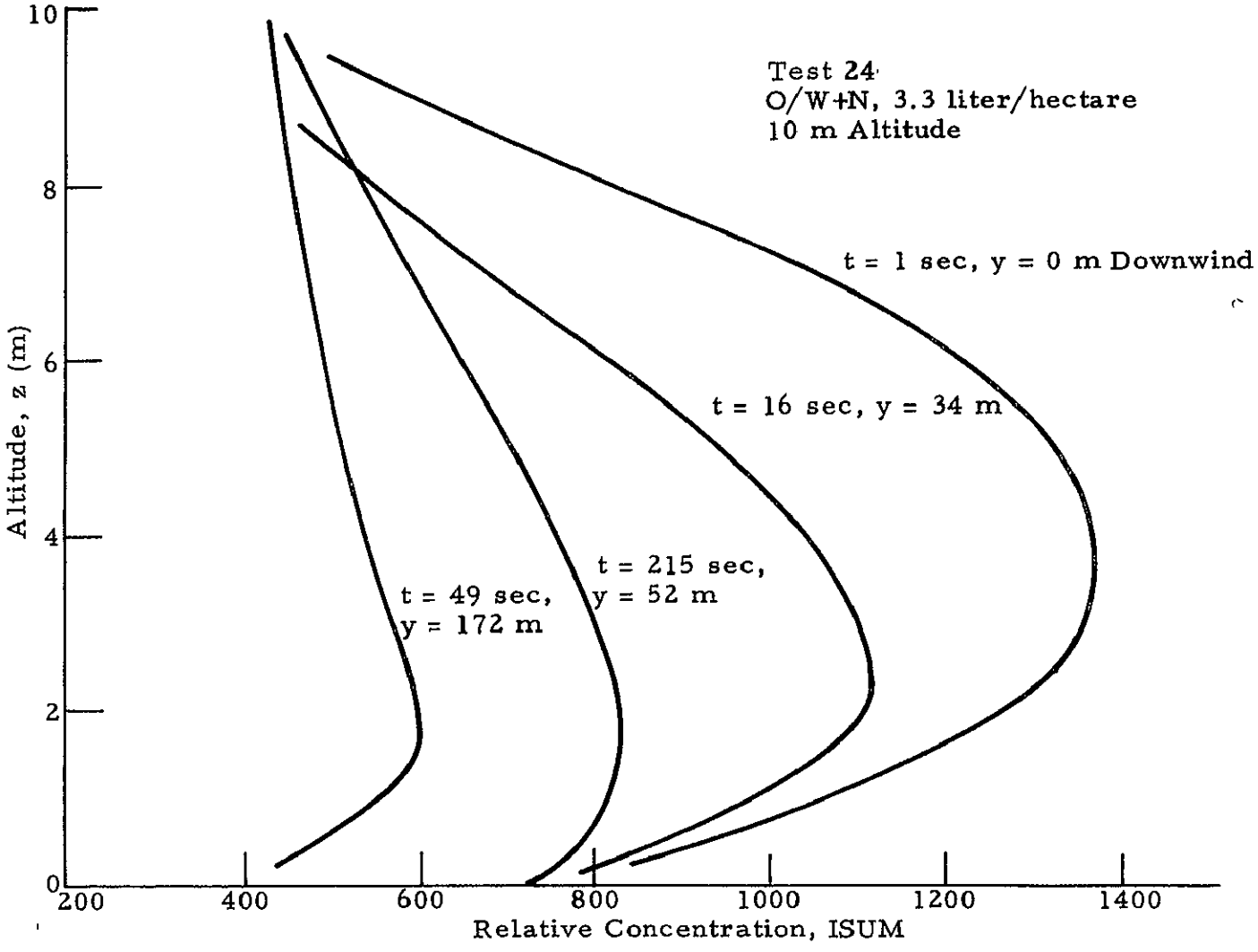

Fig. 34 - Relative Aerial Spray Concentration as a Function of Altitude and Downwind Distance

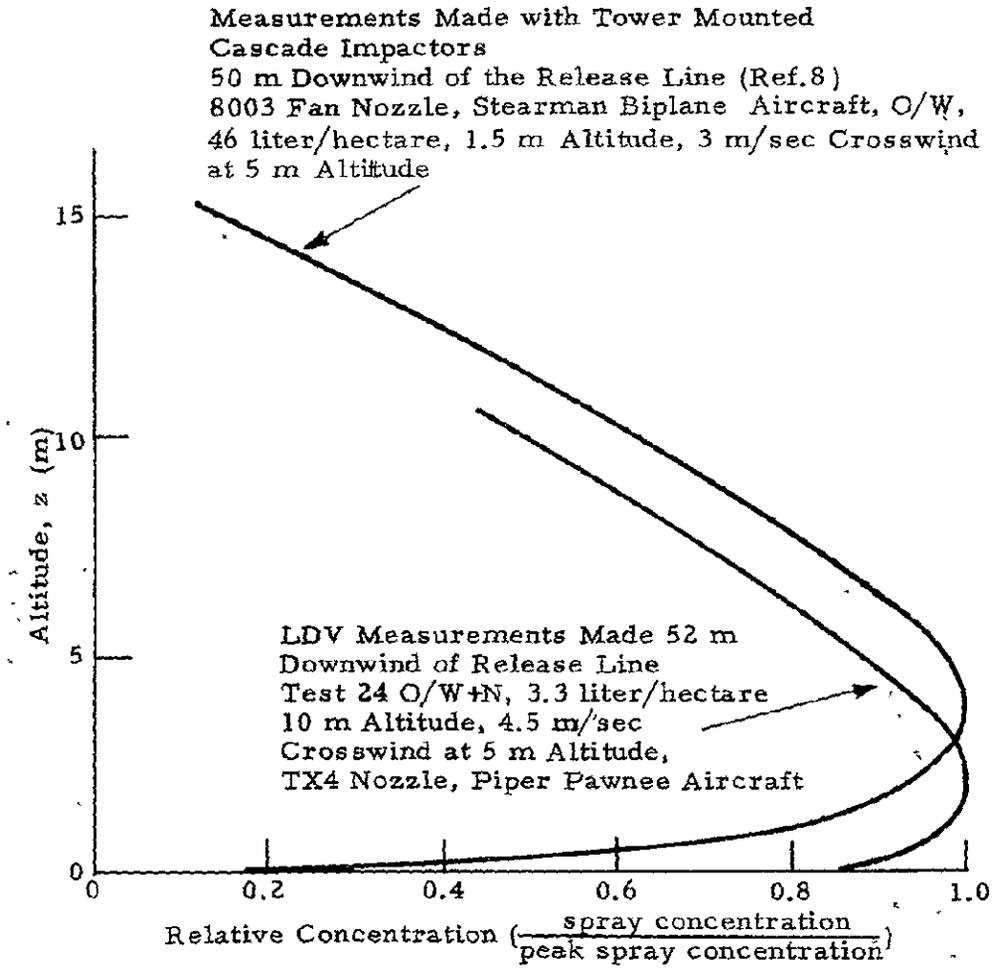

Fig. 35 - Comparison of Vertical Relative Concentration Profile Measured by the LDV and Measured by Tower Mounted Cascade Impactors

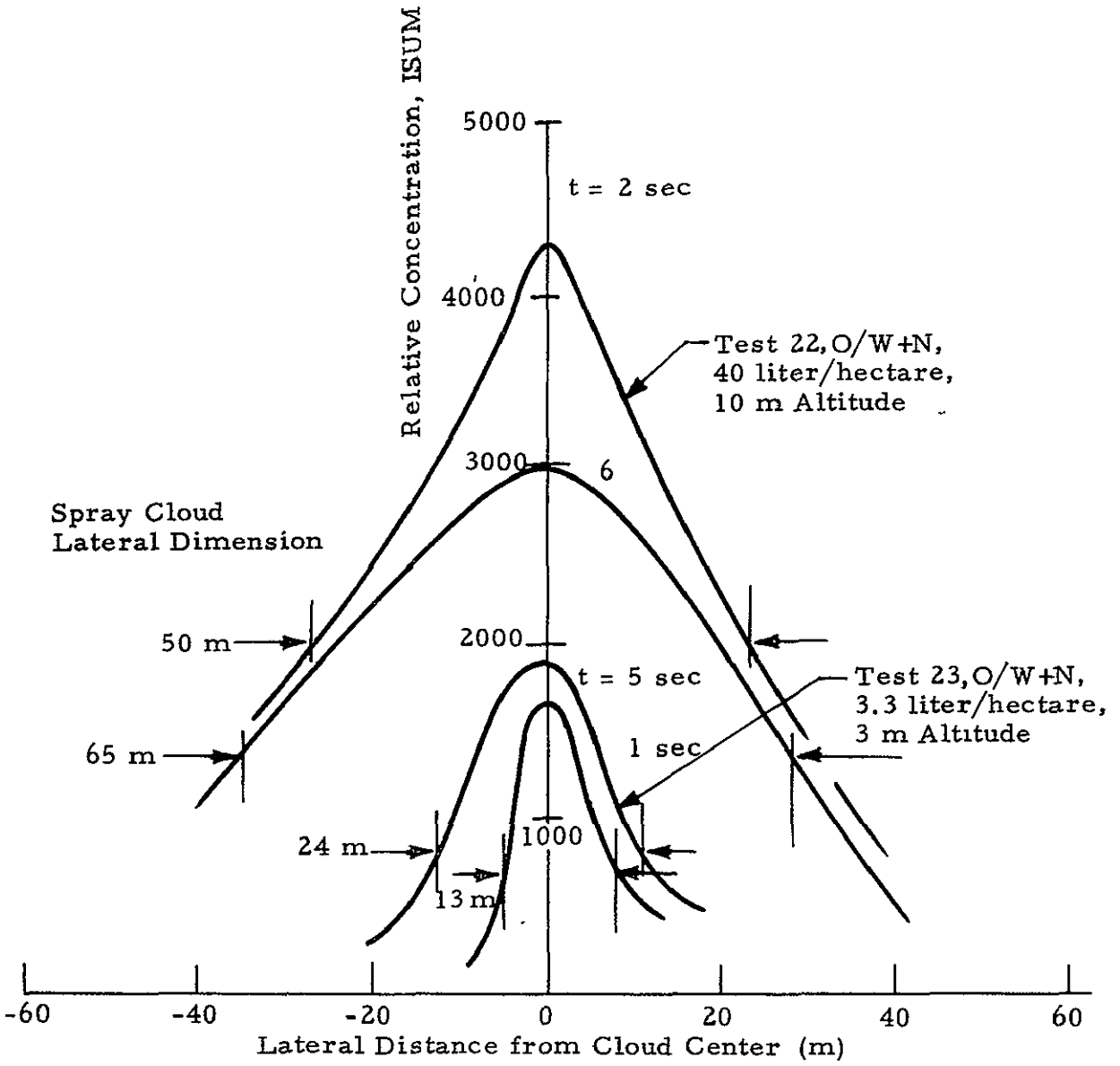

Fig. 36 - Comparison of Horizontal Relative Concentration Distribution at 3.2 m Altitude Observed for Different Spray Rates and Airplane Heights

increases slightly, approximately 10%, from 1 to 5 sec. Apparently, the effect of fallout is minimal and an upward transport of particulates across the 3.2 m altitude scan time is occurring for this test condition. The results in Fig. 36 illustrate that the LDV relative concentration measurements clearly reflect changes in spray application parameters.

4.3 Fallout of Particulates from the Spray Cloud

Integration of the observed relative concentration profile of the spray cloud across the cross section of the cloud determines the relative total mass of the cloud per unit length along the flight path. By monitoring the changes in the relative mass of the spray cloud, per unit length, the fallout rate can be determined. In this section, the fallout rate is computed from the LDV relative concentration measurements for a sample case.

The LDV spray cloud measurements, discussed earlier in Section 4.1 and 4.2, give the relative concentration of the spray cloud as a function of space and time. Neglecting temporal variations, the mass of the cloud is found by integration of the local relative concentration over the cloud cross-sectional area as illustrated in Fig. 37. Assuming conservation of mass (i.e., no evaporation of particulates) it follows that the changes in the mass of the airborne cloud determine the fraction of material deposited on the ground per unit length, F(t), defined as

$$F(t) = \frac{M(0) - M(t)}{M(0)} \tag{16}$$

where the mass per unit length of airborne particulates over a cross-sectional area, A, is given by

$$M(t) \alpha \iint_A ISUM(y, z)\, dy\, dz \Big|_t \tag{17}$$

As an example, the distribution of relative aerial spray concentration shown in Fig. 33 can be integrated to determine the variation in mass above the release point. The results, shown in Fig. 38, indicate the variation in particulate mass above the release point as a function of time. Within a few seconds after release, the mass of the airborne spray cloud above the release point has diminished to half its original value. Therefore, a significant fraction of the mass was transported from or deposited above the release point. The measurements illustrated in Fig. 38 suggests that the LDV relative concentration measurements provide a means for determining ground fallout rates.

4.4 Spray Transport

Transport of the particulates during aerial spray applications involves several mechanisms. The initial formation of the aerial spray pattern

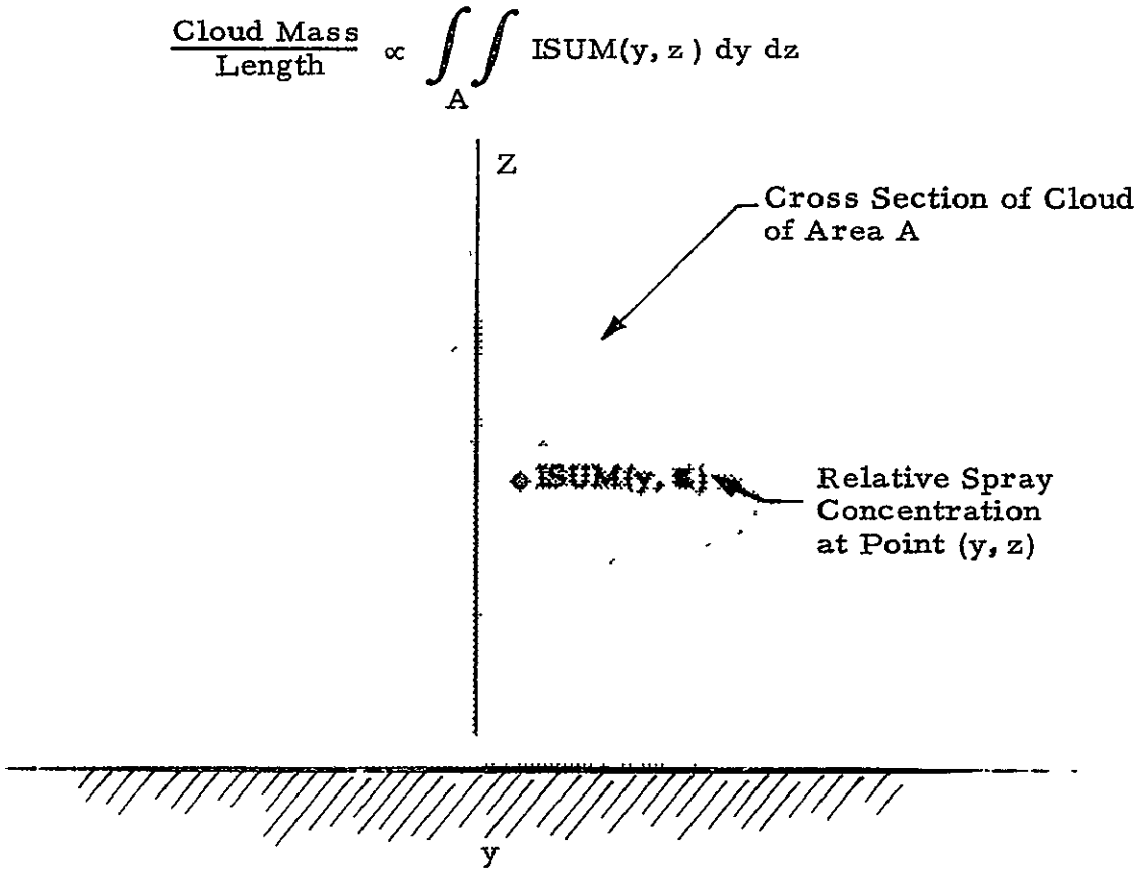

Fig. 37 - Calculation of Total Mass of Airborne Particulates

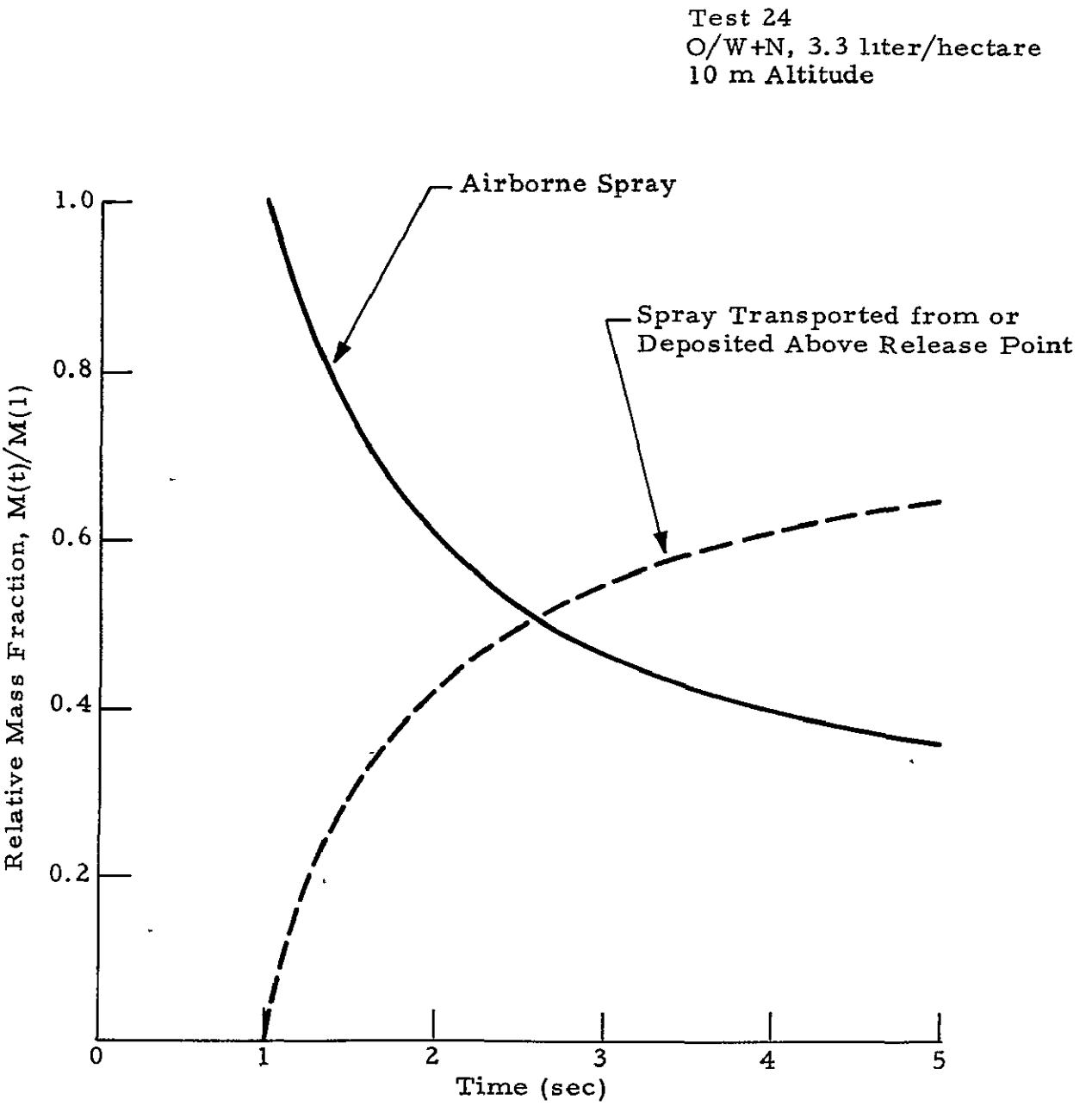

Fig. 38 - Variation in Particulate Mass Above Release Point

represents an interaction between the spray delivery system and the aircraft near wake. The heavier particles fall out of the spray cloud due to gravity, aerodynamic drag, and acceleration by the aircraft vortex wake. However, the lighter particles are not deposited immediately along the flightpath and are transported laterally by the winds and the aircraft wake vortices. Since the wind and vortex induced mass transport process reduces spray coverage and degrades the efficiency of the spray applicator, it is a primary area of interest. Therefore, one of the objectives of the present test was to identify the spray cloud, to follow its trajectory, and to show how it is transported by the ambient winds.

The lateral motion of the spray cloud is illustrated in Fig. 39. The plot shows the location of the relative concentration regions above the ambient level (ISUM > 300) as a function of time. The LDV was located 60 m upwind of the flight path and the motion of the spray cloud was observed as it drifted away from the LDV. The scan limits of the LDV are noted in Fig. 39. The estimated spatial limits of the low relative concentration region are indicated by the two dashed lines. As noted earlier in Section 4.2, the actual spatial extent of the spray cloud is given by the criteria that ISUM is midway between the peak and background values. Thus, the spatial limits of the low relative concentration region, shown by the dashed lines, are considerably larger than the actual width of the cloud. However, the trajectory of the cloud centroid can be estimated as lying midway between the low relative concentration limits. The estimated trajectory of the cloud centroid, shown by the solid line in Fig. 39, indicates a mean lateral cloud velocity of 4.9 m/sec. In comparison, a 4.8 m/sec crosswind was measured by the 5 m tower located adjacent to the sample line. The lateral velocity of the cloud is in agreement with the ambient crosswind velocity. The measurements shown in Fig. 39 demonstrate the ability of the LDV to track the location and lateral displacement of spray releases from agricultural aircraft.

Based on the distribution of the relative concentration regions spray cloud trajectories have been computed for a number of cases. The observed spray cloud trajectories are summarized in Fig. 40. They show the cross section of the cloud based on the criteria that the relative concentration at edge of the cloud, ISUM, is midway between the maximum value and the background value. The crosswind velocity, defined as the velocity along the sample line, is also shown in Fig. 40. The crosswind labeled tower was measured for a 1 min period after the release by an anemometer mounted on a 5 m tower located approximately 100 m east from the N-S sample line. The crosswind labeled LDV was measured by the LDV system operating in the finger scan mode over a 13 min period after the release. The crosswind was measured between the altitude of 3 and 6 m from y = -50 to y = 500 m along the sample line by the LDV.

The results in Fig. 40 show that initially (within 10 sec of the release), the cross section of the spray cloud is an elongated region 10 to 20 m in breadth and approximately 5 m high. Later (10 to 20 sec after release), the lateral extent of the spray cloud has increased to 40 m and the centroid of the cloud has translated as much as 80 m downwind. At 30 sec after release, the spray cloud begins to drift past the 85 m scan limit. Within 60 sec after the release, there is no evidence of the spray cloud in the region 0 to 160 m downwind of the release point. The lateral velocity of the spray cloud based

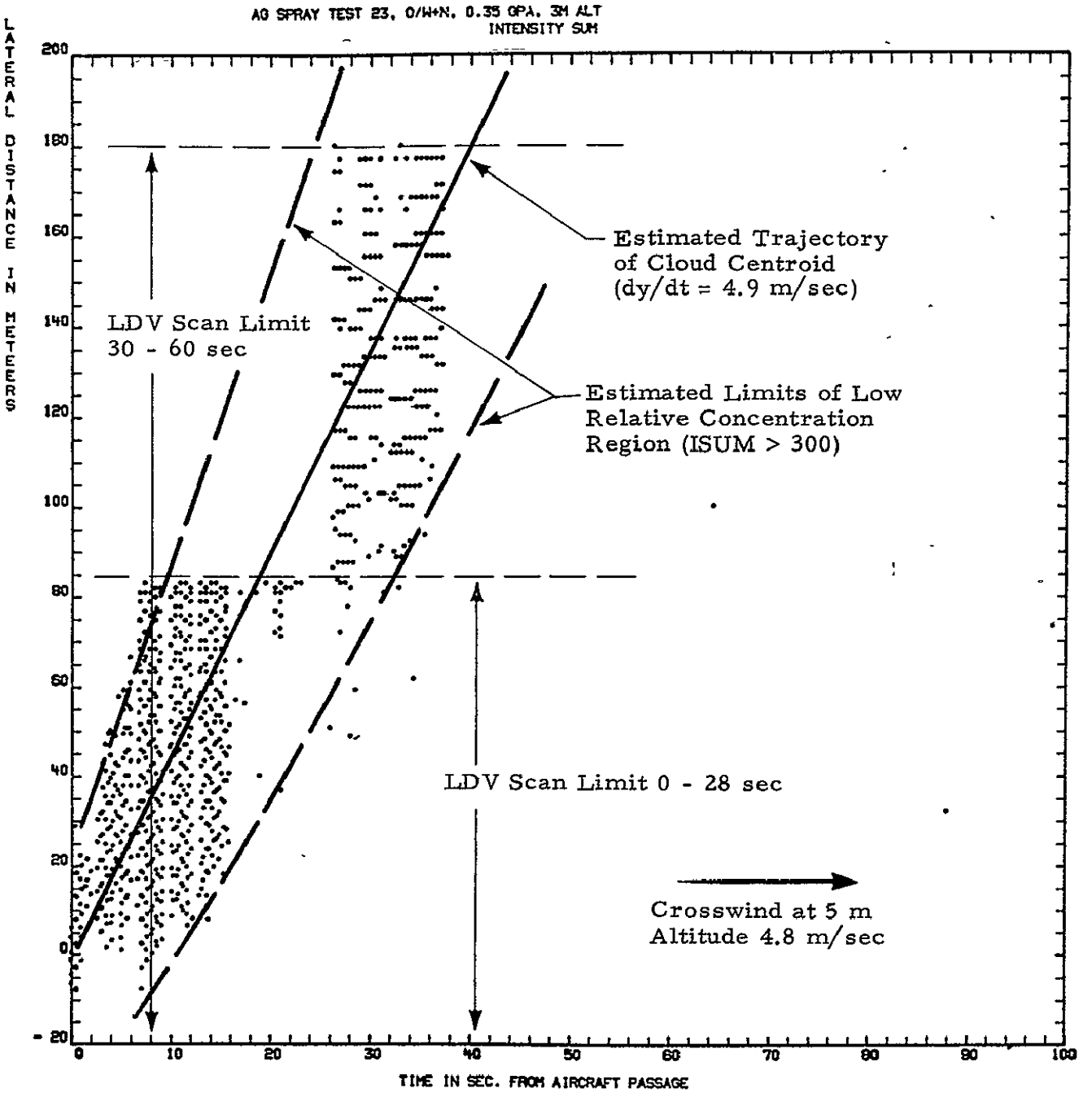

Fig. 39 - Lateral Displacement of Spray Cloud High Concentration Region for Test 23

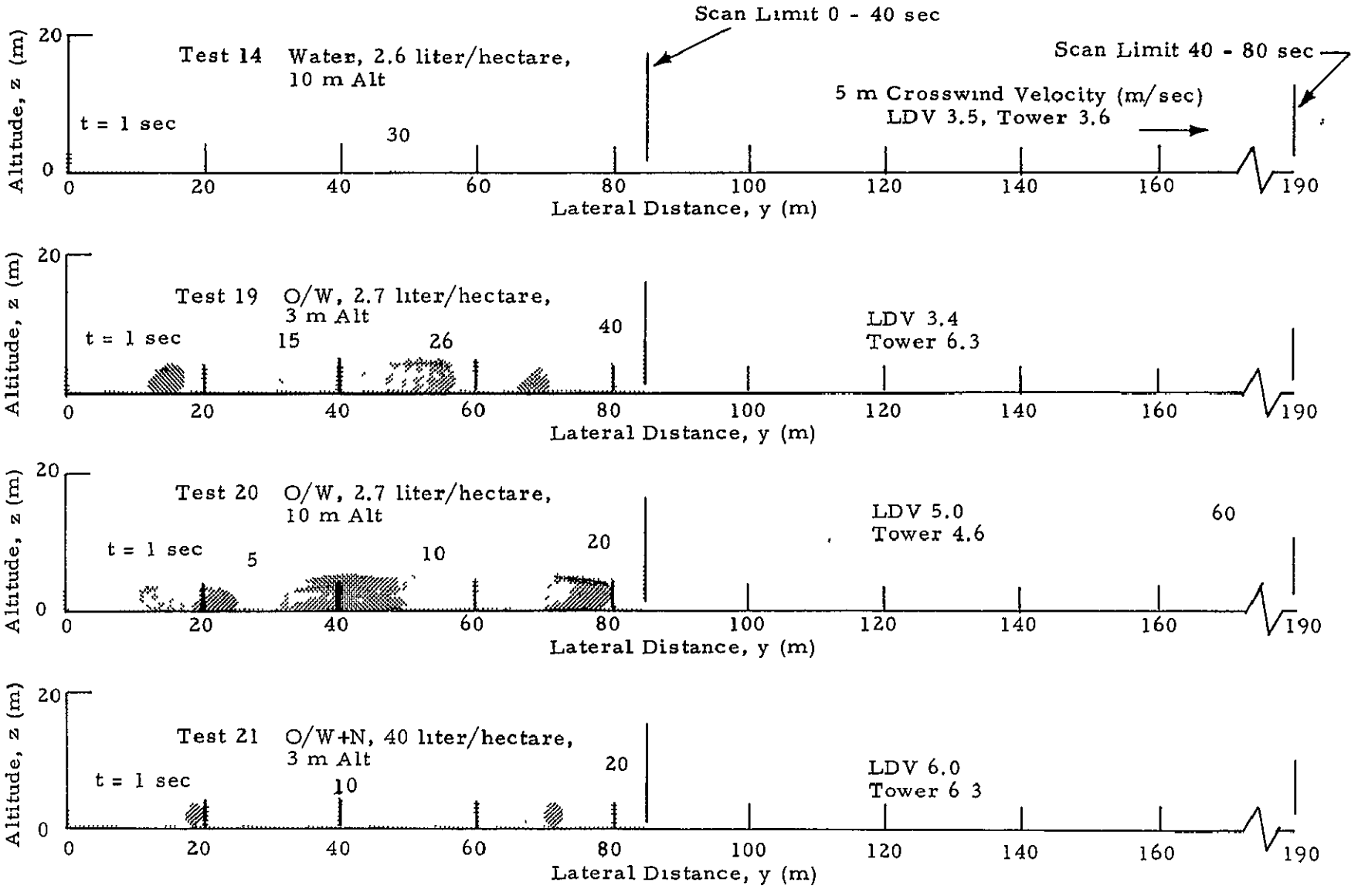

Fig. 40 - Observed Lateral Motion of Spray Cloud Cross Section

on the motion of the cloud centroid is on the order of 3 to 4 m/sec while the crosswind measured at the 5 m altitude ranges from 3 to 6 m/sec. Since the spray cloud is located close to the ground, generally less than 5 m, the crosswind observed at an altitude below 4 m may show better agreement with the observed lateral spray transport velocity.

The measurements shown in Fig. 40 include variations in spray material, spray rate, aircraft height, and crosswind velocity. With so many variables, it is difficult to isolate particular trends. However, the applications with water produced a swath pattern of consistently smaller lateral extent, lower relative concentration, and shorter lifespan than the oil in water spray applications. This is illustrated in Fig. 40, Test 14. A relatively narrow swath pattern at 10 sec and a small patch at 30 sec is observed for the water release in comparison to the large well-defined swath pattern observed for the oil-in-water runs (Tests 19-21). Additional transport measurements are shown in Appendix B.

Since the dominant spray cloud transport mechanisms illustrated in Fig. 40 are believed to be the effect of crosswind and wake vortices, the vortex wake trajectories were calculated for a typical agricultural aircraft flying in ground-effect with a moderate crosswind. These calculations were sought as a qualitative check on the lateral spray cloud trajectories shown earlier in Figs. 39 and 40.

The trailing vortex streamlines, showing the cross section of fluid transported by the wake vortices, are presented in Fig. 41 for an agricultural aircraft flying at 6 m altitude in a 4.5 m/sec crosswind. The selected crosswind profile is given in Fig. 42. The streamlines of the vortex cells were computed from a theoretical model developed at Lockheed-Huntsville to predict aircraft wake transport near the ground (Ref. 9). The vortex wake is modeled by a pair of Rankine vortices located at the aircraft altitude and with a spacing determined from the aircraft spanwise loading distribution. The effect of the ground is simulated by a pair of image vortices. The trajectory of the vortices is computed using a fourth-order Runge-Kutta technique to solve for the induced velocity field as a function of time. The streamlines of the vortices are computed by numerical integration of the vortex pair streamfunction (Ref. 10). The results of the calculations, shown in Fig. 41, indicate the drift and cross-sectional extent of the trailing vortex pair. The trailing vortex streamlines form a dividing boundary between the fluid in the freestream and the fluid which is trapped and carried along by the vortex wake. The fluid which is carried along by the wake vortex is shown by the shaded region in Fig. 41.

The fluid transported by the vortex wake is initially (t = 0 sec) confined to an elliptical region which is approximately 20 m in lateral extent and is 6 m high. Later (10 to 20 sec), two distinct regions are evident since the stagnation points of the upwind and downwind vortices are no longer joined. The upwind vortex cell is considerably larger in size than the downwind cell. The two cells are translated downwind to approximately 40 m at 10 sec and to 80 m at 20 sec. A continuous growth in the vortex cross-sectional area is observed. At 20 sec, the limits of the vortex cells extend from 30 to 100 m downwind and from the groundplane to 12 m altitude.

It is interesting to note that the wake vortex cell lateral displacement, horizontal and vertical dimensions, and cross-sectional area indicated in

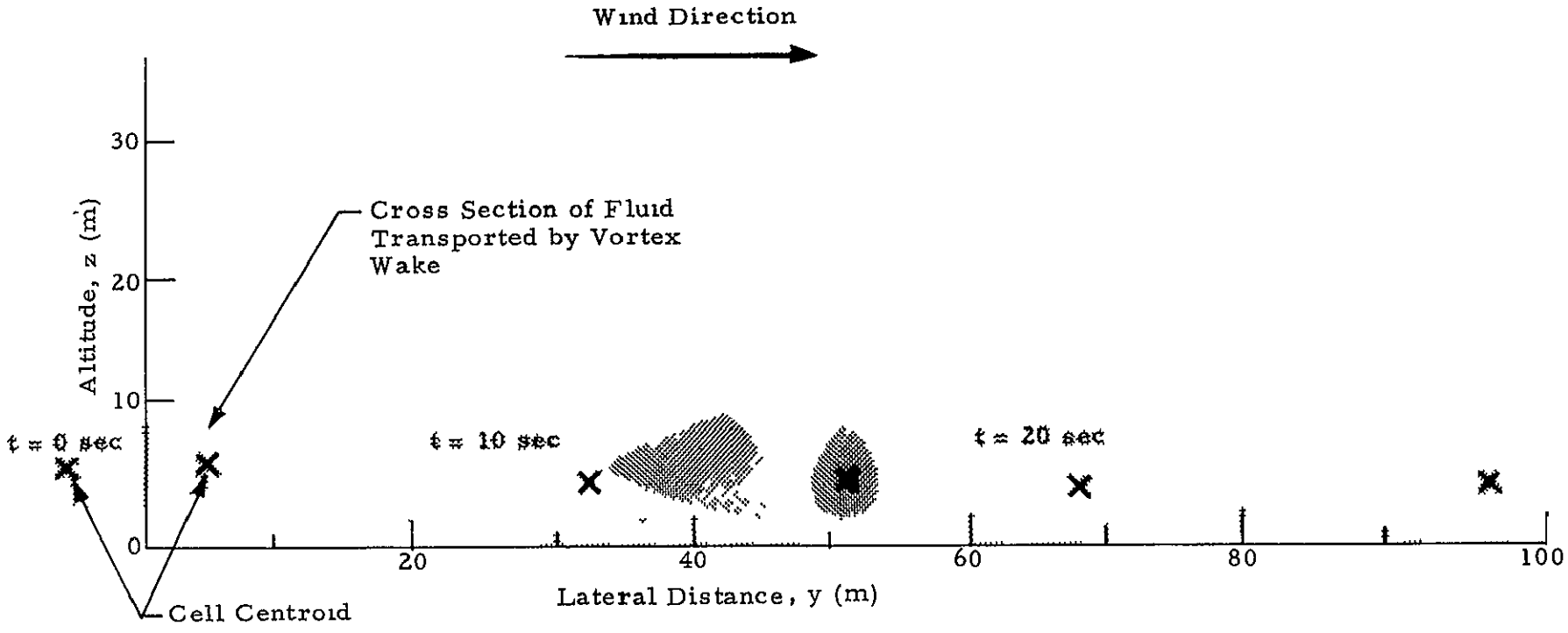

Fig. 41 - Trailing Vortex Streamlines Computed for an Agricultural Aircraft Flying at 6 m Altitude in a 4.5 m/sec Crosswind

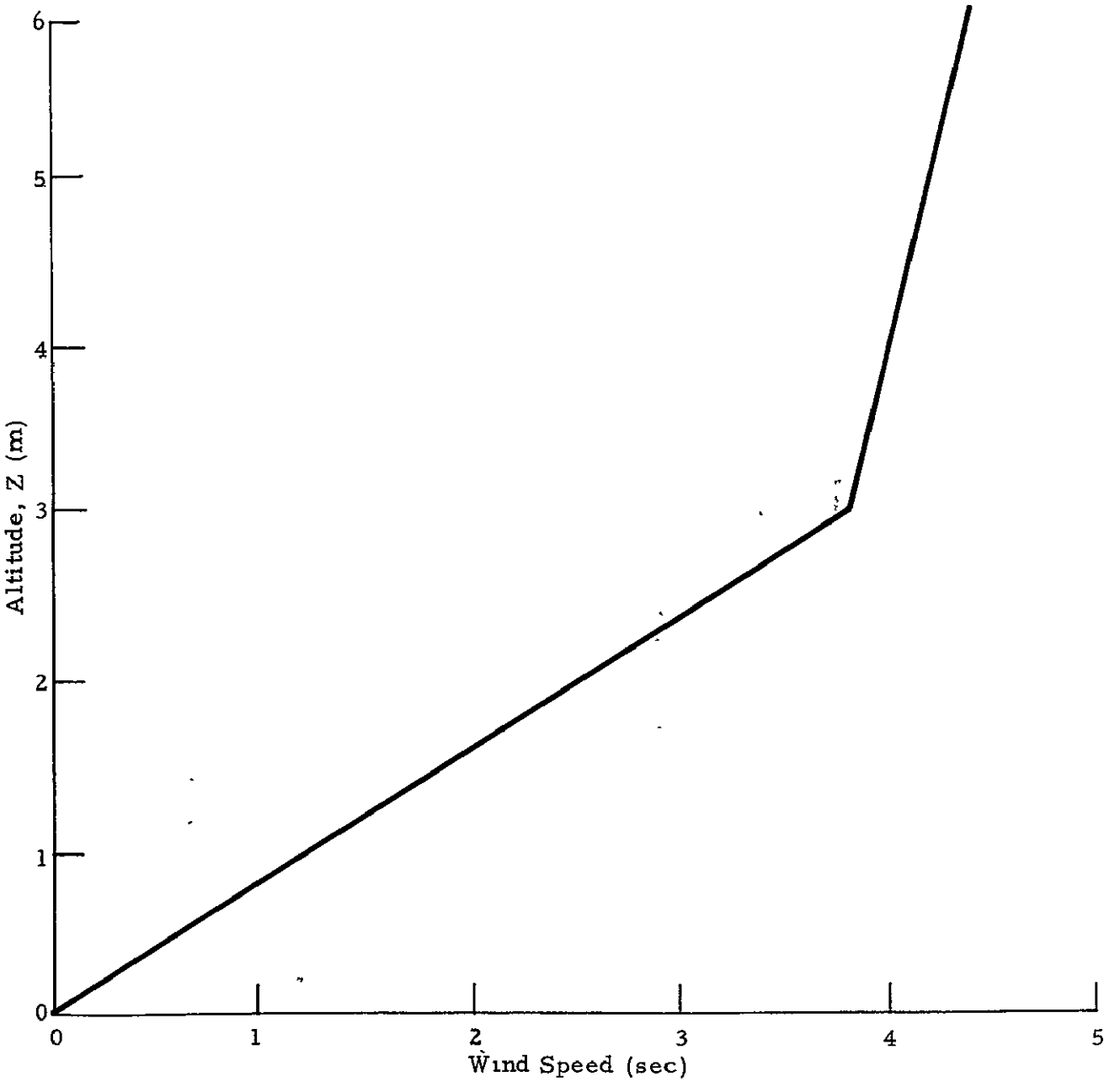

Fig. 42 - Selected Crosswind Profile for Trailing Vortex Streamline Calculation

Fig. 41 show a strong resemblance to the LDV spray transport measurements presented earlier in Fig. 40. The good agreement between the vortex streamlines and the spray cloud measurements suggest that this modeling capability be explored further.

4.5 Wind Measurement

The objective of the wind measurements was to record the atmospheric conditions which influenced the spray transport and dispersion phenomena. The wind velocity component along the sample line at the altitude and lateral location of the spray cloud was sought as a measure of the lateral transport velocity of the spray cloud. The wind speed profile up to several hundred meters altitude was sought to determine the ambient wind characteristics which influenced the dispersion and mixing of the spray material. Since wind velocity measurements were required both in the spray release zone near the ground as well as at higher altitudes, two different types of measuring techniques were used. The wind velocities near the sample line were obtained with the LDV operating in the finger scan mode. The observed line-of-sight velocity along the sample line was essentially the crosswind velocity of the spray cloud normal to the aircraft flight path (cf. Fig. 25). The ambient wind velocities were measured with the LDV operating in the VAD mode. The results obtained with these two types of wind measuring techniques are discussed in this section.

During the spray release tests, the component of velocity of the spray particles (or of the ambient aerosol) along the sample line was measured directly as the LDV line-of-sight velocity. The distribution of the line-of-sight velocity along the sample line with the LDV operating in the finger scan mode was illustrated earlier in Fig. 30. The temporal and spatial variations in the line-of-sight velocity can be observed in Fig. 30. From the distribution of the line-of-sight velocity as a function of time, range, and elevation angle, the mean velocity along the sample line was computed. The mean velocity along the sample line was taken to be the average of the line-of-sight velocity over a 13 min period starting at the spray release. The sampling points were confined between the altitude of $z = 3$ and 6 m and laterally between $y = -50$ and 500 m along the sample line. The observed wind velocity along the sample line, representative of the spray cloud lateral velocity, is given in Table 4. For comparison, the mean wind velocity measured by a propeller anemometer located on a 5 m tower located approximately 100 m east from the N-S sample line is also shown in Table 4. The propeller anemometer measurements were averaged over time periods ranging from 4 to 8 min. The wind velocities along the sample line observed by the LDV and the propeller anemometer given in Table 3 are not necessarily the same. Since the ability of the LDV to measure ambient winds is well documented, i.e., the agreement in wind speed between the LDV and propeller anemometers is better than 0.5 m/sec for 75% of the time and is always within 1 m/sec (Ref. 11), it is concluded that the scatter between the LDV and the tower mounted anemometer measurements is due to the different location of the two sensors and the different averaging periods.

In addition to the wind measurements near the sampling line, the wind profile was obtained with the LDV operating in the VAD mode. A sample wind measurement obtained prior to Test 19 with the LDV in the VAD mode is illustrated in Figs. 43 to 46. The four figures show the variation of wind speed, wind direction, down runway (17R), and cross runway (17R) wind

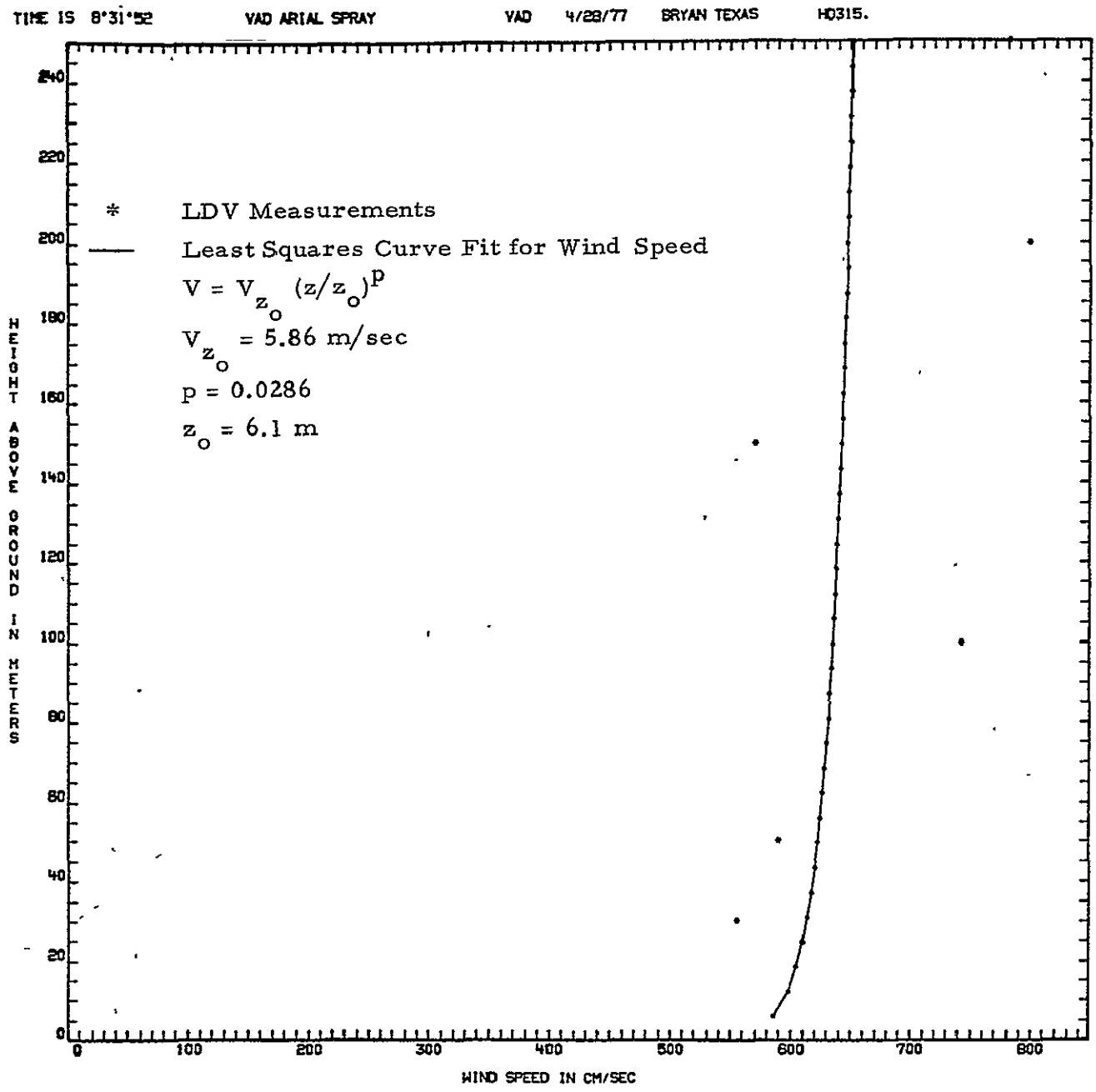

Fig. 43 - Wind Speed as a Function of Altitude

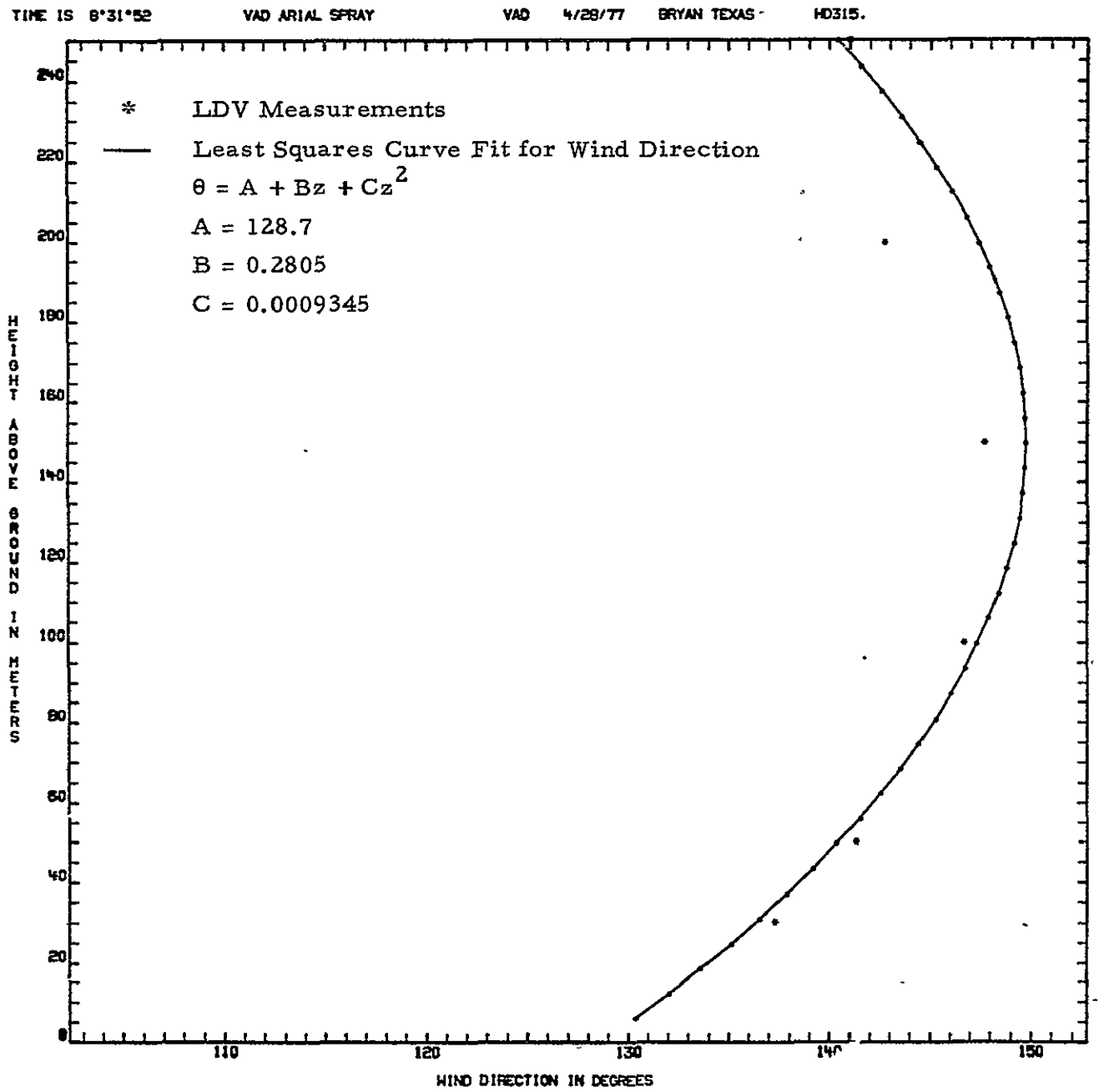

Fig. 44 - Wind Direction as a Function of Altitude

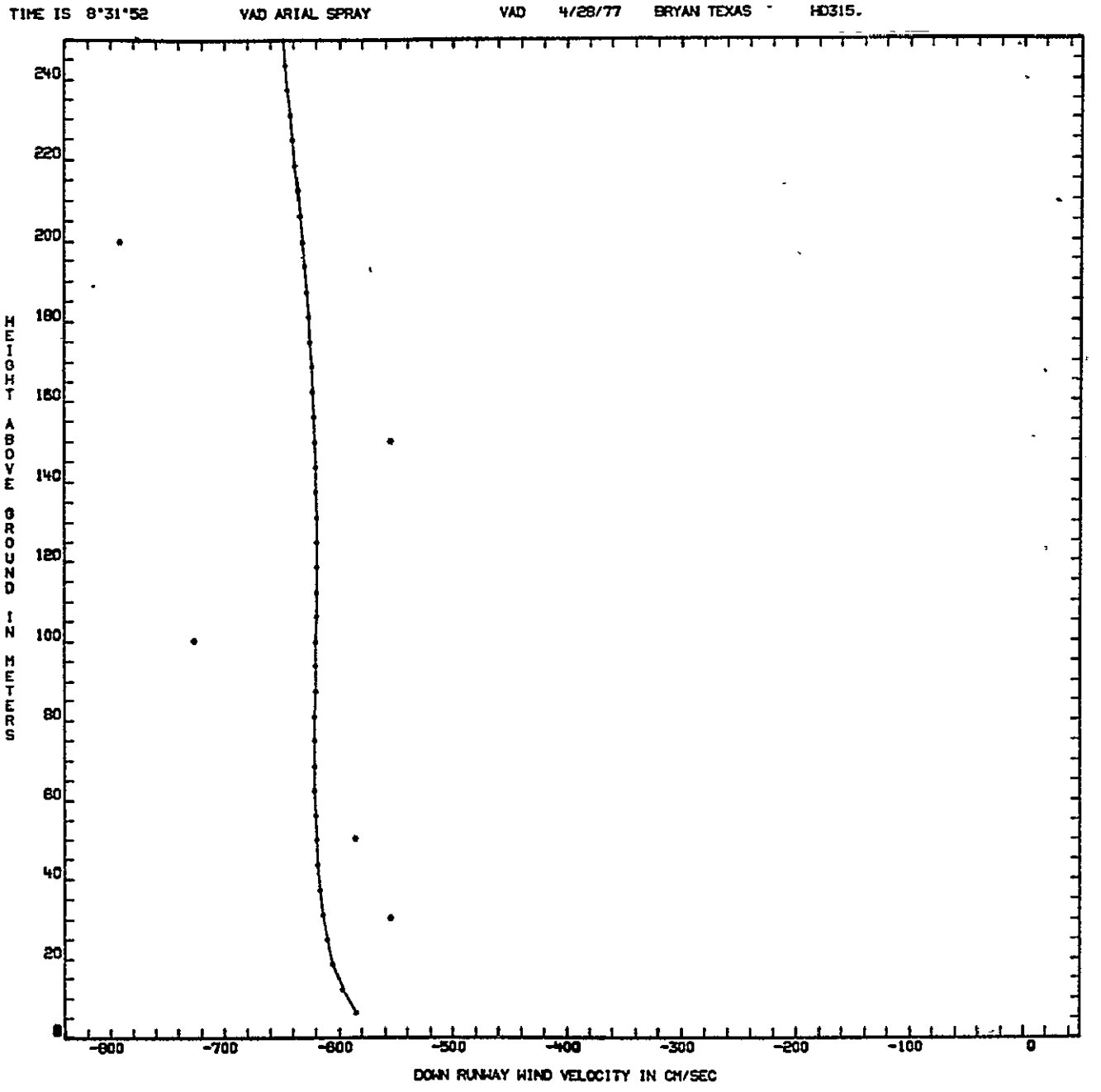

Fig. 45 - Down Runway Velocity as a Function of Altitude

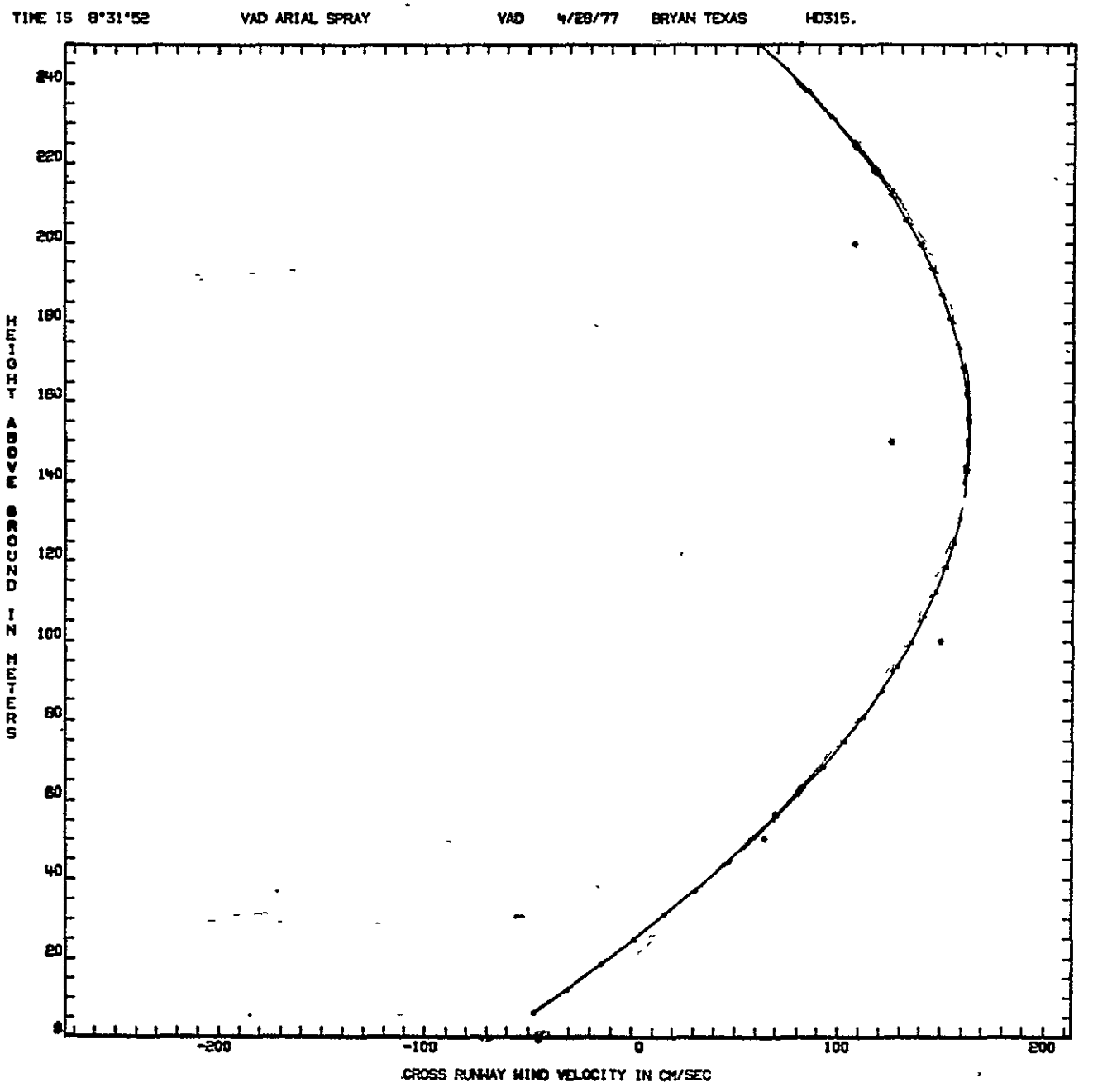

Fig. 46 - Cross Runway Wind Velocity as a Function of Altitude

Table 4

OBSERVED WIND VELOCITY ALONG SAMPLE LINE

Test No.	Observed Wind Velocity Component Along Sample Line	
	LDV (m/sec)	Tower (m/sec)
1		3.10
2		1.43
3		5.01
4	4.31	4.42
5		5.21
6		4.13
7		2.23
8		1.35
9	2.18	2.14
10	2.20	2.73
11	2.64	2.12
12	2.46	2.68
13	3.71	3.76
14	3.49	4.07
15	3.87	4.62
16	4.27	4.21
17		3.78
18	2.59	3.99
19	3.40	4.84
20	4.98	5.33
21		6.15
22	5.31	5.52
23	4.33	4.81
24	3.33	4.53
Dummy	4.84	4.94

velocity as a function of altitude, respectively. The wind measurements were made at the altitudes of 30, 50, 100, 150, 200, 250, 300 and 350 over a 40 sec period. The data points for the six lowest tower altitudes are shown by the asterisks on the plots. The wind speed measurements for all altitudes were fitted to a power law wind profile

$$V = V_{z_o} (z/z_o)^p \tag{18}$$

using a least squares curve fit to solve for the exponent, p, and the wind speed, V_{z_o}, at the reference altitude, z_o. A reference altitude of 6.1 m was selected for the calculations. The choice of z_o has no effect on the plot (i.e., z_o determines V_{z_o} but p is independent). The computed power law profile is shown by the solid line in Fig. 43. The wind direction measurements were fitted to a quadratic profile

$$\theta = A + Bz + Cz^2 \tag{19}$$

illustrated by the solid line in Fig. 44. The component wind profiles shown by the solid lines in Figs. 45 and 46 were computed from the values of V and θ calculated from Eqs. (18) and (19). Previous research has shown that the power law wind profile fitted to the 15 min mean wind measurements gives a consistent characterization of the winds (Ref. 12). However, for measurements made over shorter averaging periods, i.e., the 1 min means, it is difficult to fit the measurements to the power law wind profile and a large scatter in p is noted from run to run.

The wind profile measurements, illustrated in Figs. 43 through 46, can be combined with synoptic weather observations to determine the atmospheric conditions during the spray release. In conjunction with temperature or turbulence measurements, the wind profile measurements can be applied to determine the stability class and atmospheric turbulent mixing and diffusion parameters during the tests (Refs. 13 and 14). These parameters can complement the stability ratio based on the temperature and wind speed measurements near the ground (Ref. 15) which has been used to correlate spray drift with atmospheric turbulence (Ref. 16).

5. CONCLUSIONS AND RECOMMENDATIONS

The results of this study have shown that a mobile LDV remote sensing system is capable of locating, tracking, and providing quantitative measurements of the relative concentration of airborne spray releases up to 200 m downwind from typical agricultural aircraft applications. The LDV measurements were made of the spray cloud of an oil/water solution applied at 3 to 41 liter/hectare under 1 to 7 m/sec wind conditions from an altitude of 3 to 10 m by a Piper Pawnee aircraft.

The physical characteristics of airborne spray releases have been measured with the LDV. The LDV measurements showed a high relative particulate concentration confined to an elongated region above the release point during the release. Later, (10 to 30 sec after release) the region of high relative concentration moved downwind, closer to the ground, and increased in cross-sectional area and decreased in intensity. Within 60 sec after release, the particulate concentration near the release point returned to the ambient levels. The maximum relative spray concentration was observed within 3 m above the ground. A bell shaped distribution of relative concentration was observed in the horizontal and vertical direction through the spray cloud. The maximum relative concentration of the airborne spray cloud was approximately double for the high versus the low spray volume application (~40 versus ~3 liter/hectare). The centroid of the cross section of the spray cloud moved laterally at less than or the same velocity as the ambient wind measured at the 5 m level.

Under the present study, the feasibility of measuring airborne spray clouds with an LDV has been demonstrated and measurements have been obtained of the distribution of relative particulate concentration within the spray cloud as a function of time and space. The need exists to: (1) expand the available data base; (2) relate the physical characteristics of airborne spray clouds to ground fallout measurements; and (3) establish variations with aircraft, spray applicator, and ambient atmospheric parameters. It is anticipated that the successful completion of these tasks will improve the understanding of aerial spray transport phenomena and will result in more effective and more efficient spray applicator techniques and equipment.

REFERENCES

1. Price, R., R. Winblade, J. Mullin, P. Steen, M. McDermott, L. Kaplan and R. Kupersmith, "Agricultural Aviation Study and Program Plan," Vol. I Project Summary, 6 June 1976, NASA Headquarters.
2. Lawrence, T. R., M. C. Krause, C. E. Craven and W. F. Herget, "Remote Sensing of Smokestack Exit Velocities Using a Laser Doppler Velocimeter," AIAA Paper 75-684, presented at 10th Thermophysics Conference, Denver, May 1975.
3. Brashears, M. R., T. R. Lawrence and A. D. Zalay, "Mobile Laser Doppler System Check Out and Calibration," Report FAA-RD-77-48, Lockheed Missiles & Space Company, Huntsville, Ala., February 1977.
4. Brashears, M. R., and W. R. Eberle, "Remote Wind Measurement in Fog Using Laser Doppler Velocimetry," Report AFGL-TR-76-0313, Lockheed Missiles & Space Company, Huntsville, Ala., December 1976.
5. Thompson, J. A. L., and J. C. S. Meng, "Laser Doppler System Simulation for Sensing Aircraft Wake Vortices," Physical Dynamics Report, PD-74-058, December 1974.
6. Miller, C. R., and C. M. Sonnenschein, "Remote Measurement of Power Plant Smoke Stack Effluent Velocity," Report EPA-650/2-75-062, August 1975.
7. Lhermitte, R. M., and D. Atlas, "Precipitation Motion by Pulse Doppler Radar," Proc. 9th Weather Radar Conference, Boston, 1961, pp. 343-346.
8. Akesson, N. B., Wesley E. Yates and P. Christensen, "Aerial Dispersion of Pesticide Chemicals of Known Emissions, Particle Size and Weather Conditions," paper presented at American Chemical Society Meeting, Boston, April 1972.
9. Brashears, M. R., A. D. Zalay, L. C. Chou and K. R. Shrider, "Development of Predictive Wake Vortex Transport Model for Terminal Area Wake Vortex Avoidance," FAA-RD-76-94, May 1976.
10. Brashears, M. R., N. A. Logan, S. J. Robertson, K. R. Shrider and C. D. Walters, "Analysis of Predicted Aircraft Wake Vortex Transport and Comparison with Experiment," Report FAA-RD-74-74, Vol. I, April 1974.
11. Brashears, M. R., and W. R. Eberle, "Verification of Wind Measurement with Mobile Laser Doppler System," LMSC-HREC TR D497071, Lockheed Missiles & Space Company, Huntsville, Ala., June 1977.
12. Brashears, M. R., W. R. Eberle, A. D. Zalay, K. R. Shrider and D. A. Love, "Aircraft Wake Vortex Characteristics Measured at John F. Kennedy International Airport," FAA Report, to be published, 1977.

13. Pasquill, F., "The Estimation of the Dispersion of Windborne Material," Meteorol. Mag., Vol. 90, No. 33, 1961.

14. Skaggs, D. L., and E. Robinson, "A Comparison of Methods for Estimating Atmospheric Stability and Diffusion Coefficients," J. Air Pollution Control Assoc., Vol. 26, No. 9, September 1976, pp. 888-891.

15. Barad, M. L., "Examination of a Wind Profile Proposed by Swinbank," J. App. Meteorology, Vol. 2, 1972, pp. 747-754.

16. Christensen, P., W. E. Yates, and L. O. Myrup, "A Micrometeorological Data Acquisition System," Trans. ASAE, Vol. 15, No. 5, 1972, pp. 956-959.

APPENDIX A

SPRAY APPLICATIONS AND CONVENTIONAL DRIFT MEASUREMENTS

L. F. Bouse and J. B. Carlton
Agricultural Engineers
and
H. R. Crookshank
Research Chemist

U. S. Department of Agriculture
Science and Education Administration

College Station, Texas 77843

NOT FOR USE IN SALES PROMOTION OR ADVERTISING WHICH EXPRESSES OR IMPLIES ENDORSEMENT OF THE PRODUCT BY THE U. S. DEPARTMENT OF AGRICULTURE

SPRAY APPLICATIONS

Aerial spray treatments were selected to simulate a wide range of pesticide drift situations. Application variables included two heights of spray release, two application rates, and three types of spray solution. Each treatment was replicated twice for a total of 24 test runs.

Application Equipment

All spray solutions were applied with an aircraft (Model C Piper Pawnee) equipped with a conventional windmill-driven spray pump and thirty 4664 diaphragm Tee-Jet nozzles (Spraying Systems Co.). Stainless steel orifice discs and brass cores (no. D10-45) were used to provide a nominal low-volume application rate of 37 l/ha (≈4 gal/acre) and brass ConeJet Tips (no. TX4) were used to provide a nominal ultra-low-volume application rate of 2.81 l/ha (≈0.3 gal/acre). Both nozzle types produce hollow cone spray patterns. The D10-45 nozzles were operated at 276 kPa (40 psi) and the orifices were directed straight back to maximize the size of spray droplets produced. The TX4 nozzles were operated at 345 kPa (50 psi), and the orifices were directed straight down to decrease the droplet size.

Spray Materials

The three spray solutions used in the study were water, oil-water emulsion, and oil-water emulsion plus polymer. Reagent grade manganese sulfate was added to the water in each spray solution at a rate of 1.2 percent by weight to permit quantitative analysis of spray deposition and airborne spray. Methylene blue dye was also added to the water in each solution (0.0375 percent by weight) to permit measurements of the size and density of spray droplets deposited.

The oil-water emulsion was prepared by mixing one part of diesel oil with three parts of water. Triton X-100 was premixed with the diesel oil at the rate of 1.56 percent by volume to increase the stability of the emulsion. The emulsion was formed by circulating the mixture through a piston pump and mixing tank before loading it into the aircraft. For the spray solution consisting of oil-water emulsion plus polymer, Nalco-Trol was premixed with the water at the rate of 0.0625 percent by volume. Nalco-Trol is a polyvinyl polymer additive used to reduce the drift of pesticide sprays.

Application Rate Measurement

Since the physical properties of spray solutions affect the flow rate for a given nozzle and pressure, the flow rates were measured for each material, nozzle, and pressure combination used in the tests. The flow rates were determined by measuring the amount of solution dispensed from the aircraft hopper during a 1-minute period while actually flying the aircraft. The theoretical application rate was then calculated based on a 12.2-m (40-ft) effective swath width and a ground speed of 168 km/hr (105 mph). This swath width and speed is equivalent to an area coverage rate of 3.4 ha/min (8.5 acres/min). Measured flow rates and theoretical application rates are presented in the test log (Table 1).

Table 1. Test log for study of feasibility of measuring aerial spray with a laser Doppler velocimeter system.

Date & Time April				Test	Rep.	Spray*	Aircraft height	Nozzle	Pressure,	Flow rate,	Application rate**	Sample line
Day	Hr	Min	Sec	no.	no.	material	m	type & size	kPa	l/min	l/ha	direction
24	19	08	04	1	1	water	3	D10-45	276	127.2	37.0	N-S
24	19	44	00	2	1	water	10	D10-45	276	127.2	37.0	N-S
25	13	45	45	3	1	water	3	TX4	345	9.1	2.6	N-S
25	14	27	33	4	1	water	10	TX4	345	9.1	2.6	N-S
25	18	05	00	5	1	o/w	3	TX4	345	9.5	2.7	N-S
25	18	42	52	6	1	o/w	10	TX4	345	9.5	2.7	N-S
25	19	22	56	7	1	o/w	3	D10-45	276	141.2	41.1	N-S
25	19	56	24	8	1	o/w	10	D10-45	276	141.2	41.1	N-S
26	14	58	26	9	1	o/w+n	3	D10-45	276	137.4	40.0	SE-NW
26	15	40	24	10	1	o/w+n	10	D10-45	276	137.4	40.0	SE-NW
26	17	39	59	11	1	o/w+n	3	TX4	345	11.4	3.3	S-N
26	18	21	45	12	1	o/w+n	10	TX4	345	11.4	3.3	S-N
27	09	25	59	13	2	water	3	TX4	345	9.1	2.6	S-N
27	09	58	50	14	2	water	10	TX4	345	9.1	2.6	S-N
27	11	31	21	15	2	water	3	D10-45	276	127.2	37.0	S-N
27	12	11	08	16	2	water	10	D10-45	276	127.2	37.0	S-N
28	07	17	46	17	2	o/w	3	D10-45	276	141.2	41.1	SE-NW
28	07	50	33	18	2	o/w	10	D10-45	276	141.2	41.1	SE-NW
28	08	34	26	19	2	o/w	3	TX4	345	9.5	2.7	SE-NW
28	09	59	16	20	2	o/w	10	TX4	345	9.5	2.7	S-N
28	17	41	56	21	2	o/w+n	3	D10-45	276	137.4	40.0	S-N
28	18	16	15	22	2	o/w+n	10	D10-45	276	137.4	40.0	S-N
28	18	56	32	23	2	o/w+n	3	TX4	345	11.4	3.3	S-N
28	19	22	54	24	2	o/w+n	10	TX4	345	11.4	3.3	S-N
28	09	39	17	Dummy**	-	-	10	-	-	-	-	S-N

*Water - Contained 1.2 percent manganese sulfate and 0.0375 percent methylene blue dye.

o/w - Oil/water emulsion containing a diesel-to-water ratio of 1:3. Also contained Triton X-100 emulsifier (1.56 percent of diesel oil volume), manganese sulfate (1.2 percent of water by weight), and methylene blue dye (0.0375 percent of water by weight).

o/w+n - Same as o/w, except Nalco-Trol (polyvinyl polymer) was added to the water at the rate of 0.0625 percent by volume.

**Theoretical application rate, in liters per hectare, based on an effective spray swath width of 12.2 m (40 ft) and based on an aircraft speed of 168 km/hr (105 mph).

***Dummy run - no spray.

Test Procedures

Immediately before a test run, the aircraft was equipped with the correct nozzles, and the nozzle orientation was adjusted to the predetermined angle (downward or backward). About 95 l (25 gal) of premixed spray solution was loaded into the aircraft hopper, and the aircraft was flown briefly at an airspeed of 168 km/hr to prime the spray system and to adjust the boom pressure. When the laser Doppler velocimeter (LDV) system, conventional spray sampling equipment, and weather measurement system were readied for a test, a single spray pass was made with the aircraft over a 400-m (1/4 mi) marked course perpendicular to the laser beam and conventional sample line azimuth. The spray system was turned on at least 200 m before the aircraft passed through the laser beam and turned off about 200 m beyond the laser beam. The center of the flight path was located 760 m upwind from the LDV for tests 1 through 8 and 60 m downwind from the LDV for tests 9 through 24. Although the physical features of the test site and random fluctuations in wind direction prohibited precise alignment, an attempt was made to align the laser beam and conventional sample line parallel with the wind direction. The aircraft was flown straight and level for all spray passes at a predetermined boom height of 3 or 10 m. A captive weather balloon, tethered at the desired boom height and positioned about 20 m to one side of the flight path, was used for height guidance during most flights.

CONVENTIONAL DRIFT MEASUREMENTS

Measurements of spray deposition, spray droplet size, and airborne spray concentration were obtained for each test run. Targets for collecting quantitative samples of spray deposit and spray droplet size were placed along a line perpendicular to the flight path. The line of targets extended from a point 10 m upwind from the centerline of the flight path to a point 640 m downwind from the centerline. The spacing between target stations located from 10 m upwind from the flight path to 10 m downwind was 2 m. Beyond 10 m downwind the target stations were logarithmically spaced at 20, 40, 80, 160, 320, and 640 m.

Targets used to collect quantitative samples of spray deposit were 10-cm x 20-cm sheets of 7.5-mil-thick Mylar film, and targets used to collect samples for measurement of droplet size and density were 10-cm x 10-cm sheets of 12-mil-thick Kromekote paper. Two Mylar sheets and two Kromekote sheets were fastened to horizontal metal plates at all target stations except one; at the 640 m station, four sheets of each type were used.

Commercially available, high-volume air samplers were used to obtain samples of airborne spray concentration. One sampler was used at the 320-m downwind location and two at the 640-m downwind location. In addition, one sampler was placed about 100 m upwind from the flight path to obtain background measurements of manganese. Each sampler was equipped with a 20.3-cm x 25.4-cm (8-in. x 10-in.) glass fiber filter having a collection efficiency of 98 percent for particles as small as 0.05 μm. The height of the air intake for each sampler was about 1 m, and the airflow rate was 0.025 m^3/s.

Sample Collection and Processing

Several minutes elapsed after each spray run before retrieval of the Mylar and Kromekote sample sheets was begun and the air samplers were turned off. This time interval ranged from about 5 to 10 min, depending on the wind speed and LDV sampling time, but was always sufficient to insure that spray particles carried by the wind would have passed the last sampling station downwind from the flight path.

As each Mylar sample sheet was retrieved, it was rolled into a cylinderical shape and placed in a 600-ml, wide-mouth glass jar containing 50 ml of wash solution. The sprayed surface of the sheet was oriented to the inside of the jar so that the tracer would be exposed to the wash solution. The jars were placed in wooden trays and transported to the laboratory. In the laboratory, the jars were placed in a jar rotating machine in a horizontal position and rotated for 10 min at a speed of 6 rpm to remove the spray material and tracer from the Mylar sheet. Distilled water was used to wash the sheets from test runs in which water and tracer were sprayed. For the oil-water emulsion plus tracer and the oil-water emulsion plus polymer and tracer, a 50/50 solution of methyl alcohol and distilled water was used for the wash. About 20 ml of each resultant solution was stored for later analysis to determine the amount of manganese tracer collected on each Mylar sheet. A Model 403 atomic absorption spectrophotometer (Perkin Elmer) equipped with a standard flame atomizer was used for the initial analysis. Samples having less than 0.1 ppm of manganese were rerun with a Model 1200 instrument (Varian) equipped with a CRA-90 carbon rod atomizer. For this analysis the sample size was 2µl. Samples having less than 0.003 ppm of manganese were rerun using 4µl of solution. This procedure provided a sensitivity of greater than 0.001 ppm. Each reading was repeated three times.

The air sampler filters were placed in individual plastic bags as they were retrieved. In the laboratory, one 10-cm x 20-cm section was cut from the center portion of each filter and washed in the same manner as the Mylar sheets. A 0.1 percent solution of hydrochloric acid in distilled water was used as the wash solution for all test samples. Samples of the resulting solutions were injected directly into the spectrophotometer to determine the amount of manganese tracer collected.

Manganese concentrations obtained from the Mylar sample sheets were converted to spray deposit rates in l/ha based on the dilution ratio, concentration of tracer in the original spray solution and sample area. The average deposit rates for the samples at each target station were then determined (Table 2).

One set of Mylar sample sheets (36 sheets) was rewashed after the tests were completed to obtain a measure of the manganese residue remaining on the sheets. The average amount of residue was found to be equivalent to a deposit rate of 0.023 l/ha for the water spray and 0.028 l/ha for the oil-water emulsion and oil-water emulsion plus polymer sprays. The deposit rates shown in Table 2 for each test were corrected by subtracting the appropriate residue values. Numerical integration was then used to determine the amount of spray deposited between each sample station per meter of distance along the flight path. These deposits were expressed as percentages of the amount of spray released per meter of distance along the flight path and accumulated from the upwind to downwind ends of the spray deposit sample line (Table 3). Curves for the cumulative percentage of spray recovery were plotted on log-log paper for each LDV-aerial-spray-measurement test (Fig. 1).

Table 2. Spray deposits collected on Mylar sheets (l/ha) and Kromekote cards (LMD and droplets/cm^2)

Spray material: Water

Distance downwind from flight path, m	D10-45 nozzles: 37.03 l/ha*						TX4 nozzles: 2.62 l/ha*					
	Test no. 1, 3 m aircraft height			Test no. 2, 10 m aircraft height			Test no. 3, 3 m aircraft height			Test no. 4, 10 m aircraft height		
	l/ha	LMD μm	droplets/cm^2	l/ha	LMD μm	droplets/cm^2	l/ha	LMD μm	droplets/cm^2	l/ha	LMD μm	droplets/cm^2
-10	31.84	313	15.5	.019	-	0	.019	-	0	.008	-	0
- 8	31.84	193	30.5	.033	-	0	.009	-	0	.006	-	0
- 6	33.80	209	28.8	37.17	369	12.6	.033	-	0	.004	-	0
- 4	13.93	154	26.5	29.36	255	22.2	.007	-	0	.002	-	0
- 2	24.17	161	35.9	26.55	193	27.1	.007	-	0	.007	-	0
0	30.48	168	29.6	10.80	127	24.0	.089	160	1.0	.008	-	0
2	25.62	192	22.3	18.09	151	20.3	.069	114	1.4	2.95	-	0
4	9.30	156	21.5	23.61	230	16.1	1.92	126	0.8	.006	-	0
6	5.84	128	13.9	25.43	216	17.4	.136	97	4.2	.837	-	0
8	3.23	130	8.3	17.53	220	11.6	.238	95	4.2	2.82	115	0.3
10	1.54	105	5.9	9.16	219	8.5	1.38	63	1.9	.047	130	0.4
20	.145	102	2.3	.980	130	1.6	.094	114	0.8	.056	97	1.3
40	.061	68	0.8	.140	136	0.2	.017	-	0	.070	80	0.4
80	.023	-	0	.056	-	0	.056	-	0	.008	-	0
160	.017	-	0	.061	-	0	.013	-	0	.006	-	0
320	.023	-	0	.042	-	0	.007	-	0	.019	-	0
640	.021	-	0	.007	-	0	.040	-	0	.007	-	0

*See footnote at end of table, page A-11

continued

REPRODUCIBILITY OF THE ORIGINAL PAGE IS POOR

Table 2. (cont.)

Spray material: Oil-water emulsion

Distance downwind from flight path, m	TX4 nozzles: 2.71 l/ha*						D10-45 nozzles: 41.14 l/ha*					
	Test no. 5, 3 m aircraft height			Test no. 6, 10 m aircraft height			Test no. 7, 3 m aircraft height			Test no. 8, 10 m aircraft height		
	l/ha	LMD µm	droplets/ cm^2	l/ha	LMD µm	droplets/ cm^2	l/ha	LMD µm	droplets/ cm^2	l/ha	LMD µm	droplets/ cm^2
-10	.098	-	0	.014	-	0	.533	-	0	.122	-	0
- 8	.140	-	0	.007	-	0	44.74	316	26.2	11.41	237	19.9
- 6	.084	-	0	.033	-	0	28.28	224	61.3	13.98	210	27.0
- 4	.131	197	0.7	.032	-	0	25.90	186	79.2	8.79	163	23.6
- 2	.229	153	3.3	.079	-	0	31.51	182	112.0	3.51	157	16.3
0	.168	154	2.6	.285	173	2.9	25.39	182	93.4	4.58	163	17.4
2	.229	137	2.5	.645	129	2.5	21.83	184	53.9	6.12	184	15.1
4	.173	140	2.1	.299	153	4.4	17.48	196	28.7	10.00	207	16.3
6	.178	129	0.8	.453	111	5.6	12.06	188	30.3	8.74	240	11.8
8	.182	111	2.1	.556	120	4.7	6.36	176	19.7	3.32	244	6.5
10	.178	141	1.4	.168	119	4.0	5.56	163	22.7	1.45	212	5.0
20	.079	127	0.7	.154	100	2.5	3.46	143	12.5	.935	129	5.3
40	.079	110	0.5	.122	104	0.6	.337	107	2.8	.173	78	1.2
80	.028	118	0.4	.070	-	0	.215	78	1.2	.210	-	0
160	.108	-	0	.037	-	0	.122	-	0	.103	-	0
320	.023	-	0	.033	-	0	.131	-	0	.014	-	0
640	.021	-	0	.028	-	0	.068	-	0	.019	-	0

*See footnote at end of table, page A-11.

continued

Table 2.(cont.)

Spray material: Oil-water emulsion plus polymer

Distance downwind from flight path, m	D10-45 nozzles: 40.02 l/ha*						TX4 nozzles: 3.27 l/ha*					
	Test no. 9, 3 m aircraft height			Test no. 10, 10 m aircraft height			Test no. 11, 3 m aircraft height			Test no. 12, 10 m aircraft height		
	l/ha	LMD μm	droplets/ cm^2	l/ha	LMD μm	droplets/ cm^2	l/ha	LMD μm	droplets/ cm^2	l/ha	LMD μm	droplets/ cm^2
-10	.006	-	0	.842	-	0	.131	-	0	.014	-	0
- 8	3.18	157	18.0	1.17	-	0	1.22	143	5.8	.007	-	0
- 6	40.02	224	54.7	2.34	-	0	.598	157	6.0	.042	-	0
- 4	37.03	214	35.5	77.89	482	10.8	1.03	139	3.4	.070	-	0
- 2	42.82	220	40.5	65.54	349	23.1	.935	90	1.7	.028	-	0
0	23.05	180	35.0	24.12	217	26.5	.982	109	3.3	.075	244	0.1
2	19.35	170	57.4	18.14	163	41.8	1.17	83	6.6	.126	128	1.7
4	27.91	225	36.6	23.94	178	38.4	1.26	129	3.6	.079	105	1.3
6	20.76	186	44.4	26.37	198	33.6	1.54	113	3.5	.098	105	1.4
8	16.13	196	31.3	23.38	210	22.2	.982	134	1.1	.098	128	1.1
10	11.64	191	17.7	23.94	194	18.6	.117	119	1.8	.094	129	1.7
20	1.36	136	7.9	6.26	220	6.1	.098	180	0.4	.094	146	0.6
40	1.26	141	6.5	1.31	135	2.0	.033	-	0	.122	177	0.6
80	.028	-	0	.011	-	0	.014	-	0	.006	-	0
160	.008	-	0	.011	-	0	.007	-	0	.003	-	0
320	.006	-	0	1.08	-	0	.003	-	0	.0	-	0
640	.003	-	0	.603	-	0	.004	-	0	.004	-	0

*See footnote at end of table, page A-11

continued

Table 2. (cont.)

Spray material: Water

Distance downwind from flight path, m	TX4 nozzles: 2.62 l/ha*						D10-45 nozzles: 37.03 l/ha*					
	Test no. 13, 3 m aircraft height			Test no. 14, 10 m aircraft height			Test no. 15, 3 m aircraft height			Test no. 16, 10 m aircraft height		
	l/ha	LMD µm	droplets/ cm^2	l/ha	LMD µm	droplets/ cm^2	l/ha	LMD µm	droplets/ cm^2	l/ha	LMD µm	droplets/ cm^2
-10	.154	-	0	.019	-	0	.281	-	0	.187	-	0
- 8	.145	-	0	.136	-	0	.360	-	0	.131	-	0
- 6	.206	-	0	.094	-	0	.842	-	0	.449	-	0
- 4	.281	-	0	.075	-	0	.187	-	0	.234	-	0
- 2	.285	-	0	.070	-	0	.037	-	0	.327	-	0
0	.346	-	0	.070	-	0	1.31	327	0.1	.533	-	0
2	.496	176	2.5	.084	-	0	8.84	478	2.7	.888	-	0
4	.439	141	0.9	.089	-	0	23.05	428	8.2	4.82	489	0.6
6	.388	111	0.5	.117	-	0	25.95	370	16.1	12.34	466	3.6
8	.290	128	0.5	.192	174	0.4	9.72	256	15.1	15.43	421	3.6
10	.252	156	0.7	.154	121	0.2	12.34	278	10.6	15.10	372	5.6
20	.159	-	0	.154	156	0.3	3.23	235	4.6	7.29	265	6.4
40	.145	-	0	.117	-	0	.748	188	1.4	.888	201	1.3
80	.108	-	0	.042	-	0	.103	-	0	.159	-	0
160	.103	-	0	.060	-	0	.201	-	0	.206	-	0
320	.042	-	0	.056	-	0	.006	-	0	.019	-	0
640	.026	-	0	.020	-	0	.006	-	0	.154	-	0

*See footnote at end of table, page A-11

continued

Table 2. (cont.)

Spray material: Oil-water emulsion

Distance downwind from flight path, m	D10-45 nozzles: 41.14 l/ha*						TX4 nozzles: 2.71 l/ha*					
	Test no. 17, 3 m aircraft height			Test no. 18, 10 m aircraft height			Test no. 19, 3 m aircraft height			Test no. 20, 10 m aircraft height		
	l/ha	LMD μm	droplets/ cm^2	l/ha	LMD μm	droplets/ cm^2	l/ha	LMD μm	droplets/ cm^2	l/ha	LMD μm	droplets/ cm^2
-10	.023	-	0	.007	-	0	.103	-	0	.056	-	0
- 8	.047	-	0	.037	-	0	.084	-	0	.070	-	0
- 6	.047	-	0	.084	-	0	.079	-	0	.098	-	0
- 4	6.26	530	1.3	.065	-	0	.098	-	0	.065	-	0
- 2	55.02	357	32.7	.070	-	0	.075	-	0	.131	-	0
0	29.78	222	44.7	.070	-	0	.238	-	0	.122	-	0
2	24.92	207	66.4	.098	-	0	.519	-	0	.178	-	0
4	10.66	195	31.2	2.15	647	0.2	.519	-	0	.154	-	0
6	32.21	209	51.1	8.88	548	1.4	.982	144	2.3	.173	-	0
8	18.89	184	47.4	13.28	487	3.4	1.08	161	2.0	.122	-	0
10	12.25	190	37.9	14.91	449	3.9	.514	146	1.5	.112	-	0
20	6.12	164	6.2	18.93	276	23.5	.842	186	1.8	.042	138	0.3
40	1.45	169	6.6	3.74	250	10.5	.108	156	1.8	.168	132	4.7
80	.094	136	1.8	1.50	187	5.7	.061	129	0.2	.103	-	0
160	.065	116	0.5	.051	115	1.4	.032	-	0	.037	-	0
320	.037	-	0	.028	-	0	.014	-	0	.028	-	0
640	.015	-	0	.006	-	0	.006	-	0	.051	-	0

*See footnote at end of table, page A-11.

continued

Table 2. (cont.)

Spray material: Oil-water emulsion plus polymer

Distance downwind from flight path, m	D10-45 nozzles: 40.02 l/ha*						TX4 nozzles: 3.27 l/ha*					
	Test no. 21, 3 m aircraft height			Test no. 22, 10 m aircraft height			Test no. 23, 3 m aircraft height			Test no. 24, 10 m aircraft height		
	l/ha	LMD µm	droplets/ cm^2	l/ha	LMD µm	droplets/ cm^2	l/ha	LMD µm	droplets/ cm^2	l/ha	LMD µm	droplets/ cm^2
-10	.131	-	0	.045	-	0	.019	-	0	.022	-	0
- 8	.089	-	0	.051	-	0	.019	-	0	.033	-	0
- 6	.103	-	0	.019	-	0	.028	-	0	.075	-	0
- 4	.178	-	0	.019	-	0	.037	-	0	.014	-	0
- 2	.117	-	0	.042	-	0	.037	-	0	.051	-	0
0	.126	-	0	.075	-	0	.075	-	0	.033	-	0
2	3.38	310	2.5	.047	-	0	.065	-	0	.023	-	0
4	21.41	237	14.2	.051	-	0	.108	151	1.7	.122	-	0
6	16.46	175	21.9	.070	-	0	.131	146	1.8	.047	-	0
8	4.30	157	9.3	.051	-	0	.079	118	0.6	.028	-	0
10	4.25	182	6.3	4.44	287	0.9	.108	149	1.7	.014	-	0
20	3.27	132	4.0	6.92	185	4.7	.122	121	1.0	.103	153	0.6
40	1.17	138	2.6	1.92	137	2.8	.047	-	0	.056	188	0.2
80	1.03	137	2.6	1.17	129	1.9	.023	-	0	.108	127	0.3
160	.453	-	0	.033	-	0	.028	-	0	.051	144	0.2
320	.037	-	0	.089	-	0	.007	-	0	.007	-	0
640	.045	-	0	.054	-	0	.018	-	0	.004	-	0

*Theoretical application rate based on an effective spray swath width of 12.2 m (40 ft) and a ground speed of 168 km/hr (105 mph).

Table 3. Cumulative spray recovery measured from Mylar sheet samples

Test no.:	1	2	3	4	5	6	7	8	9	10	11	12
Spray material*:	water	water	water	water	o/w	o/w	o/w	o/w	o/w+n	o/w+n	o/w+n	o/w+n
Nozzle type**:	D10-45	D10-45	TX4	TX4	TX4	TX4	D10-45	D10-45	D10-45	D10-45	TX4	TX4
Aircraft height:	3m	10m	3m	10m	3m	10m	3m	10m	3m	10m	3m	10m
Distance from upwind end of sample line, m	Cumulative spray recovery, percentage of amount released											
2	14.0	0	0	0	0.54	0	8.97	2.27	0.64	0.40	3.17	0
4	28.5	8.18	0.03	0	1.04	0.01	23.4	7.29	9.43	1.10	7.49	0.02
6	39.0	22.8	0.06	0	1.49	0.04	34.3	11.8	25.1	17.4	11.4	0.17
8	47.3	35.1	0.06	0	2.39	0.20	45.7	14.2	41.4	46.7	16.0	0.27
10	59.4	43.3	0.28	0	3.40	1.11	57.0	15.8	54.8	64.9	20.6	0.39
12	71.7	49.7	0.62	9.02	4.41	3.69	66.3	17.9	63.4	73.5	25.7	0.76
14	79.4	58.9	6.62	18.0	5.43	6.31	74.1	21.1	73.0	82.1	31.6	1.13
16	82.7	69.6	12.8	20.5	6.30	8.36	80.0	24.8	83.0	92.3	38.3	1.42
18	84.7	79.1	13.8	31.6	7.20	11.2	83.6	27.2	90.5	102.5	44.3	1.76
20	85.7	85.0	18.7	40.3	8.10	13.1	86.0	28.1	96.1	112.1	46.9	2.10
30	87.5	96.1	40.7	41.2	11.1	17.1	94.8	30.4	109.3	142.8	48.8	3.72
50	87.9	98.4	42.9	43.7	14.1	23.5	102.2	32.6	114.5	158.1	50.5	7.65
90	88.1	99.1	44.9	46.6	17.1	31.6	104.2	33.9	119.5	163.3	50.8	12.3
170		99.7	49.0		26.5	37.6	106.4	36.0		163.3		
330		100.7	49.0		45.4	40.9	109.6	37.2		180.4		
650			57.3			43.2	114.1			233.4		

See footnote at end of table, page A-13.

continued

Table 3 (cont.)

Test no.:	13	14	15	16	17	18	19	20	21	22	23	24
Spray material*:	water	water	water	water	o/w	o/w	o/w	o/w	o/w+n	o/w+n	o/w+n	o/w+n
Nozzle type**:	TX4	TX4	D10-45	D10-45	D10-45	D10-45	TX4	TX4	D10-45	D10-45	TX4	TX4
Aircraft height:	3m	10m	3m	10m	3m	10m	3m	10m	3m	10m	3m	10m
Distance from upwind end of sample line, m	Cumulative spray recovery, percentage of amount released											
2	0.74	0.31	0.13	0.06	0	0	0.38	0.21	0.03	0.01	0	0.02
4	1.66	0.83	0.39	0.18	0.01	0.01	0.70	0.53	0.06	0.01	0	0.14
6	2.98	1.17	0.61	0.32	1.25	0.03	1.05	0.85	0.11	0.01	0.02	0.26
8	4.55	1.45	0.65	0.43	13.4	0.05	1.40	1.26	0.16	0.01	0.07	0.31
10	6.33	1.70	0.94	0.61	30.2	0.07	2.17	1.85	0.20	0.02	0.22	0.38
12	8.76	2.01	3.16	0.91	41.0	0.09	4.23	2.56	0.90	0.03	0.42	0.40
14	11.5	2.38	10.2	2.16	48.1	0.52	7.12	3.39	5.94	0.04	0.71	0.62
16	13.8	2.84	21.0	5.93	56.6	2.70	11.4	4.19	13.7	0.05	1.15	0.89
18	15.8	3.61	28.8	12.0	66.7	7.08	17.3	4.90	17.9	0.06	1.52	0.94
20	17.3	4.50	33.6	18.7	72.8	12.7	21.9	5.43	19.6	0.96	1.84	0.94
30	22.7	8.38	50.7	43.3	91.0	46.2	41.0	6.87	27.2	12.5	3.98	1.87
50	30.4	15.0	59.4	61.2	105.9	91.0	67.4	11.4	36.1	30.4	6.76	4.40
90	42.5	21.3	62.9	65.6	111.8	111.6	74.0	24.1	44.9	42.8	7.69	9.71
170	61.6	27.0	65.2	67.0	112.6	123.4	78.4	34.0	56.5	52.1		19.8
330	83.5	41.2	68.0	70.2	113.4	123.8	79.3	36.1	63.6	53.2		24.4
650	89.4	51.6		74.7	113.7			47.0	64.4	56.0		

*water - Contained 1.2 percent manganese sulfate and 0.0375 percent methylene blue dye.

o/w - Oil/water emulsion containing a diesel-to-water ratio of 1:3. Also contained Triton X-100 emulsifier (1.56 percent of diesel oil volume), manganese sulfate (1.2 percent of water by weight), and methylene blue dye (0.0375 percent of water by weight).

o/w+n - Same as o/w, except Nalco-Trol (polyvinyl polymer) was added to the water at the rate of 0.0625 percent by volume.

**Nozzle types shown are Spraying Systems Co. The TX4 nozzles were operated at 345 kPa (50 psi) and directed straight down. The D10-45 nozzles were operated at 276 kPa (40 psi) and directed straight back.

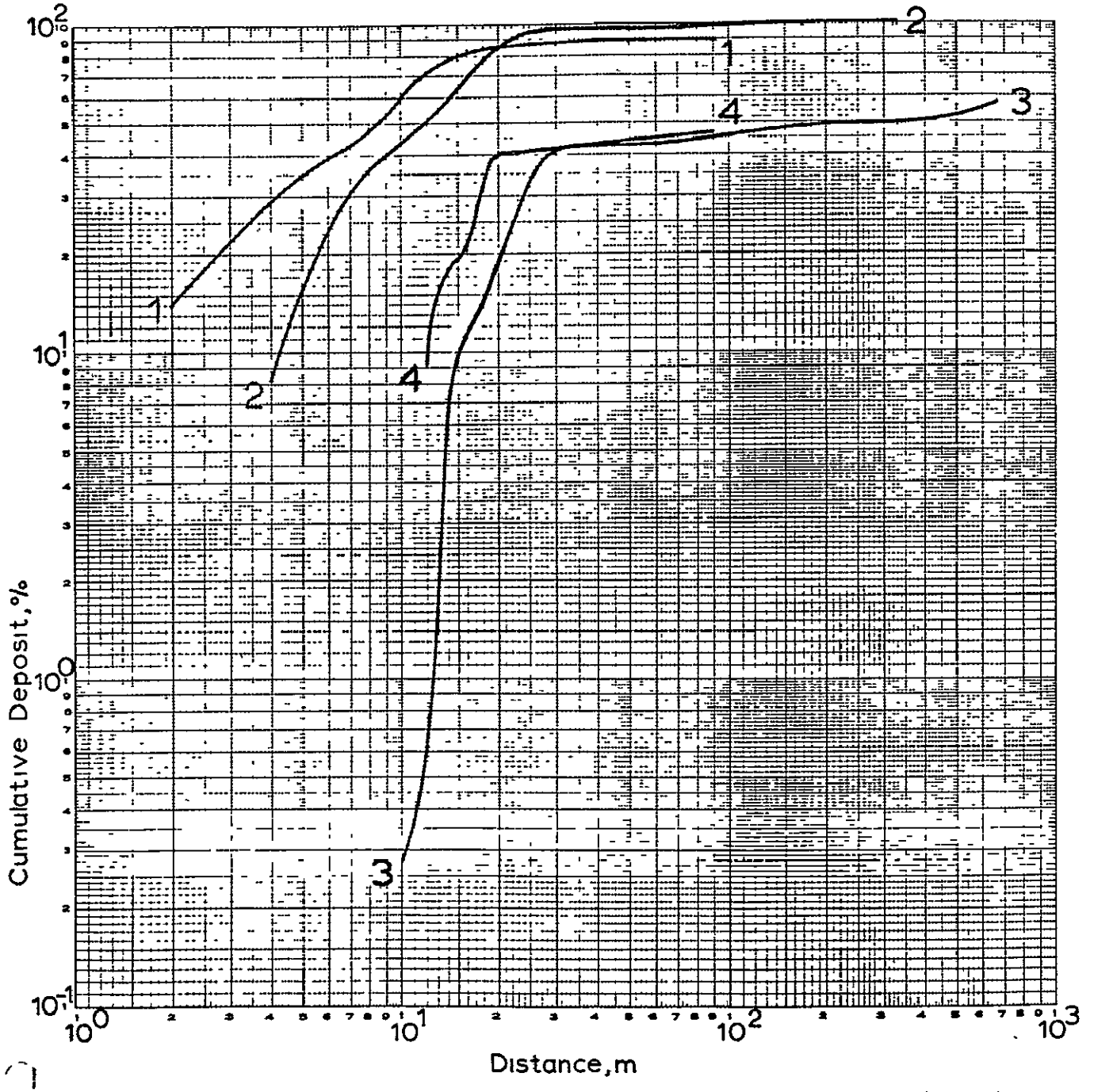

Fig. 1 - Cumulative percentage spray recovery measured from Mylar sheet samples for test numbers 1-24.

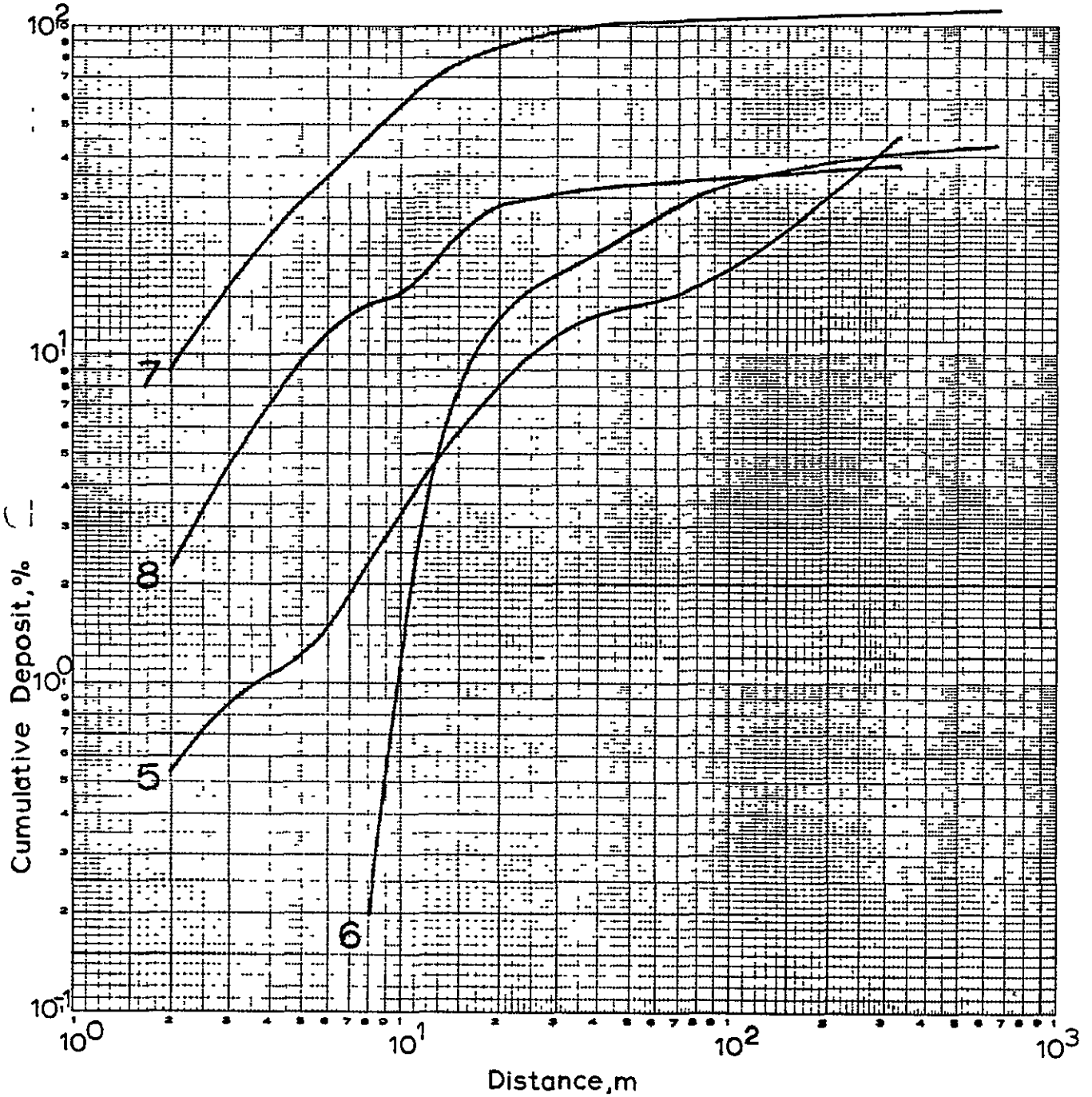
Cumulative Deposit, %
Distance, m
7
8
5
6
10^2
10^1
10^0
10^{-1}
10^0
10^1
10^2
10^3

Fig. 1 (cont.)

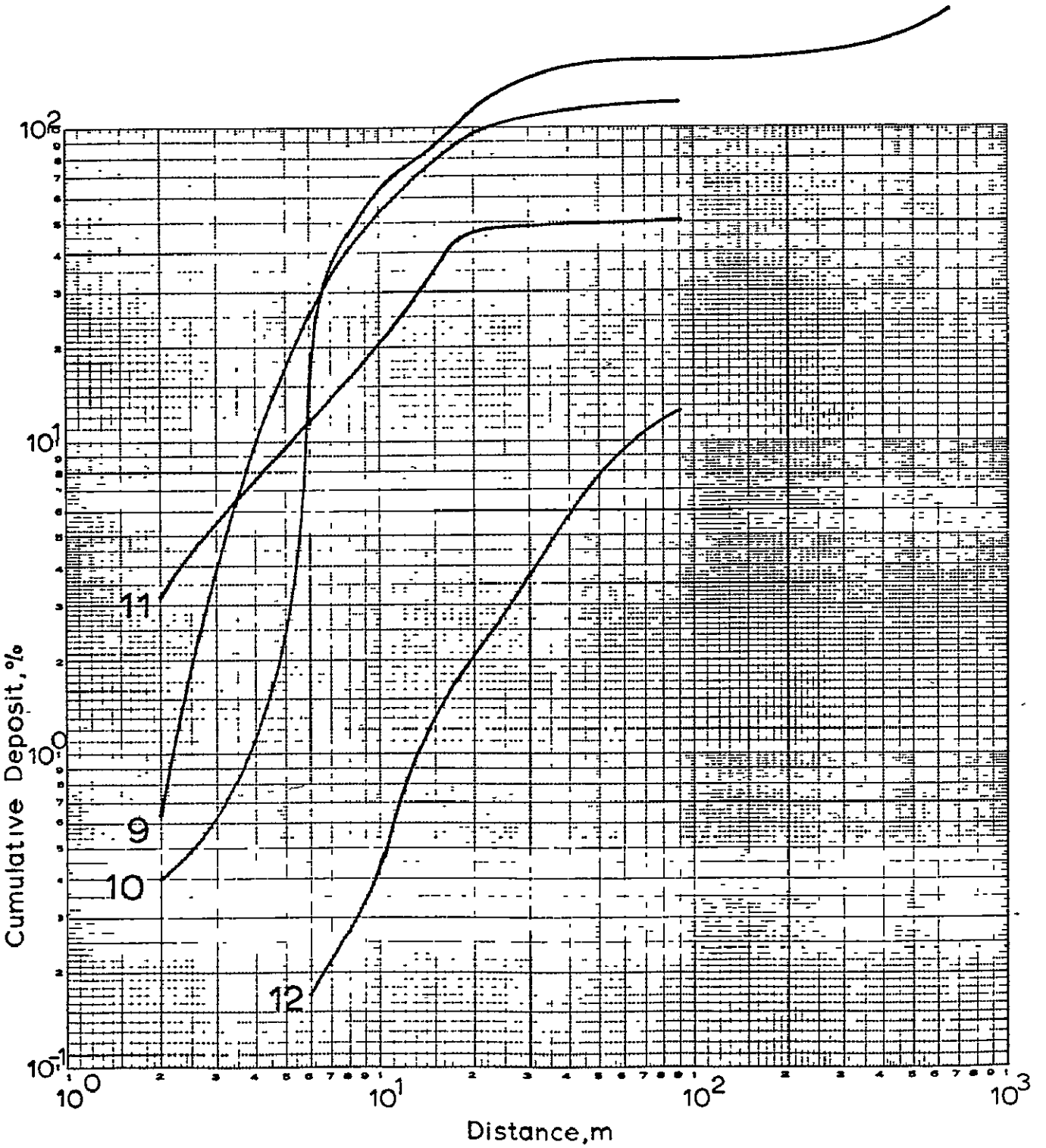

Fig. 1 (cont.)

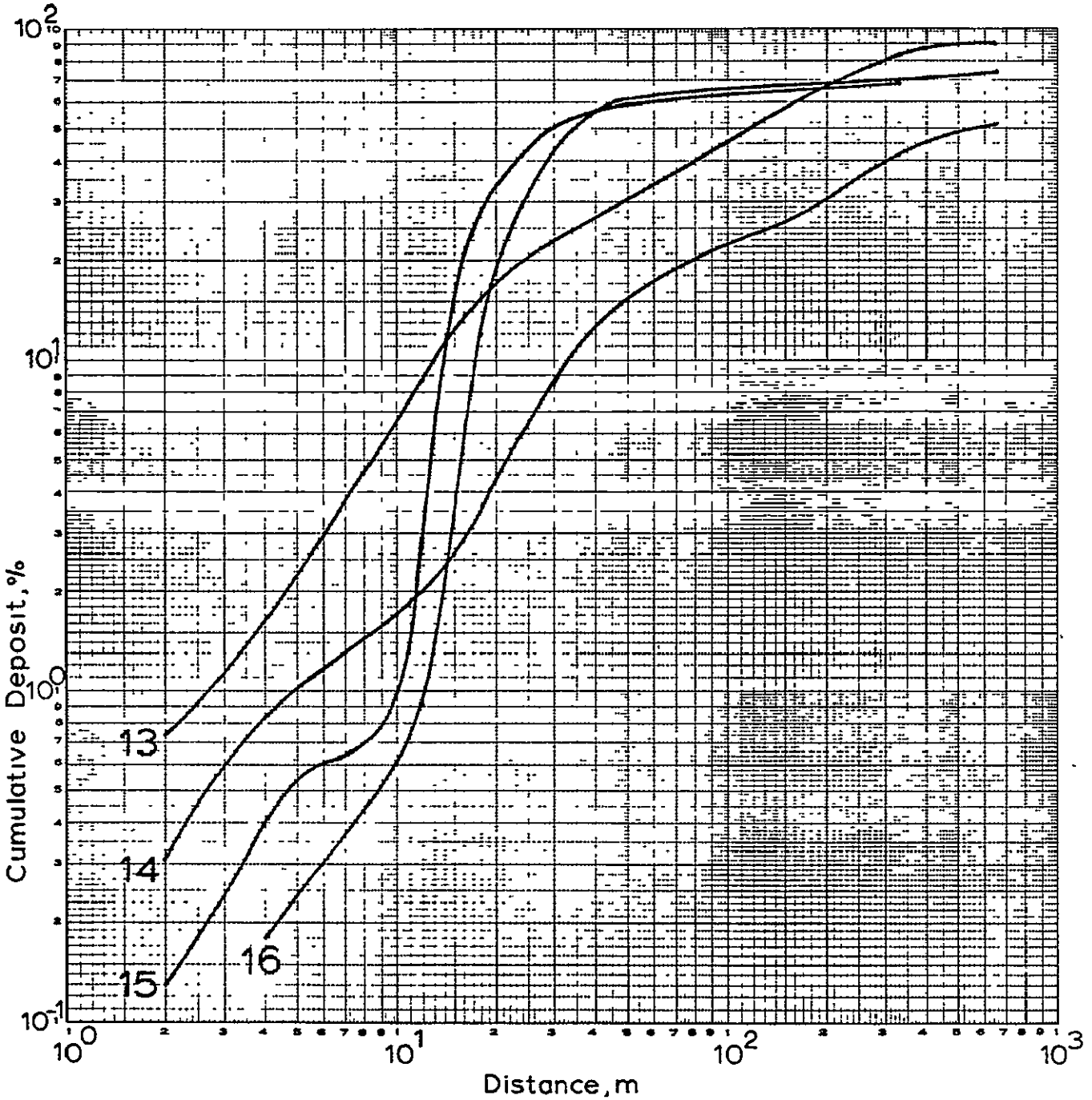

Fig. 1 (cont.)

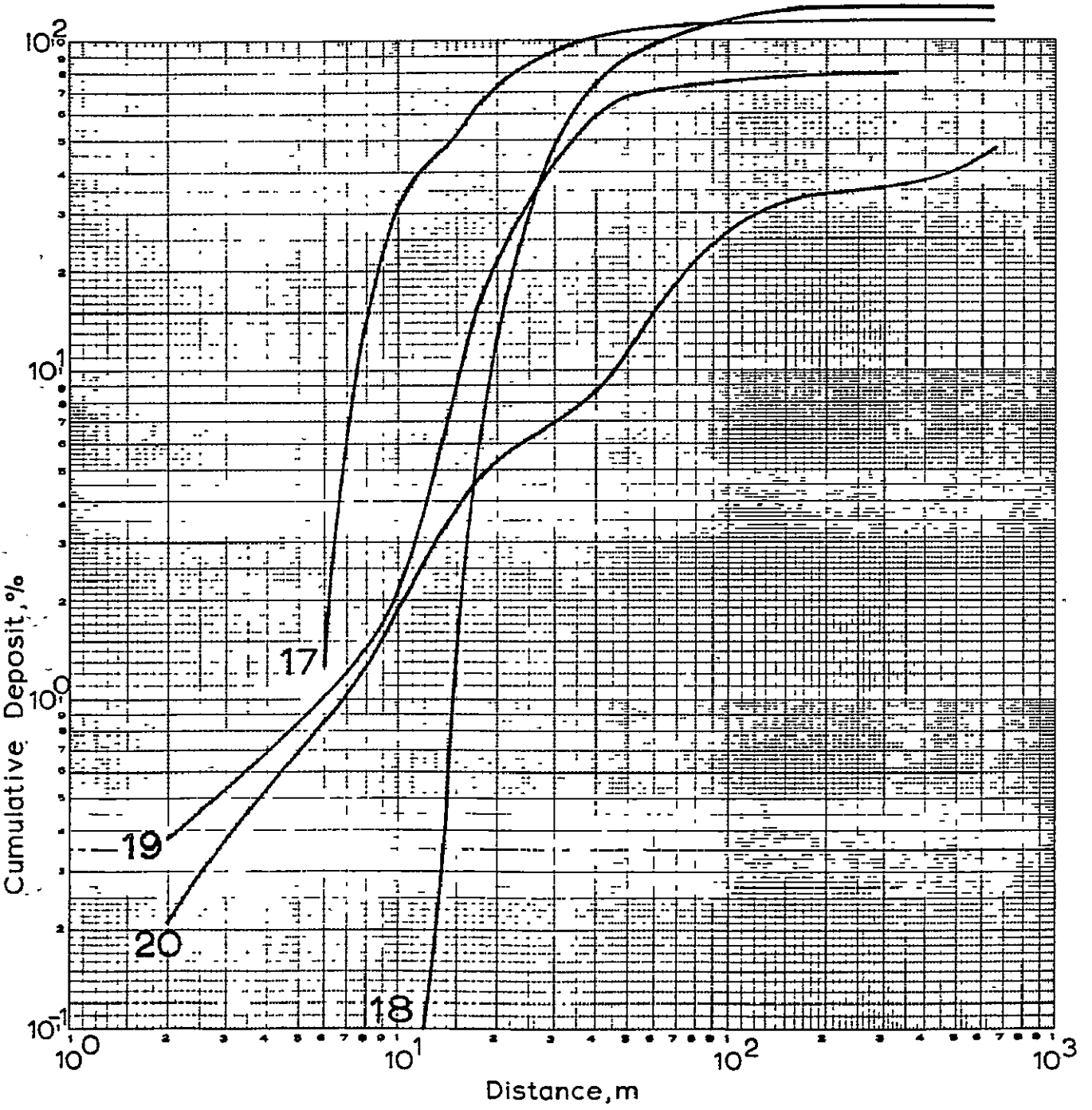

Fig. 1 (cont.)

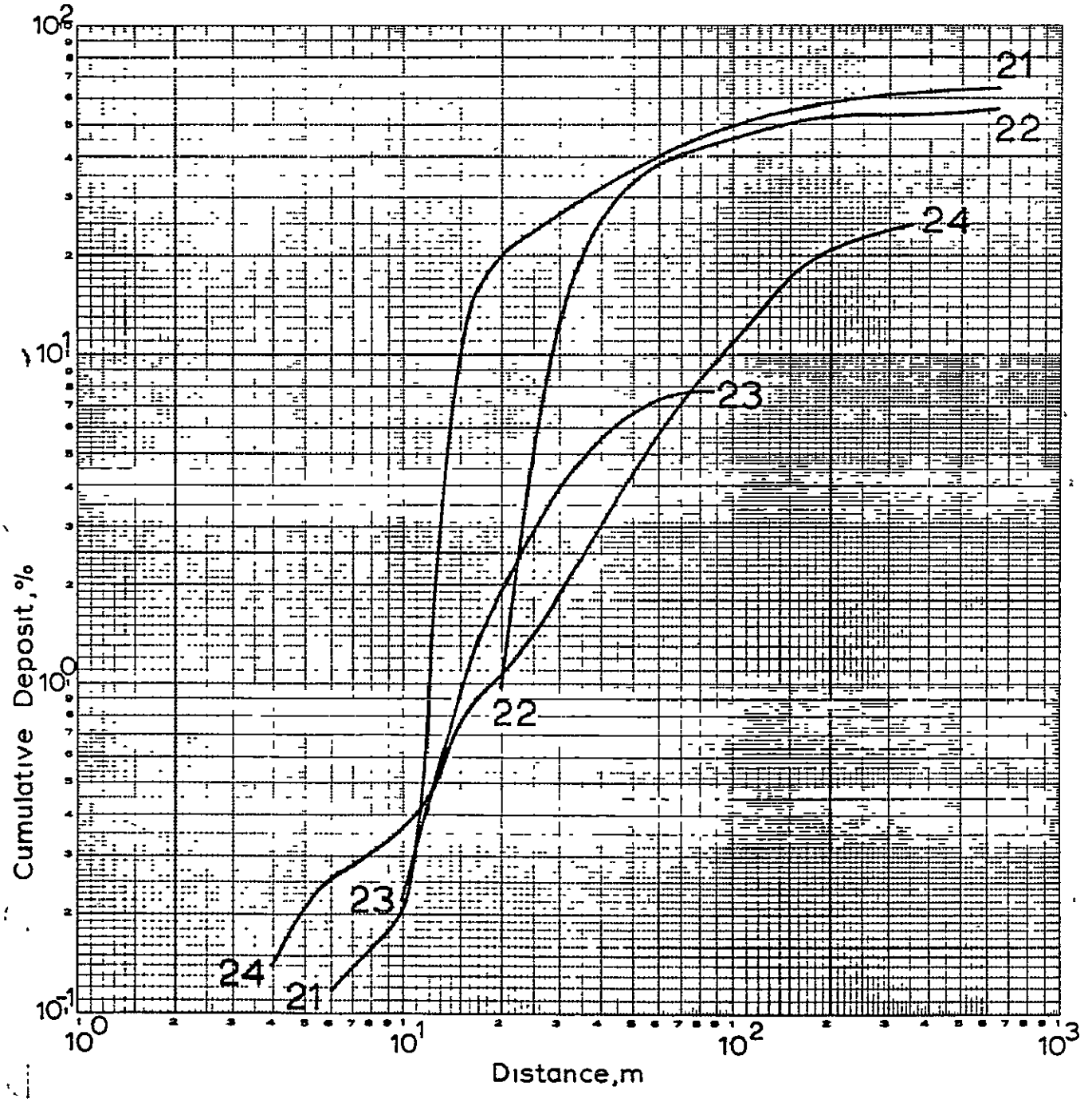

Fig. 1 (cont.)

Manganese concentrations obtained from the glass-fiber filters in the air samplers were expressed as ppm of manganese deposit per filter. These values are presented in Table 4 but are of questionable value since many of the upwind samples contained more manganese than the downwind samples. Evidently, improper handling of the filters resulted in sample contamination.

Droplet Size Measurement

The Kromekote cards used to collect droplet-size samples were processed by counting the number of droplet stains in 50μm size classes in six 1.27-cm x 1.27-cm (0.5-in. x 0.5-in.) areas on each card. The stains were magnified with a 20X microprojector while the counts were made. Spread factors were developed for each of the spray solutions used in the test by measuring stains on Kromekote paper from deposits of uniform droplets of known size. The spread factors were used to convert the droplet stain size classes to droplet-diameter size classes. The number of droplets in each size class was pooled for the 10-cm x 10-cm cards at each of the target locations. The length mean (average) droplet diameter (LMD) and the number of droplets per cm^2 were then determined at each target station for each test. These data are represented in Table 2.

WEATHER MEASUREMENTS

A weather tower and instrument trailer were located about 100 m northeast of the laser van along the edge of the NW-SE runway. Wind speed, azimuth, and elevation angle were measured at a height of 5 m. Ambient temperature was measured at heights of 10 m and 2.5 m. Relative humidity was also measured at the 2.5 m height. A Vector Vane system, (Meteorology Research, Inc.) provided an analog output for wind speed, azimuth, and elevation angle. Copper-constantan thermocouples housed in radiation shields were used for the ambient temperature measurements and a Model 2013 Relative Humidity system (Texas Electronics, Inc.) was used for the humidity measurements. Output signals from the weather instruments were appropriately scaled with precision potentiometers and recorded with a Model PD 2064 data acquisition system (Esterline Angus).

Recording and Data Reduction Procedures

The digital printer on the data acquisition system was turned on about 12-s before the aircraft would pass through the laser beam. It was operated in continuous mode, providing a record of each weather variable at 6-s intervals for about 3 min. After the 3-min period, the printer was operated manually to provide a printout every 15-s until all airborne spray would have passed beyond the last sampling station downwind from the flight path. The total sampling time for the weather data for each test ranged from 4 to 8 min, depending on the wind speed observed during the test.

One-min averages and test means were calculated from the printout data obtained for each test. In addition, the temperature lapse between the 10-m and 2.5-m heights, the deviation of the wind direction from the sample line, and the stability ratio (SR) were calculated from the data for each 1-min average and each test mean (Table 5). The SR is an indicator of air turbulence and has been related to spray drift in previous studies at the University of California. The SR is defined as follows:

Table 4. Airborne spray measurements from high-volume air samplers (ppm manganese sulfate/10-cm x 20-cm section of glass-fiber filter*).

Test no.**	Air sampler location with respect to flight path		
	100 m upwind	320 m downwind	640 m downwind
1	0.067	0.040	0.032
2	0.024	0.087	0.026
3	0.034	0.045	0.038
4	0.034	0.022	0.023
5	0.068	0.042	0.116
6	0.078	0.027	0.029
7	0.190	0.080	0.071
8	0.059	0.071	0.072
9	0.091	0.050	0.044
10	0.036	0.038	0.045
11	0.052	0.072	0.086
12	0.033	0.024	0.058
13	0.032	0.076	0.066
14	0.068	0.023	0.018
15	0.076	0.037	0.056
16	0.041	0.042	0.054
17	0.040	0.039	0.043
18	0.054	0.066	0.032
19	0.039	0.038	0.035
20	0.041	0.044	0.048
21	***	0.030	0.037
22	***	0.028	0.033
23	***	0.016	0.031
24	***	0.038	0.026

*Average for two air samples at 640 m downwind.

**See table 1, page A-4 for description of tests.

***Sample not obtained.

Table 5. Weather data for study of feasibility of measuring aerial spray with a laser Doppler velocimeter system (1-minute averages and test means)

Test no.*	Time, min	Air temperature at 2.5m, °C	Air temperature $T_{10m} - T_{2.5m}$,** °C	Relative humidity, %	Wind speed at 5m, m/s	Wind elevation angle, deg.	Wind deviation from sample line, deg.	Stability ratio
1	0 - 1	22.28	0.40	51.3	3.00	-2.7	-12.4	0.45
	1 - 2	22.27	0.39	54.5	3.22	2.3	- 9.1	0.37
	2 - 3	22.47	0.39	49.3	2.95	4.7	- 7.4	0.45
	3 - 4	22.61	0.28	49.6	2.89	-0.9	- 4.7	0.34
	4 - 5	22.56	0.40	47.7	2.88	-2.7	- 4.5	0.48
	5 - 6	22.64	0.40	49.0	3.76	-2.4	0.1	0.28
	Mean	22.47	0.38	50.3	3.12	-0.3	- 6.3	0.39
2	0 - 1	21.23	0.23	53.8	1.40	-0.4	-15.8	1.18
	1 - 2	21.28	0.14	54.5	1.58	-3.7	-16.5	0.56
	2 - 3	21.22	0.04	52.3	1.45	-1.0	-20.0	0.19
	3 - 4	21.16	0.14	48.2	1.39	0.4	-21.0	0.72
	4 - 5	21.22	0.07	53.2	1.37	-0.1	-18.2	0.37
	5 - 6	21.24	0.13	53.4	1.34	-0.7	-18.6	0.72
	6 - 7	21.21	0.13	55.9	1.96	-0.5	-16.6	0.34
	Mean	21.22	0.13	53.1	1.50	-0.9	-18.1	0.58
3	0 - 1	21.32	-0.76	31.7	3.97	-1.5	23.9	-0.48
	1 - 2	21.49	-0.88	31.2	4.74	-0.3	25.9	-0.39
	2 - 3	21.93	-0.81	33.4	5.51	4.9	- 0.8	-0.27
	3 - 4	21.60	-0.41	33.1	6.21	2.5	- 2.8	-0.11
	Mean	21.59	-0.72	32.4	5.11	1.4	11.6	-0.31
4	0 - 1	22.07	-0.45	26.1	6.36	0.9	-16.3	-0.11
	1 - 2	21.46	-0.03	26.4	4.19	-0.8	-21.1	-0.02
	2 - 3	21.82	-0.04	22.3	4.84	-1.4	-25.6	-0.02
	3 - 4	22.32	-0.16	25.5	3.75	3.7	-26.6	-0.11
	Mean	21.92	-0.17	25.1	4.78	0.6	-22.4	-0.07

See footnotes at end of table, page A-28.

continued

Table 5 (cont.)

Test no.*	Time, min	Air temperature at 2.5m, °C	Air temperature $T_{10m} - T_{2.5m}$,** °C	Relative humidity, %	Wind speed at 5m, m/s	Wind elevation angle, deg.	Wind deviation from sample line, deg.	Stability ratio
5	0 - 1	22.48	0.14	25.1	5.00	1.6	1.0	0.06
	1 - 2	22.19	0.01	26.8	4.70	0.3	-2.9	0.00
	2 - 3	22.10	0.09	27.5	5.39	-0.5	-5.6	0.03
	3 - 4	22.08	0.07	28.6	5.83	-1.2	-12.3	0.02
	Mean	22.21	0.08	27.0	5.23	0.1	-5.0	0.03
6	0 - 1	21.98	-0.29	28.8	4.97	-2.3	18.3	-0.12
	1 - 2	21.93	-0.03	29.5	4.19	-0.1	8.0	-0.02
	2 - 3	22.14	-0.04	30.7	3.79	0.0	5.9	-0.03
	3 - 4	22.04	0.00	30.6	3.80	-0.2	5.3	0.00
	Mean	22.02	-0.09	29.9	4.19	-0.7	9.4	-0.05
7	0 - 1	20.95	-0.04	28.1	2.33	-1.3	7.3	-0.07
	1 - 2	20.83	0.04	28.4	2.36	-1.6	9.8	0.07
	2 - 3	20.87	-0.07	27.4	2.30	-1.7	9.3	-0.13
	3 - 4	20.66	0.24	27.9	2.05	-0.9	12.8	0.57
	4 - 5	20.80	0.06	27.2	1.96	2.9	10.6	0.16
	5 - 6	20.77	-0.04	30.2	2.71	1.5	17.6	-0.05
	6 - 7	20.65	0.15	27.2	2.28	-0.2	17.2	0.29
	Mean	20.79	0.05	28.0	2.28	-0.2	12.1	0.12
8	0 - 1	19.63	0.06	33.4	1.14	-1.0	18.3	0.47
	1 - 2	19.60	0.11	31.0	1.32	-2.5	14.9	0.63
	2 - 3	19.65	-0.02	35.1	1.27	-2.8	10.4	-0.12
	3 - 4	19.63	0.25	32.9	1.79	-2.5	15.1	0.78
	4 - 5	19.65	0.10	32.2	1.41	-1.8	16.1	0.50
	5 - 6	19.80	0.50	33.1	1.30	-2.0	15.6	0.30
	6 - 7	19.65	-0.05	31.9	1.79	-1.5	12.9	-0.16
	7 - 8	19.80	-0.05	34.4	1.16	-1.9	14.7	-0.37
	Mean	19.68	0.05	33.0	1.40	-3.0	14.7	0.26

See footnotes at end of table, page A-28.

continued

Table 5 (cont.)

Test no.*	Time, min	Air temperature at 2.5m, °C	Air temperature $T_{10m} - T_{2.5m}$,** °C	Relative humidity, %	Wind Speed at 5m, m/s	Wind Elevation angle, deg.	Wind Deviation from sample line, deg.	Stability ratio
9	0 - 1	26.08	-0.65	22.2	2.03	-15.3	-38.8	-1.58
	1 - 2	25.91	-0.66	22.2	2.41	- 7.4	-52.6	-1.14
	2 - 3	25.89	-0.73	23.7	2.45	- 5.1	-57.0	-1.22
	3 - 4	26.06	-0.76	22.0	2.49	- 8.1	-32.9	-1.23
	4 - 5	26.47	-0.74	24.4	2.27	12.8	-31.4	-1.44
	5 - 6	25.83	-0.68	21.1	3.64	- 8.0	-49.9	-0.51
	6 - 7	25.45	-0.72	25.5	3.56	-11.7	-14.3	-0.57
	7 - 8	25.37	-0.40	22.2	2.96	-16.2	-30.7	-0.45
	Mean	25.88	-0.67	22.9	2.73	- 7.4	-38.4	-1.02
10	0 - 1	26.19	-0.73	24.7	1.74	- 8.8	63.7	-2.40
	1 - 2	26.62	-0.79	24.7	2.18	- 4.9	35.9	-1.66
	2 - 3	26.92	-1.08	24.9	2.58	- 9.0	-23.0	-1.63
	3 - 4	26.75	-0.80	24.6	2.35	0.3	-66.1	-1.45
	4 - 5	27.75	-2.15	24.3	2.66	10.8	19.7	-3.04
	5 - 6	26.90	-1.50	23.9	3.69	0.2	3.6	-1.10
	6 - 7	25.75	-0.75	24.4	3.89	2.0	-13.0	-0.50
	Mean	26.70	-1.11	24.5	2.73	- 1.4	3.0	-1.68
11	0 - 1	25.42	-0.46	24.4	2.28	- 5.7	8.6	-0.88
	1 - 2	25.80	-0.62	23.0	2.32	8.8	16.9	-1.16
	2 - 3	25.73	-0.49	20.5	2.51	- 7.5	37.0	-0.78
	3 - 4	26.38	-0.68	23.6	2.37	- 4.1	54.3	-1.21
	4 - 5	26.78	-0.78	23.4	2.17	6.5	27.2	-1.66
	5 - 6	26.80	-0.56	24.2	2.30	- 5.4	- 3.8	-1.06
	Mean	26.15	-0.60	23.2	2.31	- 1.2	23.4	-1.13

See footnotes at end of table, page A-28.

continued

Table 5 (cont.)

Test no.*	Time, min	Air temperature at 2.5m, °C	Air temperature $T_{10m} - T_{2.5m}$,** °C	Relative humidity, %	Wind Speed at 5m, m/s	Wind Elevation angle, deg.	Wind Deviation from sample line, deg.	Stability ratio
12	0 - 1	25.99	-0.66	23.1	2.93	- 0.9	19.1	-0.77
	1 - 2	25.74	-0.39	23.3	2.82	- 5.3	30.6	-0.49
	2 - 3	25.85	-0.46	24.7	2.83	- 4.2	23.9	-0.57
	3 - 4	25.71	-0.40	24.9	2.80	- 5.1	39.1	-0.51
	4 - 5	26.17	-0.64	27.6	3.33	- 0.9	35.6	-0.58
	5 - 6	26.05	-0.65	26.9	2.75	- 7.2	20.8	-0.86
	6 - 7	26.35	-0.65	27.2	3.33	10.7	9.7	-0.59
	Mean	25.98	-0.55	25.4	2.97	- 1.8	25.5	-0.62
13	0 - 1	18.87	-0.47	74.6	3.90	2.8	-21.4	-0.31
	1 - 2	19.16	-0.39	76.6	4.02	- 2.1	- 9.9	-0.24
	2 - 3	18.83	-0.03	74.2	3.69	- 2.8	-13.0	-0.02
	3 - 4	19.10	-0.17	74.8	3.78	0.0	- 4.9	-0.12
	Mean	18.99	-0.27	75.0	3.85	- 0.5	-12.3	-0.18
14	0 - 1	21.01	-0.50	70.1	4.20	- 1.7	-30.6	-0.28
	1 - 2	21.20	-0.33	67.1	4.59	2.7	-12.8	-0.16
	2 - 3	21.26	-0.65	69.3	4.14	3.0	-35.1	-0.38
	3 - 4	21.44	-0.60	66.8	4.49	0.9	-23.6	-0.30
	4 - 5	20.87	-0.50	65.0	5.08	- 2.1	-24.3	-0.19
	Mean	21.16	-0.52	67.7	4.50	0.6	-25.3	-0.26
15	0 - 1	23.86	-0.55	57.8	5.63	- 1.0	-22.2	-0.17
	1 - 2	24.47	-0.72	58.0	5.15	3.4	-10.9	-0.27
	2 - 3	23.76	-0.88	56.9	5.09	- 3.6	-20.0	-0.34
	3 - 4	23.38	-0.63	55.9	4.22	- 1.5	-10.8	-0.35
	4 - 5	23.45	-0.60	71.1	4.38	- 1.6	-31.7	-0.31
	Mean	23.78	-0.68	60.0	4.89	- 0.9	19.1	-0.28

See footnotes at end of table, page A-28.

continued

Table 5 (cont.)

Test no.*	Time, min	Air temperature at 2.5m, °C	Air temperature $T_{10m} - T_{2.5m}$,** °C	Relative humidity, %	Wind Speed at 5m, m/s	Wind Elevation angle, deg.	Wind Deviation from sample line, deg.	Stability ratio
16	0 - 1	24.74	-0.32	54.2	4.13	3.3	- 5.3	-0.19
	1 - 2	24.61	-0.58	49.9	4.11	-2.1	1.6	-0.34
	2 - 3	23.93	-0.31	51.0	4.25	-3.7	-19.1	-0.17
	3 - 4	24.72	-0.48	49.8	4.11	-3.0	-43.8	-0.28
	4 - 5	24.87	-0.54	52.1	5.42	-3.1	-18.8	-0.18
	Mean	24.57	-0.45	51.4	4.40	-1.7	-17.1	-0.23
17	0 - 1	14.30	0.20	86.5	3.47	-6.4	14.6	0.17
	1 - 2	14.35	0.16	86.8	3.46	-6.3	15.8	0.13
	2 - 3	14.36	0.14	83.5	3.53	-5.1	13.3	0.11
	3 - 4	14.48	0.10	86.0	3.82	-4.7	3.4	0.07
	4 - 5	14.37	0.00	84.4	4.31	1.5	4.1	0.00
	5 - 6	14.60	0.00	82.4	4.38	-2.1	5.7	0.00
	Mean	14.41	0.10	85.0	3.83	-3.9	9.5	0.07
18	0 - 1	15.52	-0.20	77.5	4.01	-2.9	5.2	-0.12
	1 - 2	15.45	-0.15	78.9	4.01	-4.3	2.8	-0.09
	2 - 3	15.50	-0.10	79.5	4.00	-1.6	0.6	-0.06
	3 - 4	15.78	-0.28	81.5	3.67	-2.5	1.5	-0.21
	4 - 5	15.78	-0.14	75.1	4.19	-3.3	- 3.5	-0.08
	Mean	15.61	-0.17	78.5	3.98	-2.9	1.3	-0.11
19	0 - 1	17.45	-0.37	70.1	5.53	-3.8	-25.3	-0.12
	1 - 2	17.38	-0.23	72.0	5.49	-1.8	-25.5	-0.08
	2 - 3	17.36	-0.28	70.2	5.66	-4.3	-27.0	-0.09
	3 - 4	17.53	-0.30	68.3	4.69	3.4	-27.9	-0.14
	4 - 5	17.67	-0.40	71.1	5.54	-1.6	-24.0	-0.13
	Mean	17.48	-0.32	70.3	5.38	-3.0	-25.9	-0.11

See footnotes at end of table, A-28.

continued

Table 5 (cont.)

Test no.*	Time, min	Air temperature at 2.5m, °C	Air temperature $T_{10m} - T_{2.5m}$,** °C	Relative humidity, %	Wind speed at 5m, m/s	Wind elevation angle, deg.	Wind deviation from sample line, deg.	Stability ratio
20	0 - 1	20.67	-0.58	63.4	4.48	0.1	-18.6	-0.25
	1 - 2	20.77	-0.53	63.8	5.25	-2.7	- 4.9	-0.19
	2 - 3	20.90	-0.58	64.0	5.46	2.1	- 6.6	-0.19
	3 - 4	20.83	-0.60	66.6	5.95	-1.4	1.1	-0.17
	4 - 5	20.75	-0.45	63.6	5.45	-0.2	-12.5	-0.15
	Mean	20.78	-0.55	64.3	5.39	-0.4	- 8.3	-0.19
21	0 - 1	27.98	-0.98	35.5	6.48	0.4	14.3	-0.23
	1 - 2	27.87	-0.81	36.2	6.46	-1.0	21.9	-0.19
	2 - 3	28.13	-0.95	35.4	5.96	-0.4	13.2	-0.27
	3 - 4	27.86	-0.76	37.2	6.19	-0.9	- 4.7	-0.20
	Mean	27.96	-0.88	36.1	6.27	-0.5	11.2	-0.22
22	0 - 1	26.94	-0.80	37.8	5.61	1.6	29.5	-0.25
	1 - 2	26.76	-0.61	38.8	6.39	-2.3	25.2	-0.15
	2 - 3	26.72	-0.82	37.4	6.10	-1.2	21.5	-0.22
	3 - 4	27.05	-0.77	38.0	6.23	-1.3	22.4	-0.20
	Mean	26.87	-0.75	38.0	6.08	-0.8	24.7	-0.20
23	0 - 1	25.92	-0.58	41.5	5.95	-2.4	19.0	-0.16
	1 - 2	26.27	-0.77	41.3	4.77	-1.0	8.9	-0.34
	2 - 3	26.47	-0.82	40.7	4.63	1.6	17.6	-0.38
	3 - 4	26.18	-0.60	42.9	4.81	-1.4	7.6	-0.26
	4 - 5	26.30	-0.57	39.5	4.43	-5.6	3.7	-0.29
	Mean	26.23	-0.67	41.2	4.91	-1.8	11.4	-0.28

See footnotes at end of table, page A-28.

continued

Table 5 (cont.)

Test no.*	Time, min	Air temperature at 2.5m, °C	Air temperature $T_{10m} - T_{2.5m}$,** °C	Relative humidity, %	Wind Speed at 5m, m/s	Wind Elevation angle, deg.	Wind Deviation from sample line, deg.	Stability ratio
24	0 - 1	25.36	-0.47	44.0	4.90	-0.4	15.2	-0.20
	1 - 2	25.16	-0.31	43.6	4.96	-4.6	21.0	-0.13
	2 - 3	25.26	-0.52	43.8	4.81	-2.6	28.5	-0.22
	3 - 4	25.40	-0.64	42.9	4.92	-2.1	24.7	-0.26
	Mean	25.30	-0.49	43.6	4.90	-2.4	22.3	-0.20
Dummy	0 - 1	19.91	-0.55	65.6	4.54	1.1	3.5	-0.27
	1 - 2	19.83	-0.62	66.6	5.43	-2.4	- 3.8	-0.21
	2 - 3	19.49	-0.39	68.9	4.39	-2.2	8.4	-0.20
	3 - 4	19.87	-0.62	66.4	5.19	-3.1	12.6	-0.23
	4 - 5	19.98	-0.58	65.1	5.19	4.0	- 8.4	-0.22
	Mean	19.82	-0.55	66.5	4.95	-0.5	2.4	-0.22

* See table 1, page A-3 for description of tests.

** T_{10m} refers to temperature at height of 10m above ground.

$T_{2.5m}$ refers to temperature at height of 2.5m above ground.

$$SR = \frac{T_{10m} - T_{2.5m}}{U_2} \times 10^5,$$

where T_{10m} and $T_{2.5m}$ are the ambient temperatures at 10 m and 2.5 m, and U is the wind speed measured at 5 m in cm/s. Positive values of SR greater than 0.1 indicate stable air conditions, which result in little vertical air mixing; negative values (less than -0.1) indicate unstable air conditions, which result in a larger amount of vertical mixing; and values between 0.1 and -0.1 indicate neutral air conditions.

Appendix B

AERIAL SPRAY CROSS-SECTION PLOTS MEASURED BY LASER DOPPLER VELOCIMETER SYSTEM

The aerial spray cross-section plots are presented in this section for runs 9, 10, 14, 15, 18, 19, 20 and the dummy run (no spray release). The symbols on the ISUM plots follow the convention discussed earlier (Table 3) and each plot is labeled on the top showing the test number, spray material, spray rate, aircraft altitude, and time (in seconds) after aircraft passage. The aerial spray cross-section plots illustrate the general downward and lateral motion of the spray cloud discussed in more detail in Section 4.

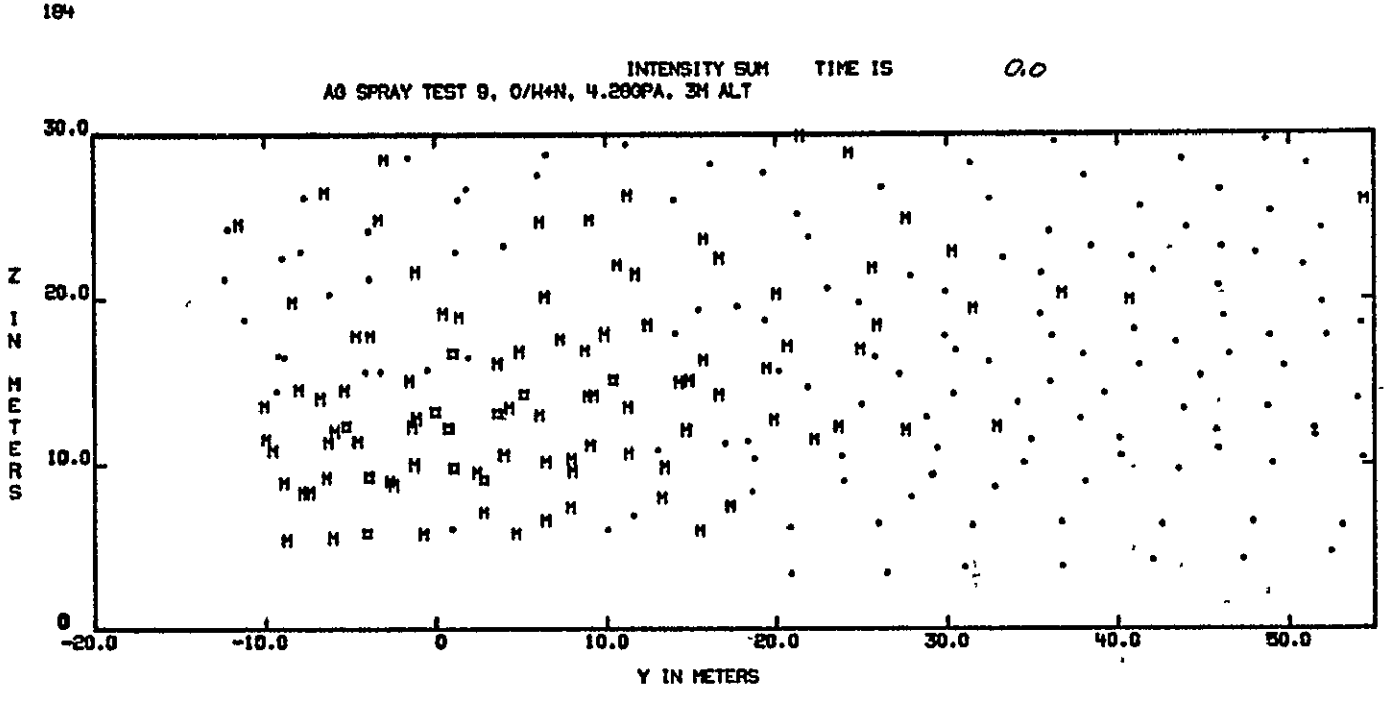
184
INTENSITY SUM TIME IS 0.0
AG SPRAY TEST 9, O/H4N, 4.280PA, 3M ALT
30.0
20.0
10.0
0
Z IN METERS
-20.0
-10.0
0
10.0
20.0
30.0
40.0
50.0
Y IN METERS

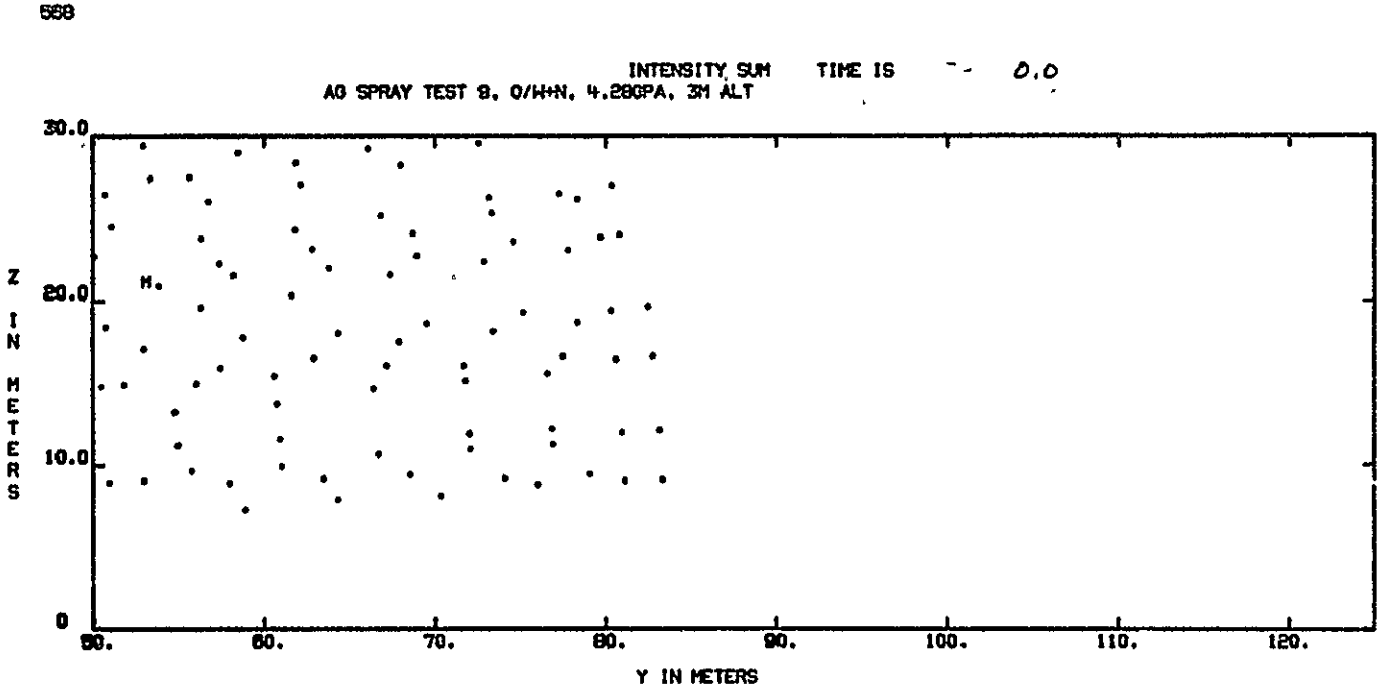
568
INTENSITY SUM TIME IS 0.0
AG SPRAY TEST 8, O/H+N, 4.28GPA, 3M ALT
30.0
20.0
10.0
0
Z IN METERS
H.
50.
60.
70.
80.
90.
100.
110.
120.
Y IN METERS

REPRODUCIBILITY OF THE
ORIGINAL PAGE IS POOR

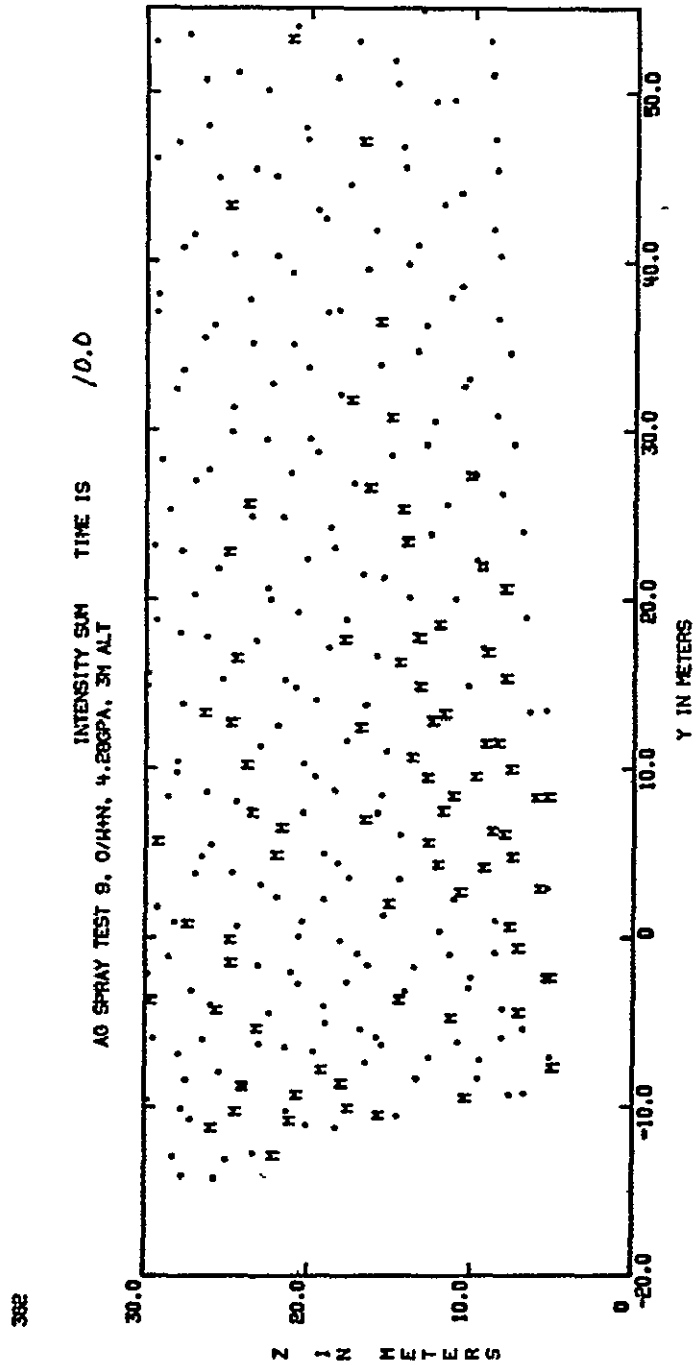

REPRODUCIBILITY OF THE
ORIGINAL PAGE IS POOR

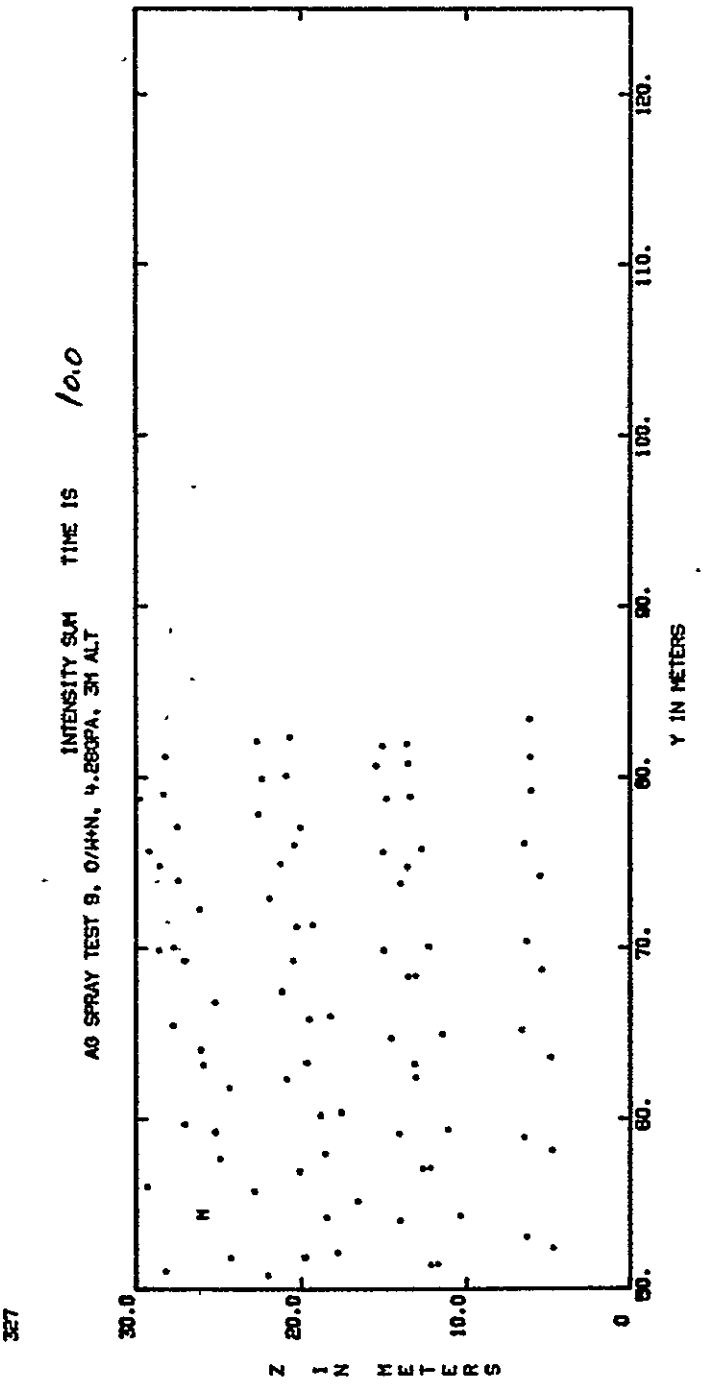

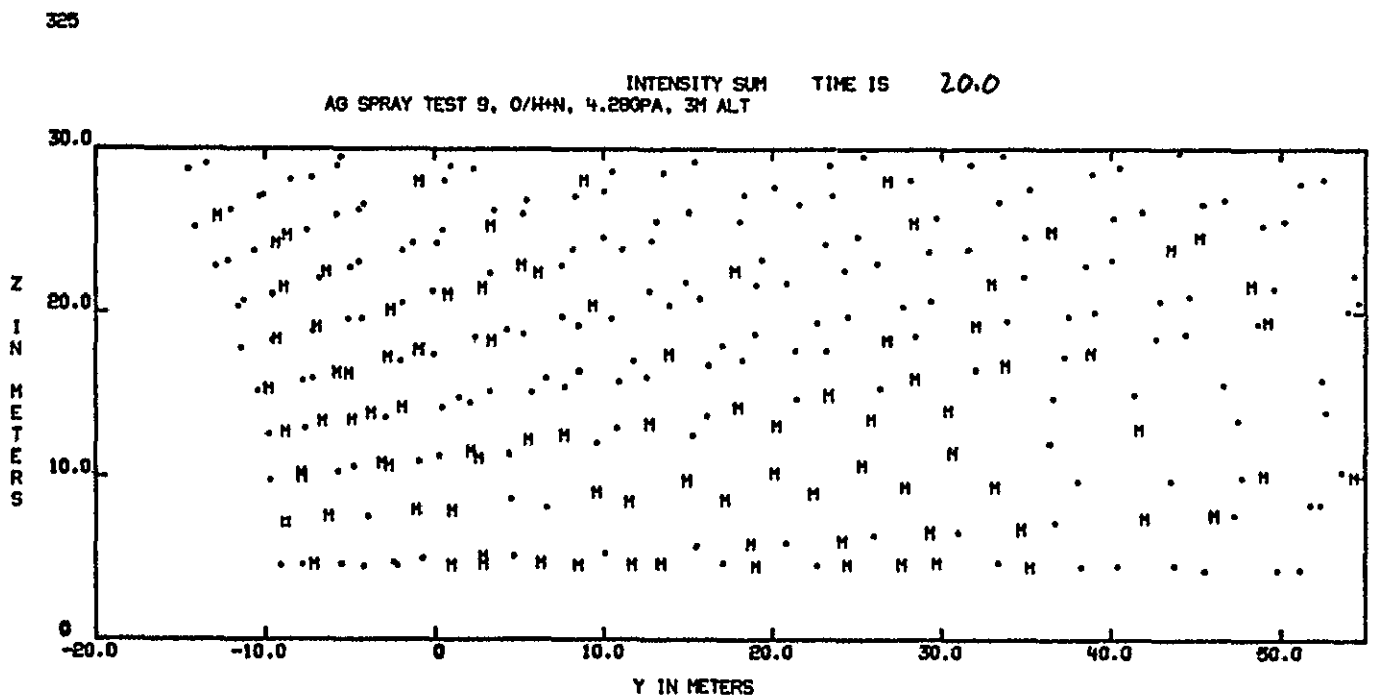
325
INTENSITY SUM TIME IS 20.0
AG SPRAY TEST 9, O/H+N, 4.28OPA, 3M ALT
30.0
20.0
10.0
0
Z IN METERS
-20.0
-10.0
0
10.0
20.0
30.0
40.0
50.0
Y IN METERS

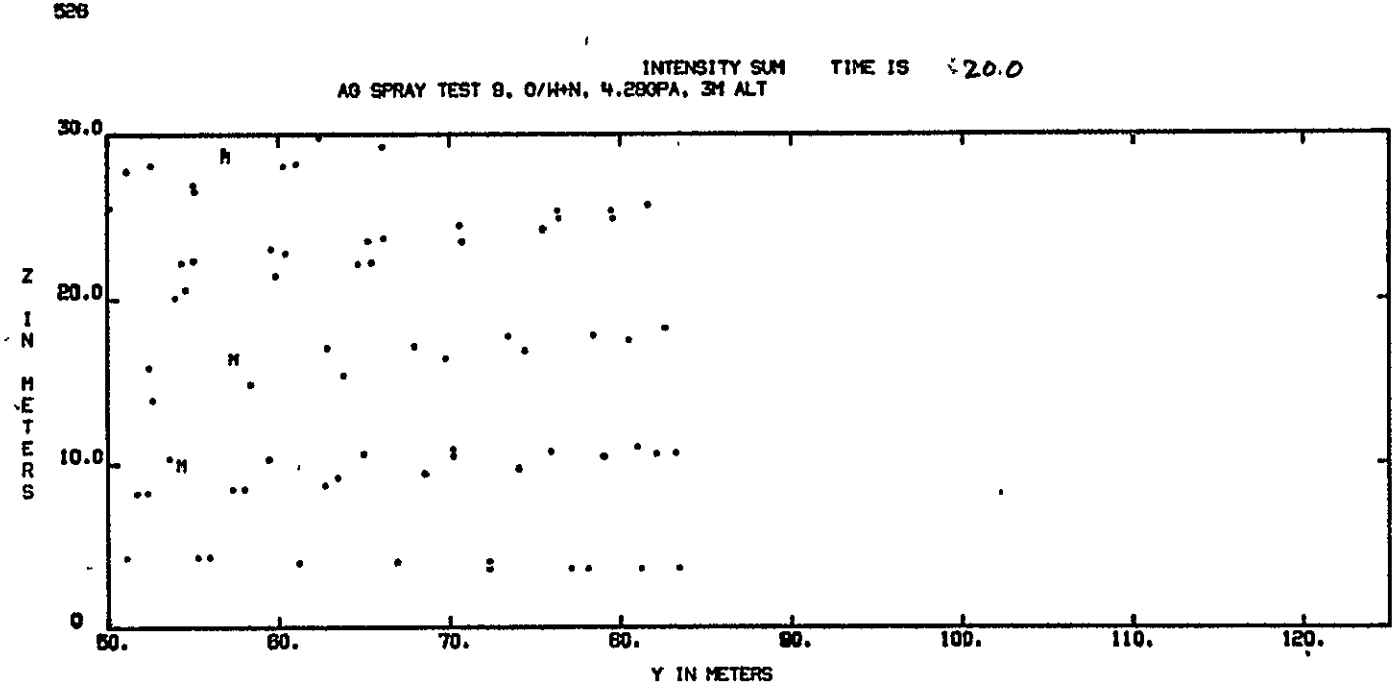
528
INTENSITY SUM TIME IS 20.0
AG SPRAY TEST 9, O/H+N, 4.280PA, 3M ALT
30.0
20.0
10.0
0
Z IN METERS
50.
60.
70.
80.
90.
100.
110.
120.
Y IN METERS

REPRODUCIBILITY OF THE
ORIGINAL PAGE IS POOR

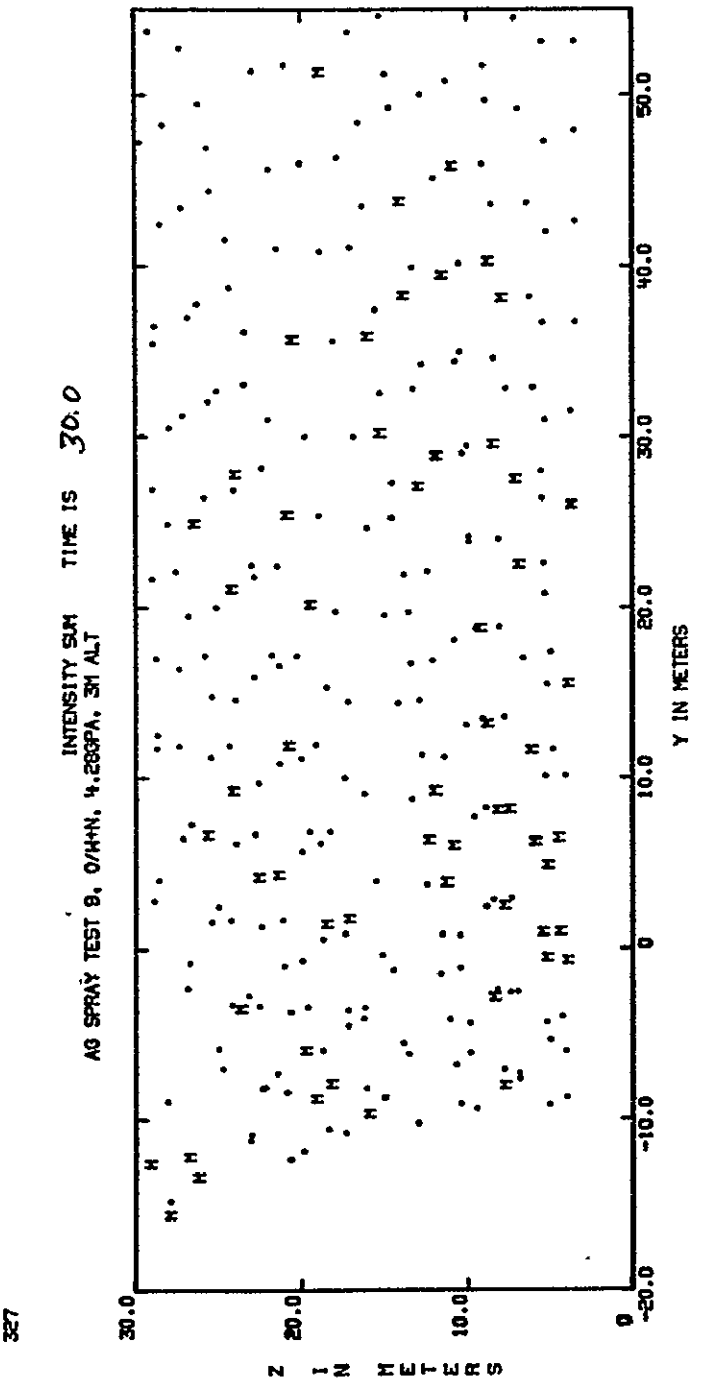

REPRODUCIBILITY OF THE
ORIGINAL PAGE IS POOR

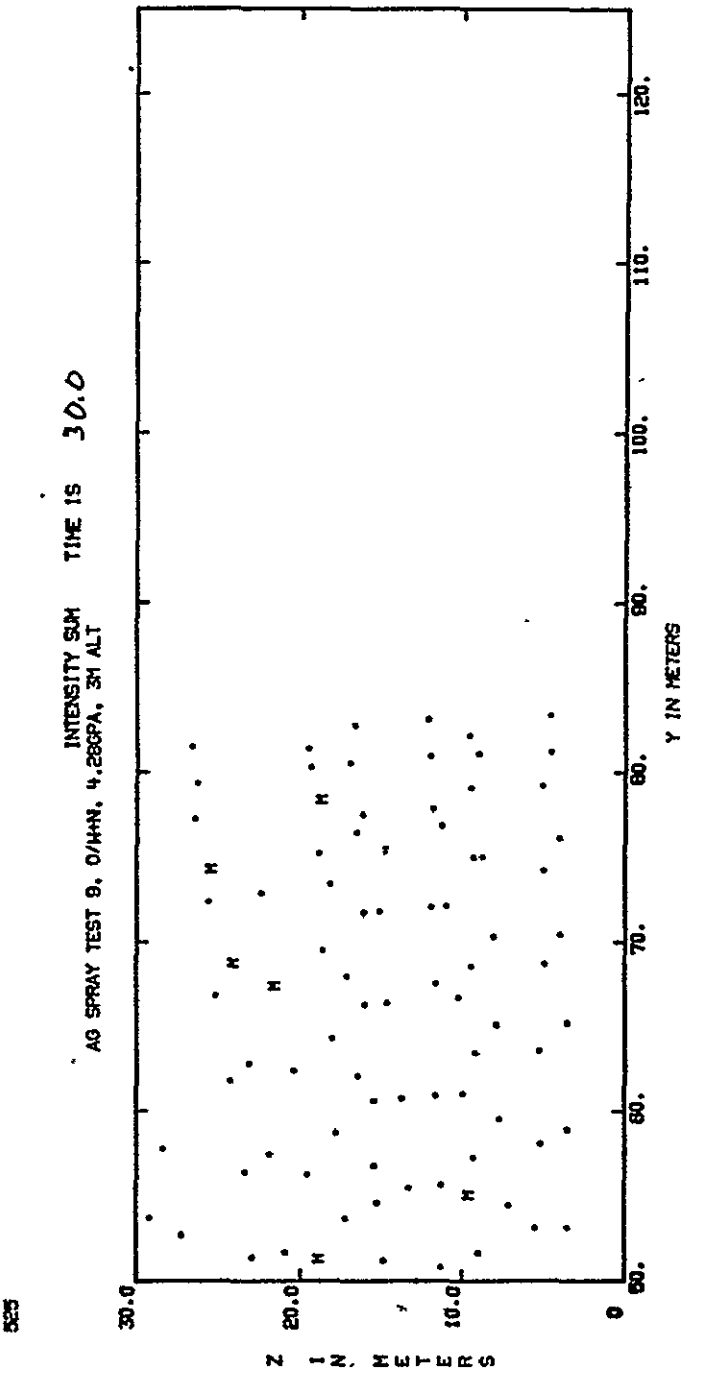

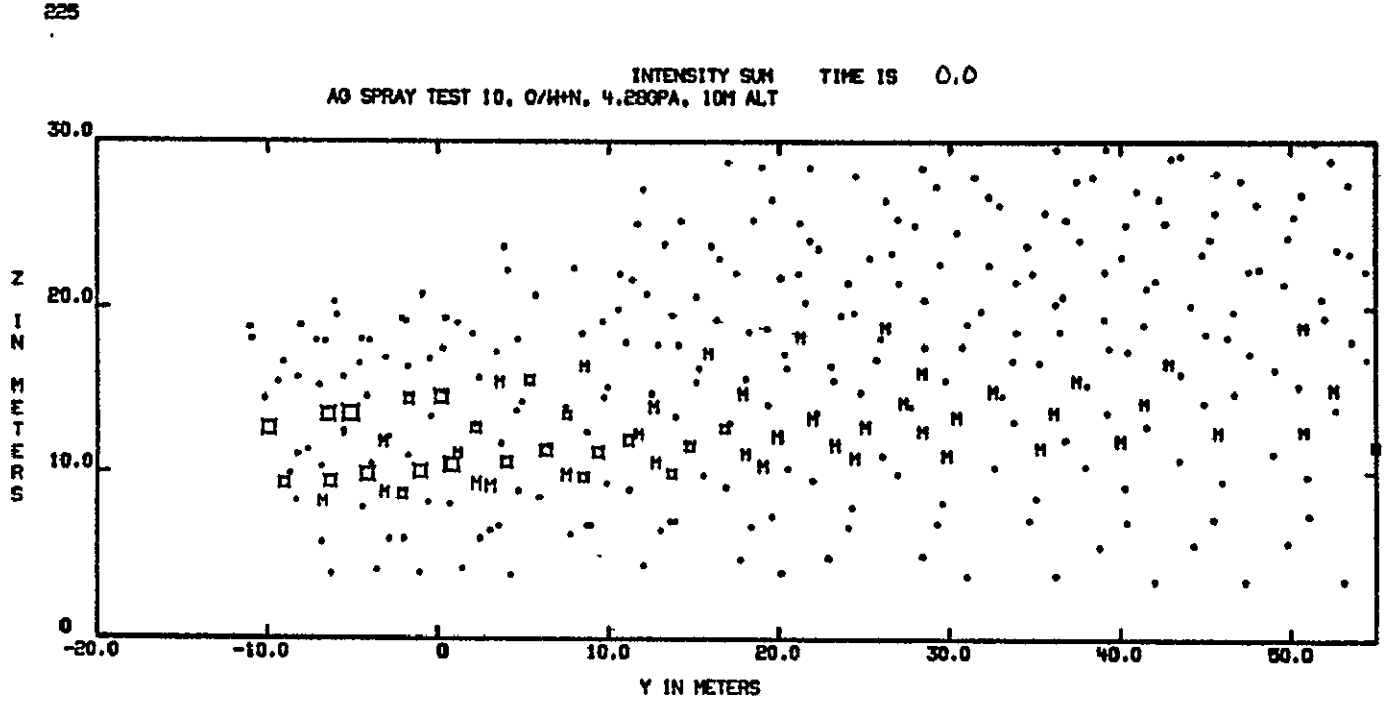
225
INTENSITY SUM TIME IS 0.0
AG SPRAY TEST 10, O/H+N, 4.280PA, 10M ALT
30.0
20.0
10.0
0
Z IN METERS
-20.0
-10.0
0
10.0
20.0
30.0
40.0
50.0
Y IN METERS

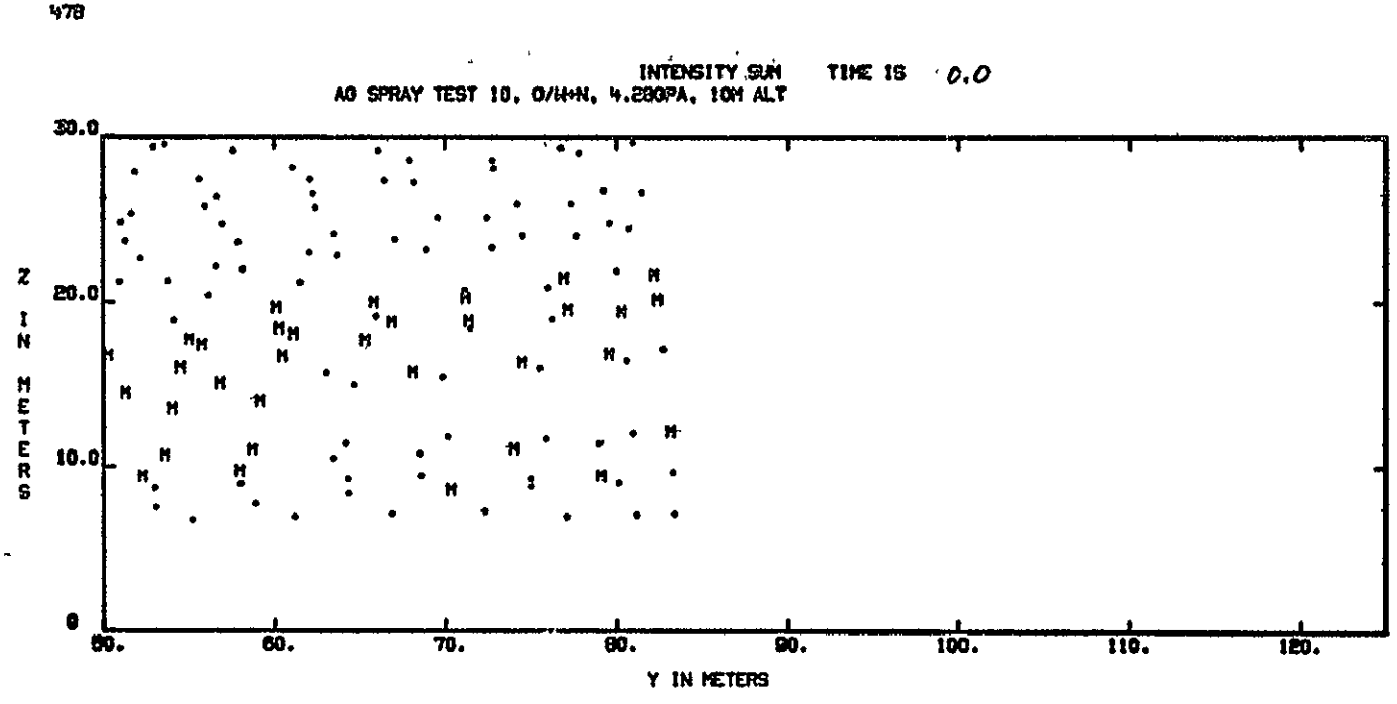
478
INTENSITY SUN TIME IS 0.0
AG SPRAY TEST 10, O/H+N, 4.200PA, 10M ALT
30.0
20.0
10.0
0
Z IN METERS
50.
60.
70.
80.
90.
100.
110.
120.
Y IN METERS

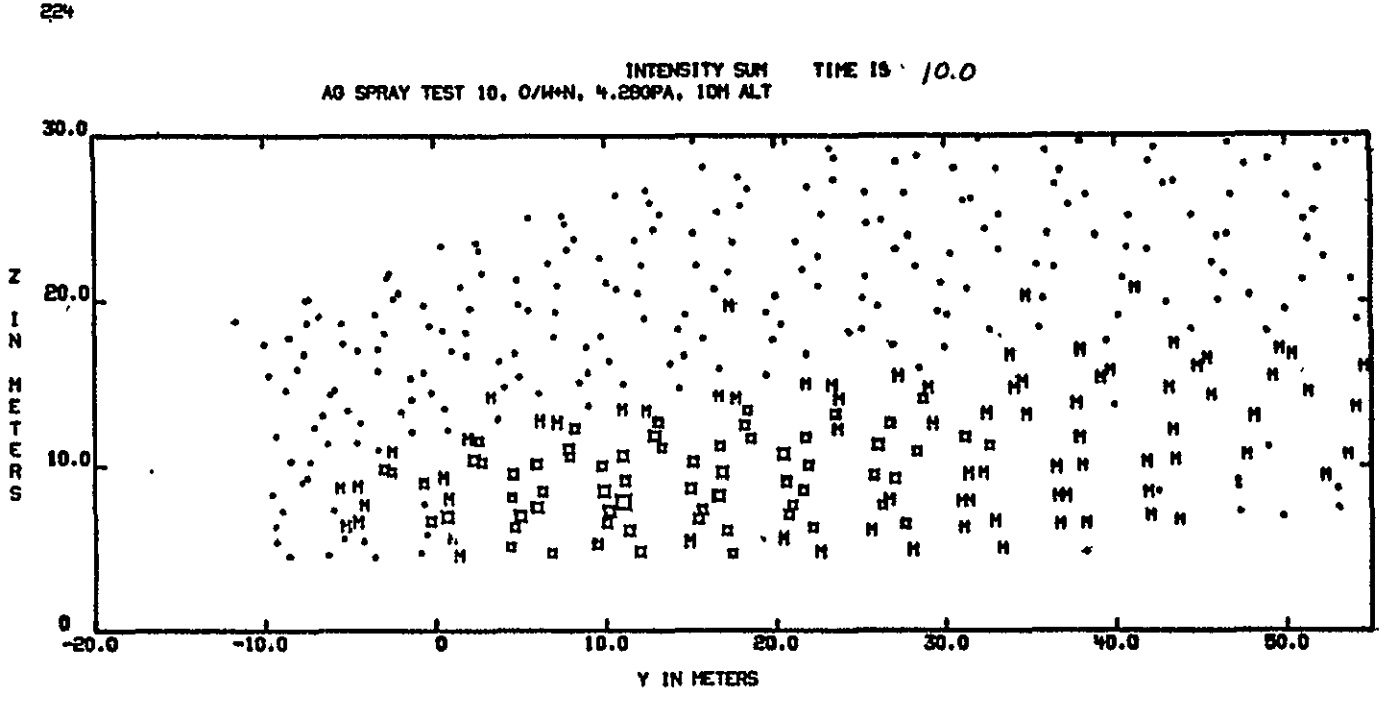
224
INTENSITY SUM TIME IS 10.0
AG SPRAY TEST 10, O/W+N, 4.280PA, 10M ALT
30.0
20.0
10.0
0
Z IN METERS
-20.0
-10.0
0
10.0
20.0
30.0
40.0
50.0
Y IN METERS

REPRODUCIBILITY OF THE
ORIGINAL PAGE IS POOR

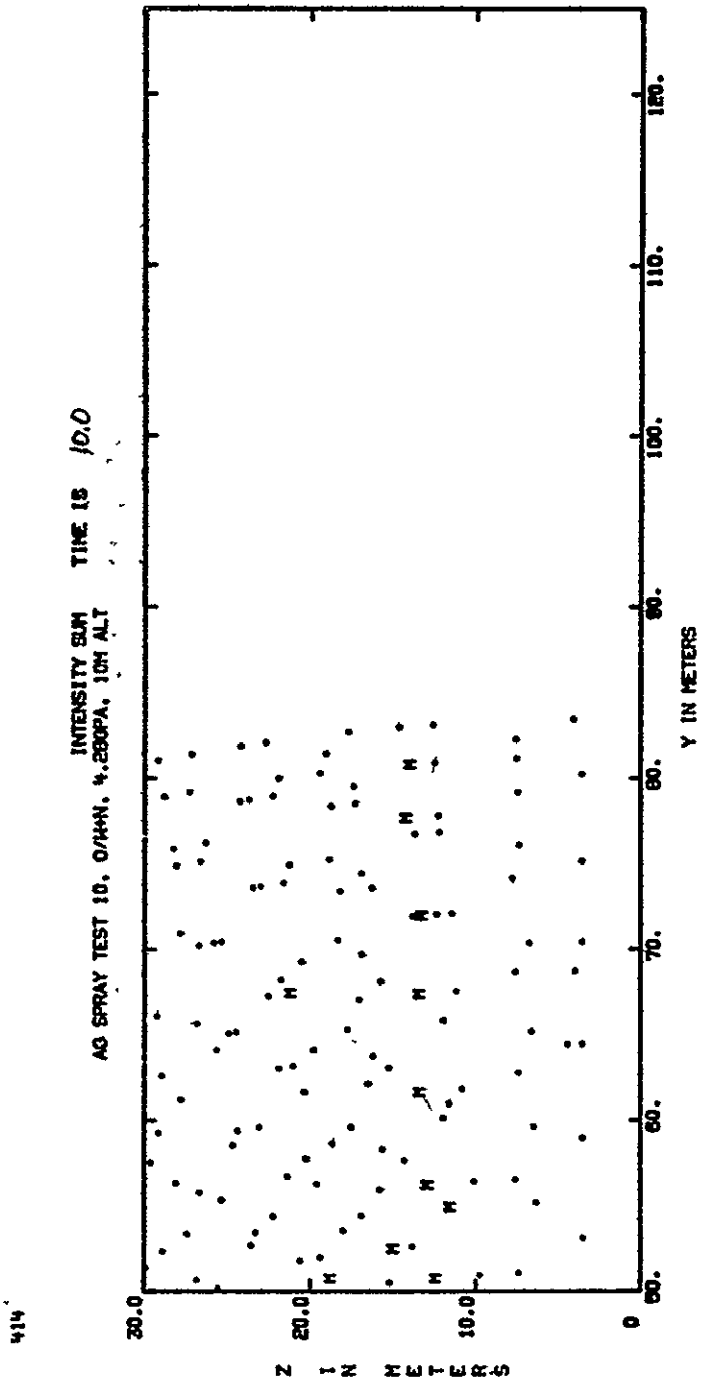

207

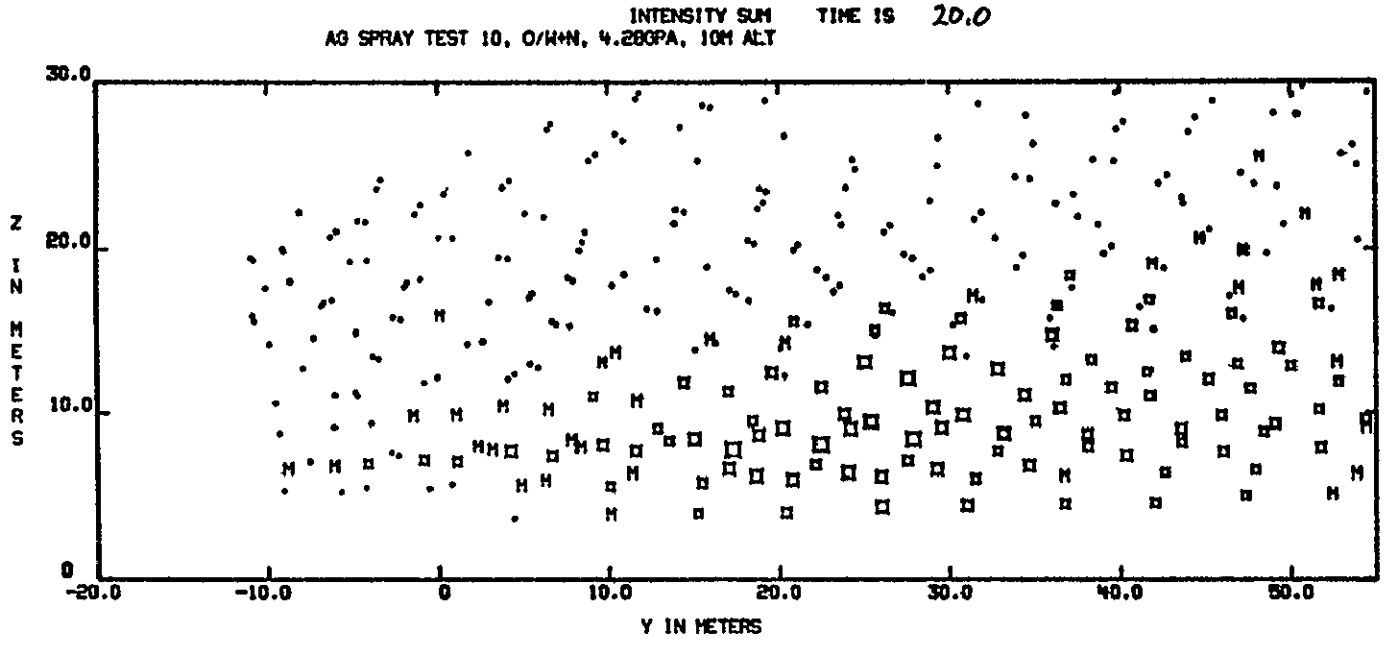
INTENSITY SUM TIME IS 20.0
AG SPRAY TEST 10, O/W+N, 4.280PA, 10M ALT
30.0
20.0
10.0
0
Z IN METERS
-20.0
-10.0
0
10.0
20.0
30.0
40.0
50.0
Y IN METERS

REPRODUCIBILITY OF THE
ORIGINAL PAGE IS POOR

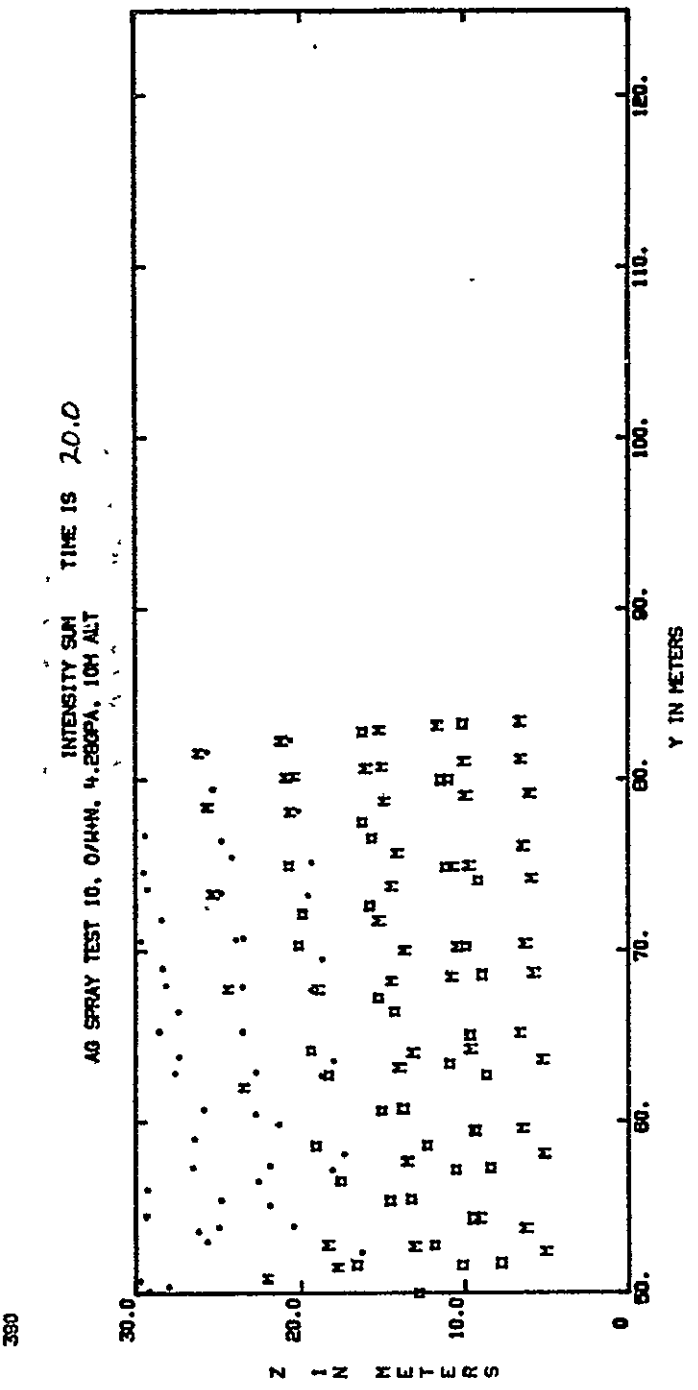

193

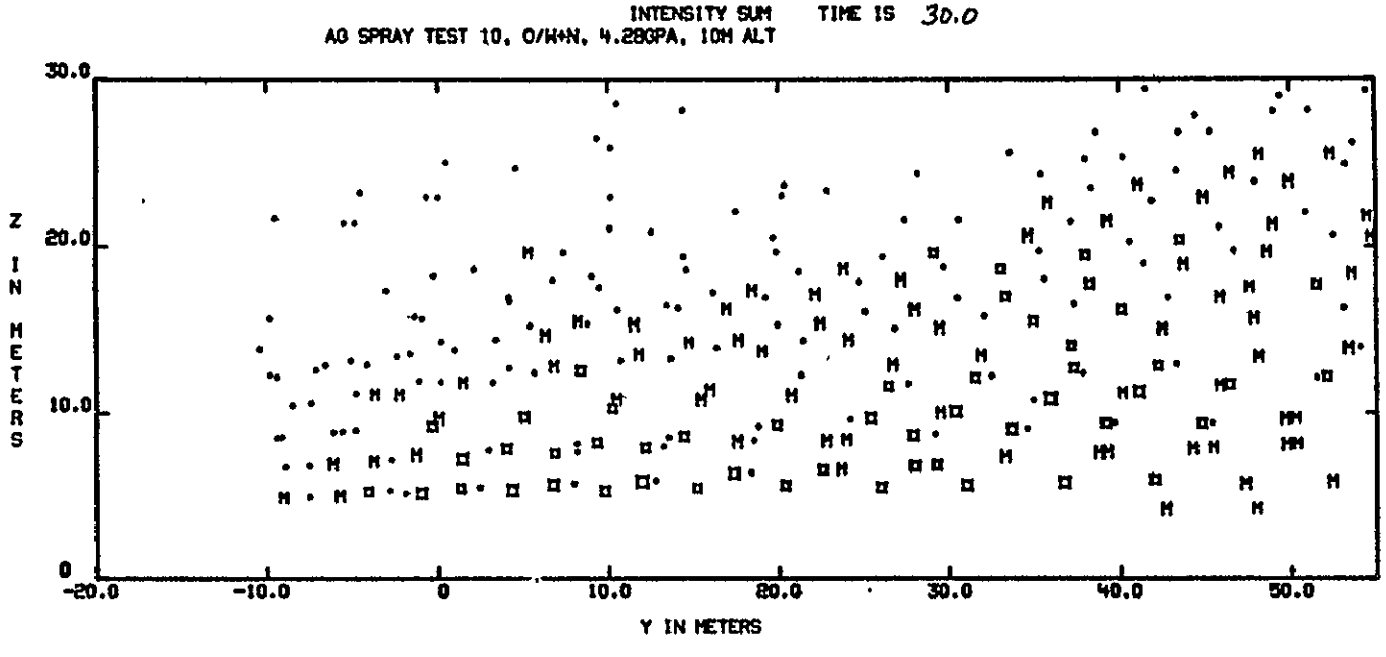
INTENSITY SUM TIME IS 30.0
AG SPRAY TEST 10, O/W+N, 4.28GPA, 10M ALT
30.0
20.0
10.0
0
Z IN METERS
-20.0
-10.0
0
10.0
20.0
30.0
40.0
50.0
Y IN METERS

REPRODUCIBILITY OF THE
ORIGINAL PAGE IS POOR

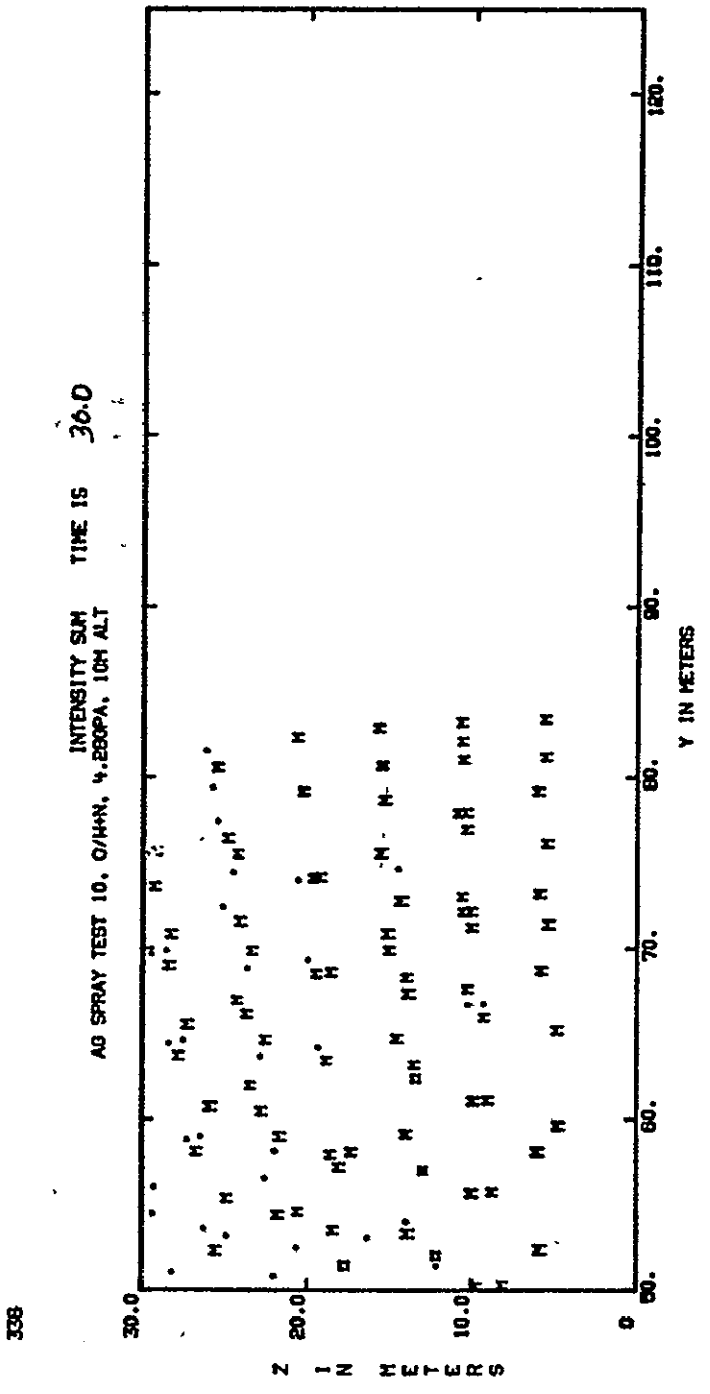

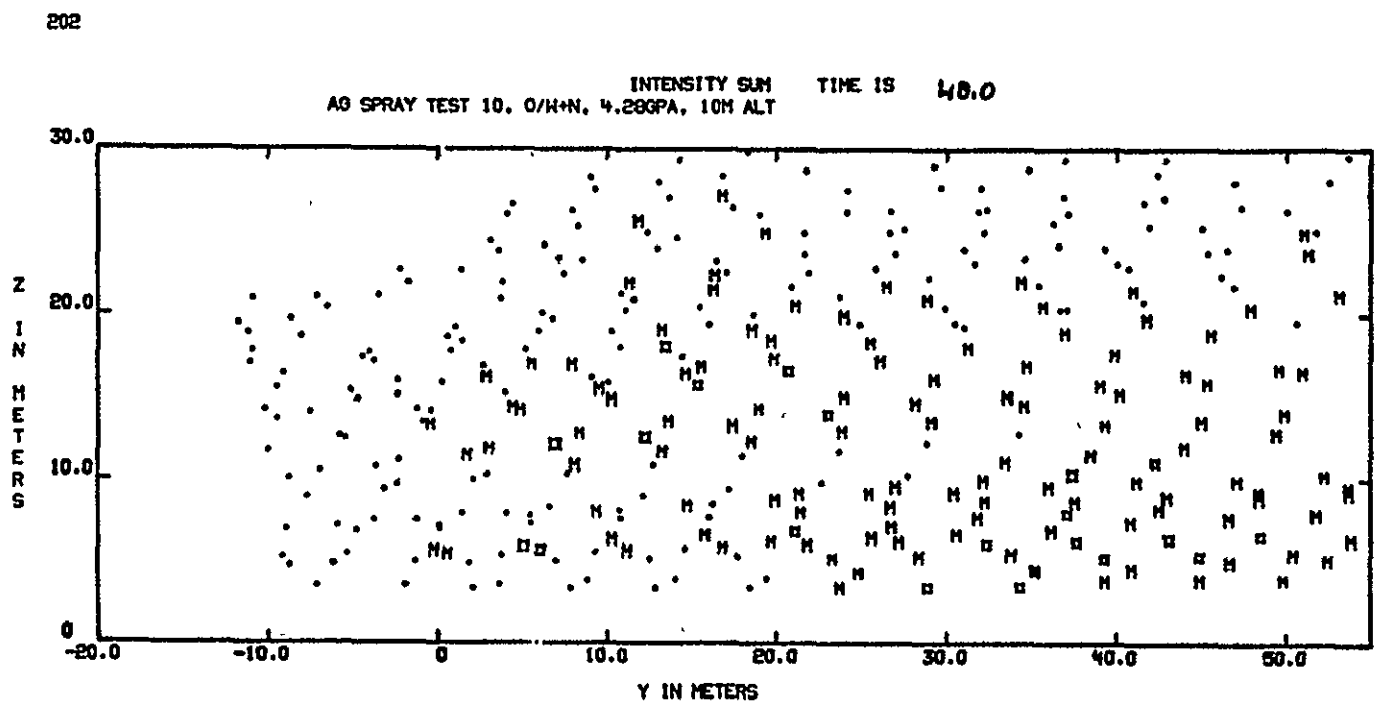
202
INTENSITY SUM TIME IS 48.0
AG SPRAY TEST 10. O/H+N, 4.28GPA, 10M ALT
30.0
20.0
10.0
0
Z IN METERS
-20.0
-10.0
0
10.0
20.0
30.0
40.0
50.0
Y IN METERS

REPRODUCIBILITY OF THE
ORIGINAL PAGE IS POOR

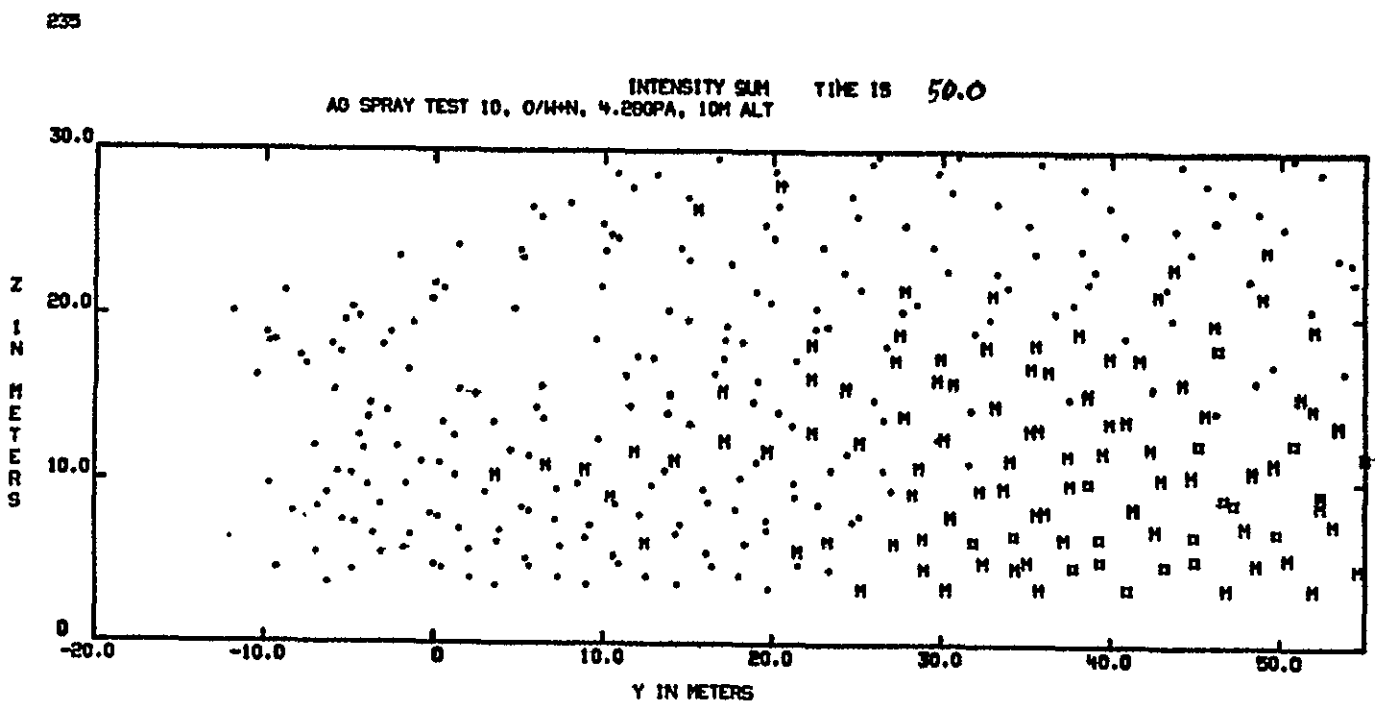
235
INTENSITY SUM TIME IS 50.0
AG SPRAY TEST 10, O/W+N, 4.2BOPA, 10M ALT
30.0
20.0
10.0
0
Z IN METERS
-20.0
-10.0
0
10.0
20.0
30.0
40.0
50.0
Y IN METERS

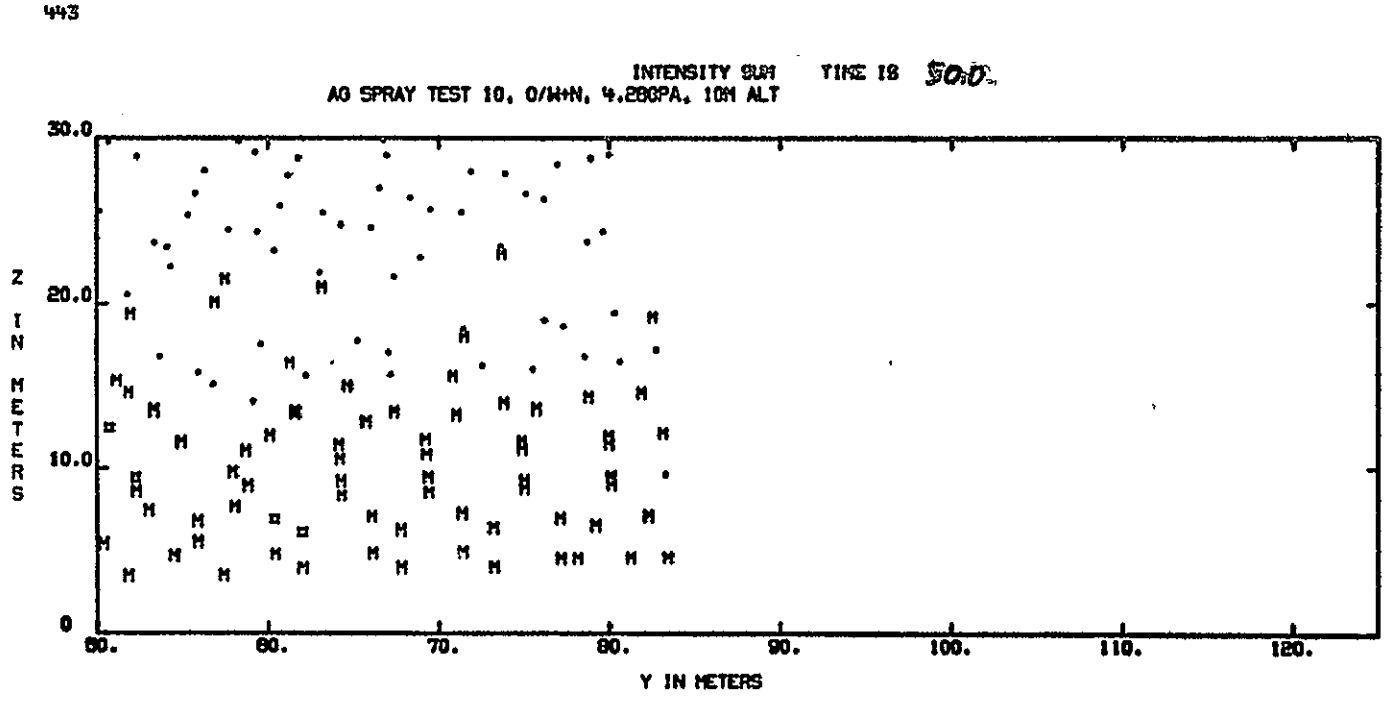
443
INTENSITY SUM
TIME IS 500.
AG SPRAY TEST 10, O/W+N, 4.28GPA, 10M ALT
30.0
20.0
10.0
0
Z IN METERS
50.
60.
70.
80.
90.
100.
110.
120.
Y IN METERS

37

INTENSITY SUM TIME IS 10.0

AG SPRAY TEST 14, WATER, .280PA, 10M ALT

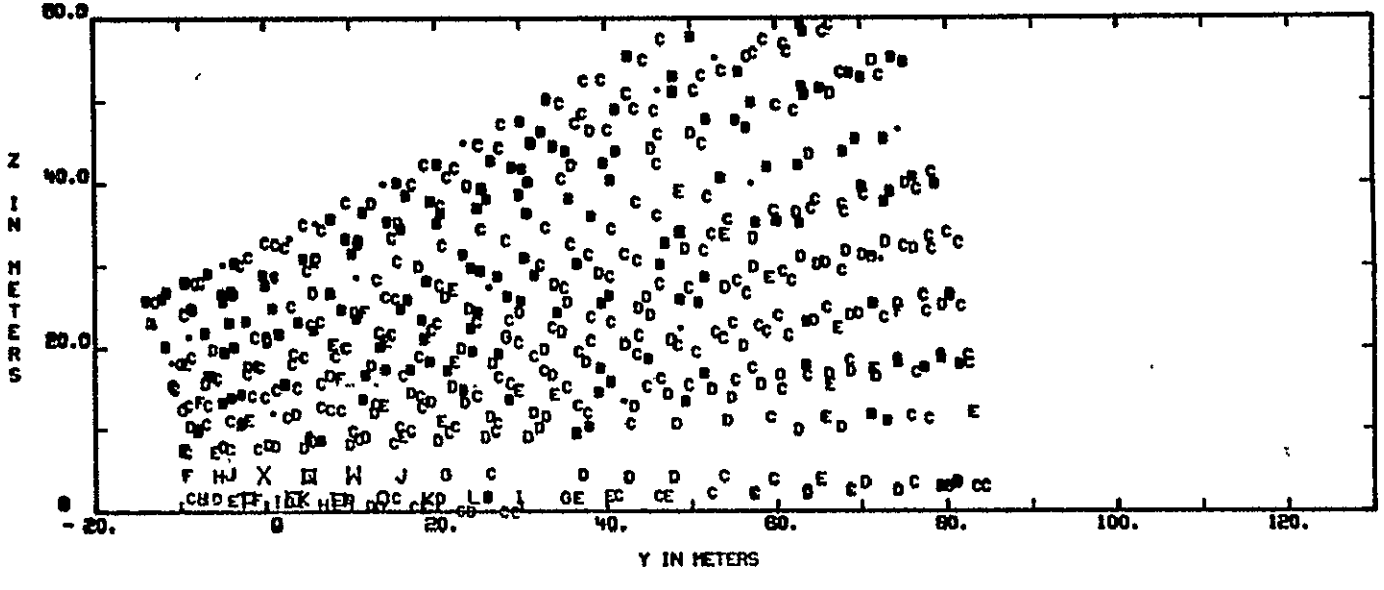

REPRODUCIBILITY OF THE
ORIGINAL PAGE IS POOR

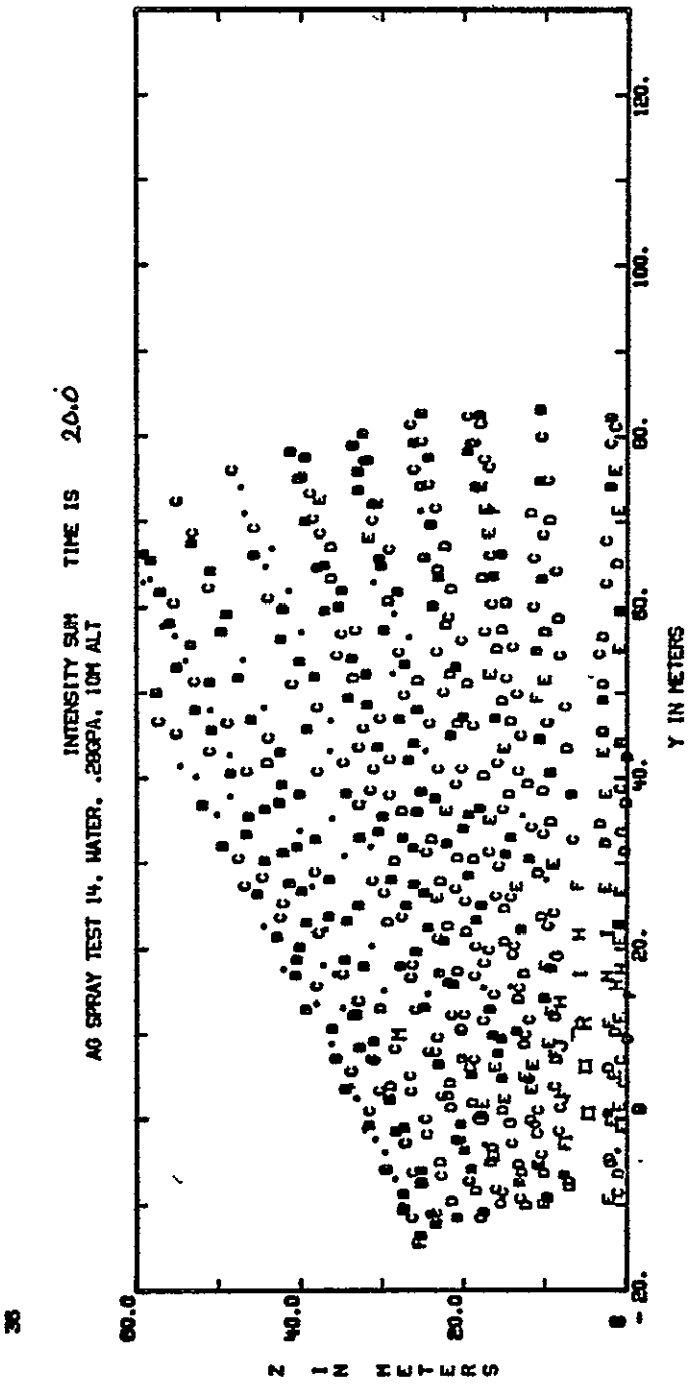

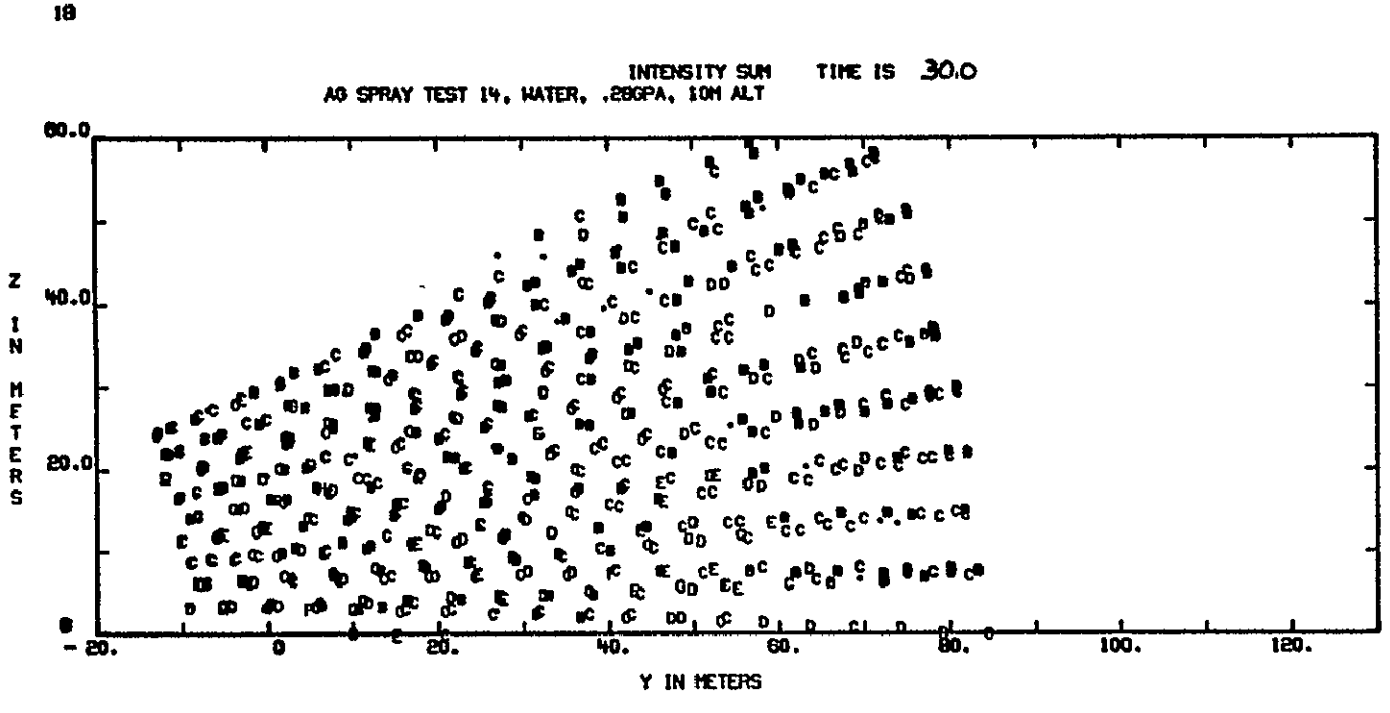
10
INTENSITY SUM TIME IS 30.0
AG SPRAY TEST 14, WATER, .28GPA, 10M ALT
60.0
40.0
20.0
0
Z IN METERS
-20.
0
20.
40.
60.
80.
100.
120.
Y IN METERS

REPRODUCIBILITY OF THE
ORIGINAL PAGE IS POOR

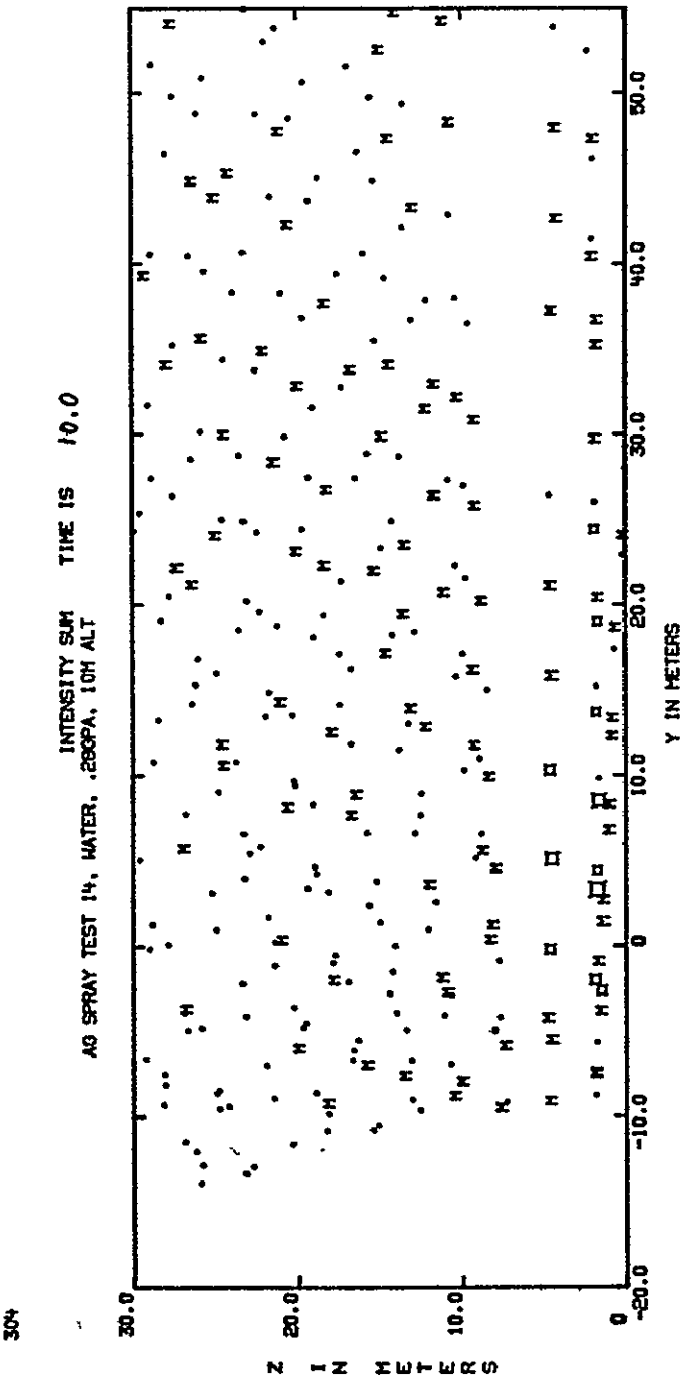

522

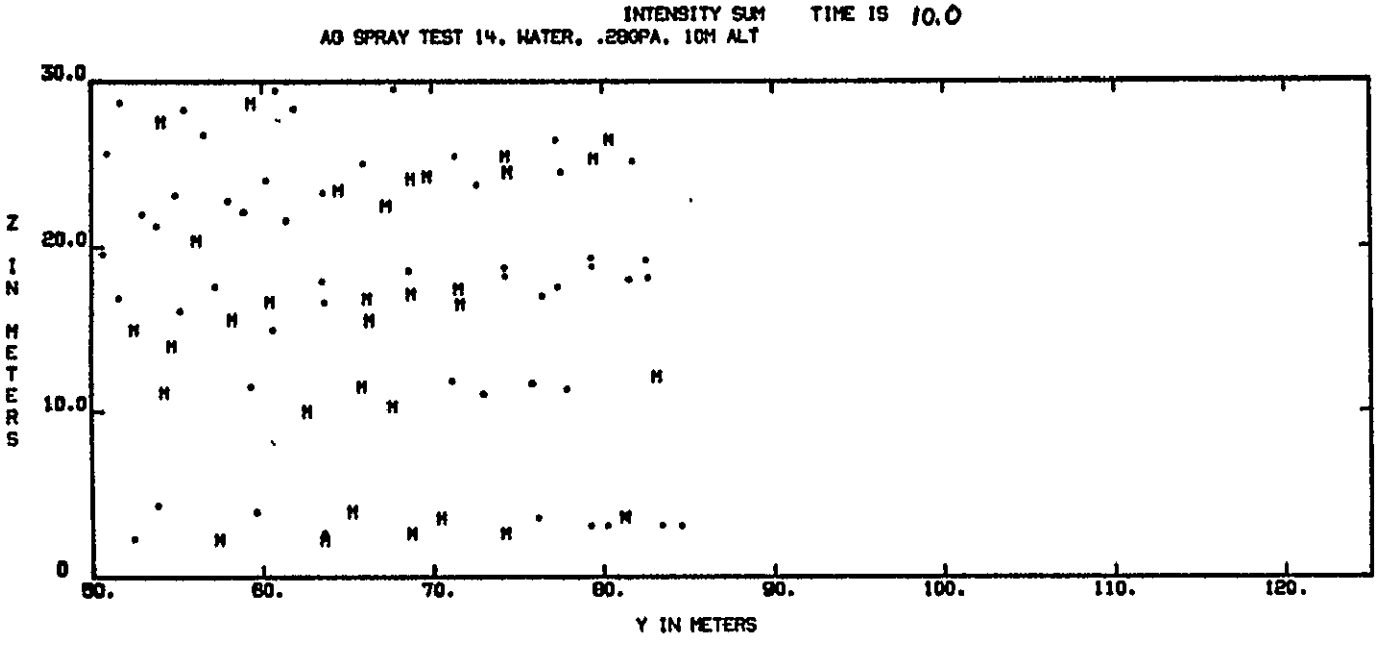
INTENSITY SUM TIME IS 10.0
AO SPRAY TEST 14, WATER, .280PA, 10M ALT
30.0
20.0
10.0
0
Z IN METERS
50.
60.
70.
80.
90.
100.
110.
120.
Y IN METERS

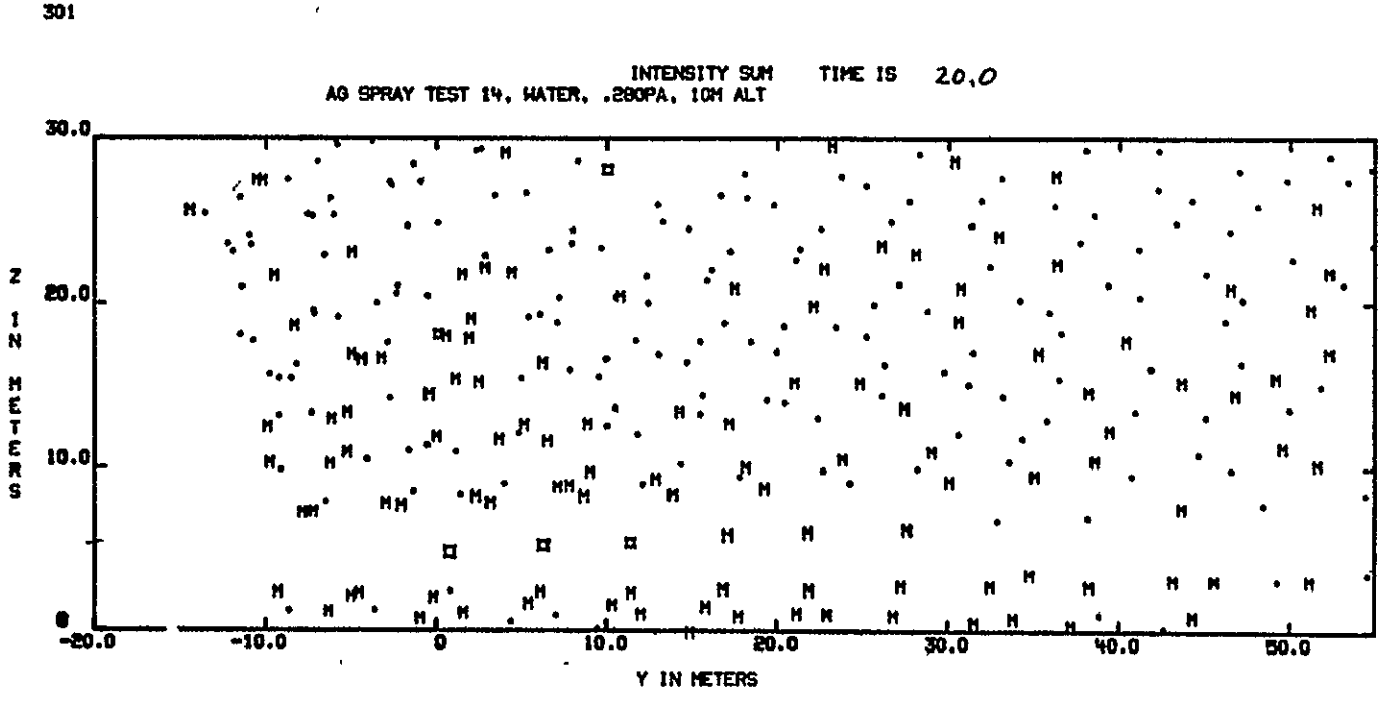
301
INTENSITY SUM TIME IS 20.0
AG SPRAY TEST 14, WATER, .280PA, 10M ALT
30.0
20.0
10.0
0
Z IN METERS
-20.0
-10.0
0
10.0
20.0
30.0
40.0
50.0
Y IN METERS

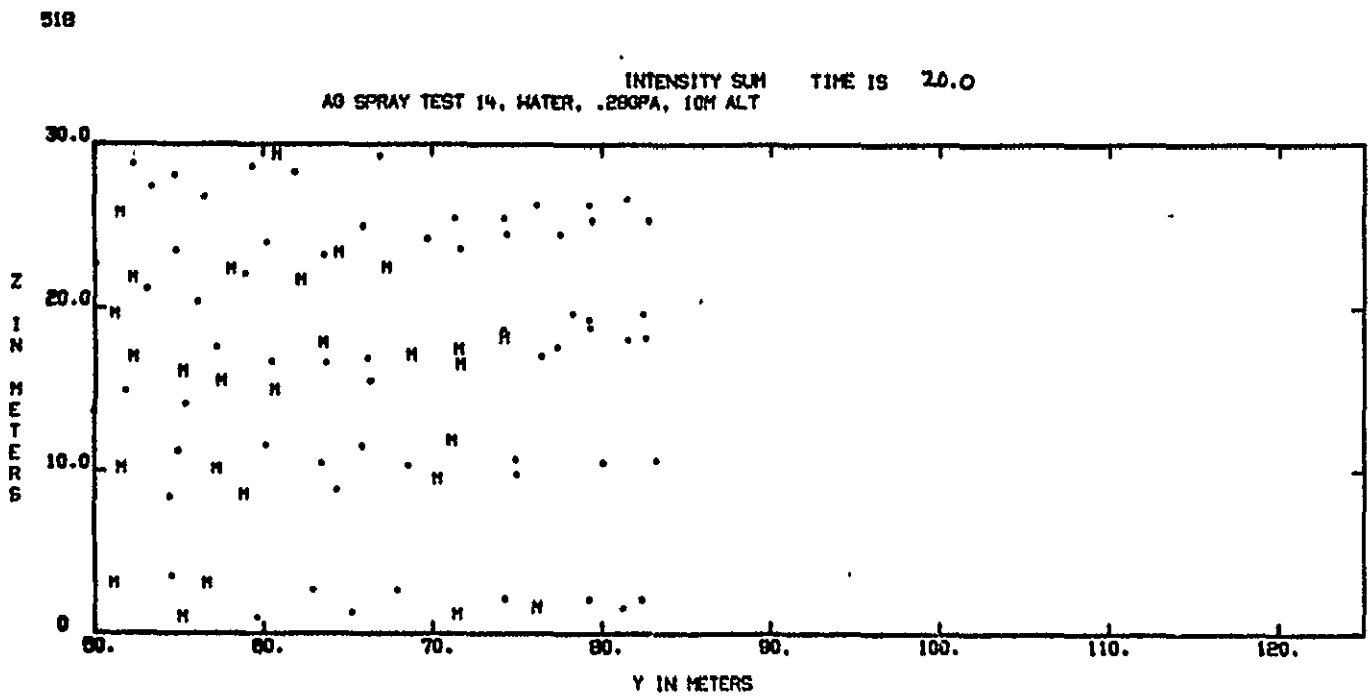
518
INTENSITY SUM TIME IS 20.0
AG SPRAY TEST 14, WATER, .28OPA, 10M ALT
30.0
20.0
10.0
0
Z IN METERS
50.
60.
70.
80.
90.
100.
110.
120.
Y IN METERS

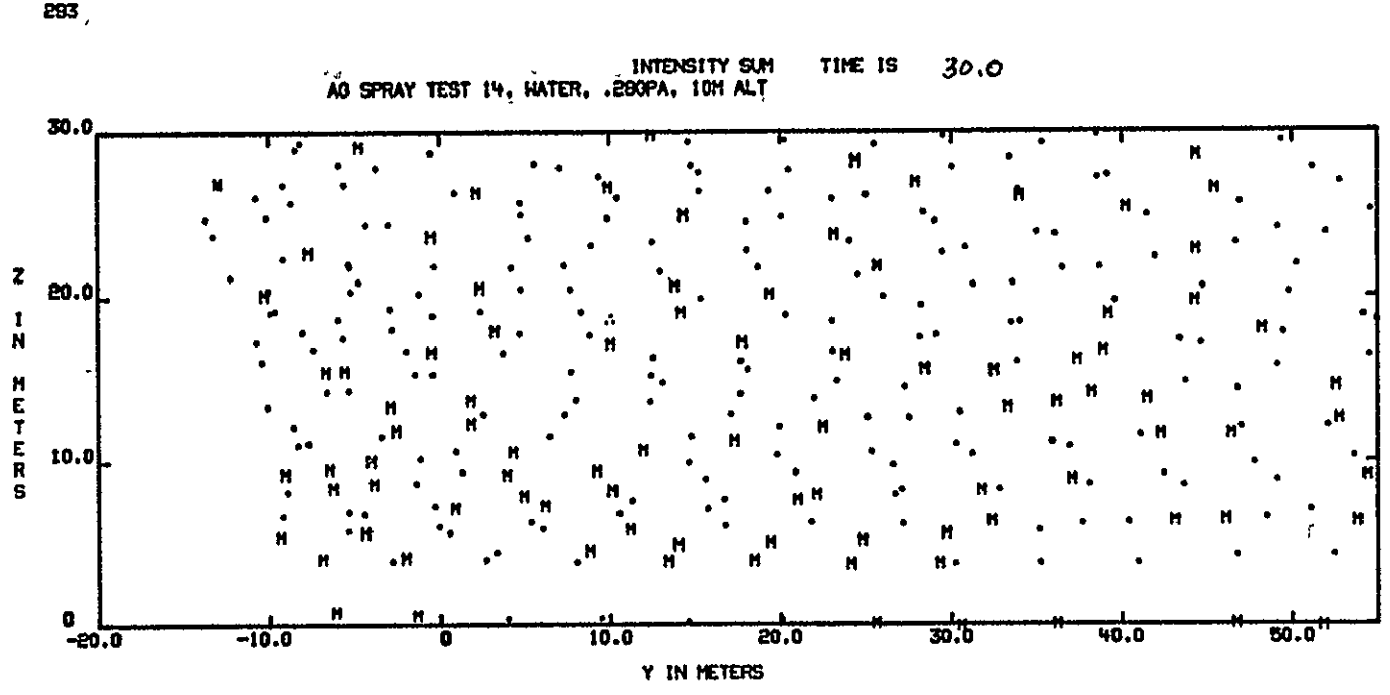
293
INTENSITY SUM TIME IS 30.0
AO SPRAY TEST 14, WATER, .280PA, 10M ALT
30.0
20.0
10.0
0
Z IN METERS
-20.0
-10.0
0
10.0
20.0
30.0
40.0
50.0
Y IN METERS

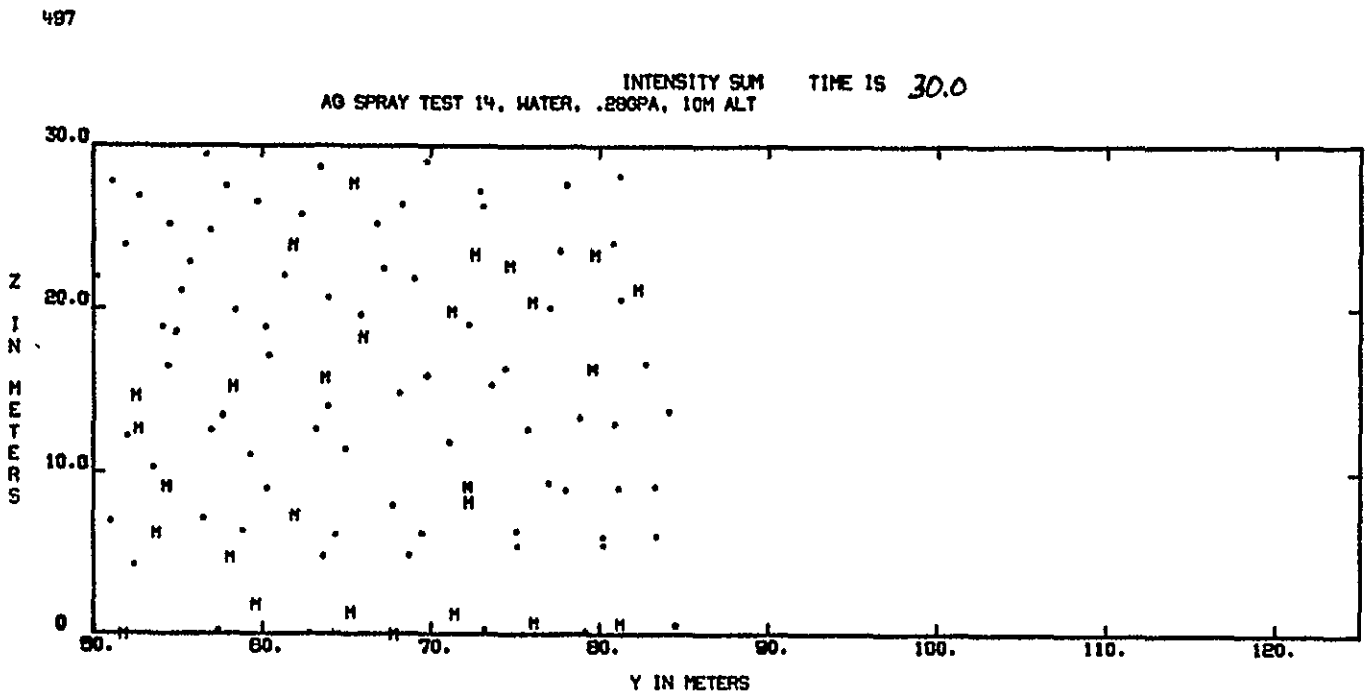
497
INTENSITY SUM TIME IS 30.0
AG SPRAY TEST 14, WATER, .28GPA, 10M ALT
30.0
20.0
10.0
0
Z IN METERS
50.
60.
70.
80.
90.
100.
110.
120.
Y IN METERS

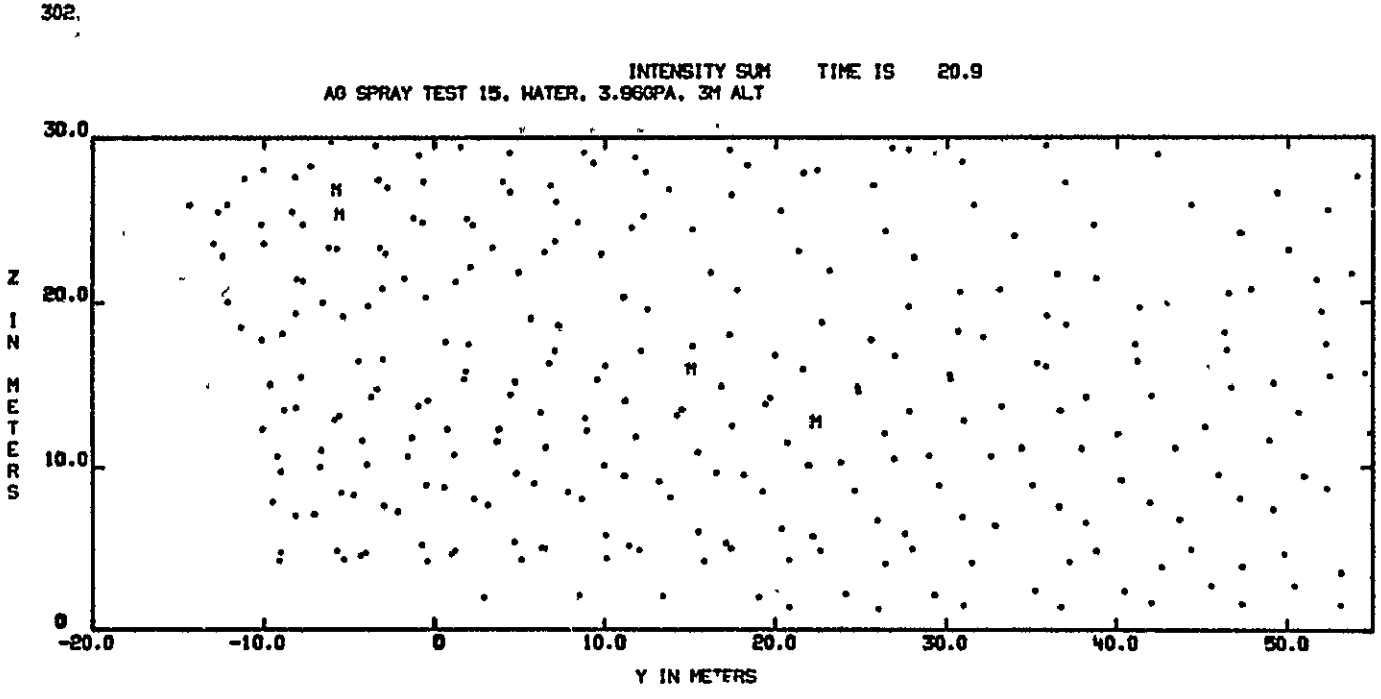
302.
INTENSITY SUM TIME IS 20.9
AG SPRAY TEST 15, WATER, 3.96GPA, 3M ALT
30.0
20.0
10.0
0
Z IN METERS
-20.0
-10.0
0
10.0
20.0
30.0
40.0
50.0
Y IN METERS

REPRODUCIBILITY OF THE
ORIGINAL PAGE IS POOR

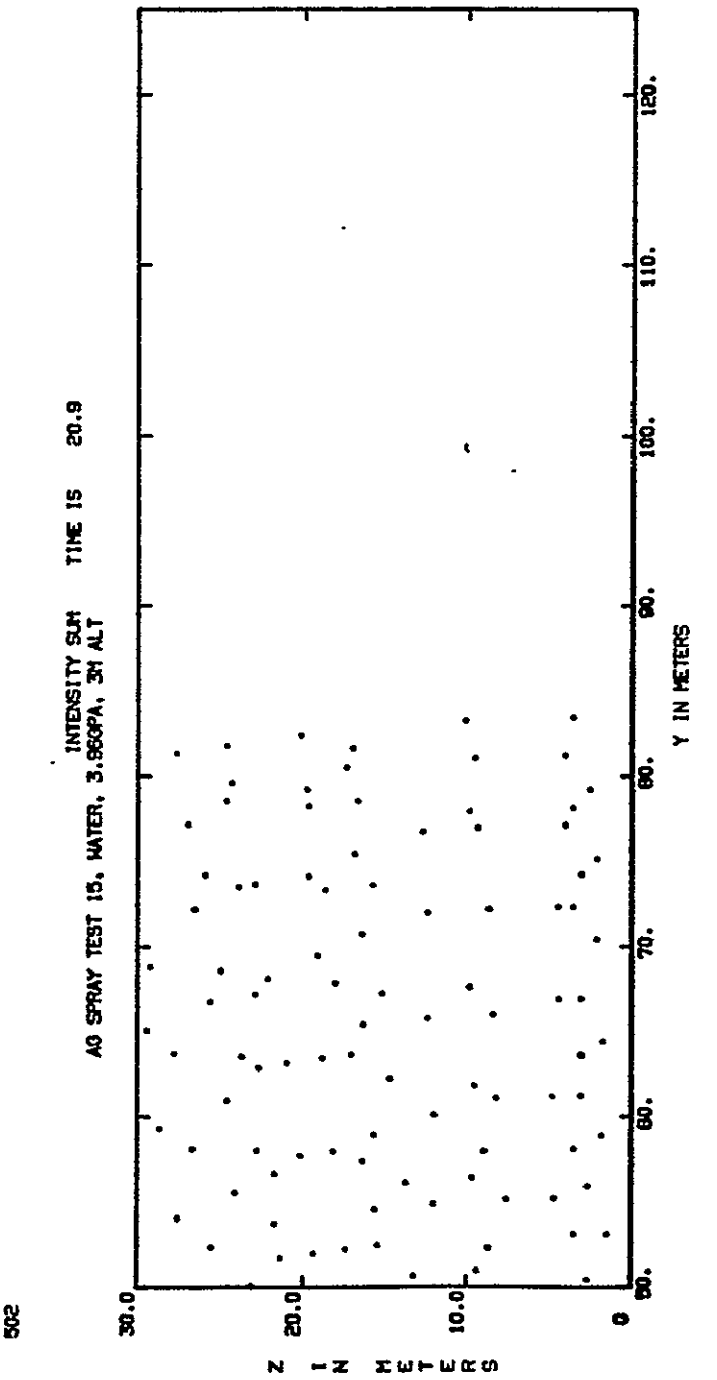

REPRODUCIBILITY OF THE
ORIGINAL PAGE IS POOR

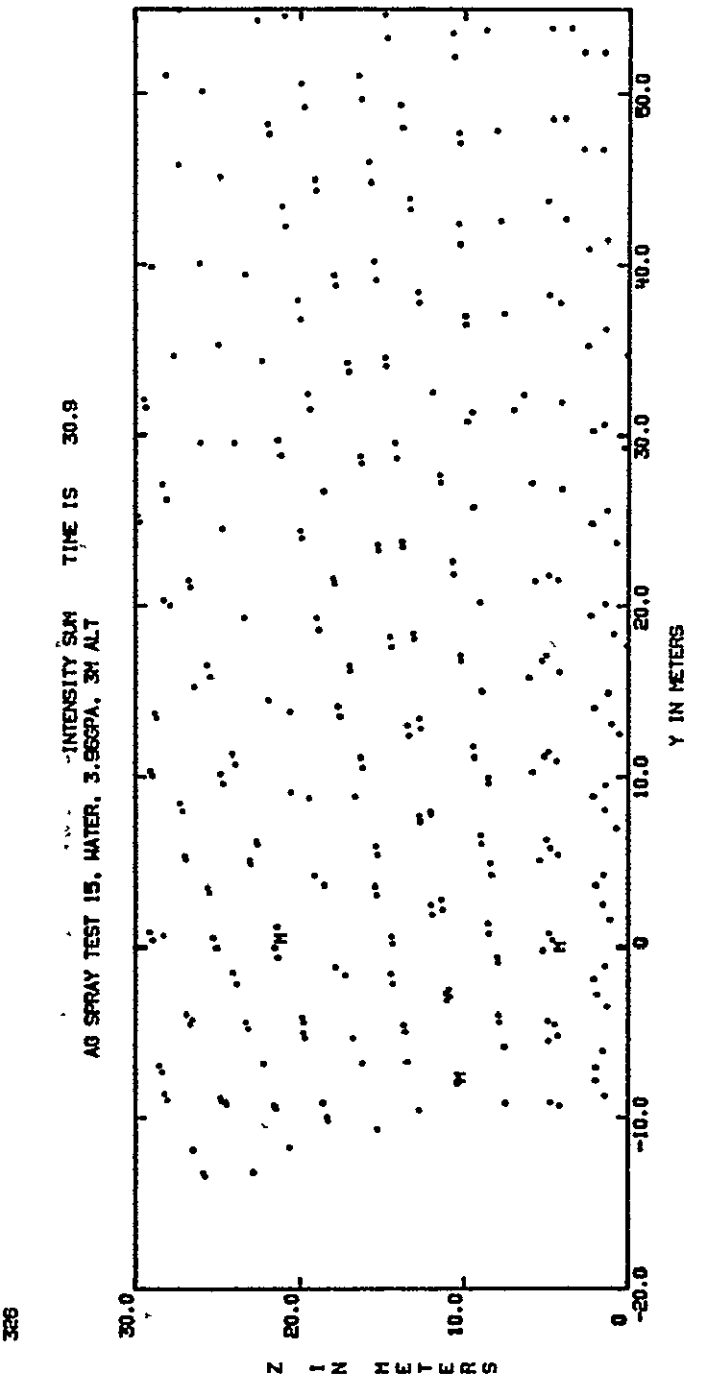

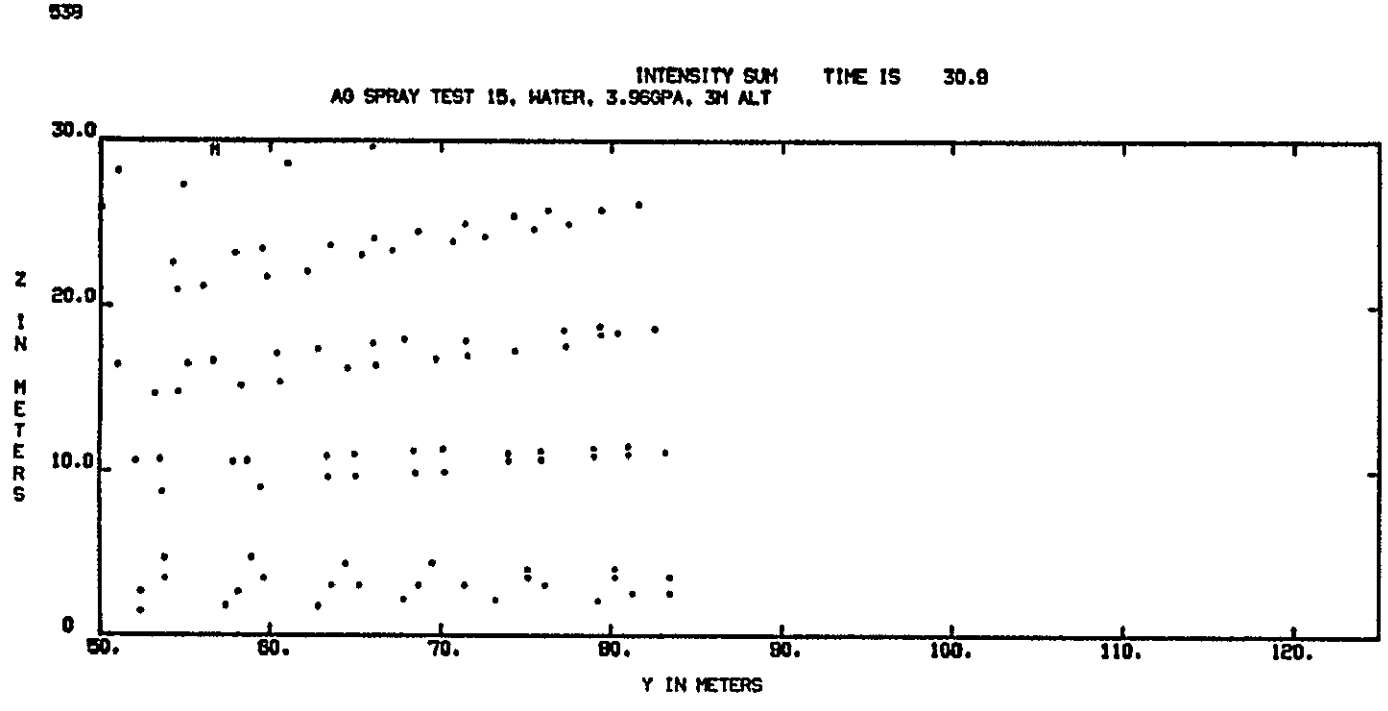
539
INTENSITY SUM TIME IS 30.8
AG SPRAY TEST 15, WATER, 3.96GPA, 3M ALT
30.0
20.0
10.0
0
Z IN METERS
50.
60.
70.
80.
90.
100.
110.
120.
Y IN METERS

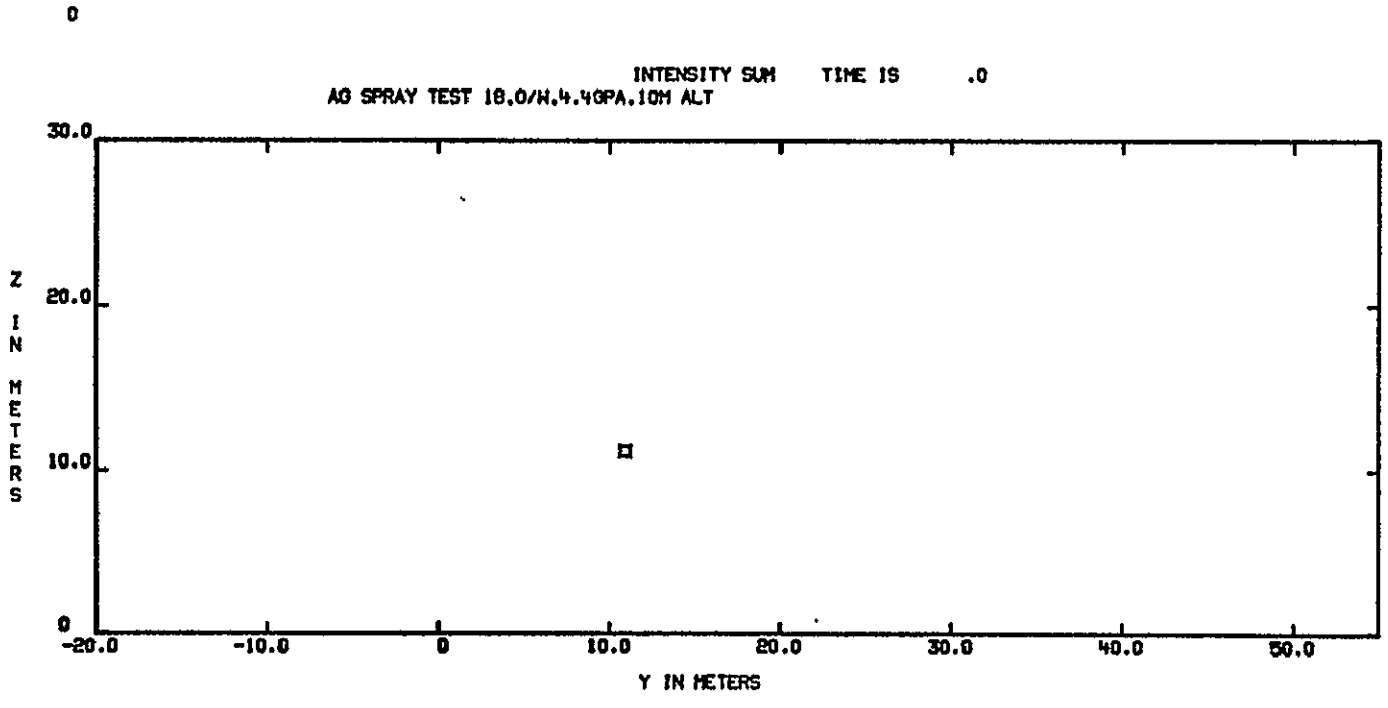
0
INTENSITY SUM TIME IS .0
AG SPRAY TEST 18.0/H,4.4GPA,10M ALT
30.0
20.0
10.0
0
Z IN METERS
-20.0
-10.0
0
10.0
20.0
30.0
40.0
50.0
Y IN METERS

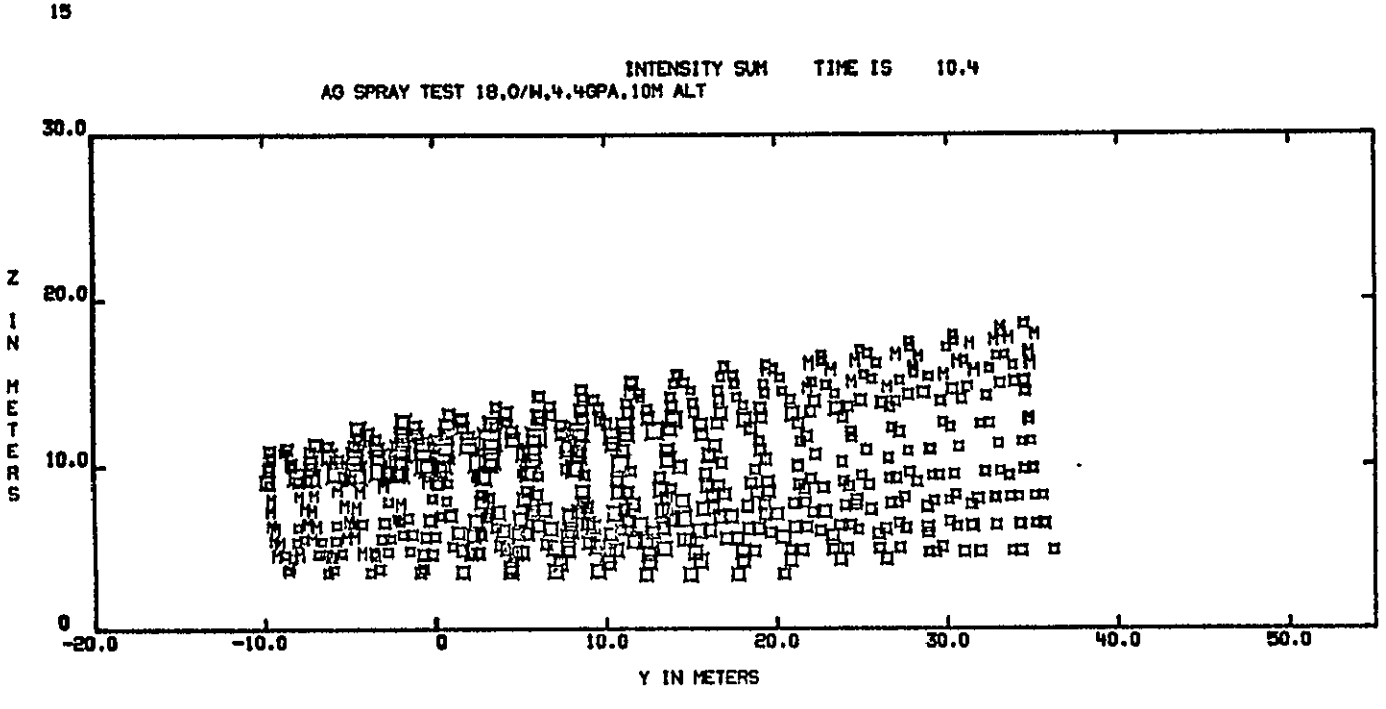
15
INTENSITY SUM TIME IS 10.4
AG SPRAY TEST 18.0/H,4.4GPA,10M ALT
30.0
20.0
10.0
0
Z IN METERS
-20.0
-10.0
0
10.0
20.0
30.0
40.0
50.0
Y IN METERS

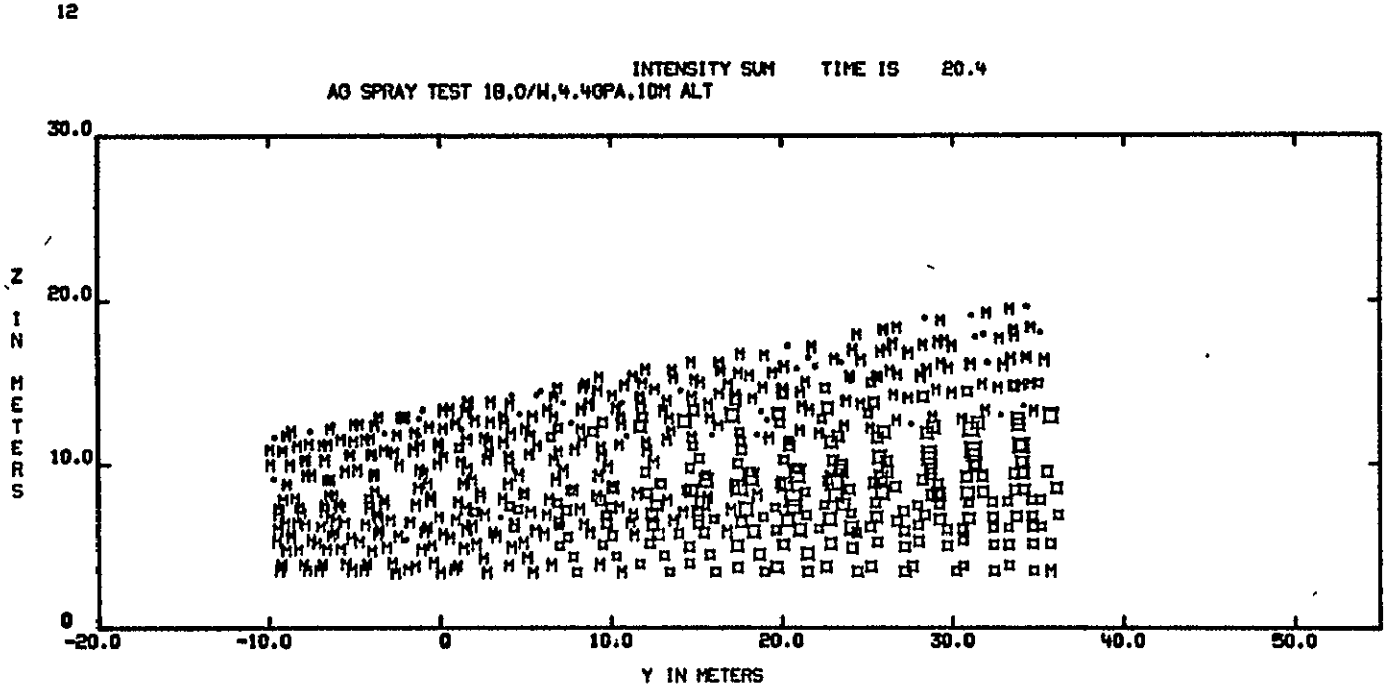
12
INTENSITY SUM TIME IS 20.4
AG SPRAY TEST 18.0/H,4.40PA,10M ALT
30.0
20.0
10.0
0
Z IN METERS
-20.0
-10.0
0
10.0
20.0
30.0
40.0
50.0
Y IN METERS

REPRODUCIBILITY OF THE
ORIGINAL PAGE IS POOR

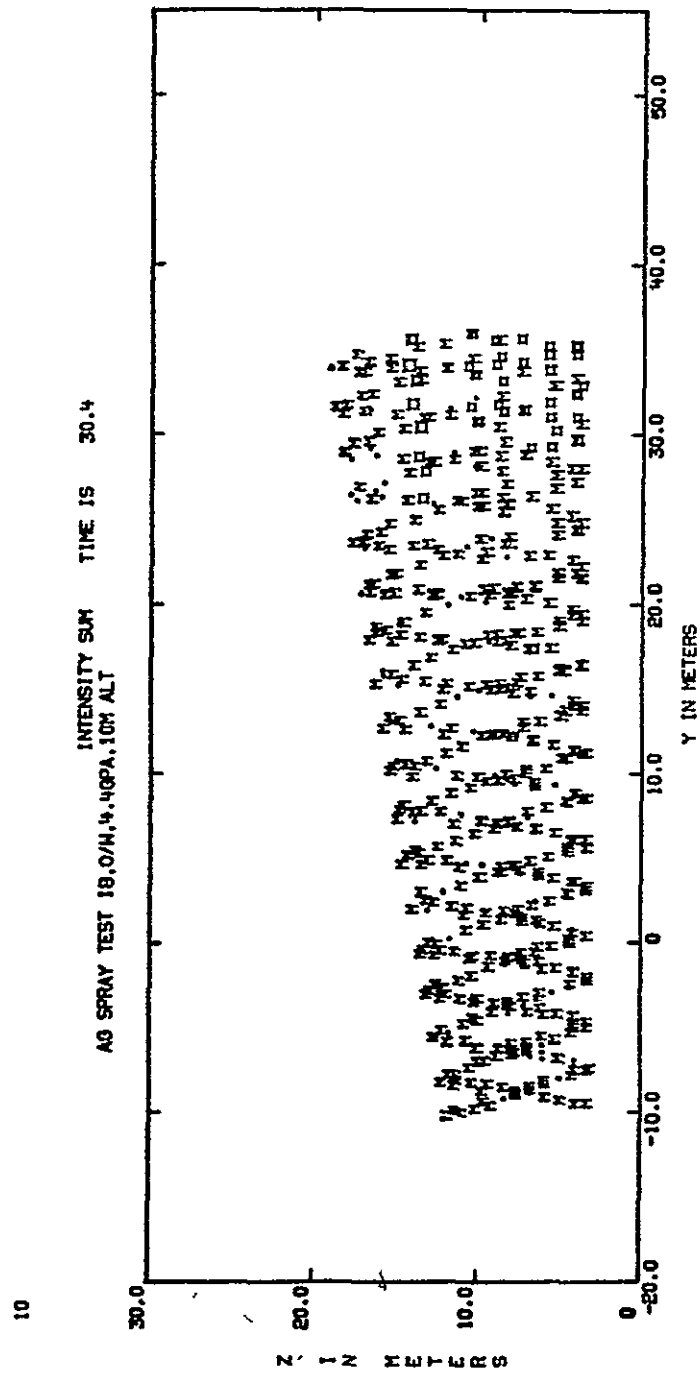

REPRODUCIBILITY OF THE
ORIGINAL PAGE IS POOR

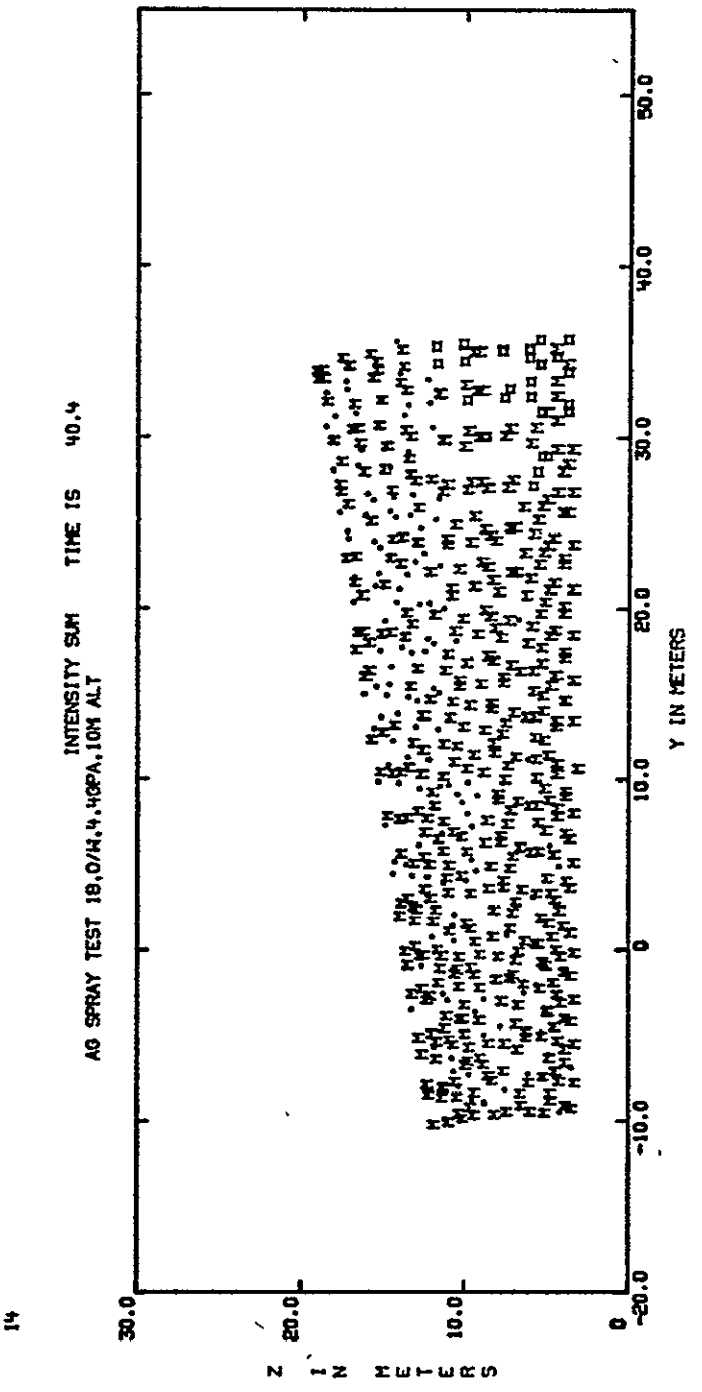

9

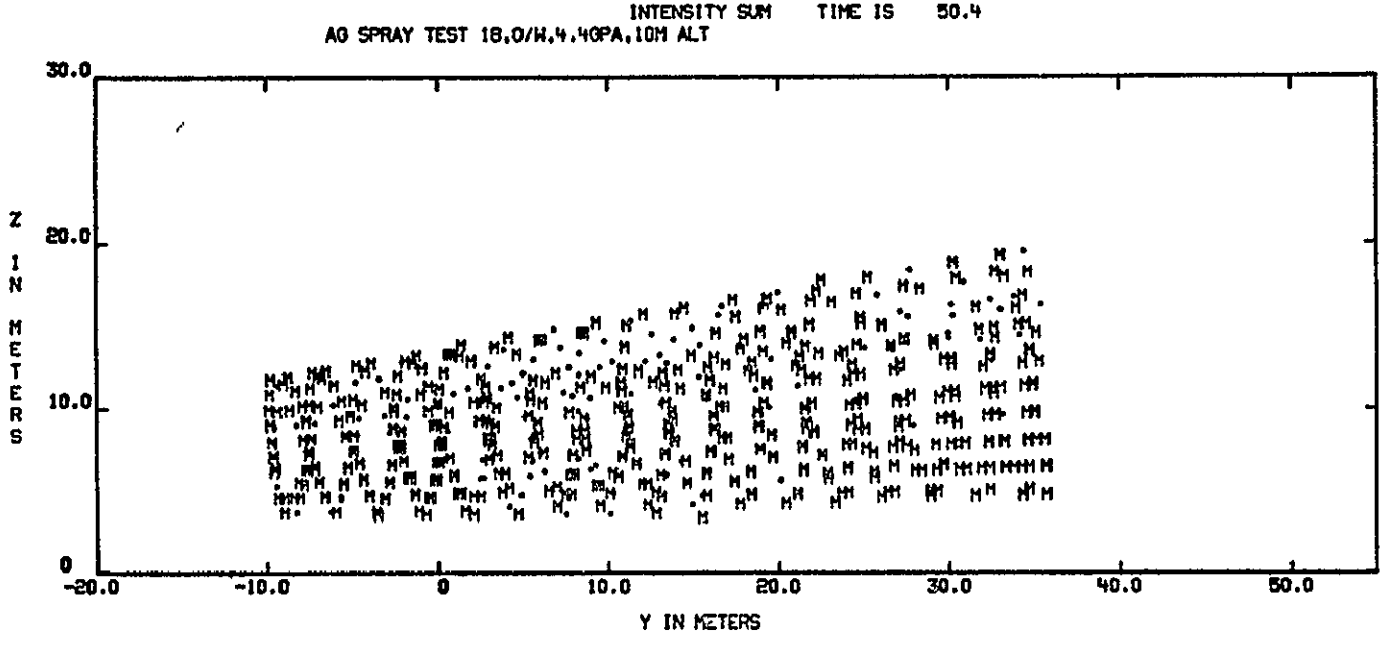
INTENSITY SUM TIME IS 50.4
AG SPRAY TEST 18.0/H,4.4GPA,10M ALT
30.0
20.0
10.0
0
Z IN METERS
-20.0
-10.0
0
10.0
20.0
30.0
40.0
50.0
Y IN METERS

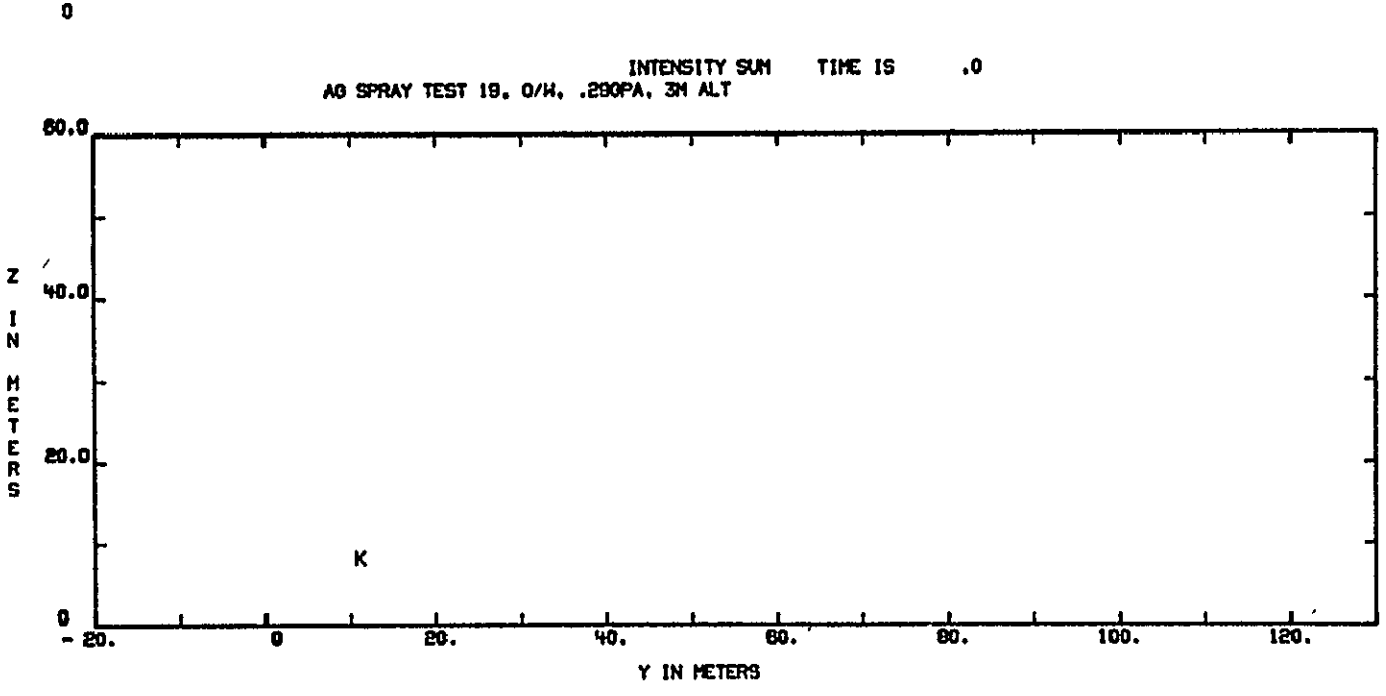
0
INTENSITY SUM TIME IS .0
AG SPRAY TEST 19. O/H, .290PA, 3M ALT
60.0
40.0
20.0
0
Z IN METERS
K
-20.
0
20.
40.
60.
80.
100.
120.
Y IN METERS

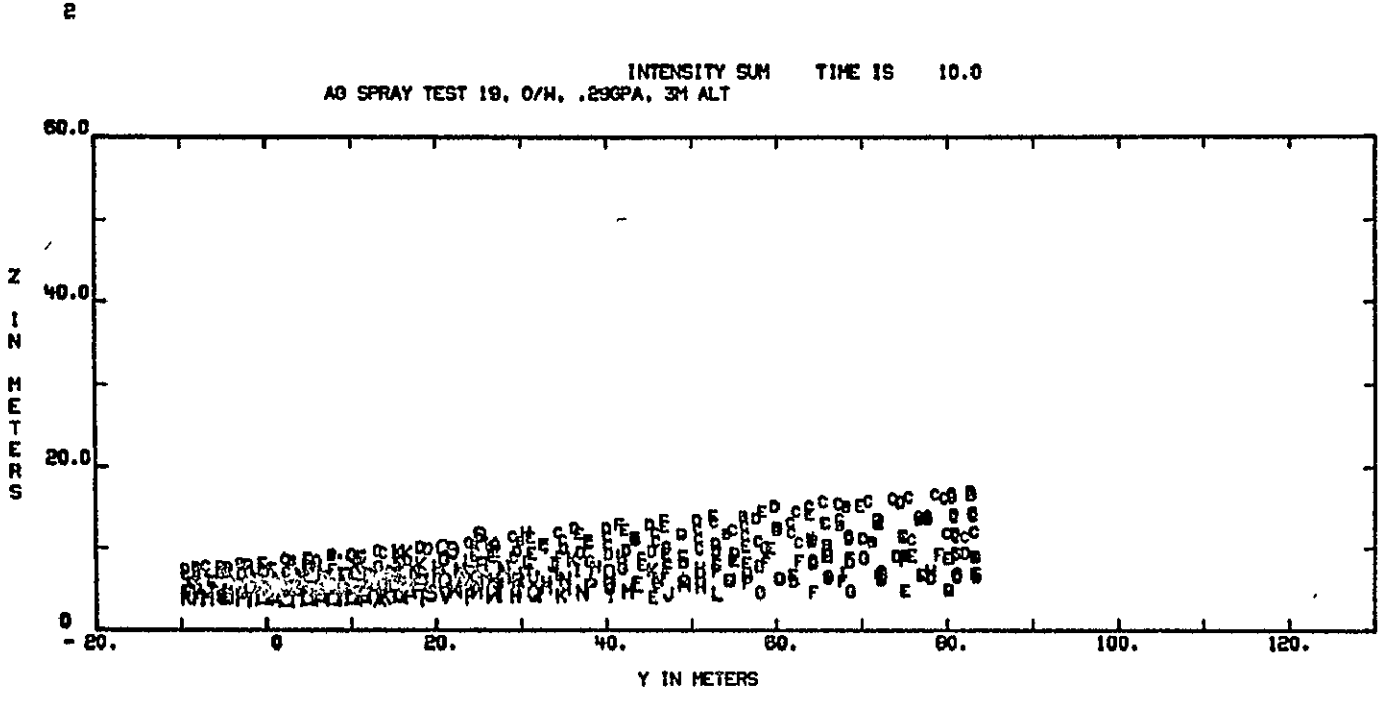
2
INTENSITY SUM TIME IS 10.0
AG SPRAY TEST 19, O/H, .29GPA, 3M ALT
60.0
40.0
20.0
0
Z IN METERS
-20.
0
20.
40.
60.
80.
100.
120.
Y IN METERS

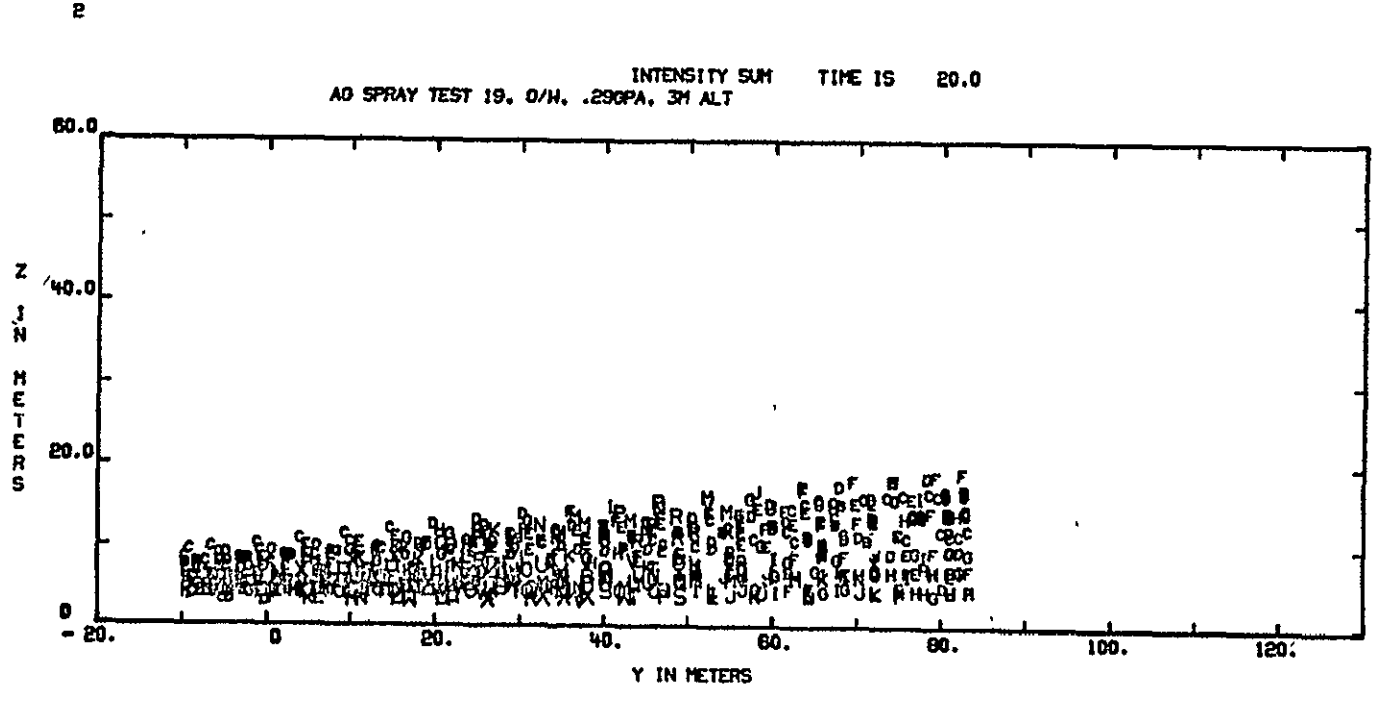
2
INTENSITY SUM TIME IS 20.0
AO SPRAY TEST 19. O/H, .290PA, 3M ALT
60.0
40.0
20.0
0
Z IN METERS
-20.
0
20.
40.
60.
80.
100.
120.
Y IN METERS

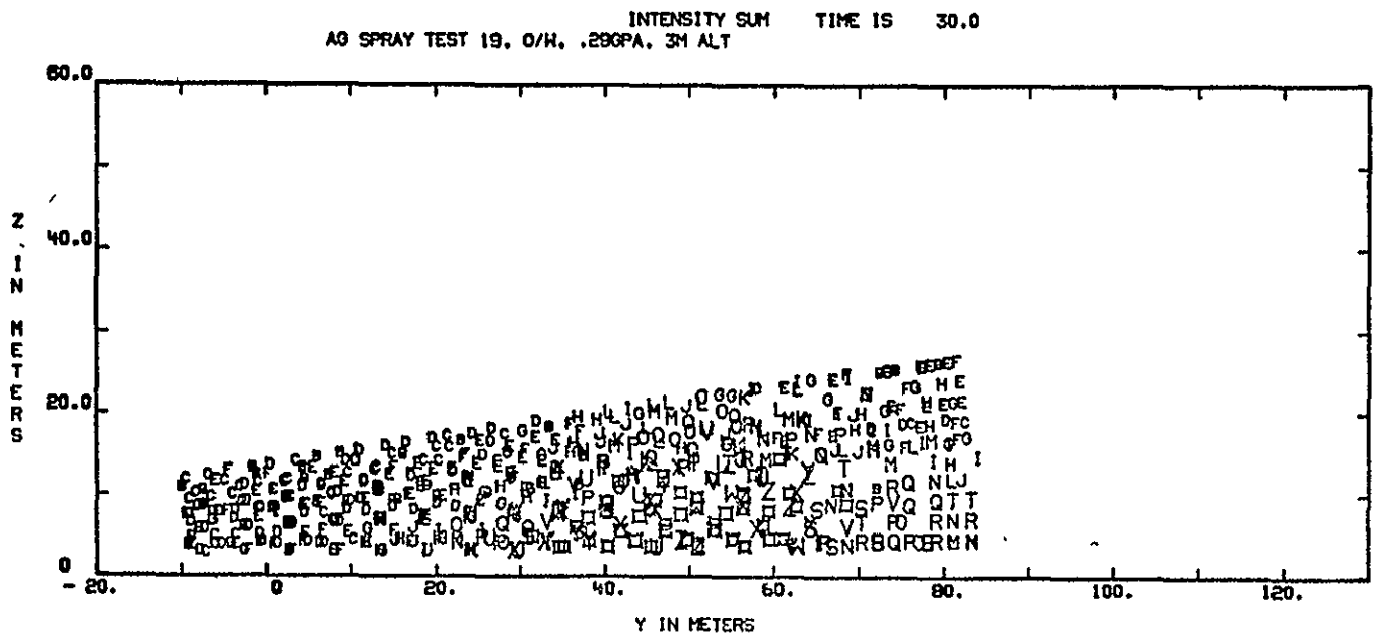
INTENSITY SUM TIME IS 30.0
AG SPRAY TEST 19, O/H, .29GPA, 3M ALT
60.0
40.0
20.0
0
Z IN METERS
-20.
0
20.
40.
60.
80.
100.
120.
Y IN METERS

REPRODUCIBILITY OF THE
ORIGINAL PAGE IS POOR

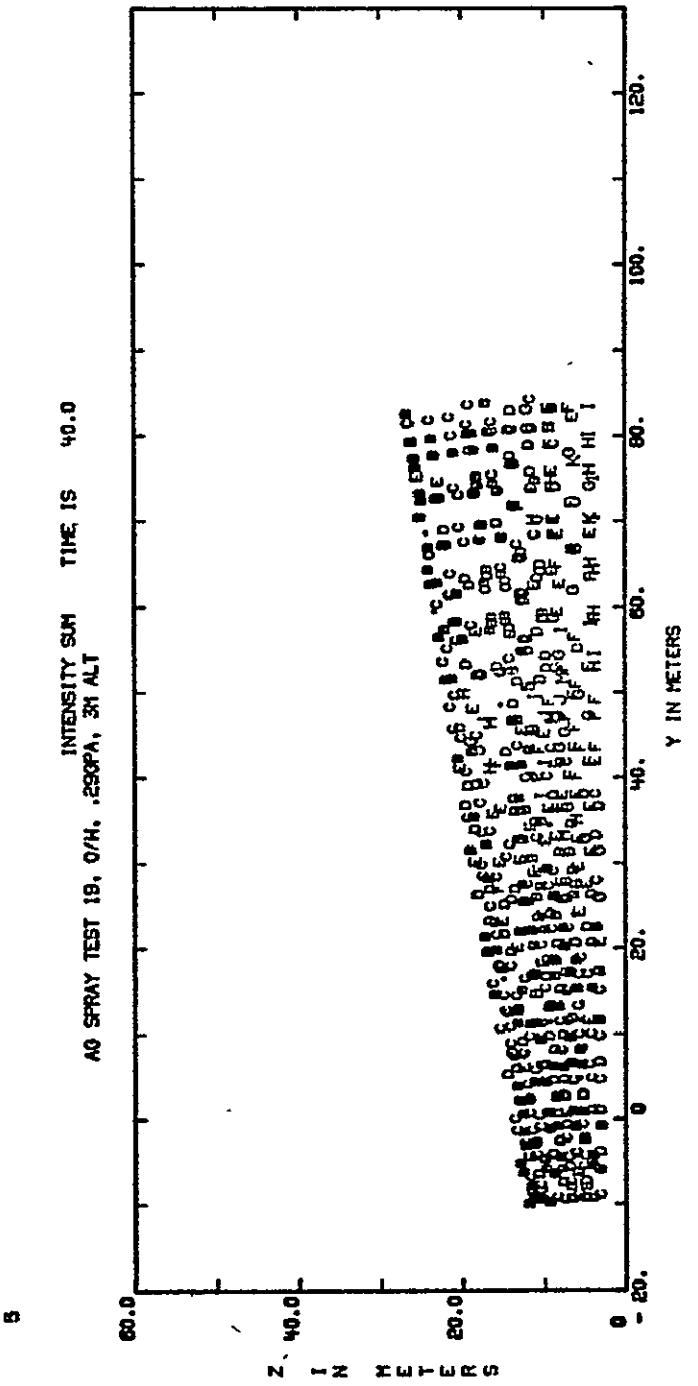

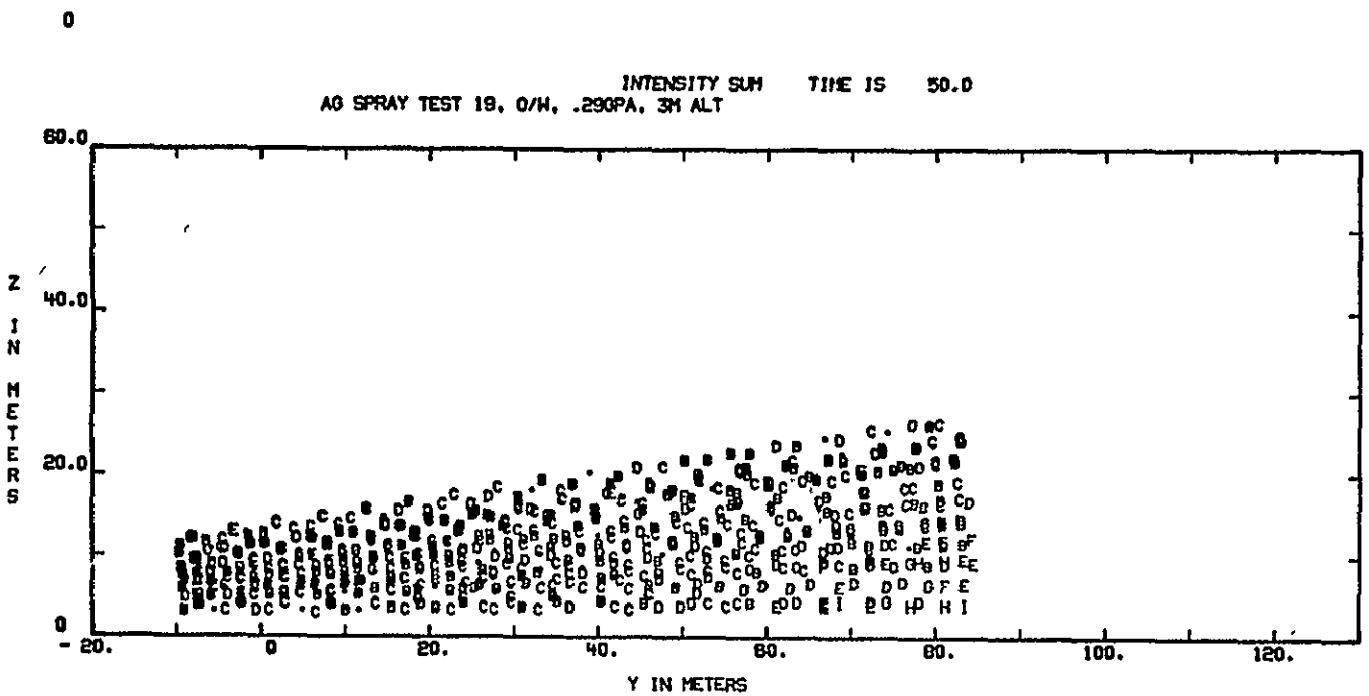
0
INTENSITY SUM TIME IS 50.0
AG SPRAY TEST 19, O/W, .290PA, 3M ALT
60.0
40.0
20.0
0
Z IN METERS
-20.
0
20.
40.
60.
80.
100.
120.
Y IN METERS

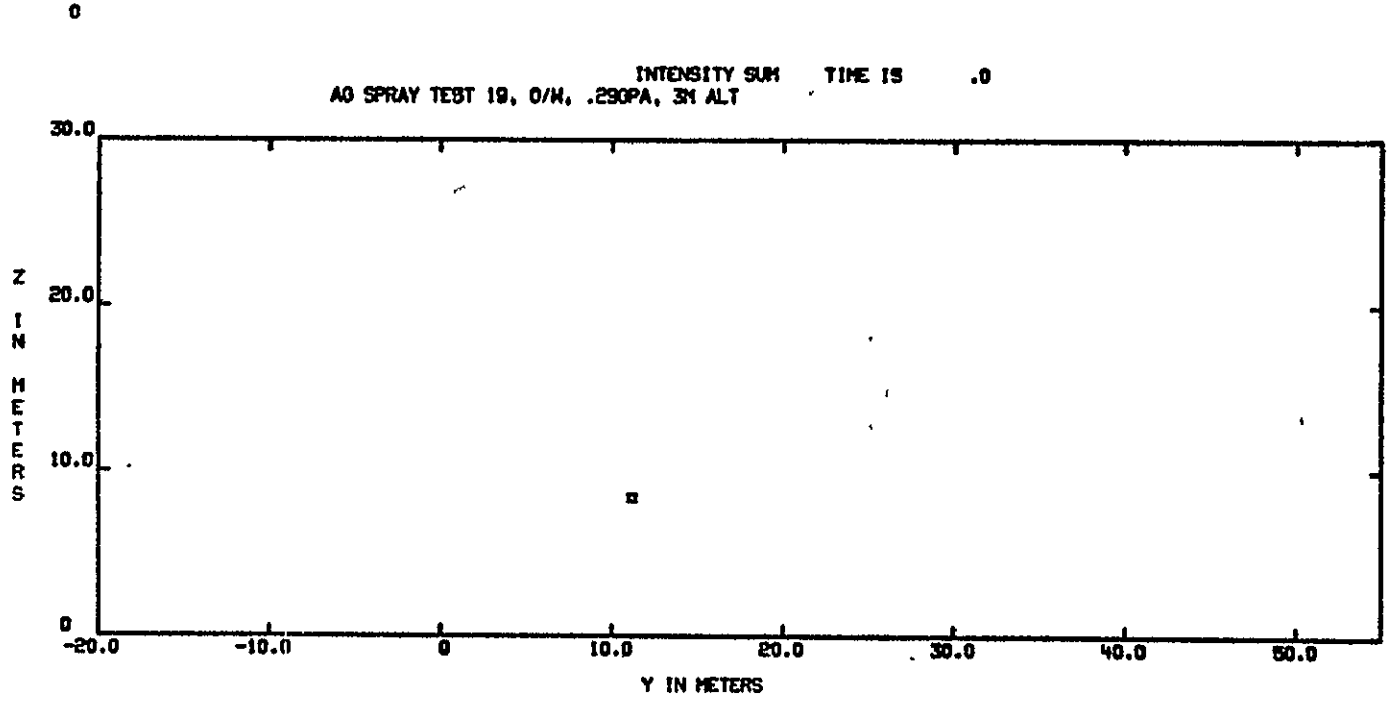
INTENSITY SUM TIME IS .0
AO SPRAY TEST 19, O/H, .290PA, 3M ALT
30.0
20.0
10.0
0
Z IN METERS
-20.0
-10.0
0
10.0
20.0
30.0
40.0
50.0
Y IN METERS

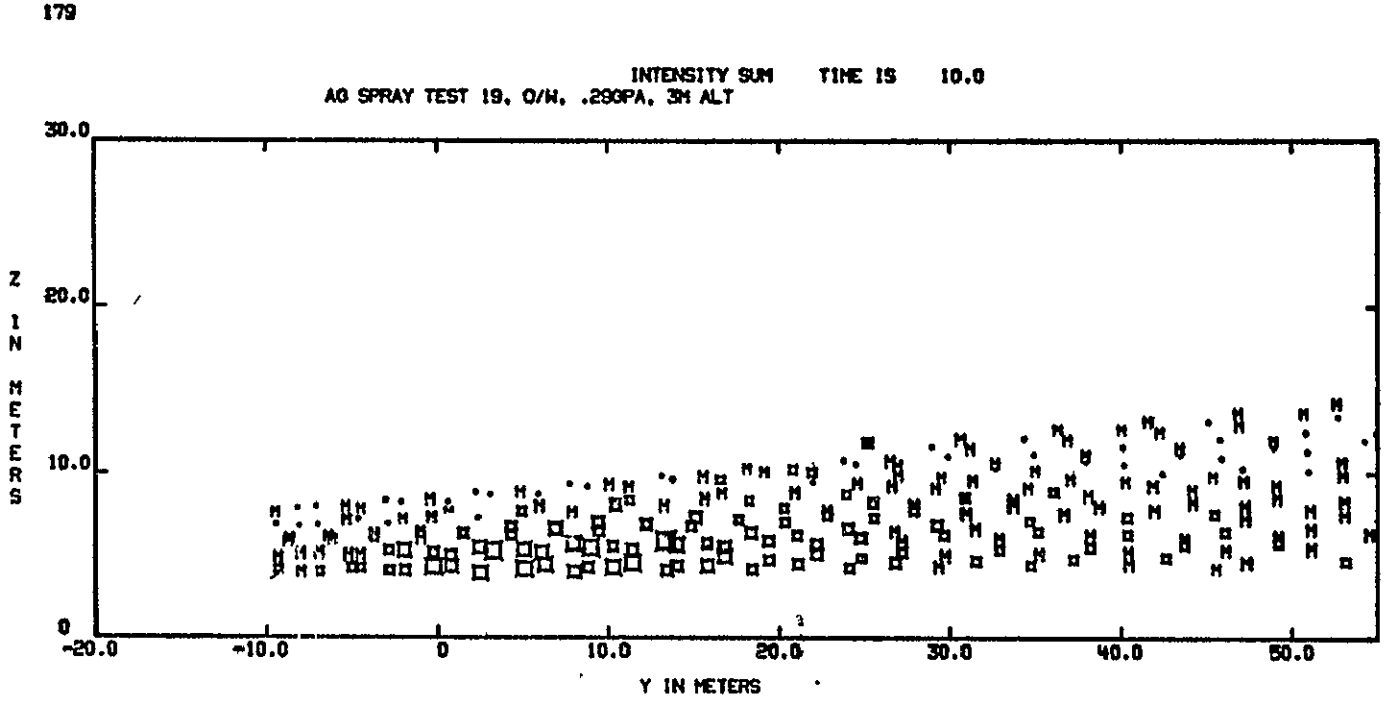
179
INTENSITY SUM TIME IS 10.0
AG SPRAY TEST 19, O/H, .290PA, 3M ALT
30.0
20.0
10.0
0
Z IN METERS
-20.0
-10.0
0
10.0
20.0
30.0
40.0
50.0
Y IN METERS

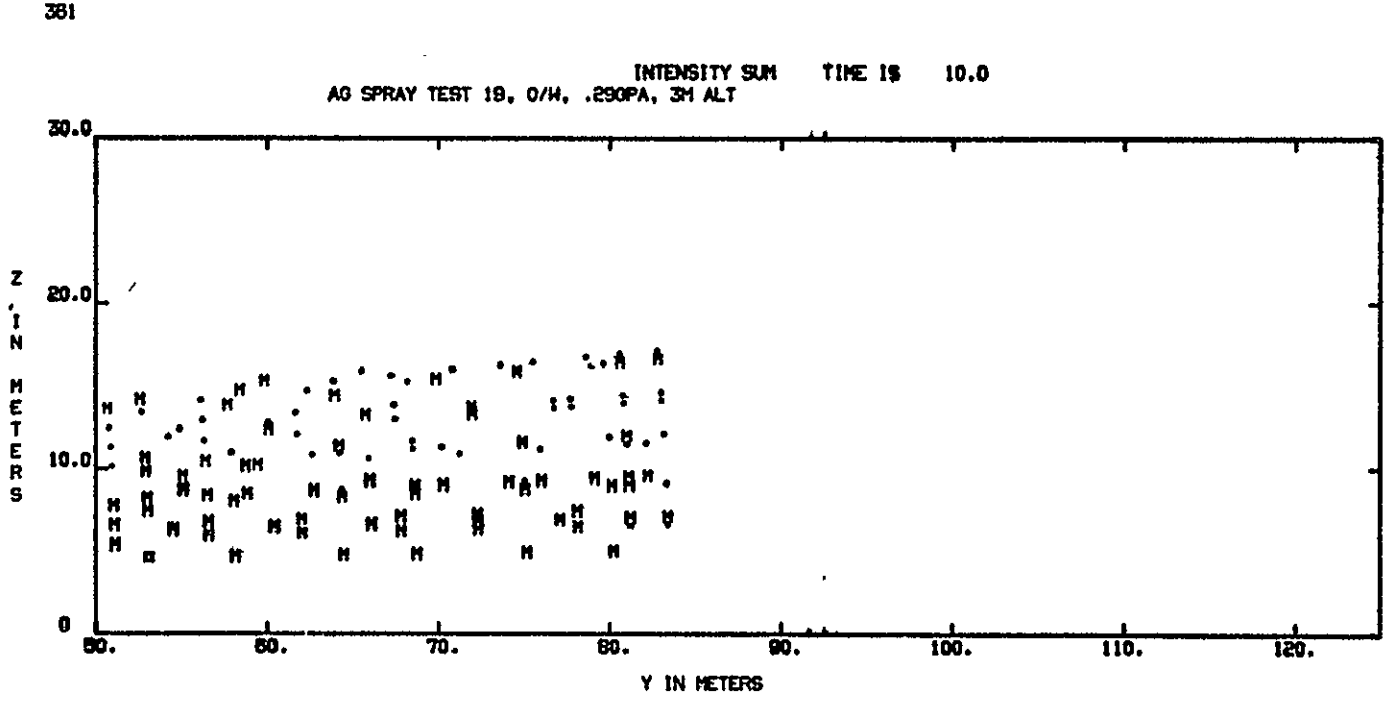
381
INTENSITY SUM TIME IS 10.0
AG SPRAY TEST 19, O/H, .290PA, 3M ALT
30.0
20.0
10.0
0
Z IN METERS
50.
60.
70.
80.
90.
100.
110.
120.
Y IN METERS

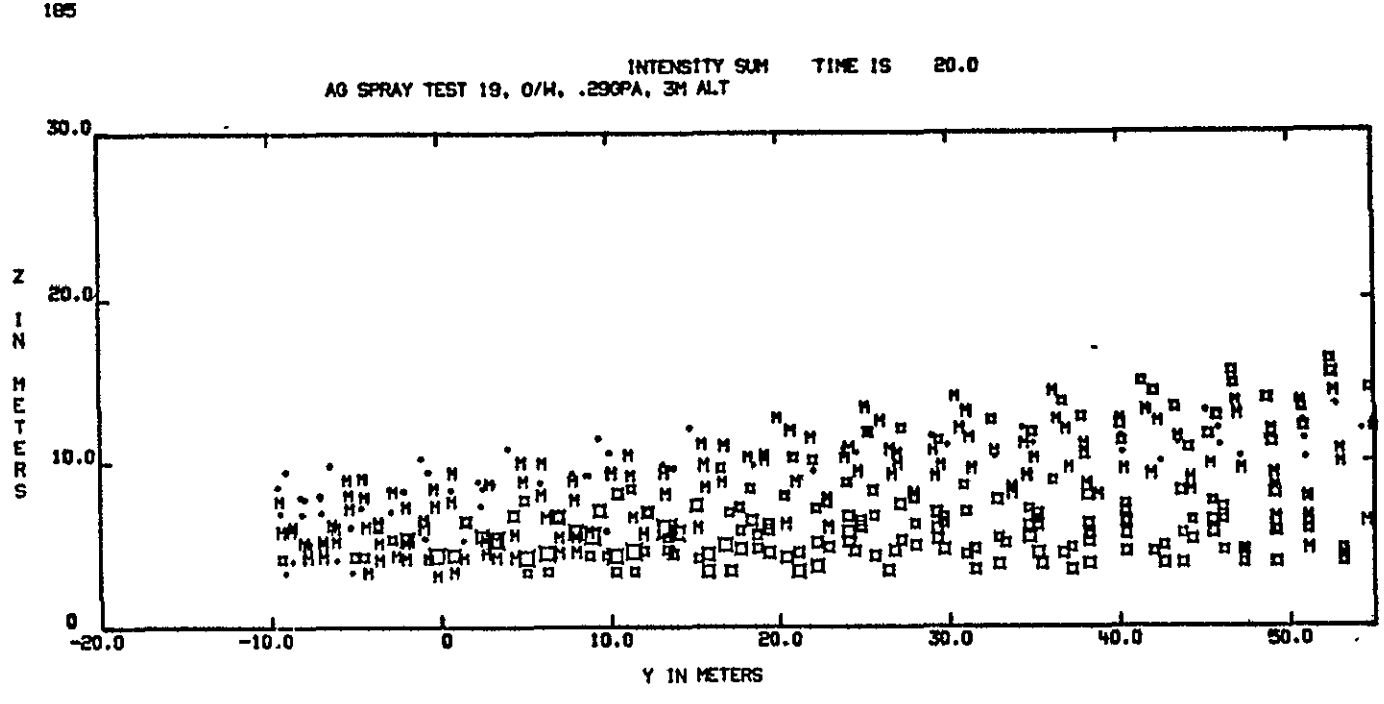
185
INTENSITY SUM TIME IS 20.0
AG SPRAY TEST 19, O/H, .290PA, 3M ALT
30.0
20.0
10.0
0
Z IN METERS
-20.0
-10.0
0
10.0
20.0
30.0
40.0
50.0
Y IN METERS

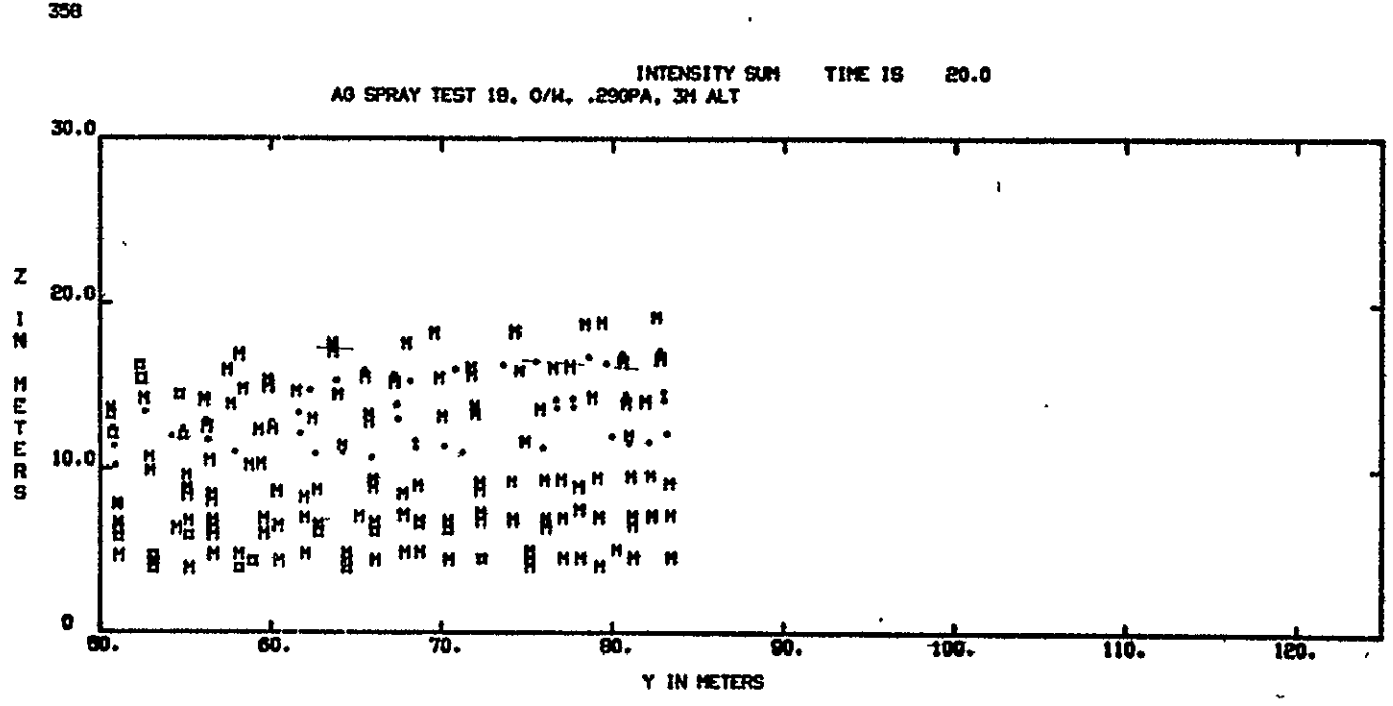
358
INTENSITY SUM TIME IS 20.0
AG SPRAY TEST 18, O/W, .290PA, 3M ALT
30.0
20.0
10.0
0
Z IN METERS
50.
60.
70.
80.
90.
100.
110.
120.
Y IN METERS

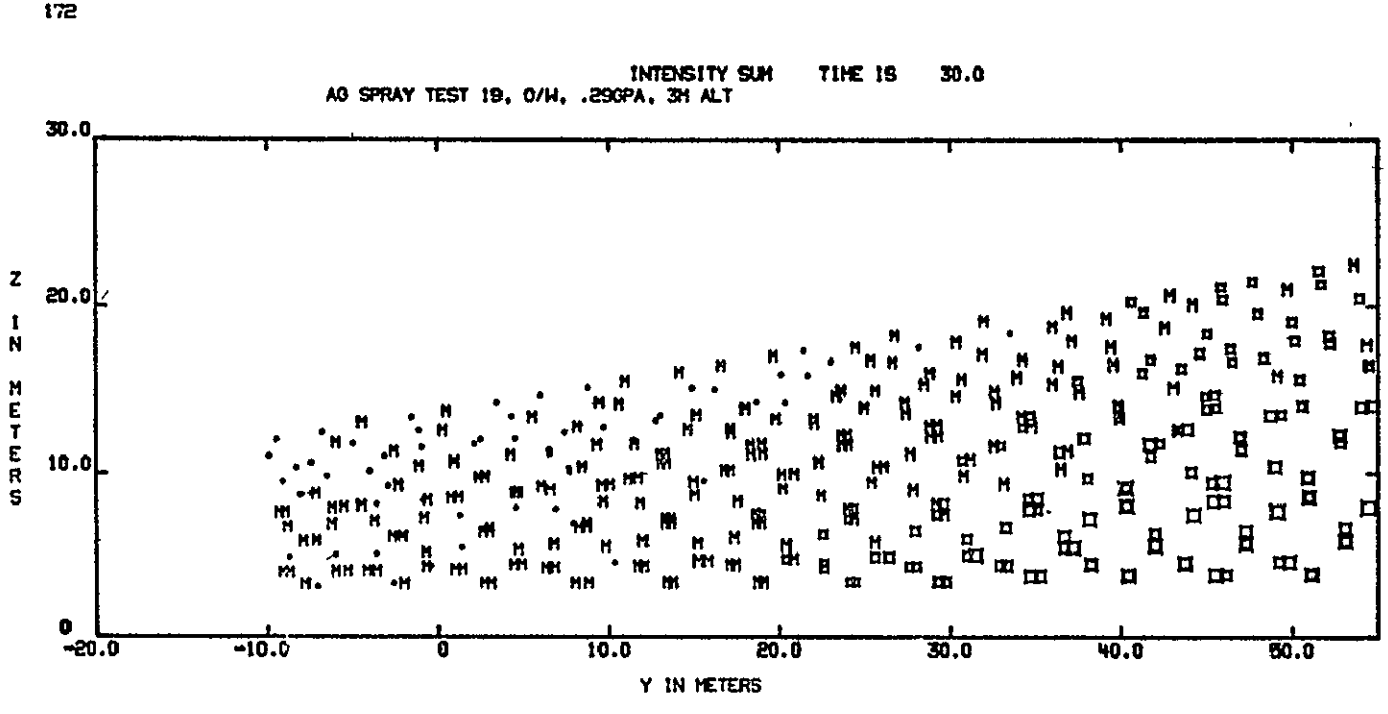
172
INTENSITY SUM TIME IS 30.0
AG SPRAY TEST 19, O/W, .29GPA, 3M ALT
30.0
20.0
10.0
0
Z IN METERS
-20.0
-10.0
0
10.0
20.0
30.0
40.0
50.0
Y IN METERS

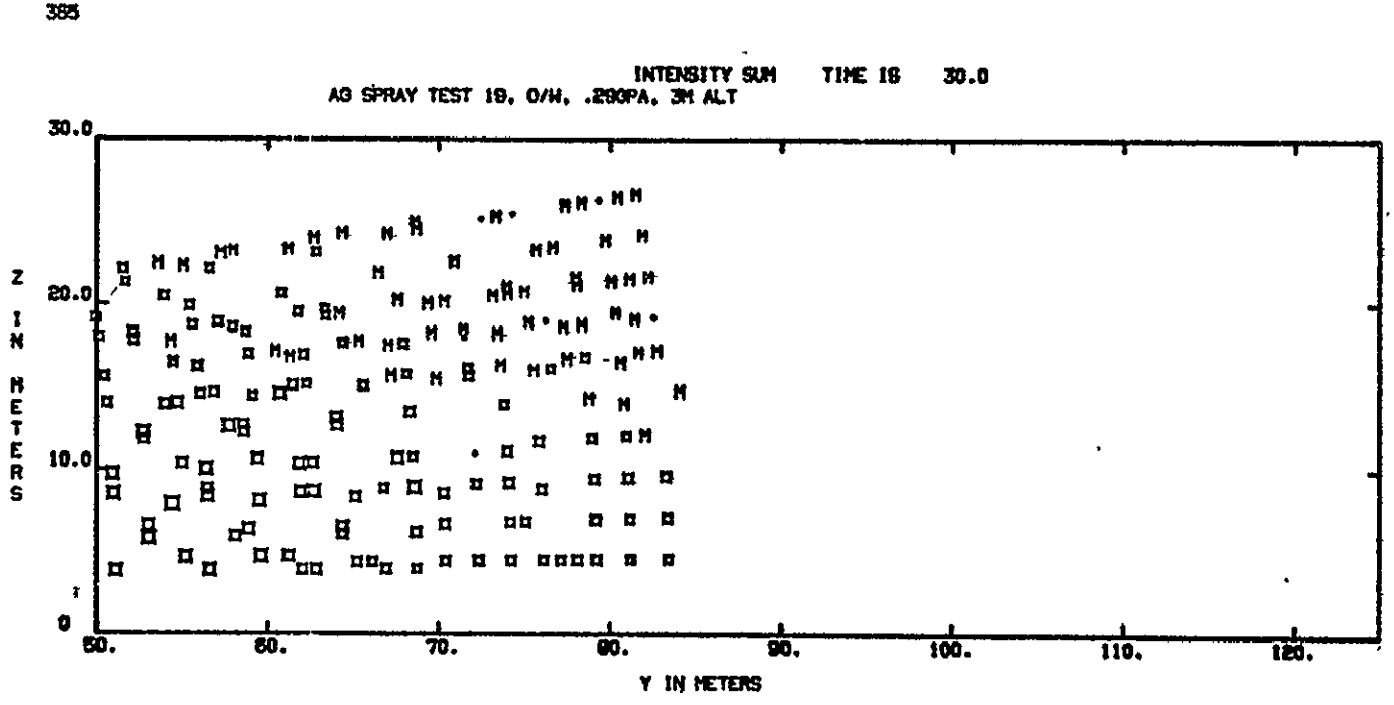
385
INTENSITY SUM TIME IS 30.0
AG SPRAY TEST 19, O/W, .290PA, 3M ALT
30.0
20.0
10.0
0
Z IN METERS
50.
60.
70.
80.
90.
100.
110.
120.
Y IN METERS

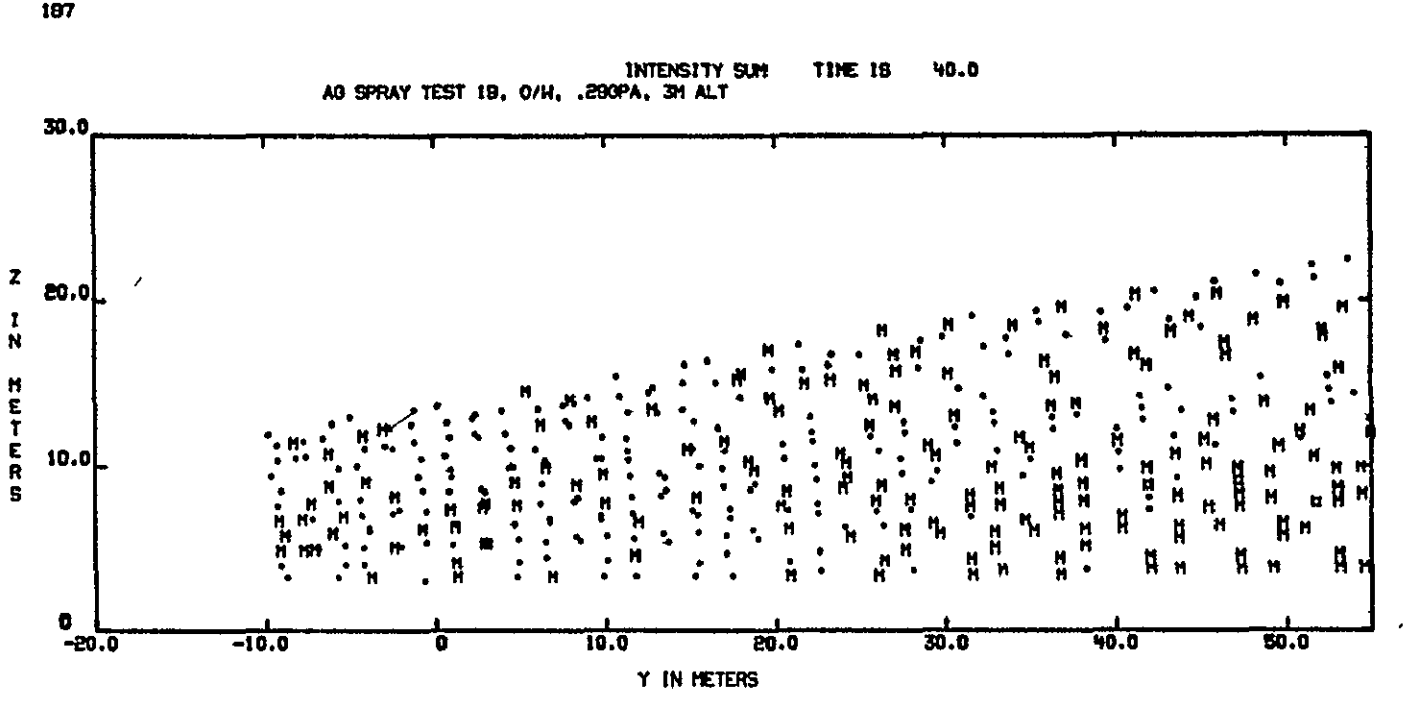
187
INTENSITY SUM TIME IS 40.0
AG SPRAY TEST 18, O/H, .290PA, 3M ALT
30.0
20.0
10.0
0
Z IN METERS
-20.0
-10.0
0
10.0
20.0
30.0
40.0
50.0
Y IN METERS

REPRODUCIBILITY OF THE
ORIGINAL PAGE IS POOR

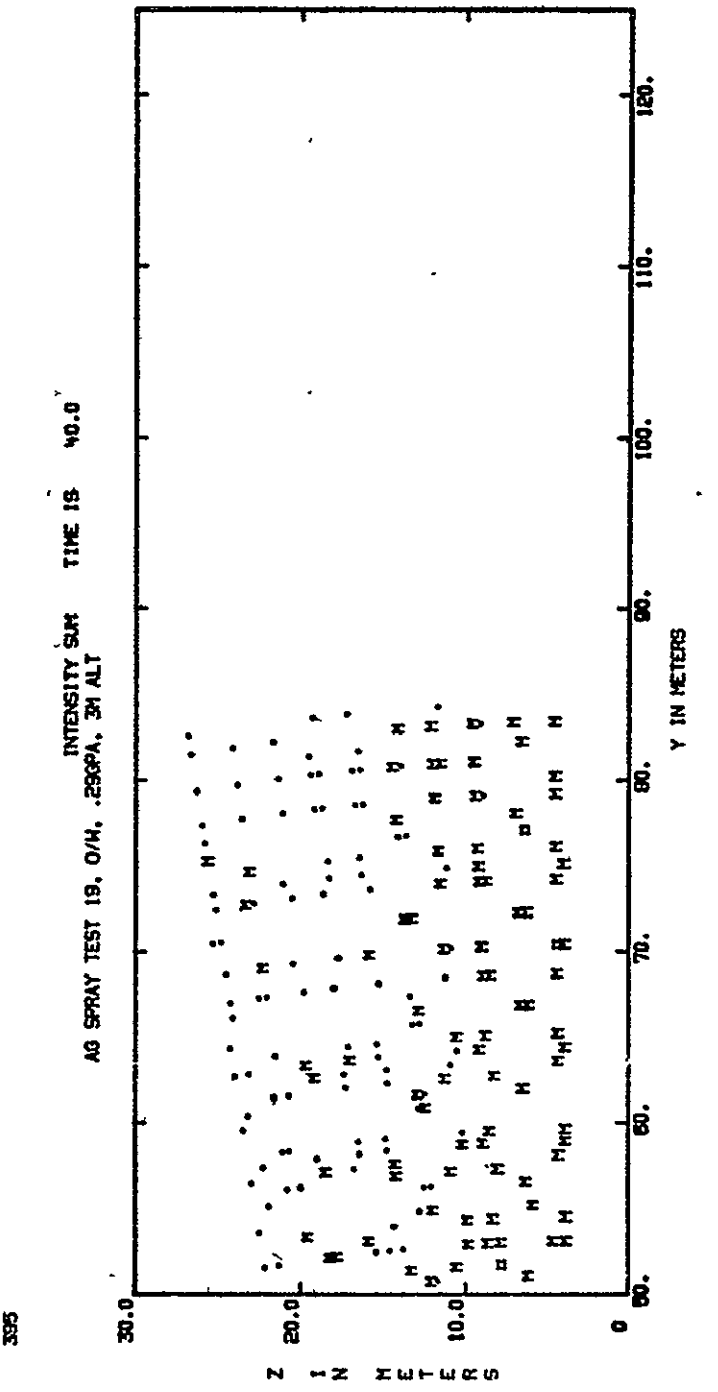

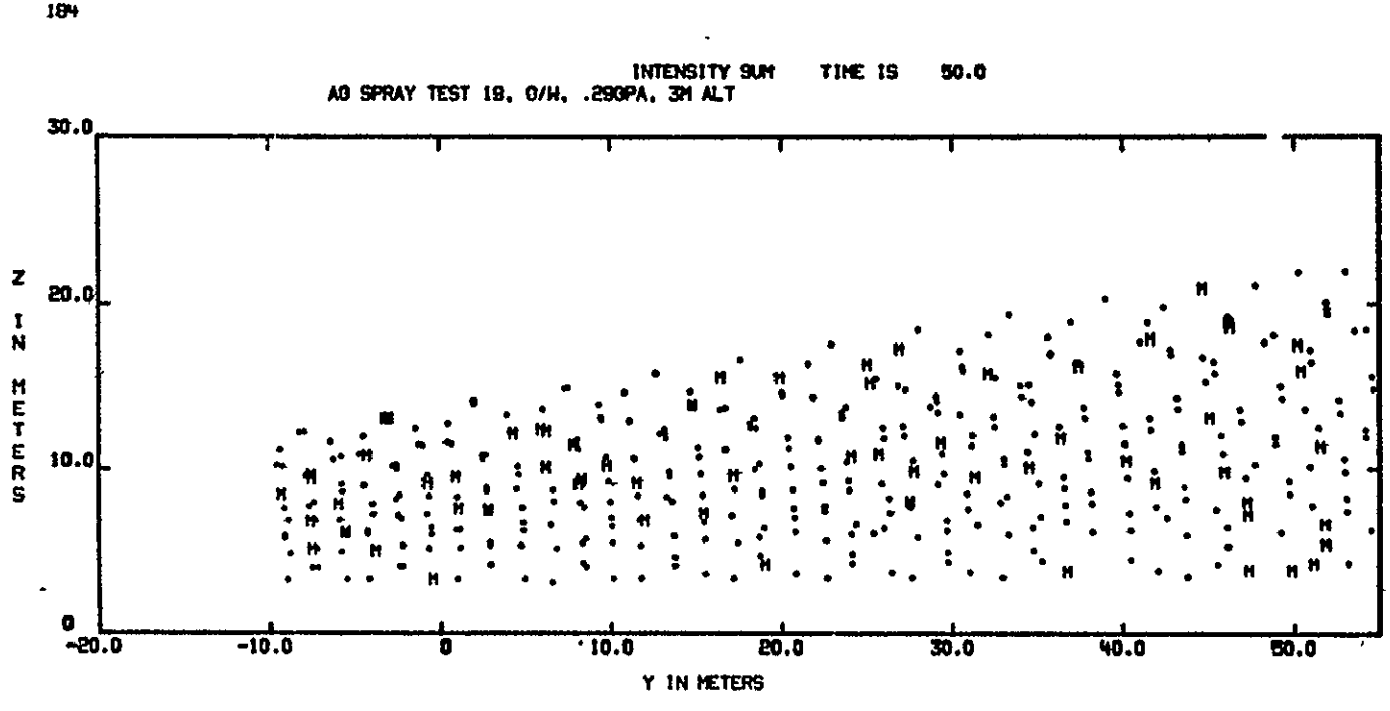
184
INTENSITY SUM TIME IS 50.0
AO SPRAY TEST 18, O/W, .290PA, 3M ALT
30.0
20.0
10.0
0
Z IN METERS
-20.0
-10.0
0
10.0
20.0
30.0
40.0
50.0
Y IN METERS

REPRODUCIBILITY OF THE
ORIGINAL PAGE IS POOR

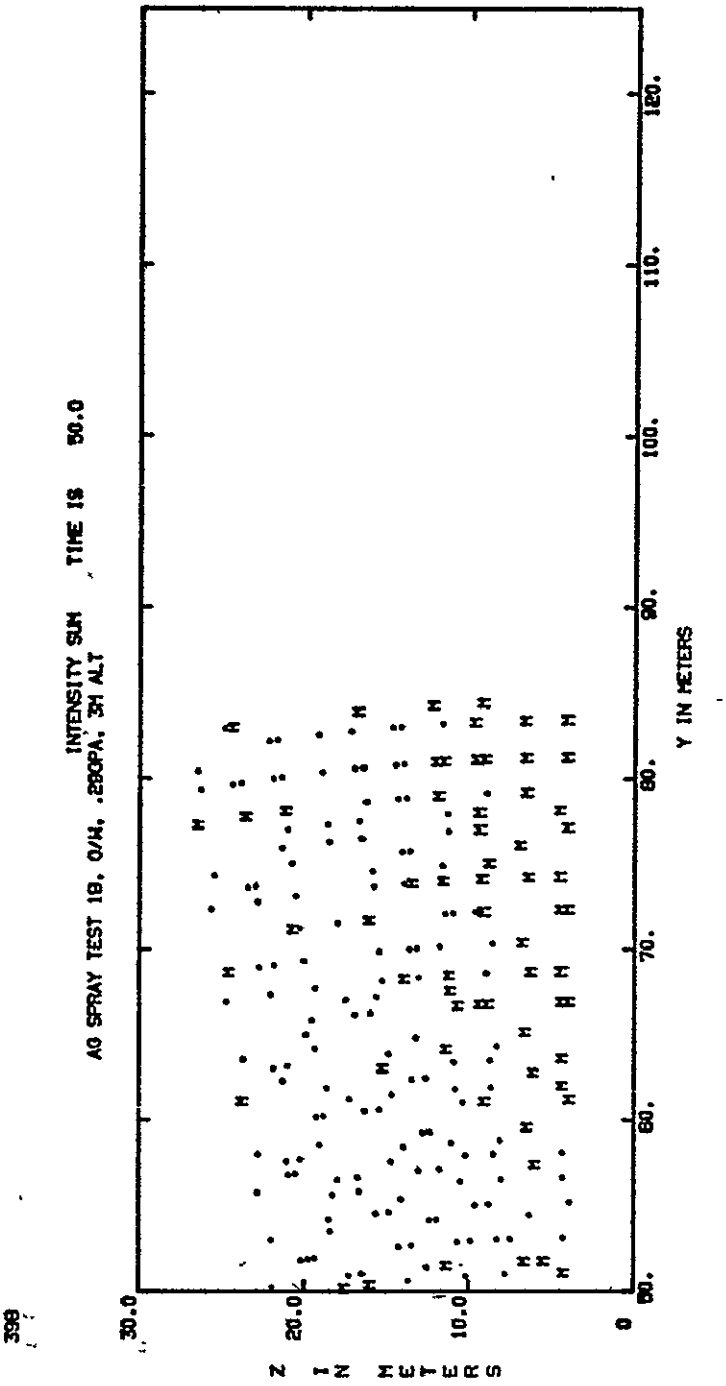

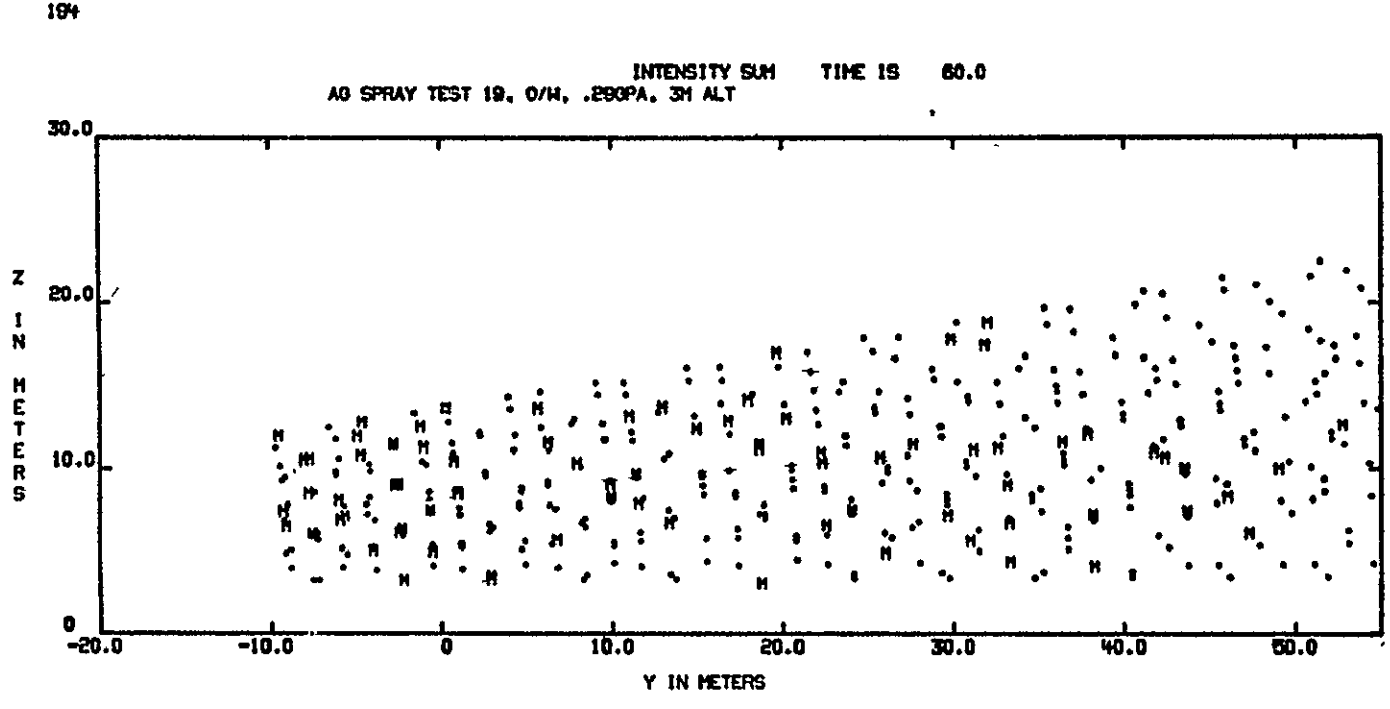
194
INTENSITY SUM TIME IS 60.0
AG SPRAY TEST 19, O/H, .290PA, 3M ALT
30.0
20.0
10.0
0
Z IN METERS
-20.0
-10.0
0
10.0
20.0
30.0
40.0
50.0
Y IN METERS

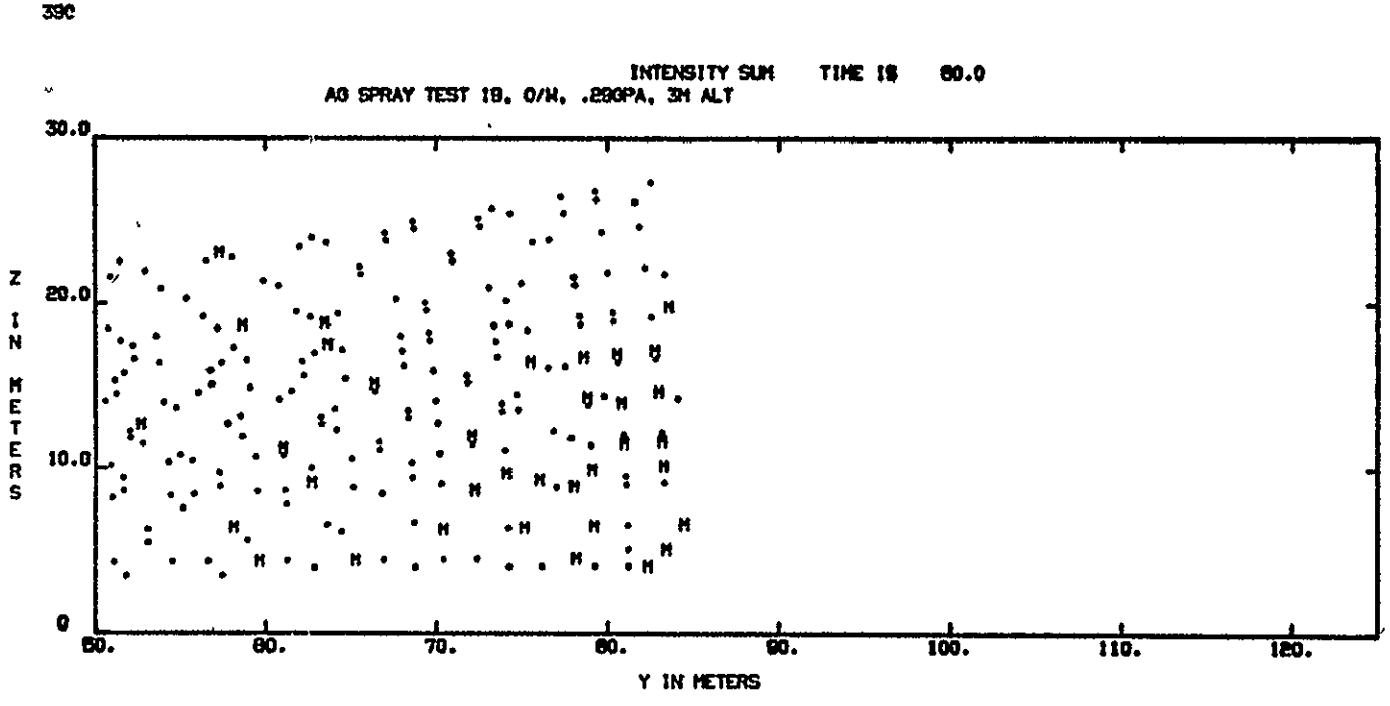
INTENSITY SUM TIME IS 60.0
AG SPRAY TEST 19, O/W, .290PA, 3M ALT
30.0
20.0
10.0
0
Z IN METERS
50.
60.
70.
80.
90.
100.
110.
120.
Y IN METERS

REPRODUCIBILITY OF THE
ORIGINAL PAGE IS POOR

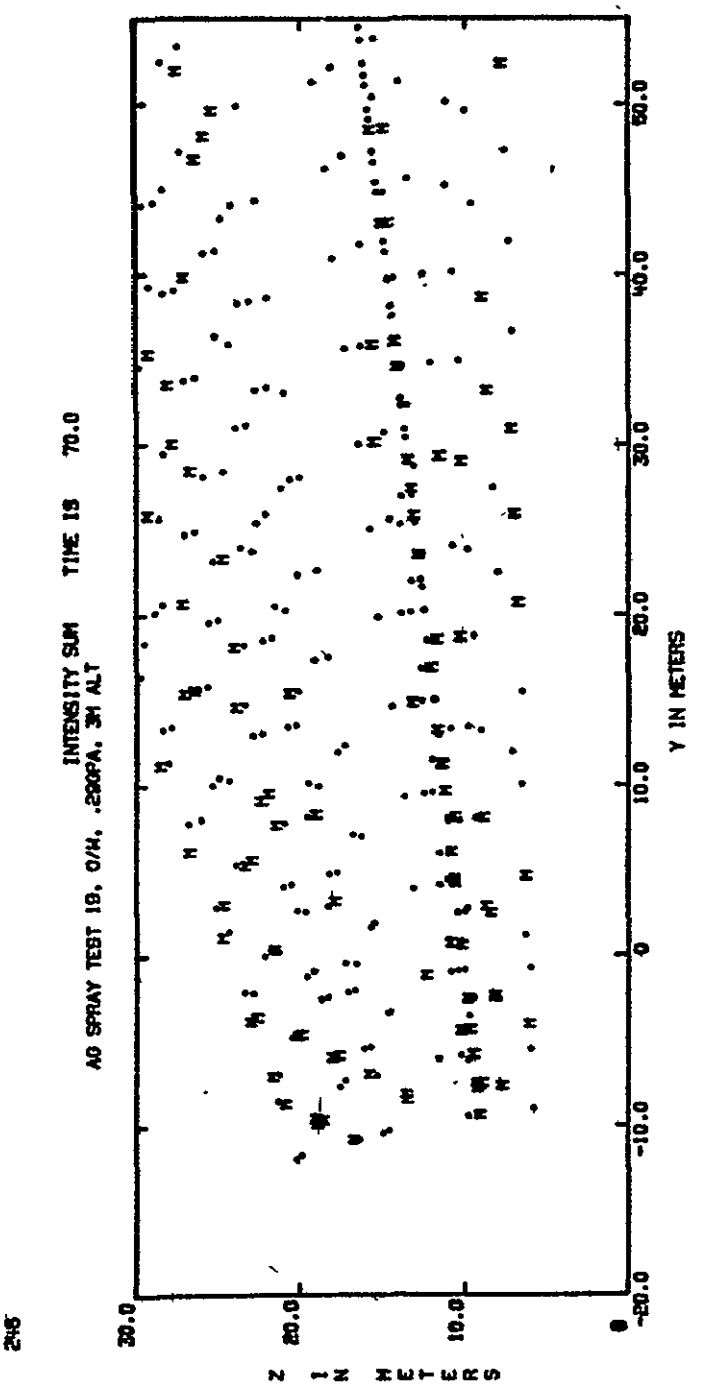

REPRODUCIBILITY OF THE
ORIGINAL PAGE IS POOR

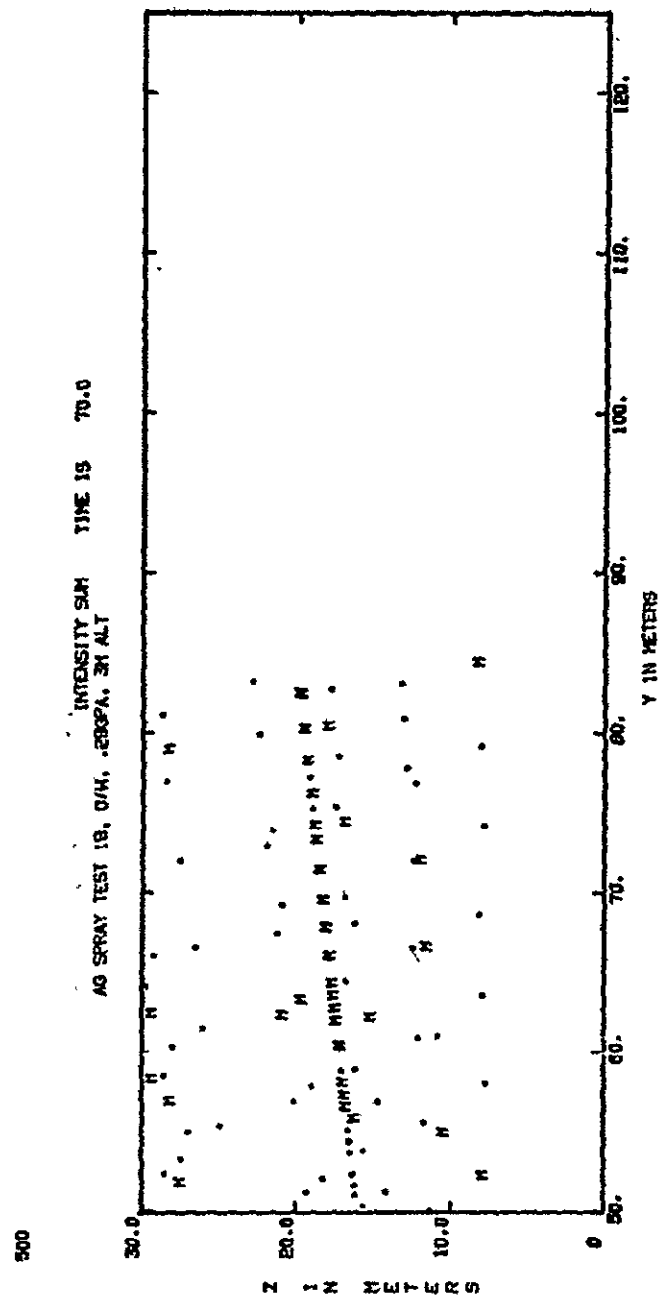

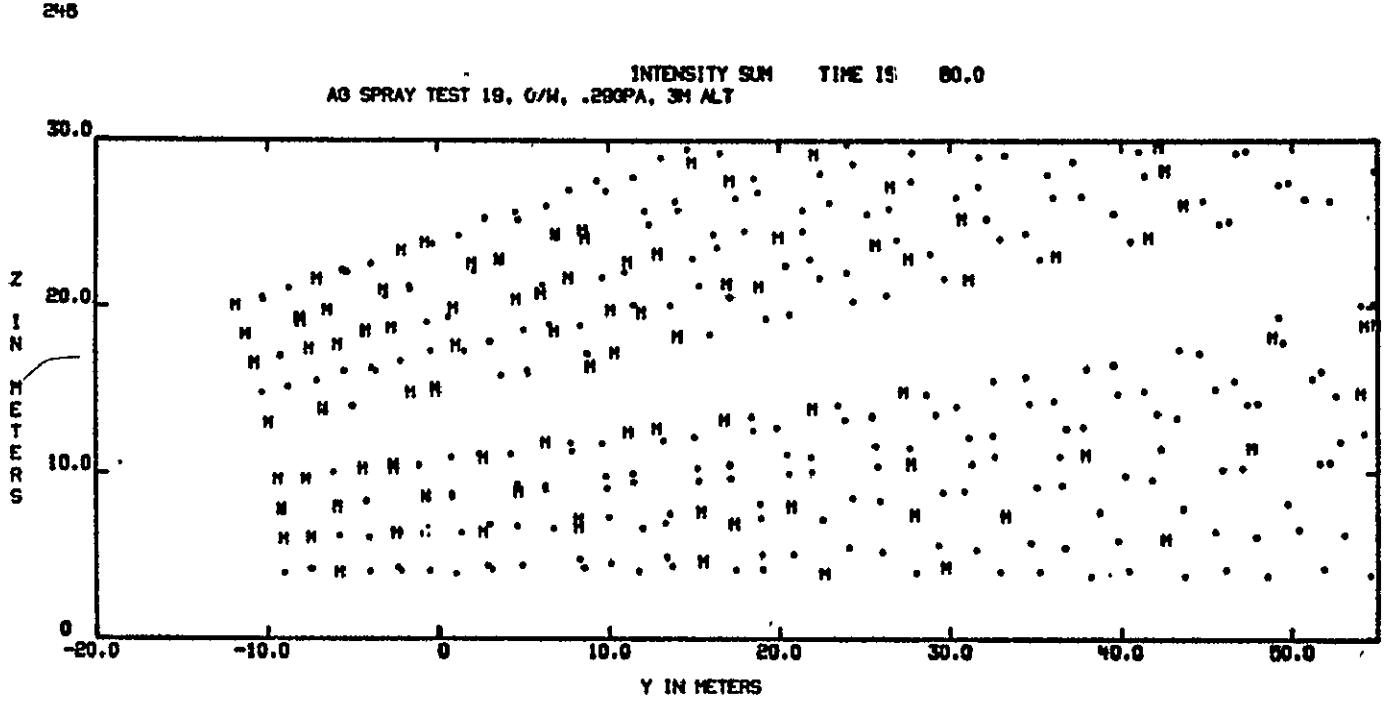
248
INTENSITY SUM TIME IS 80.0
AG SPRAY TEST 19, O/W, .280PA, 3M ALT
30.0
20.0
10.0
0
Z IN METERS
-20.0
-10.0
0
10.0
20.0
30.0
40.0
50.0
Y IN METERS

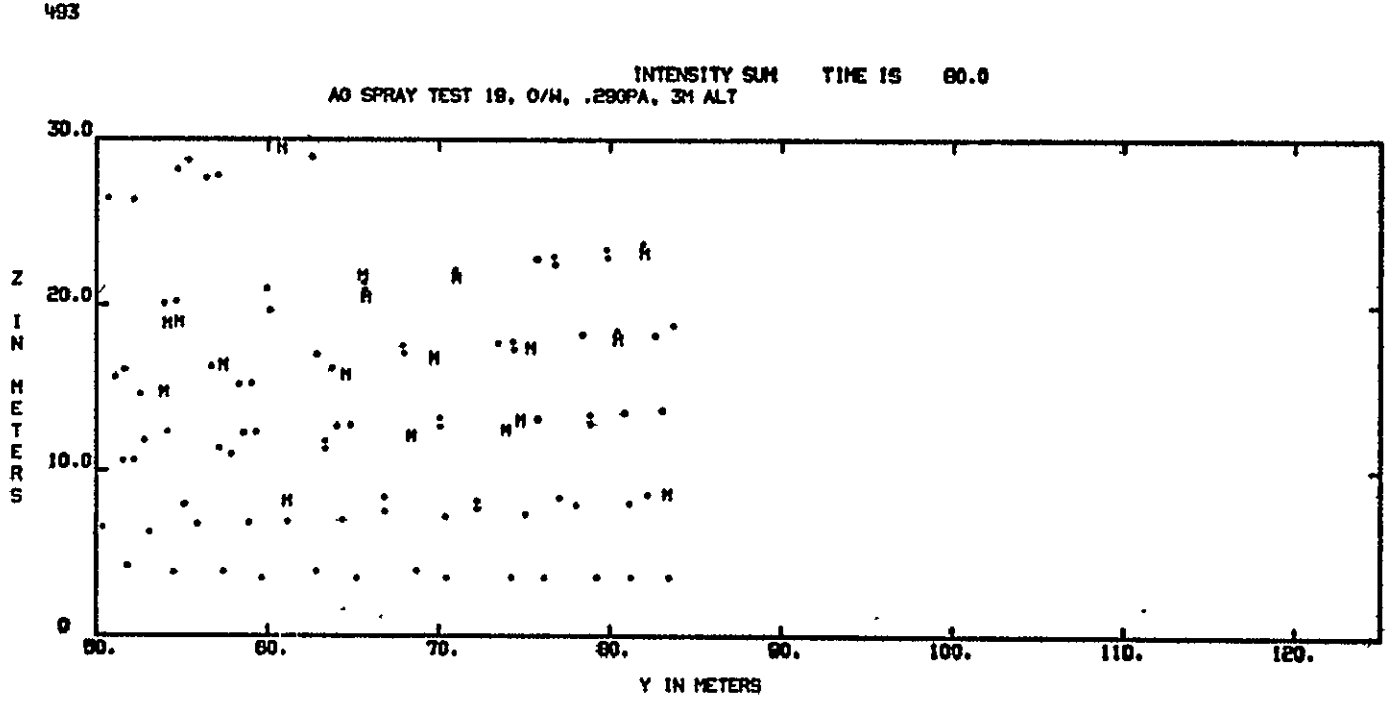
493
INTENSITY SUM TIME IS 60.0
AO SPRAY TEST 19, O/H, .290PA, 3M ALT
30.0
20.0
10.0
0
Z IN METERS
50.
60.
70.
80.
90.
100.
110.
120.
Y IN METERS

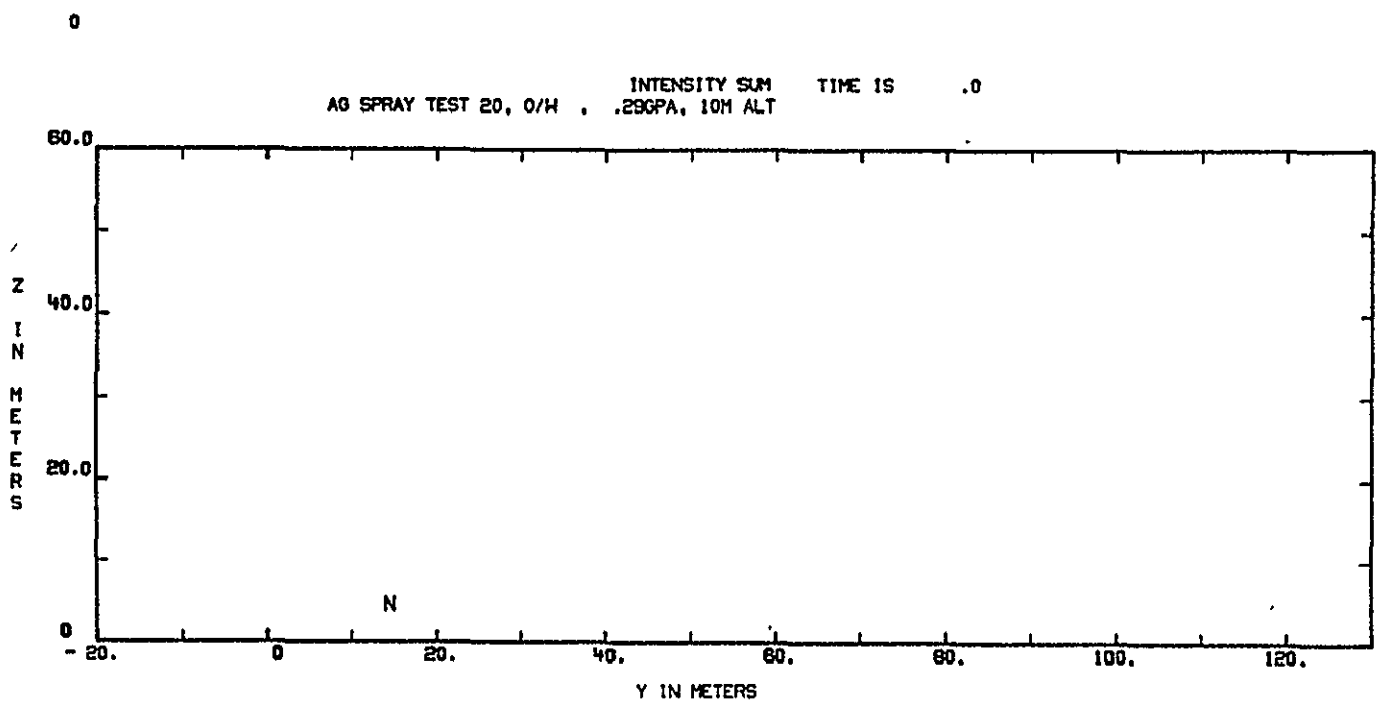
0
INTENSITY SUM TIME IS .0
AG SPRAY TEST 20, O/H , .29GPA, 10M ALT
60.0
40.0
20.0
0
Z IN METERS
N
- 20.
0
20.
40.
60.
80.
100.
120.
Y IN METERS

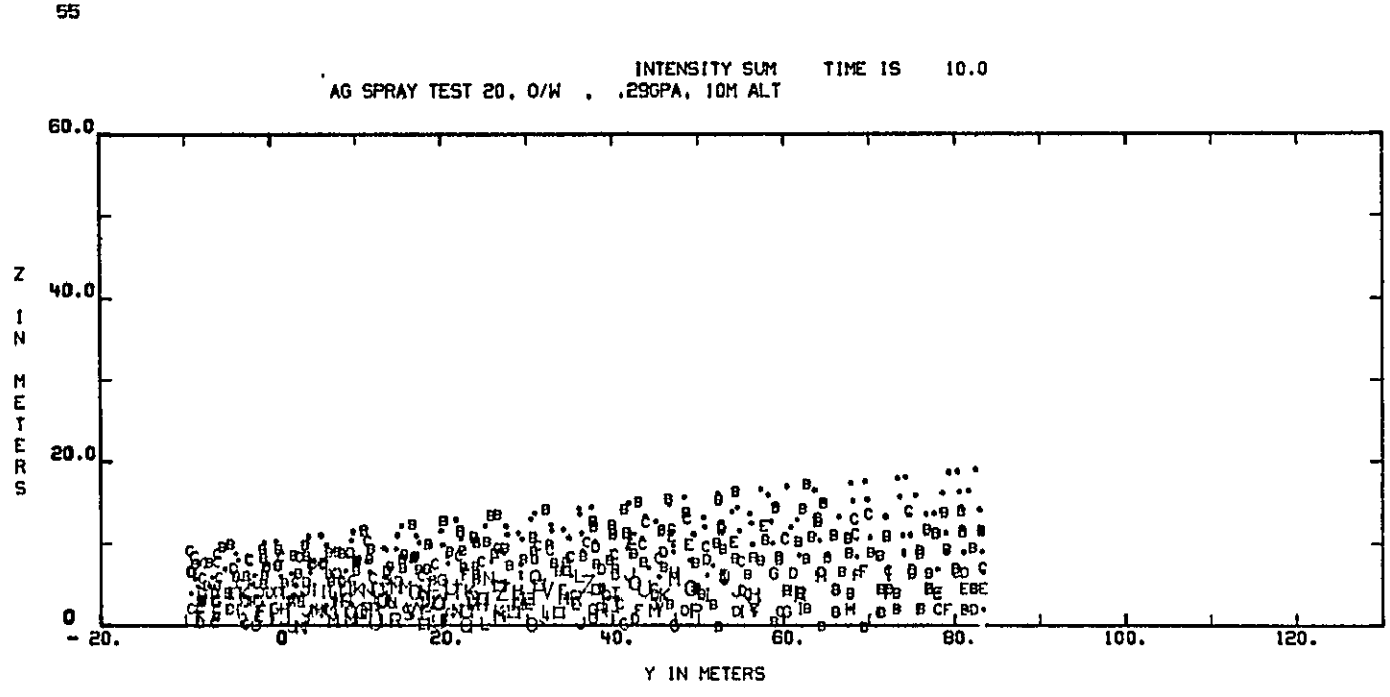
55
INTENSITY SUM TIME IS 10.0
AG SPRAY TEST 20, O/W , .29GPA, 10M ALT
60.0
40.0
20.0
0
Z IN METERS
-20.
0
20.
40.
60.
80.
100.
120.
Y IN METERS

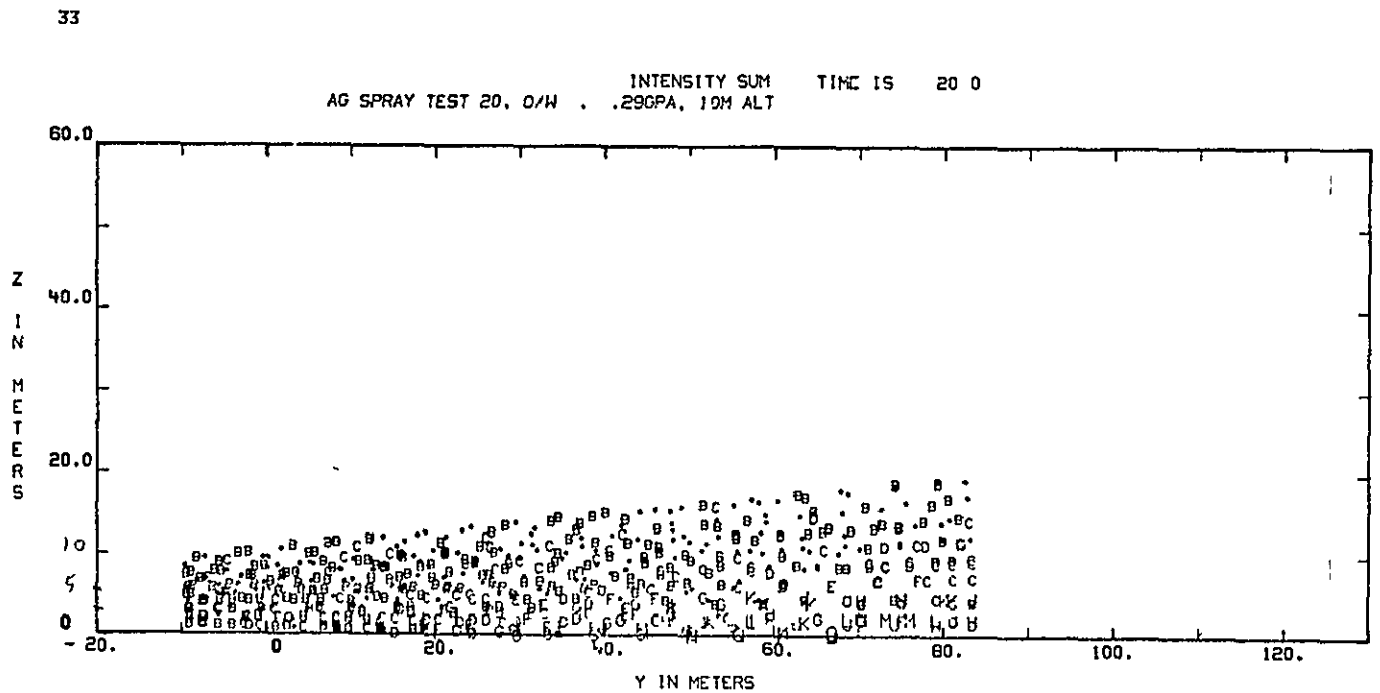
33
INTENSITY SUM TIME IS 20 0
AG SPRAY TEST 20, O/W . .29GPA, 10M ALT
60.0
40.0
20.0
10
5
0
Z IN METERS
-20.
0
20.
40.
60.
80.
100.
120.
Y IN METERS

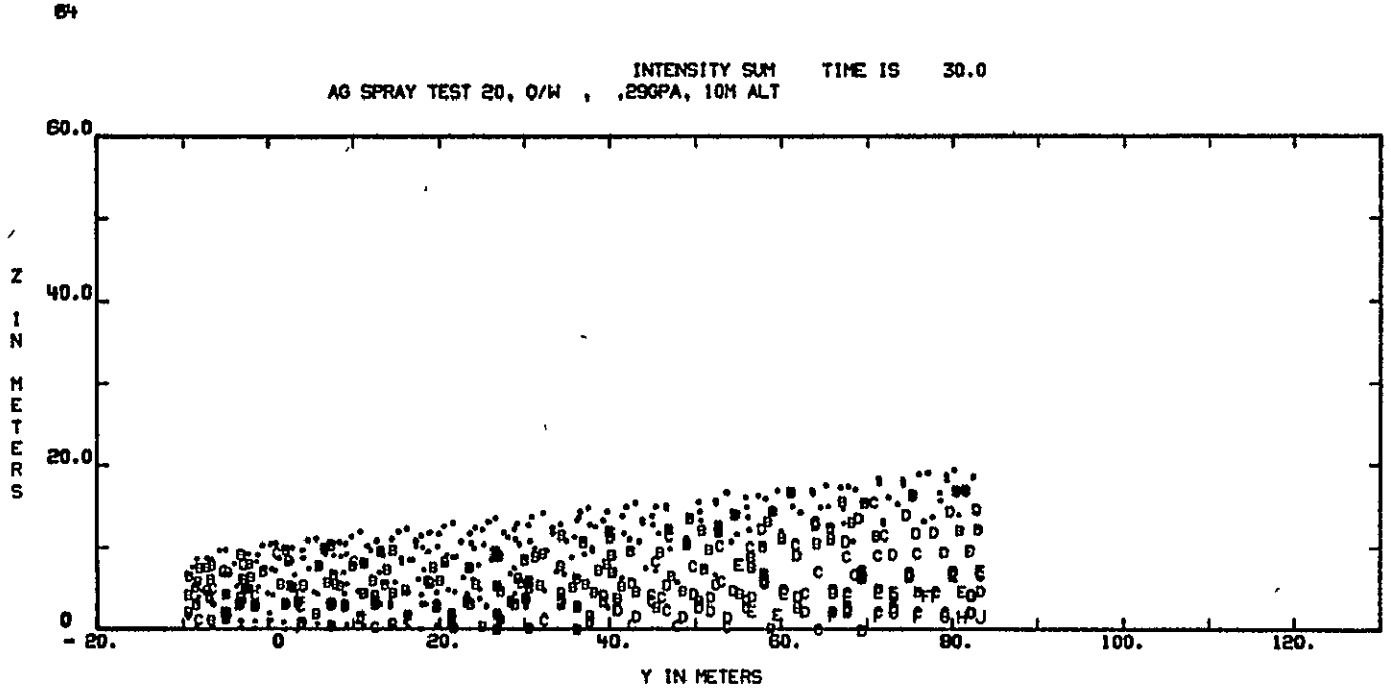
64
INTENSITY SUM TIME IS 30.0
AG SPRAY TEST 20, O/W , .29GPA, 10M ALT
60.0
40.0
20.0
0
Z IN METERS
-20.
0
20.
40.
60.
80.
100.
120.
Y IN METERS

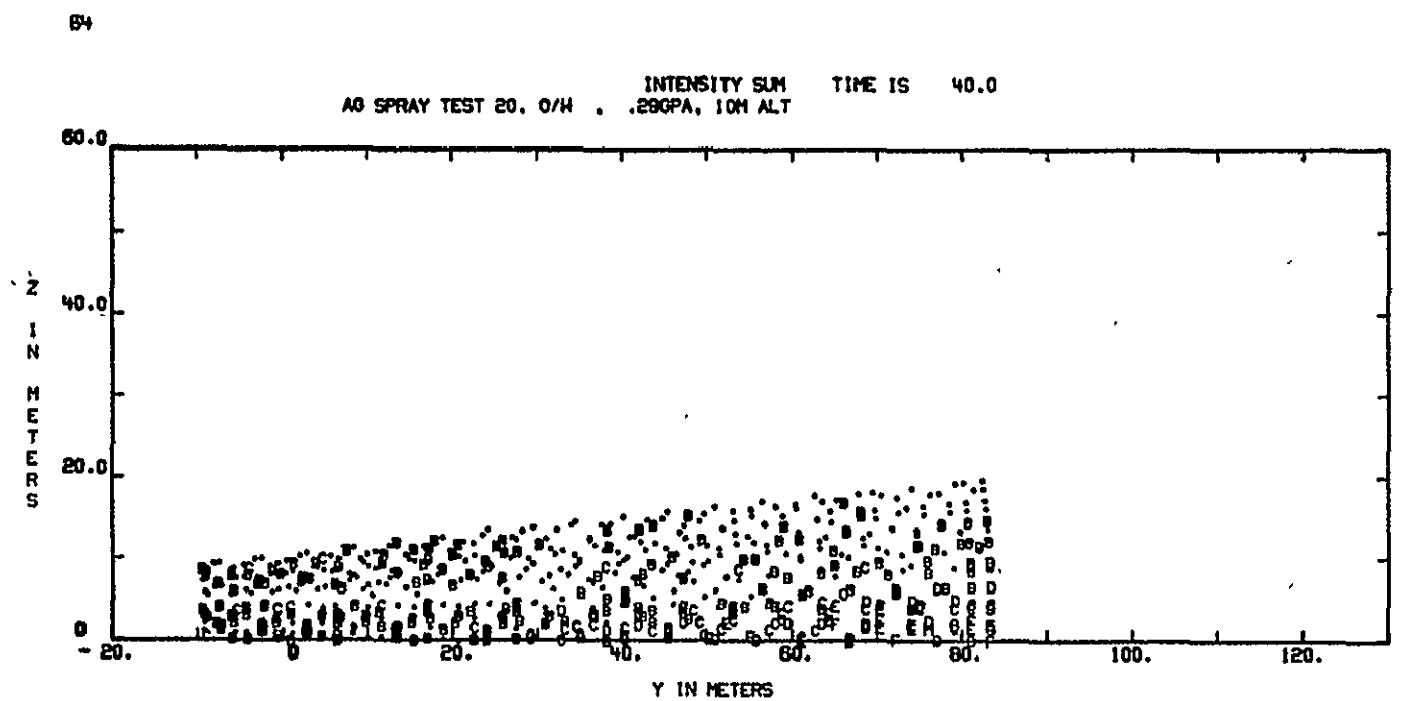
B4
INTENSITY SUM TIME IS 40.0
AG SPRAY TEST 20. O/H . .29GPA, 10M ALT
60.0
40.0
20.0
0
Z IN METERS
-20.
0
20.
40.
60.
80.
100.
120.
Y IN METERS

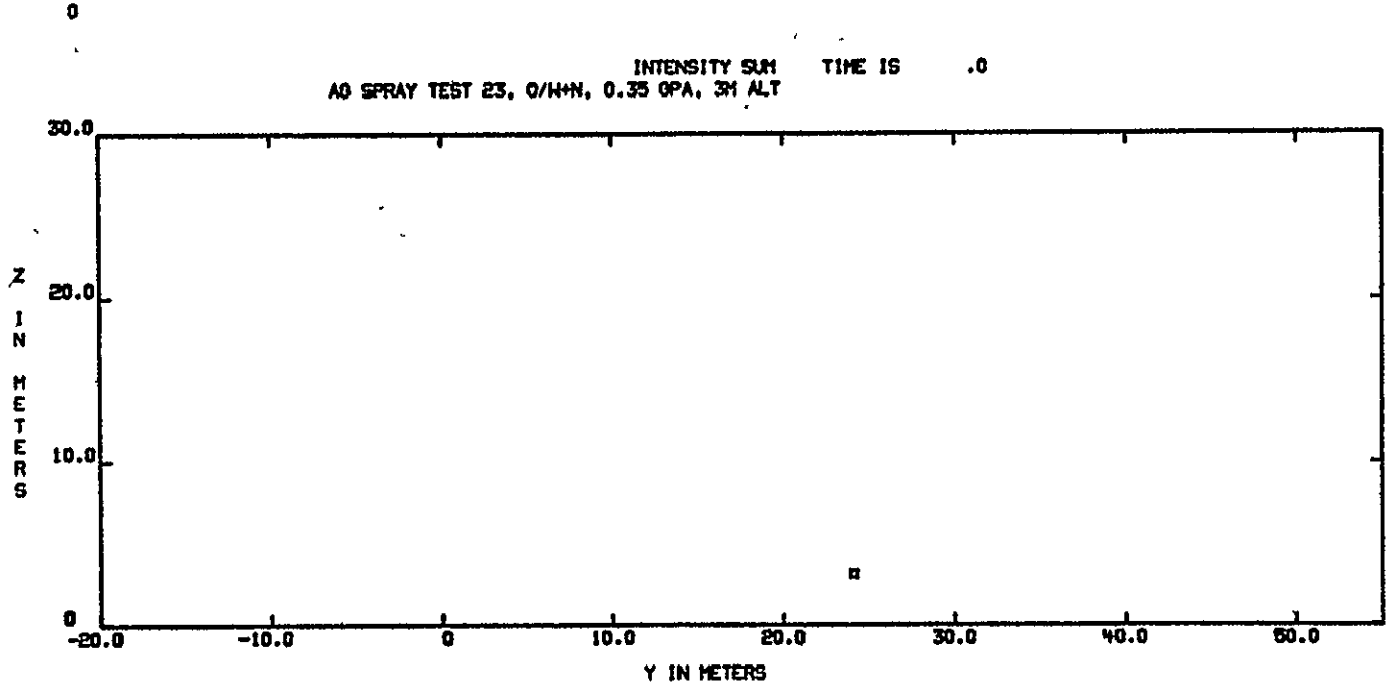
INTENSITY SUM TIME IS .0
A0 SPRAY TEST 23, O/W+N, 0.35 GPA, 3M ALT
30.0
20.0
10.0
0
Z IN METERS
-20.0
-10.0
0
10.0
20.0
30.0
40.0
50.0
Y IN METERS

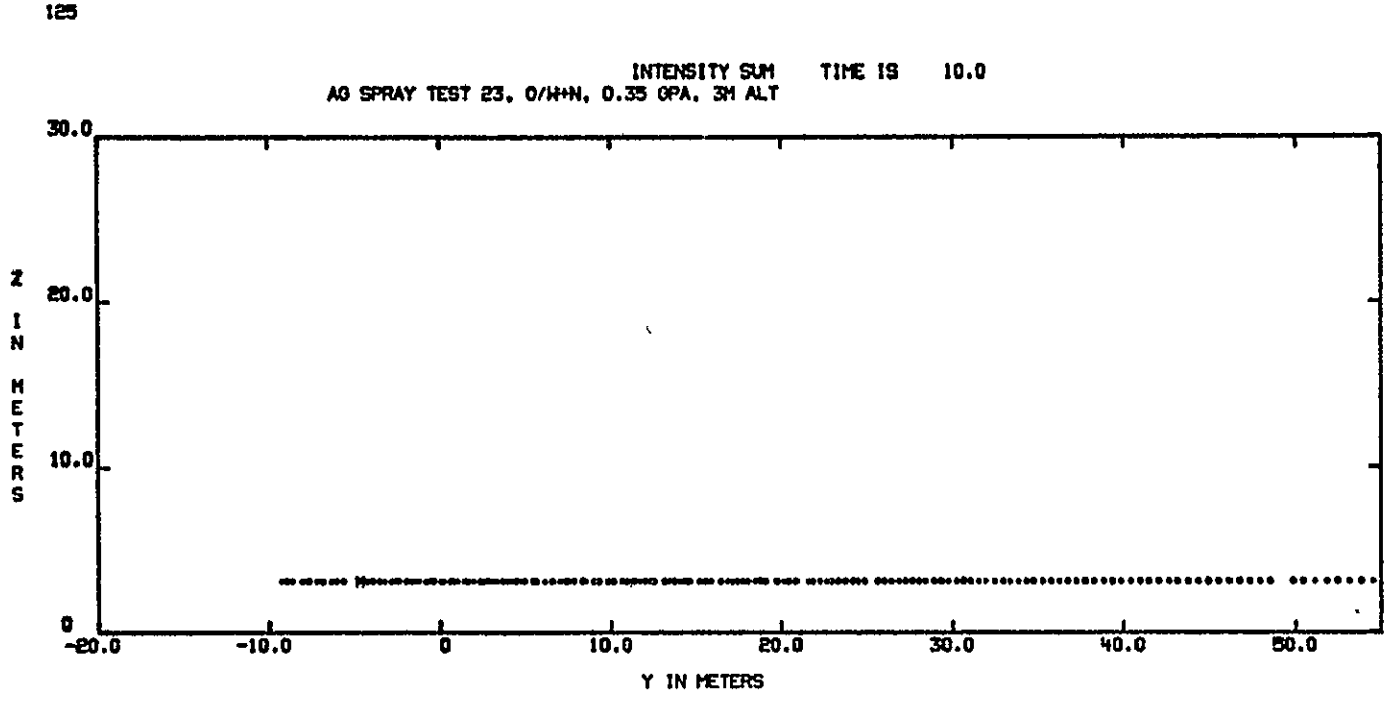
125
INTENSITY SUM TIME IS 10.0
AG SPRAY TEST 23, O/H+N, 0.35 GPA, 3M ALT
30.0
20.0
10.0
0
Z IN METERS
-20.0
-10.0
0
10.0
20.0
30.0
40.0
50.0
Y IN METERS

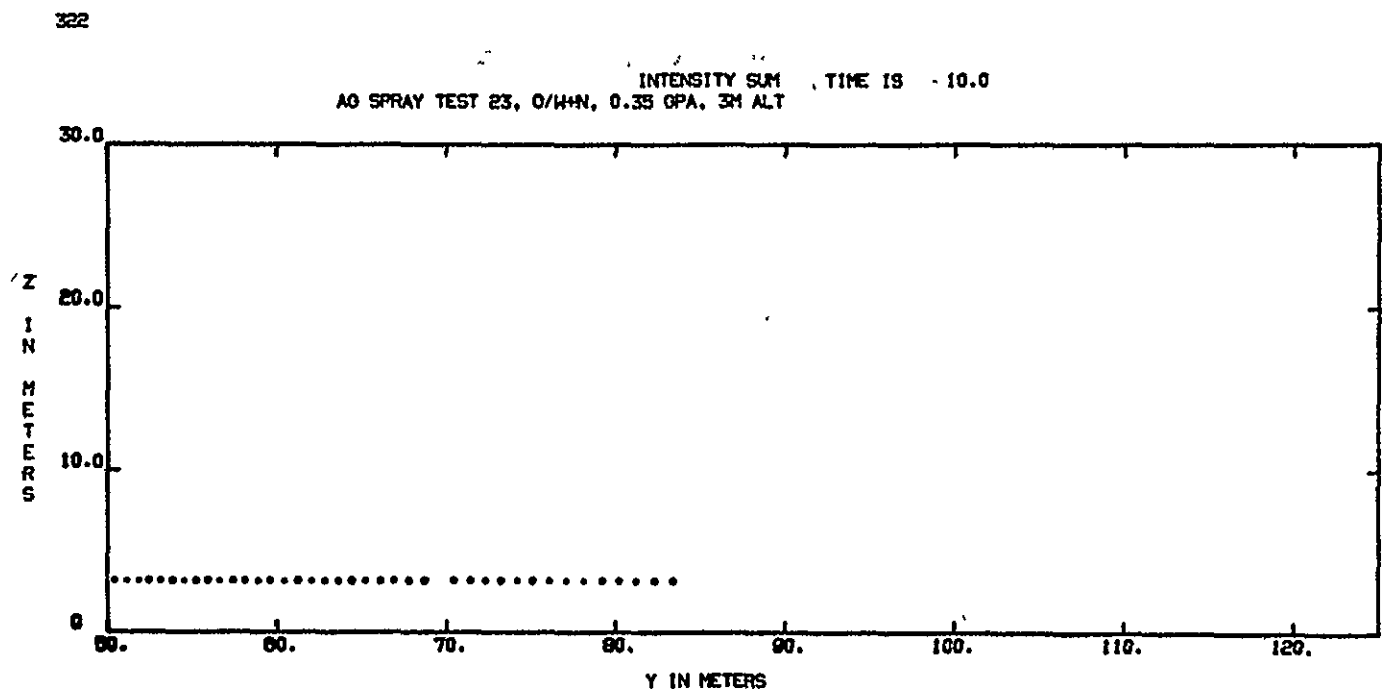
322
INTENSITY SUM , TIME IS -10.0
AO SPRAY TEST 23, O/HHN, 0.35 GPA, 3M ALT
30.0
20.0
10.0
0
Z IN METERS
50.
60.
70.
80.
90.
100.
110.
120.
Y IN METERS

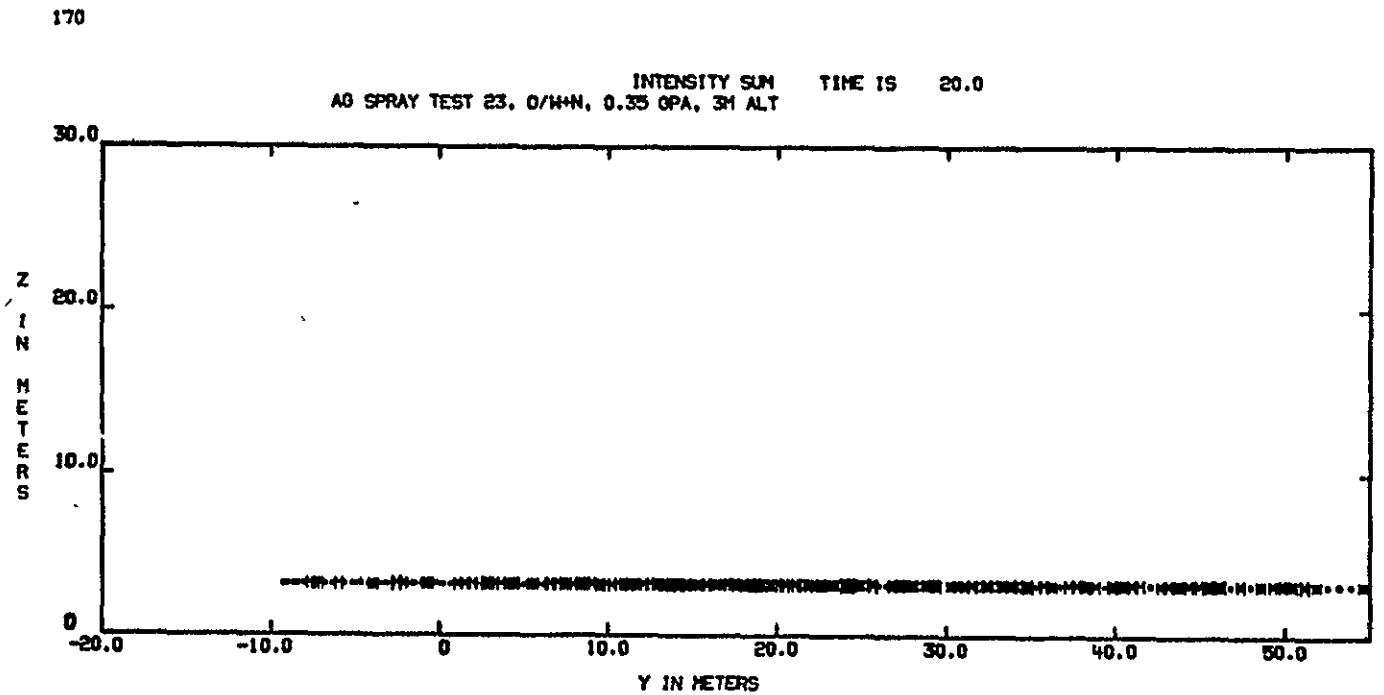
170
INTENSITY SUM TIME IS 20.0
AG SPRAY TEST 23, O/H+N, 0.35 GPA, 3M ALT
30.0
20.0
10.0
0
Z IN METERS
-20.0
-10.0
0
10.0
20.0
30.0
40.0
50.0
Y IN METERS

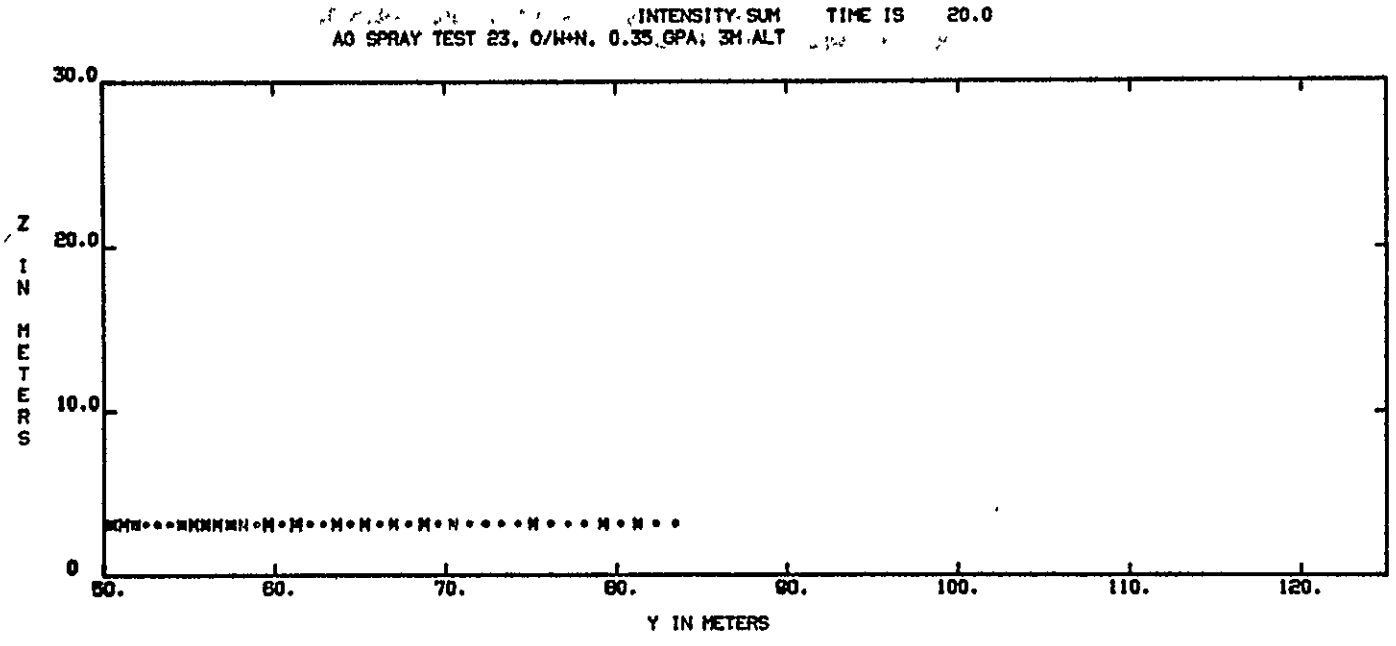
INTENSITY SUM TIME IS 20.0
AO SPRAY TEST 23, O/W+N, 0.35 GPA; 3M ALT
30.0
20.0
10.0
0
Z IN METERS
50.
60.
70.
80.
90.
100.
110.
120.
Y IN METERS

C-3

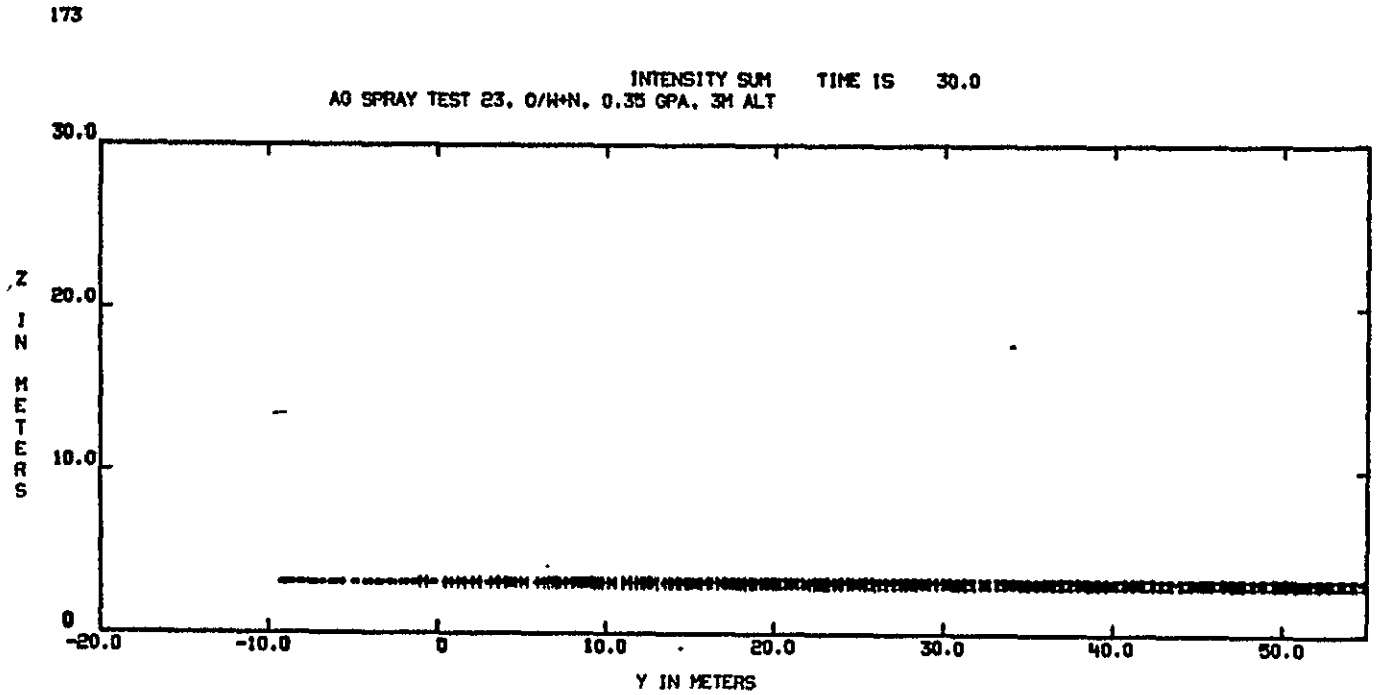
173
INTENSITY SUM TIME IS 30.0
AO SPRAY TEST 23, O/H+N, 0.35 GPA, 3M ALT
30.0
20.0
10.0
0
Z IN METERS
-20.0
-10.0
0
10.0
20.0
30.0
40.0
50.0
Y IN METERS

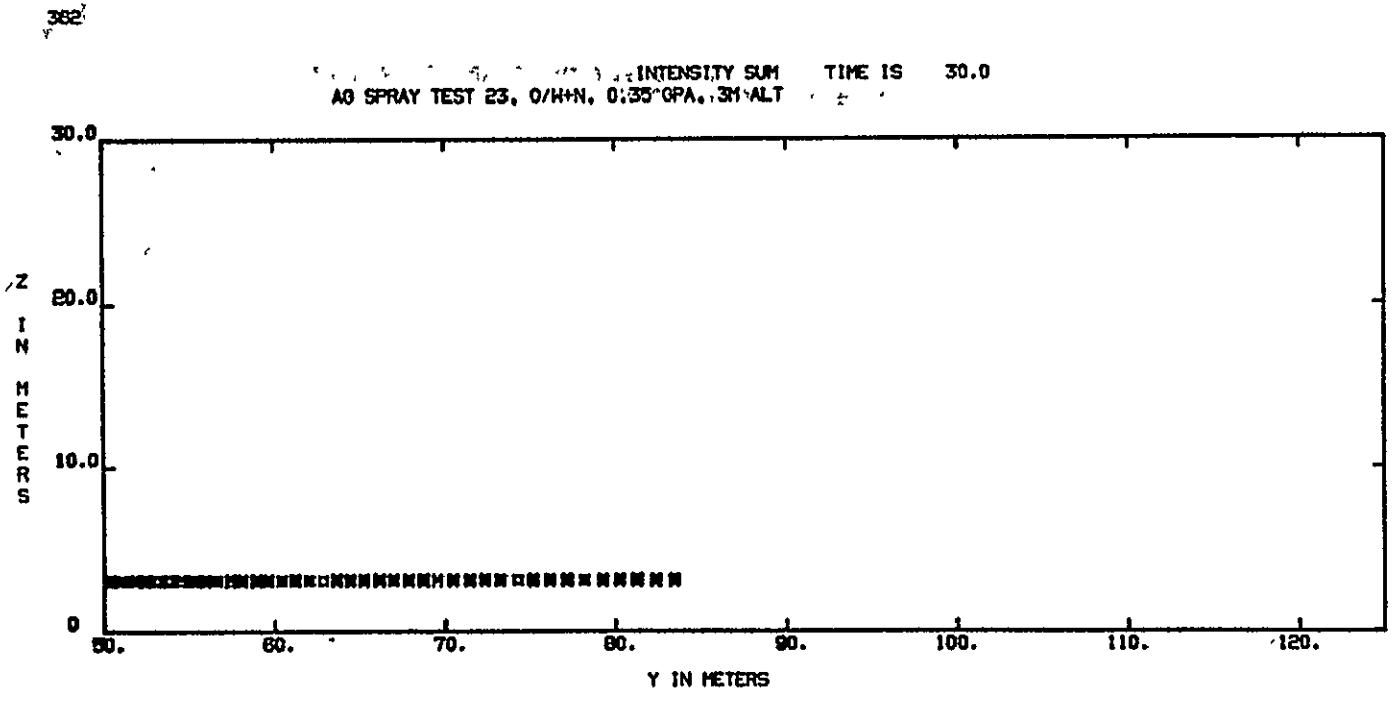
382
INTENSITY SUM TIME IS 30.0
A0 SPRAY TEST 23, O/H+N, 0.35 GPA, 3M ALT
30.0
20.0
10.0
0
Z IN METERS
50.
60.
70.
80.
90.
100.
110.
120.
Y IN METERS

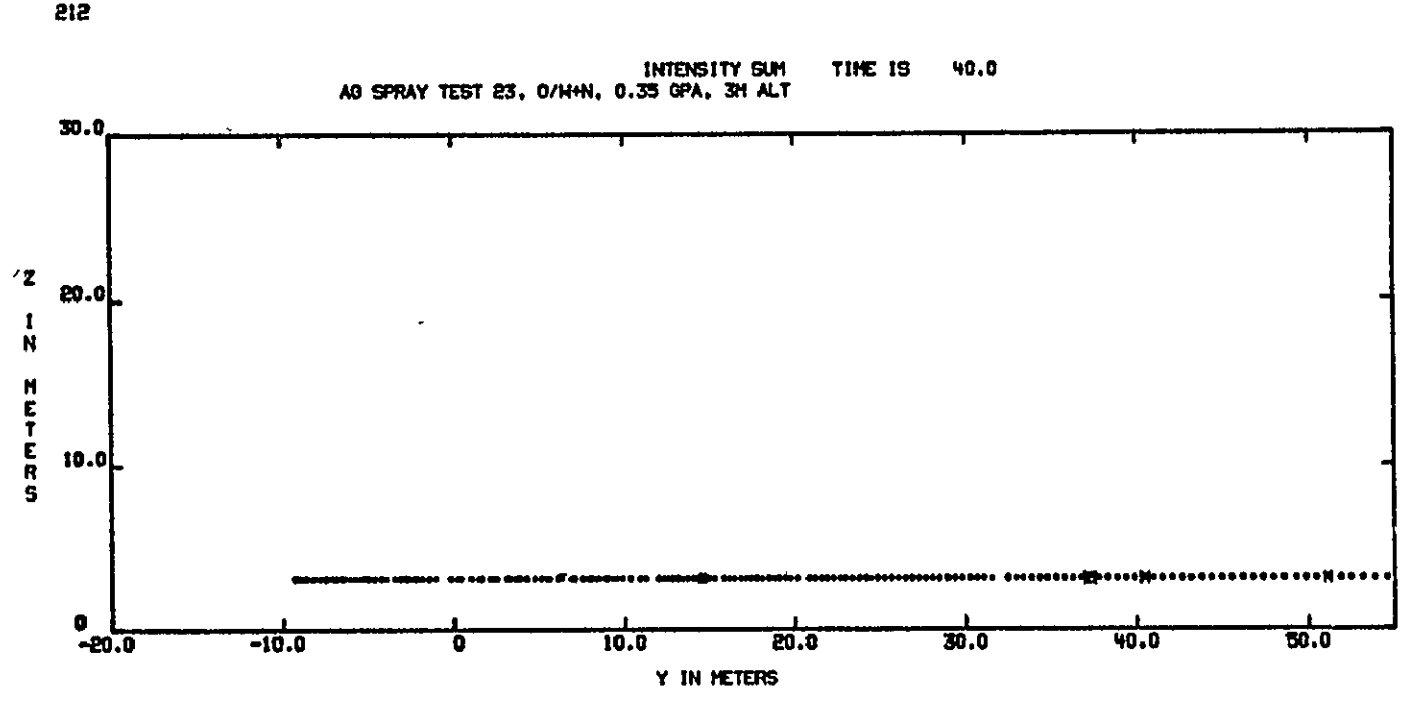
212
INTENSITY SUM TIME IS 40.0
AG SPRAY TEST 23, O/W+N, 0.35 GPA, 3M ALT
30.0
20.0
10.0
0
Z IN METERS
-20.0
-10.0
0
10.0
20.0
30.0
40.0
50.0
Y IN METERS

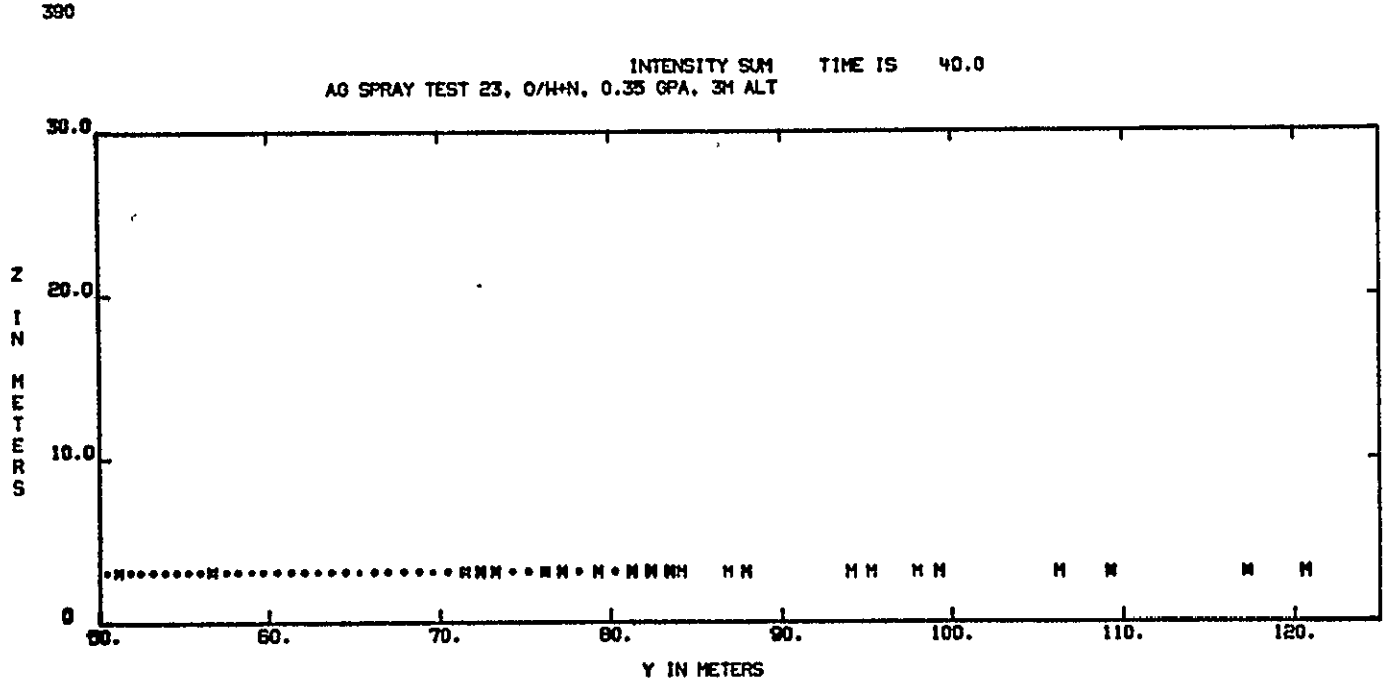
390
INTENSITY SUM TIME IS 40.0
AG SPRAY TEST 23, O/H+N, 0.35 GPA, 3M ALT
30.0
20.0
10.0
0
Z IN METERS
50.
60.
70.
80.
90.
100.
110.
120.
Y IN METERS

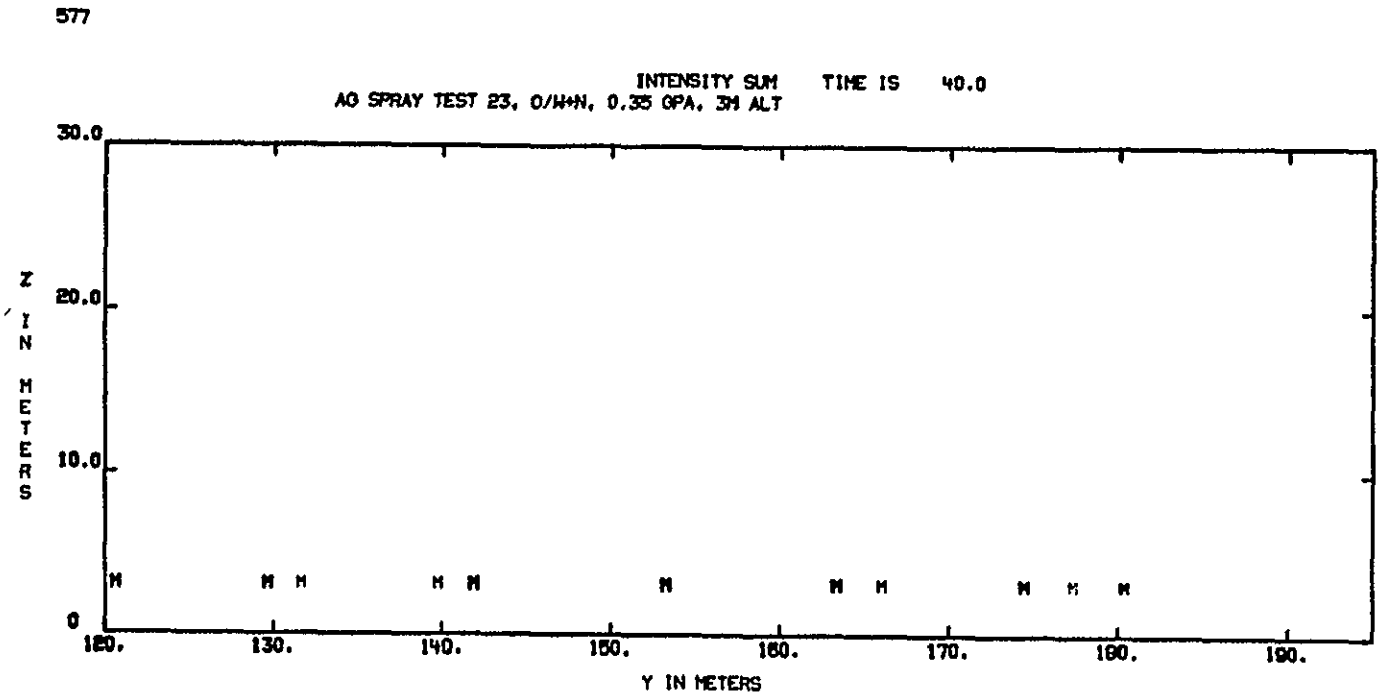
577
INTENSITY SUM TIME IS 40.0
AG SPRAY TEST 23, O/W+N, 0.35 GPA, 3M ALT
30.0
20.0
10.0
0
Z IN METERS
120.
130.
140.
150.
160.
170.
180.
190.
Y IN METERS

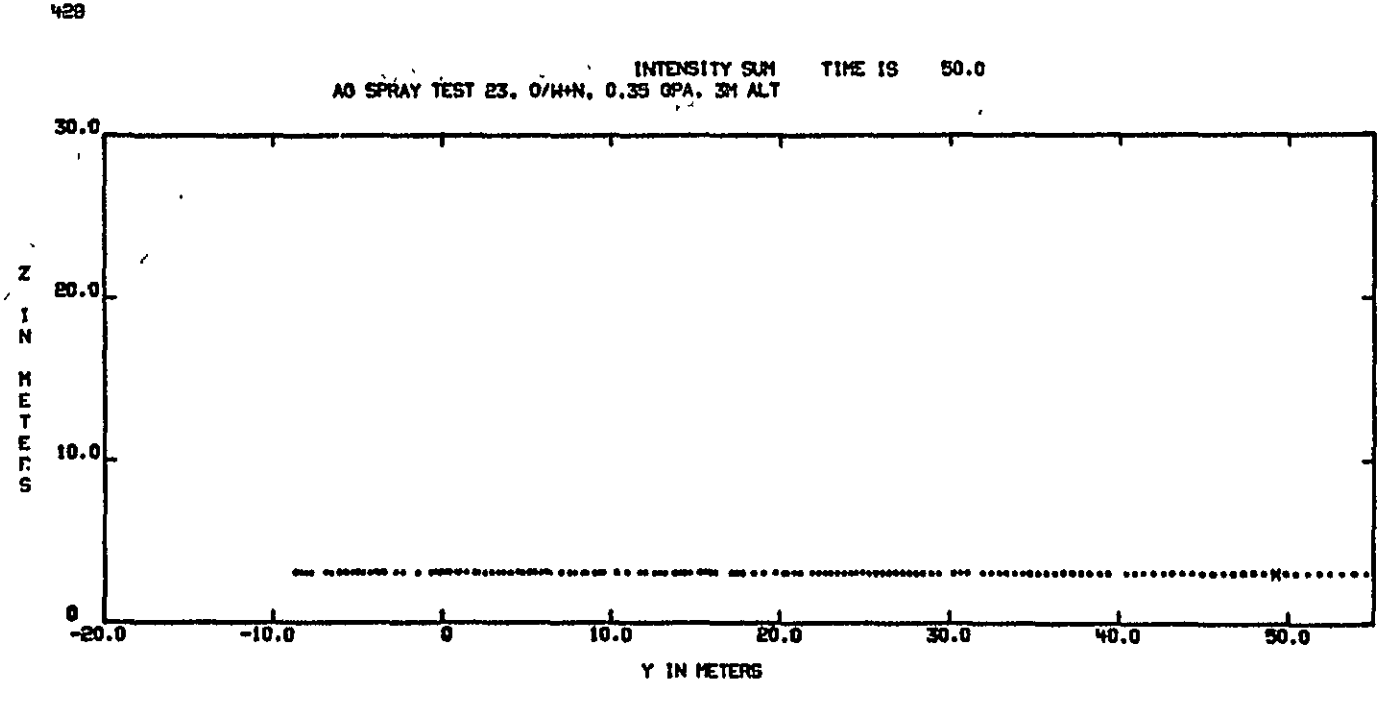
428
INTENSITY SUM TIME IS 50.0
AG SPRAY TEST 23, O/W+N, 0.35 GPA, 3M ALT
30.0
20.0
10.0
0
Z IN METERS
-20.0
-10.0
0
10.0
20.0
30.0
40.0
50.0
Y IN METERS

REPRODUCIBILITY OF THE
ORIGINAL PAGE IS POOR

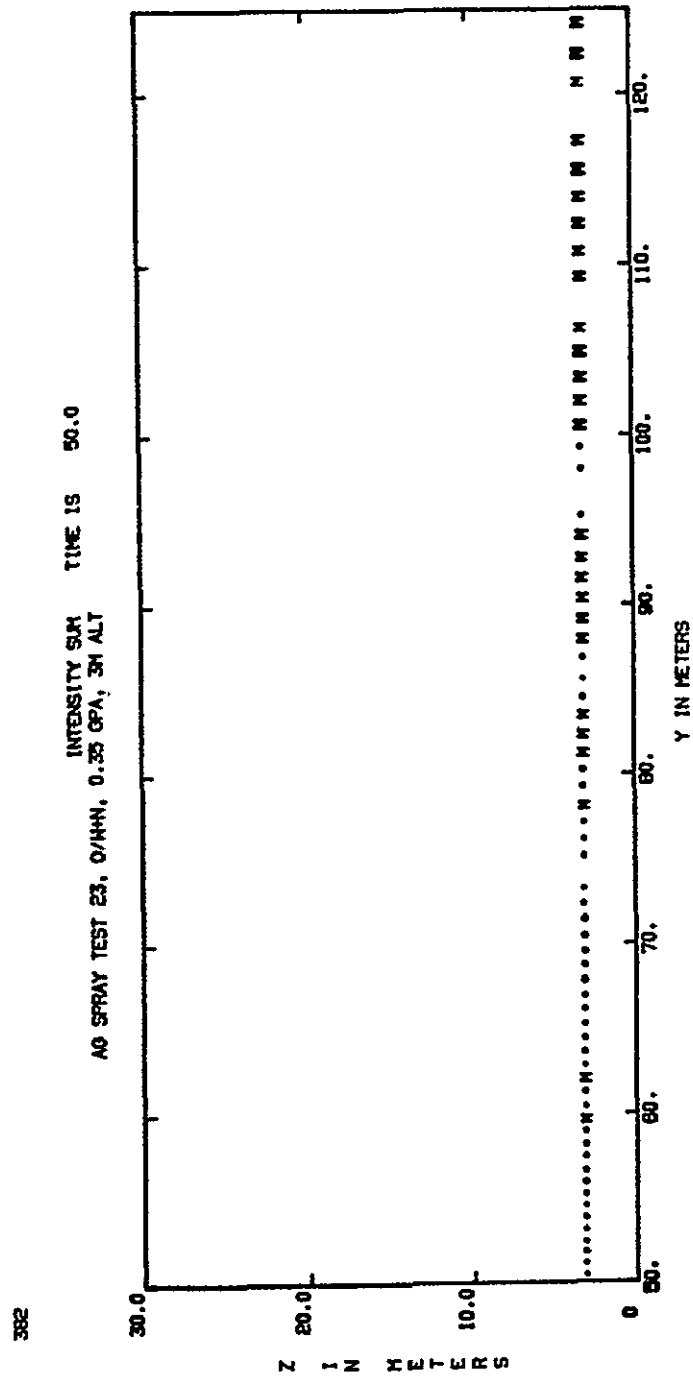

REPRODUCIBILITY OF THE
ORIGINAL PAGE IS POOR

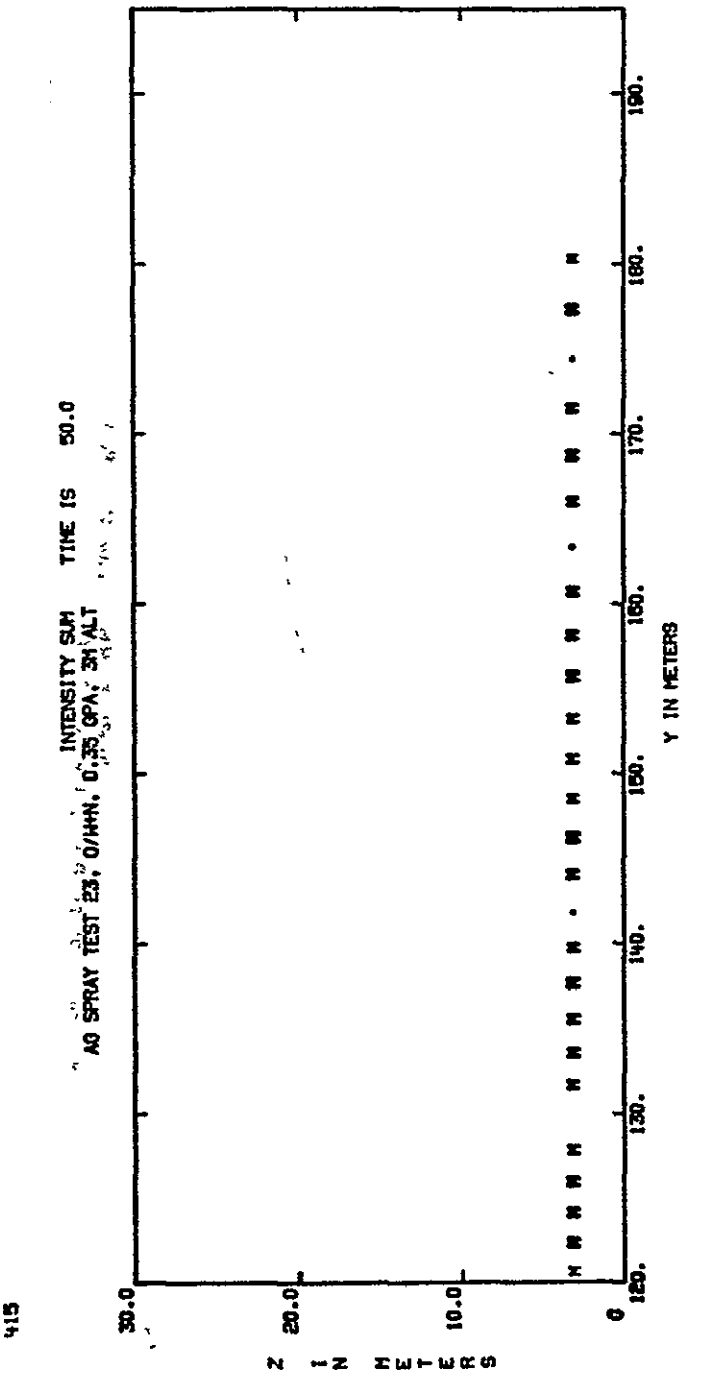

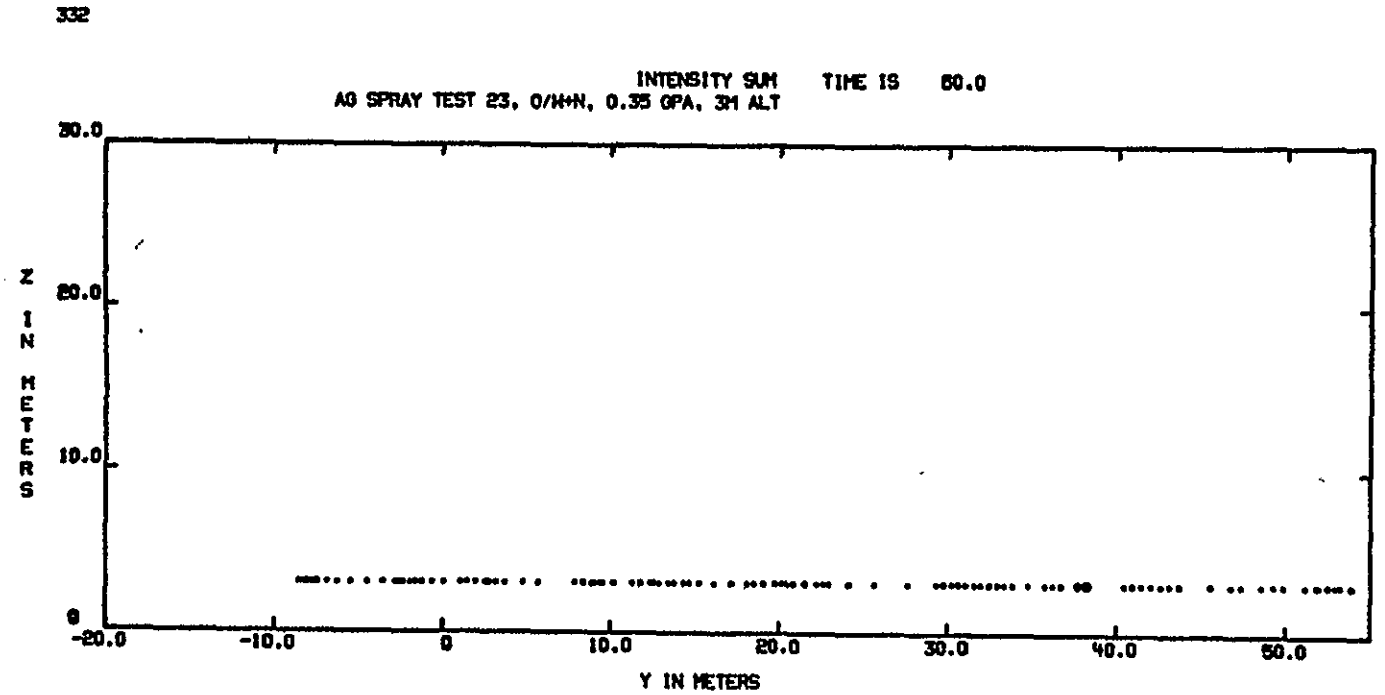
332
INTENSITY SUM TIME IS 60.0
AG SPRAY TEST 23, O/W+N, 0.35 GPA, 3M ALT
30.0
20.0
10.0
0
Z IN METERS
-20.0
-10.0
0
10.0
20.0
30.0
40.0
50.0
Y IN METERS

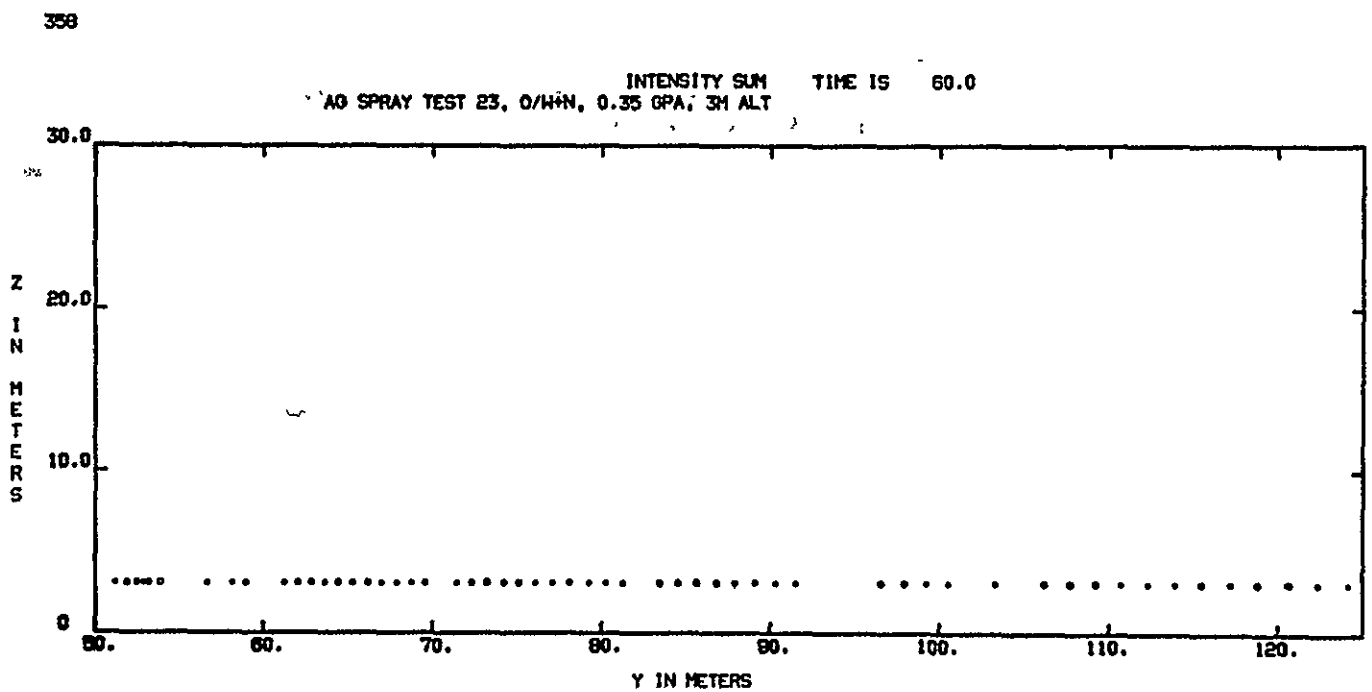
358
INTENSITY SUM TIME IS 60.0
AG SPRAY TEST 23, O/HN, 0.35 GPA, 3M ALT
30.0
20.0
10.0
0
Z IN METERS
50.
60.
70.
80.
90.
100.
110.
120.
Y IN METERS

REPRODUCIBILITY OF THE
ORIGINAL PAGE IS POOR

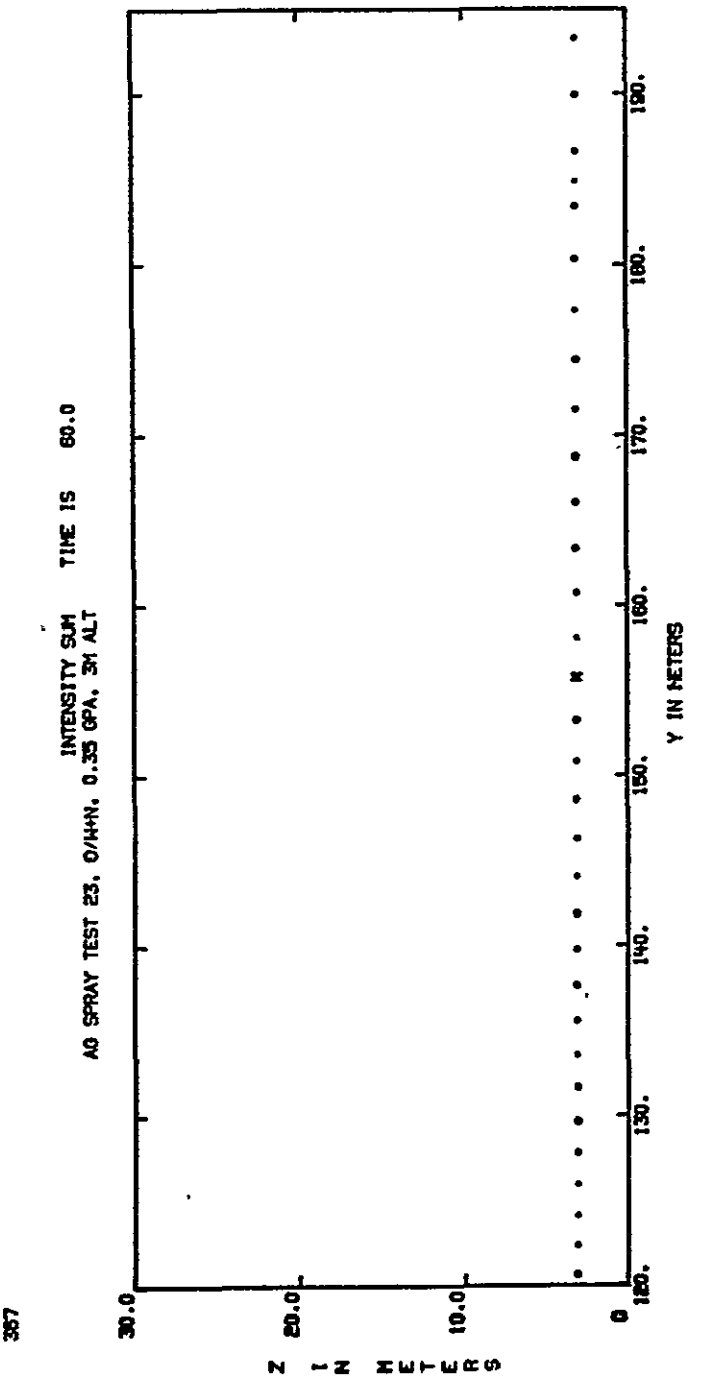

REPRODUCIBILITY OF THE
ORIGINAL PAGE IS POOR

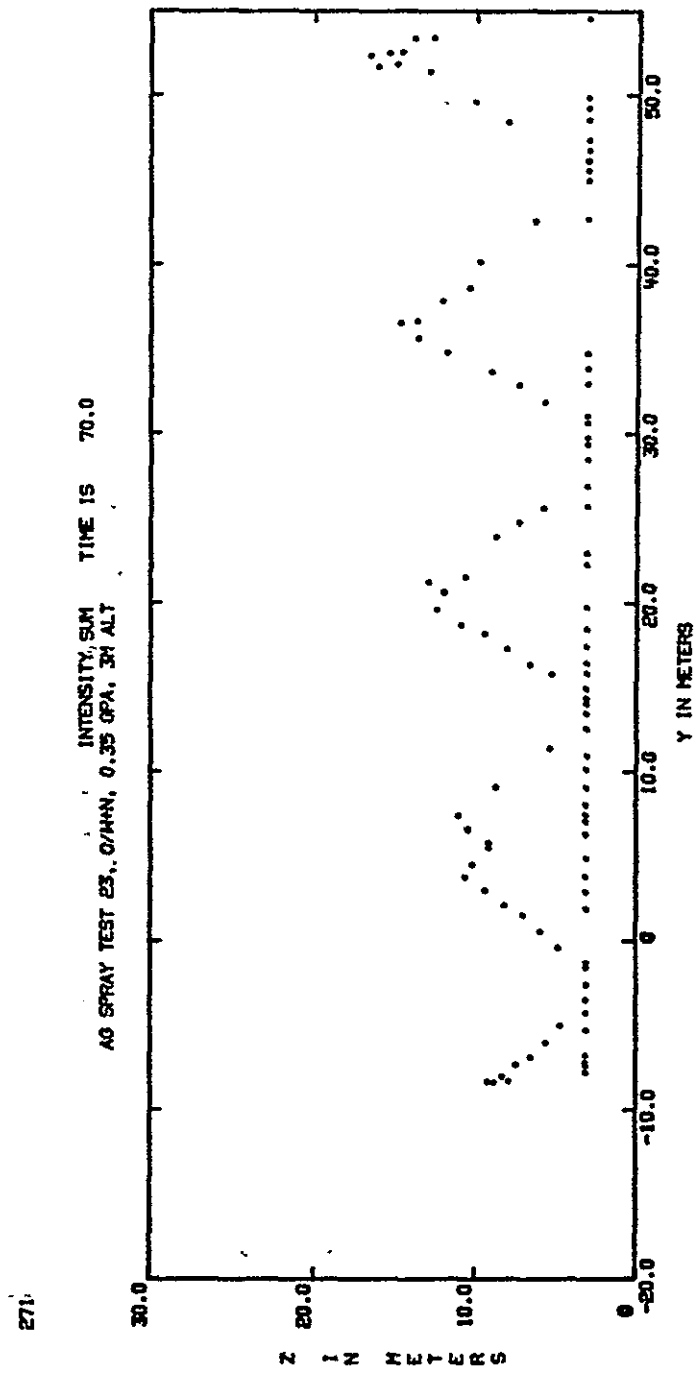

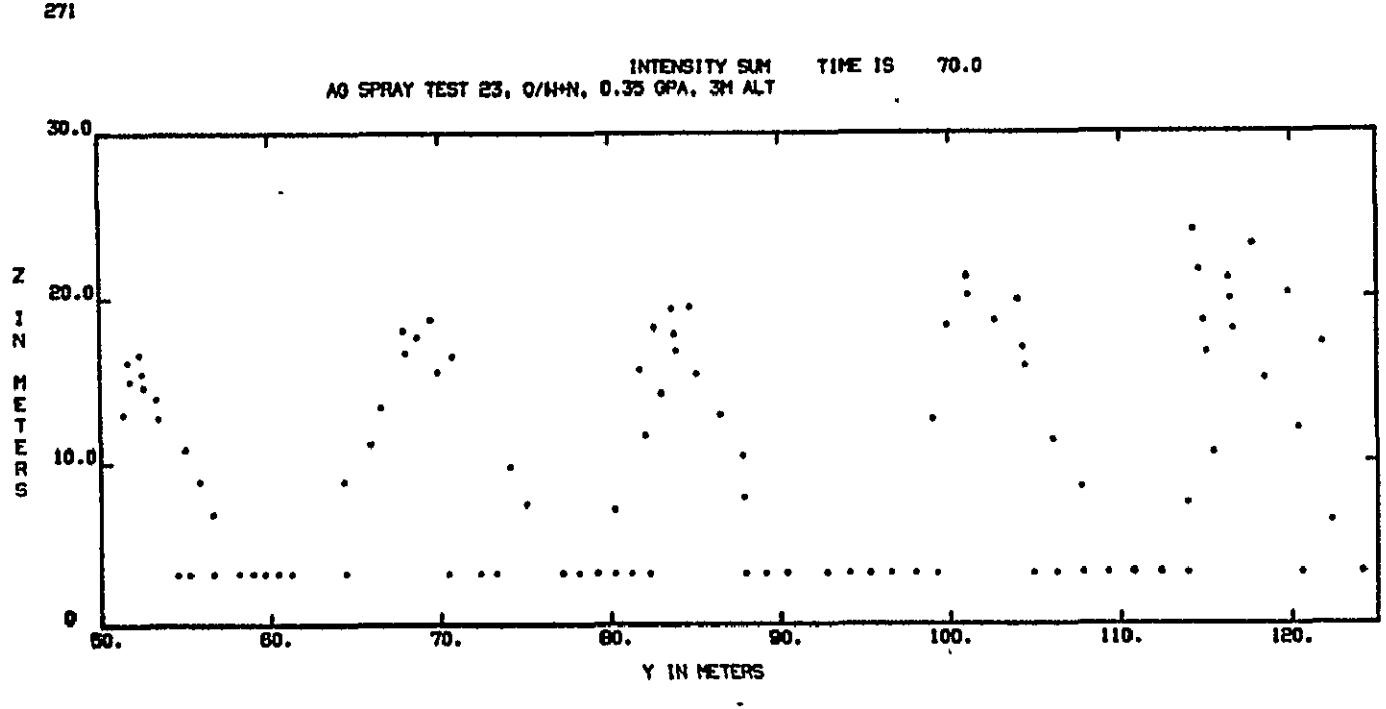
271
INTENSITY SUM TIME IS 70.0
AG SPRAY TEST 23, O/H+N, 0.35 GPA, 3M ALT
30.0
20.0
10.0
0
Z IN METERS
50.
60.
70.
80.
90.
100.
110.
120.
Y IN METERS

REPRODUCIBILITY OF THE
ORIGINAL PAGE IS POOR

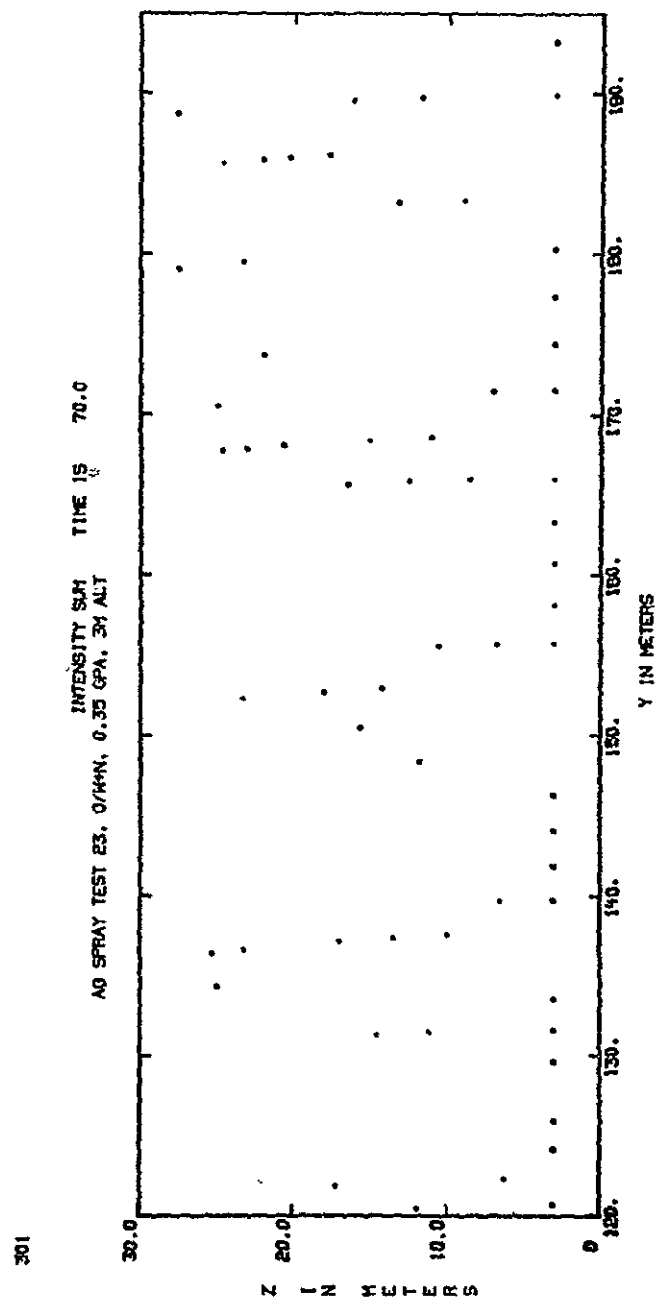

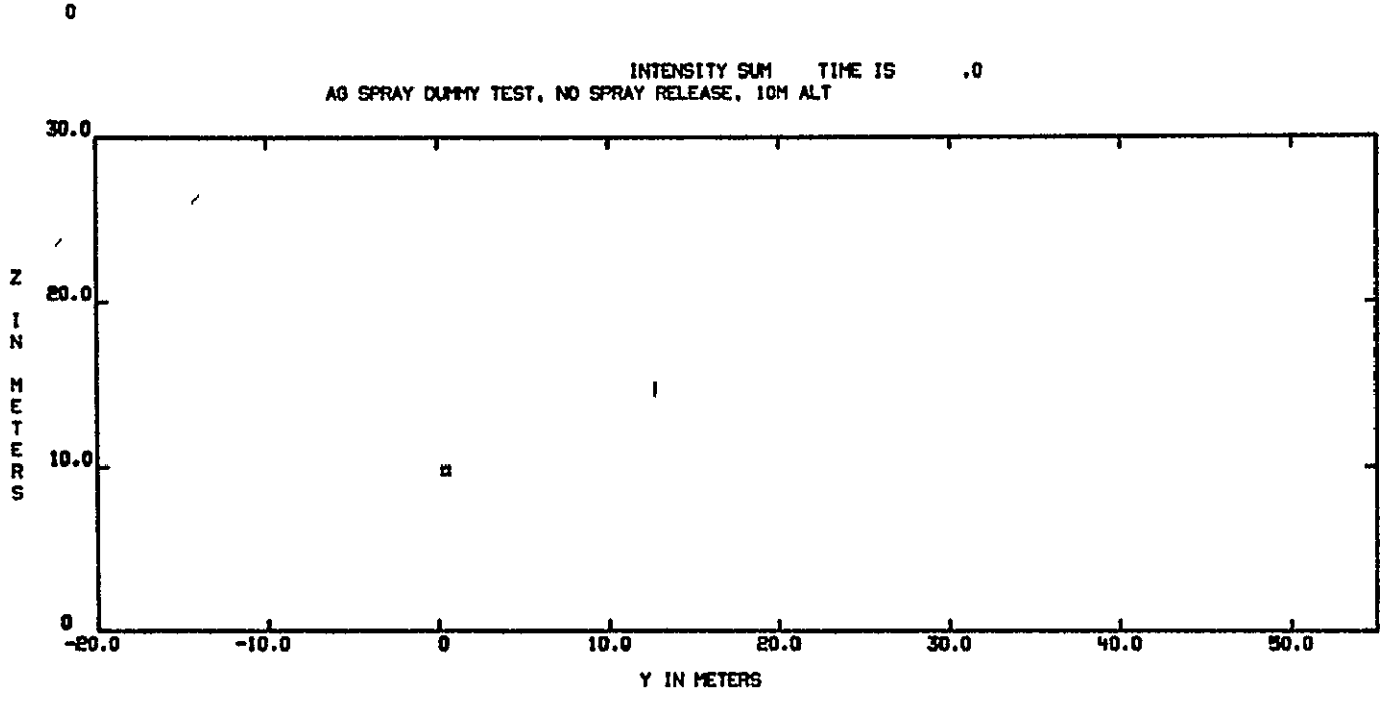
0
INTENSITY SUM TIME IS .0
AG SPRAY DUMMY TEST, NO SPRAY RELEASE, 10M ALT
30.0
20.0
10.0
0
Z IN METERS
-20.0
-10.0
0
10.0
20.0
30.0
40.0
50.0
Y IN METERS

REPRODUCIBILITY OF THE
ORIGINAL PAGE IS POOR

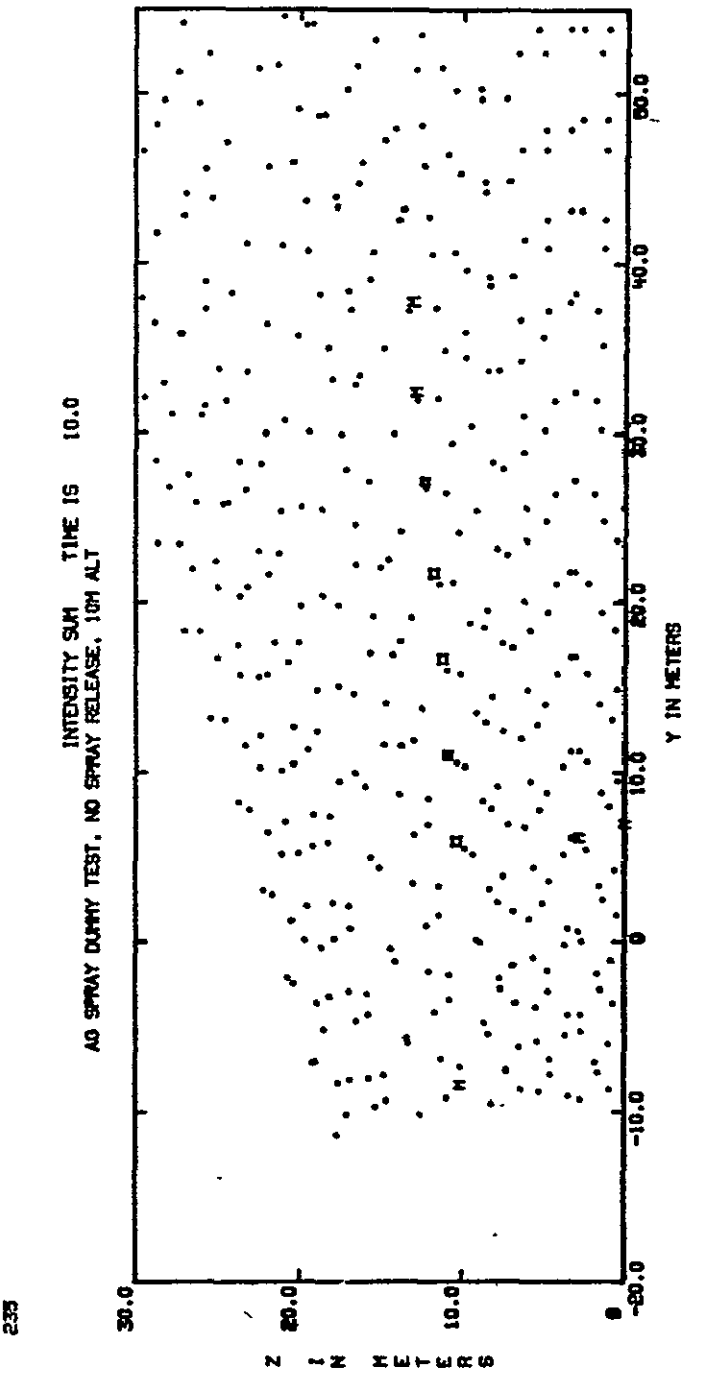

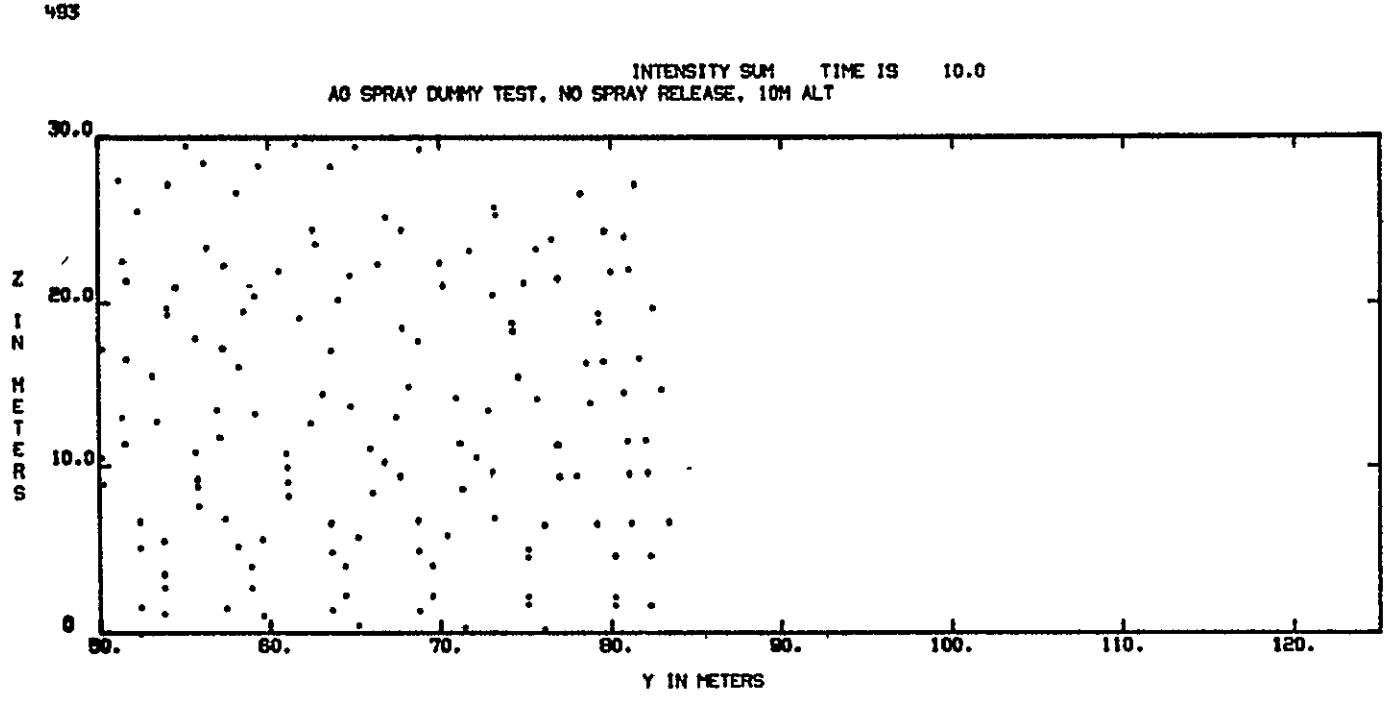
493
INTENSITY SUM TIME IS 10.0
AG SPRAY DUMMY TEST, NO SPRAY RELEASE, 10M ALT
30.0
20.0
10.0
0
Z IN METERS
50.
60.
70.
80.
90.
100.
110.
120.
Y IN METERS

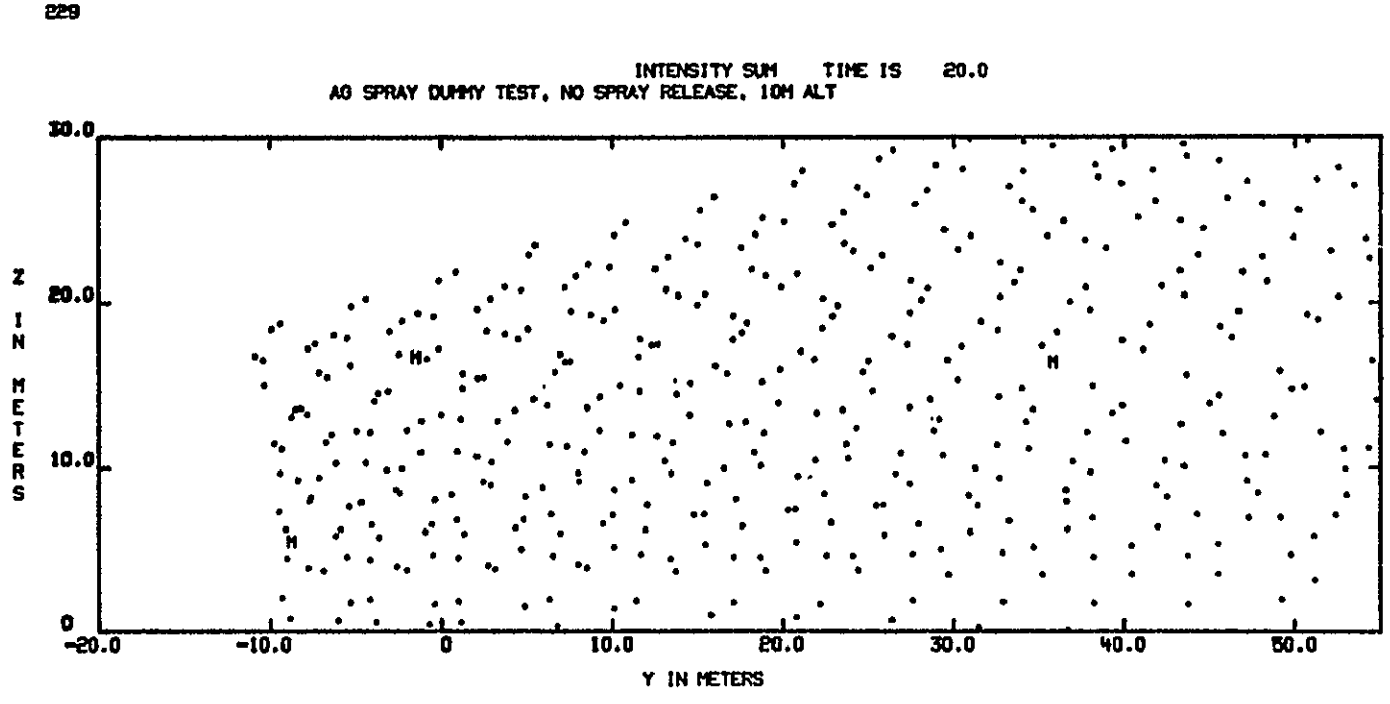
229
INTENSITY SUM TIME IS 20.0
AG SPRAY DUMMY TEST, NO SPRAY RELEASE, 10M ALT
30.0
20.0
10.0
0
Z IN METERS
-20.0
-10.0
0
10.0
20.0
30.0
40.0
50.0
Y IN METERS

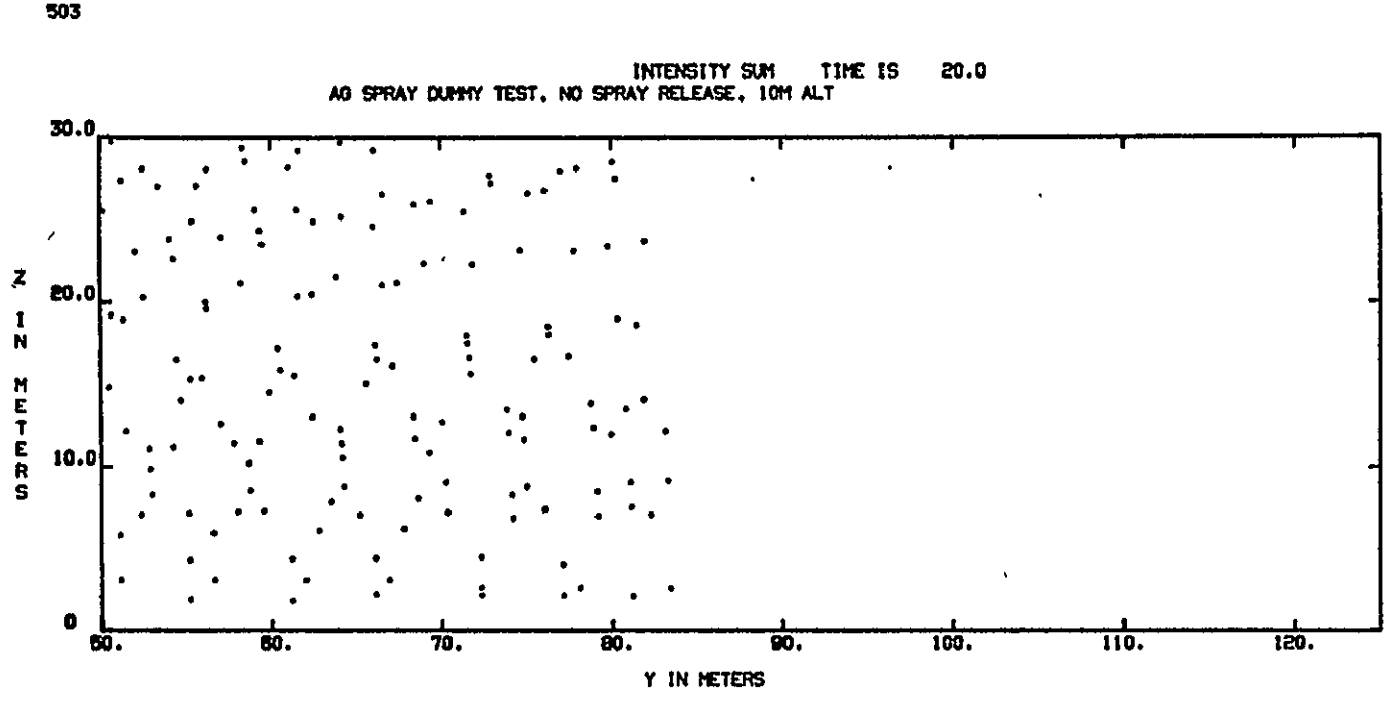
503
INTENSITY SUM TIME IS 20.0
AG SPRAY DUMMY TEST, NO SPRAY RELEASE, 10M ALT
30.0
20.0
10.0
0
Z IN METERS
50.
60.
70.
80.
90.
100.
110.
120.
Y IN METERS

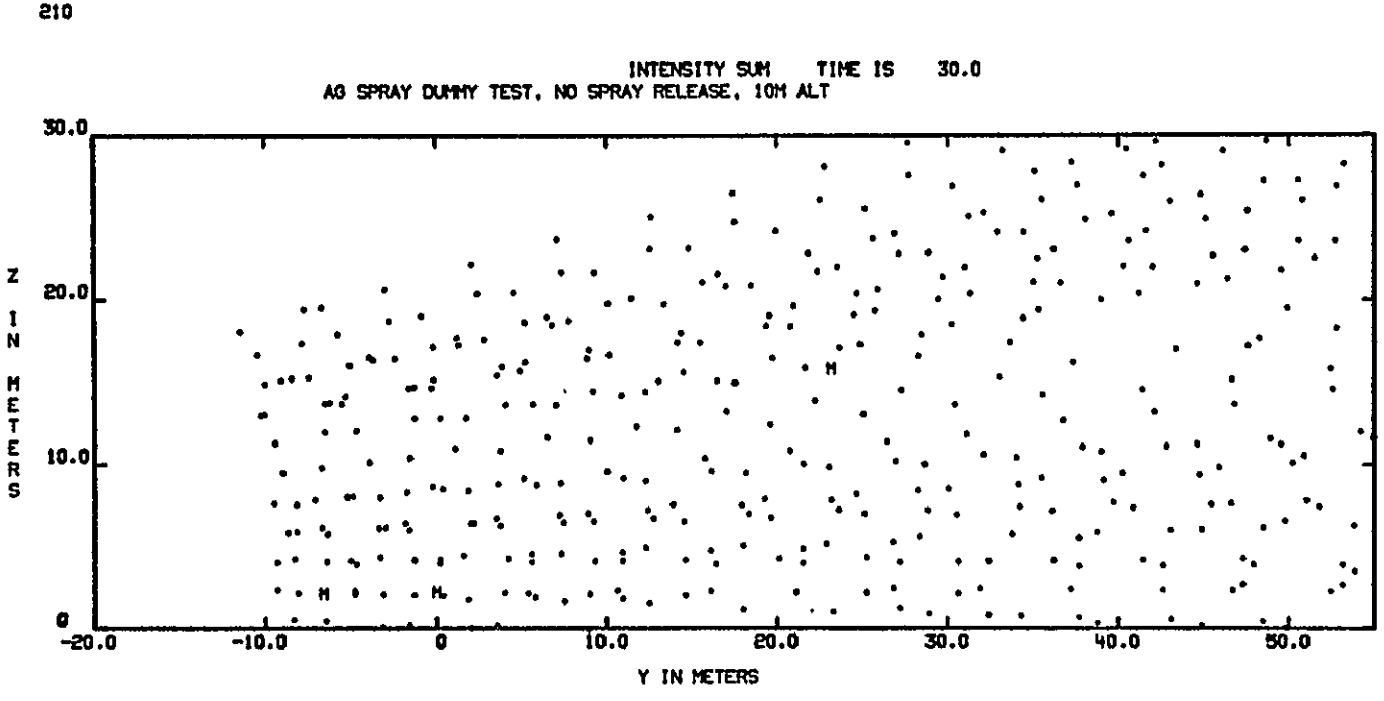
210
INTENSITY SUM TIME IS 30.0
AG SPRAY DUMMY TEST, NO SPRAY RELEASE, 10M ALT
30.0
20.0
10.0
0
Z IN METERS
-20.0
-10.0
0
10.0
20.0
30.0
40.0
50.0
Y IN METERS

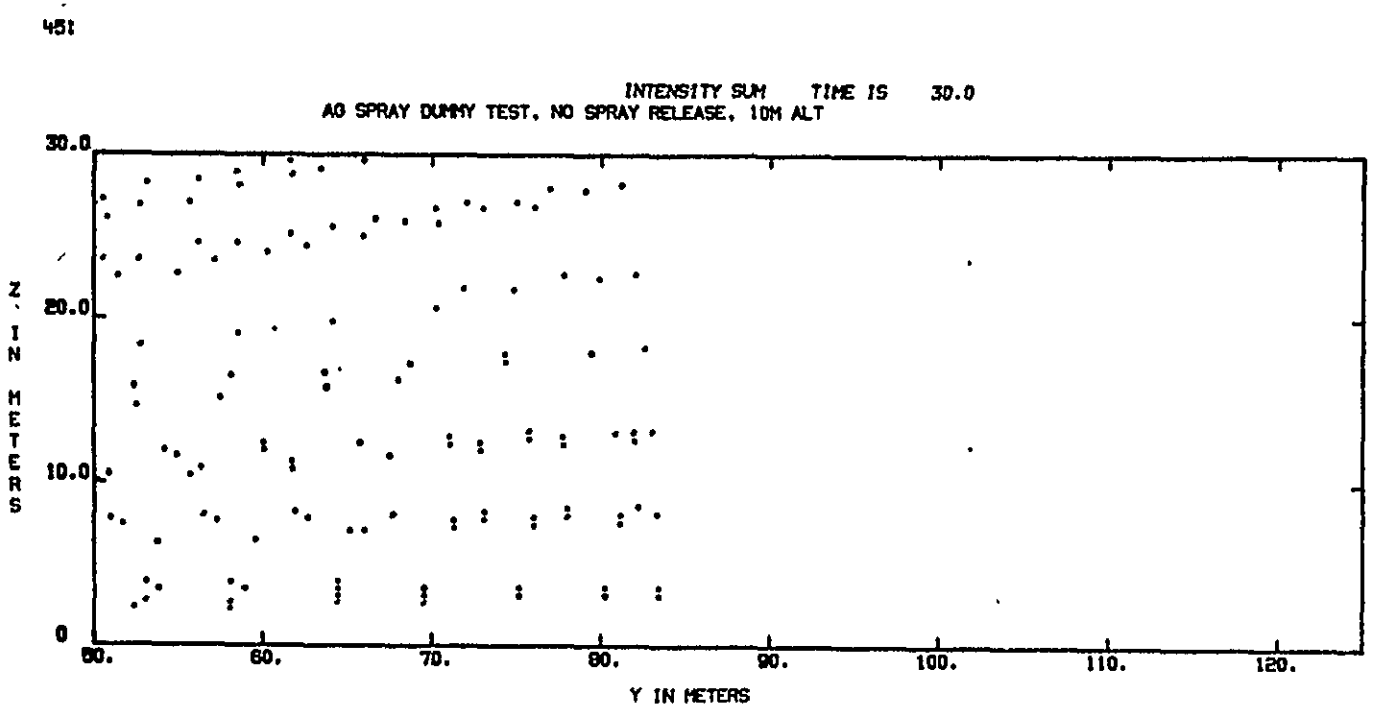
451
INTENSITY SUM TIME IS 30.0
AG SPRAY DUMMY TEST, NO SPRAY RELEASE, 10M ALT
30.0
20.0
10.0
0
Z IN METERS
50.
60.
70.
80.
90.
100.
110.
120.
Y IN METERS

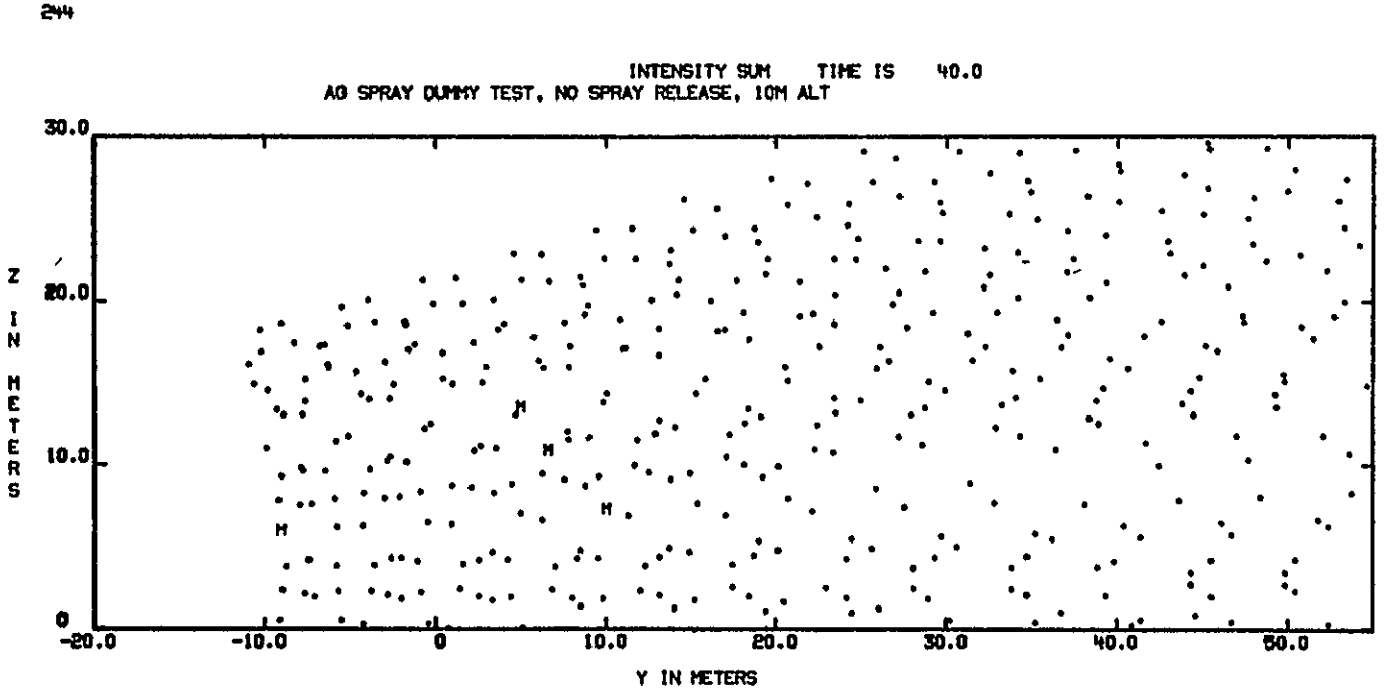
244
INTENSITY SUM TIME IS 40.0
AG SPRAY DUMMY TEST, NO SPRAY RELEASE, 10M ALT
30.0
20.0
10.0
0
Z IN METERS
-20.0
-10.0
0
10.0
20.0
30.0
40.0
50.0
Y IN METERS

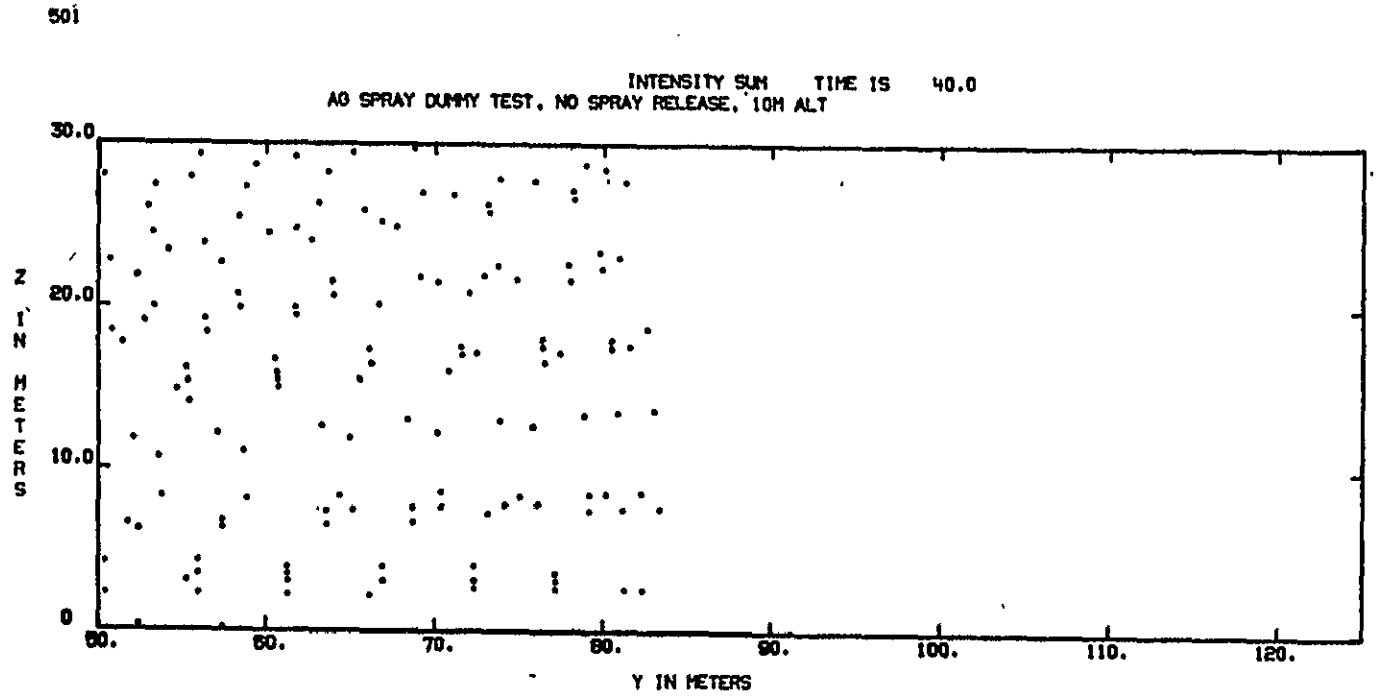
501
INTENSITY SUM TIME IS 40.0
AG SPRAY DUMMY TEST, NO SPRAY RELEASE, 10M ALT
30.0
20.0
10.0
0
Z IN METERS
50.
60.
70.
80.
90.
100.
110.
120.
Y IN METERS

217

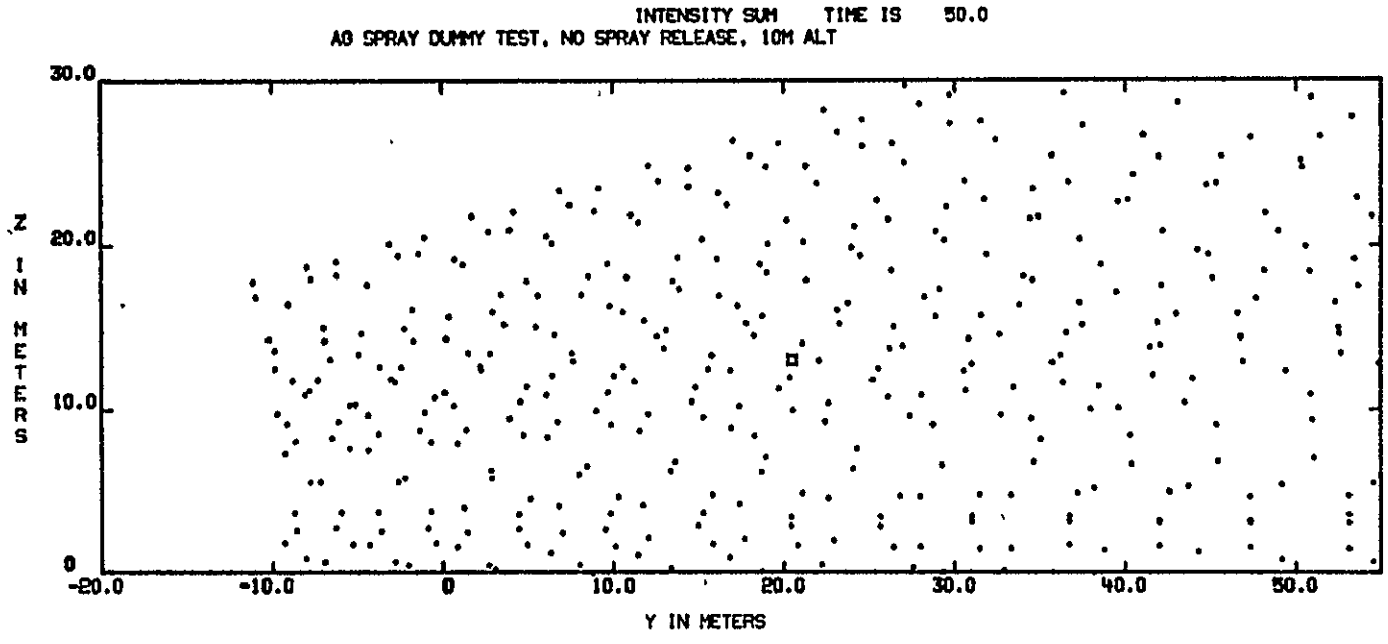
INTENSITY SUM TIME IS 50.0
AG SPRAY DUMMY TEST, NO SPRAY RELEASE, 10M ALT
30.0
20.0
10.0
0
Z IN METERS
-20.0
-10.0
0
10.0
20.0
30.0
40.0
50.0
Y IN METERS

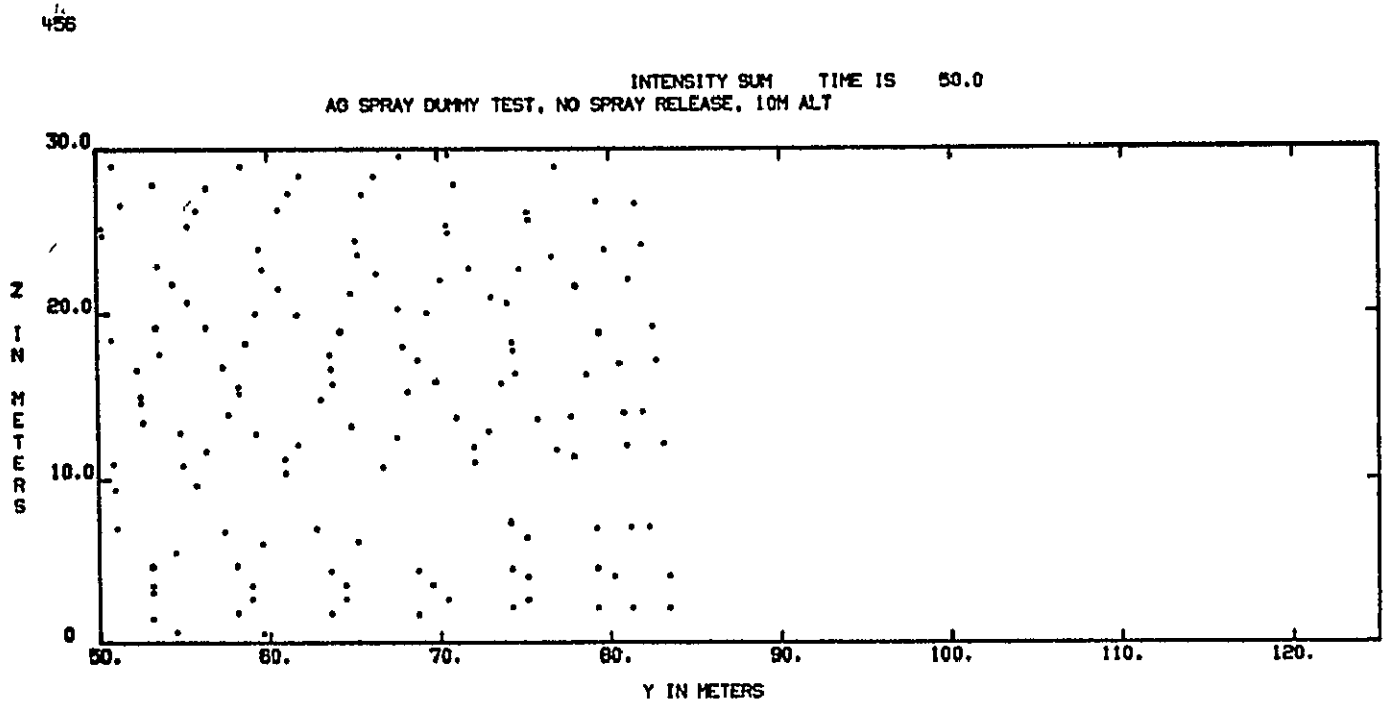
456
INTENSITY SUM TIME IS 50.0
AG SPRAY DUMMY TEST, NO SPRAY RELEASE, 10M ALT
30.0
20.0
10.0
0
Z IN METERS
50.
60.
70.
80.
90.
100.
110.
120.
Y IN METERS

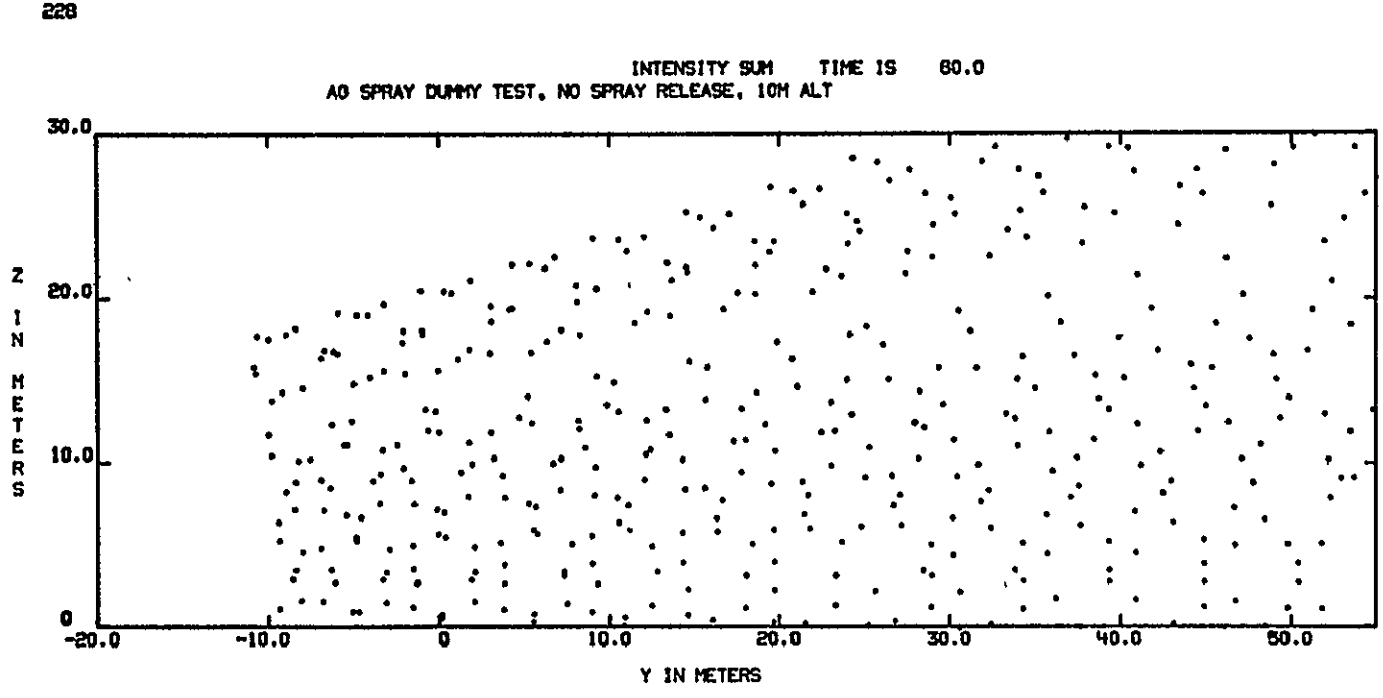
228
INTENSITY SUM TIME IS 60.0
A0 SPRAY DUMMY TEST, NO SPRAY RELEASE, 10M ALT
30.0
20.0
10.0
0
Z IN METERS
-20.0
-10.0
0
10.0
20.0
30.0
40.0
50.0
Y IN METERS

REPRODUCIBILITY OF THE
ORIGINAL PAGE IS POOR

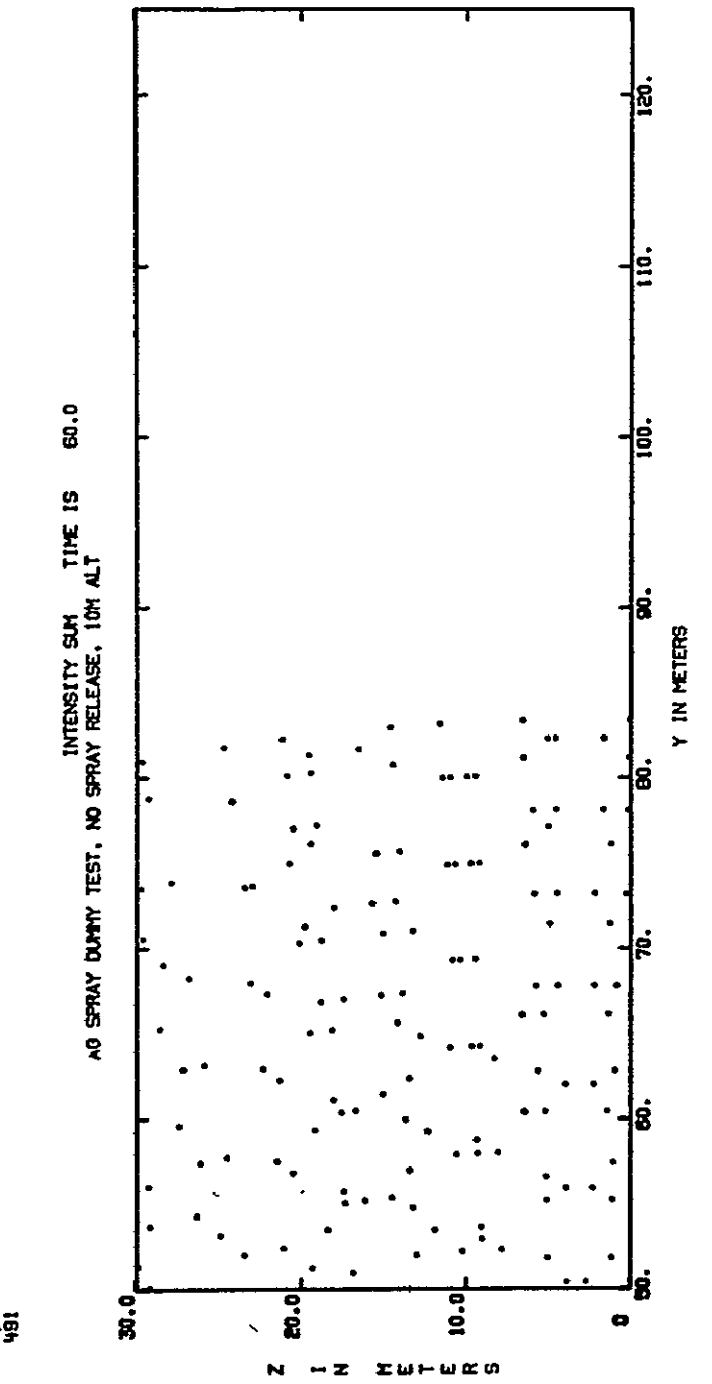

REPRODUCIBILITY OF THE
ORIGINAL PAGE IS POOR

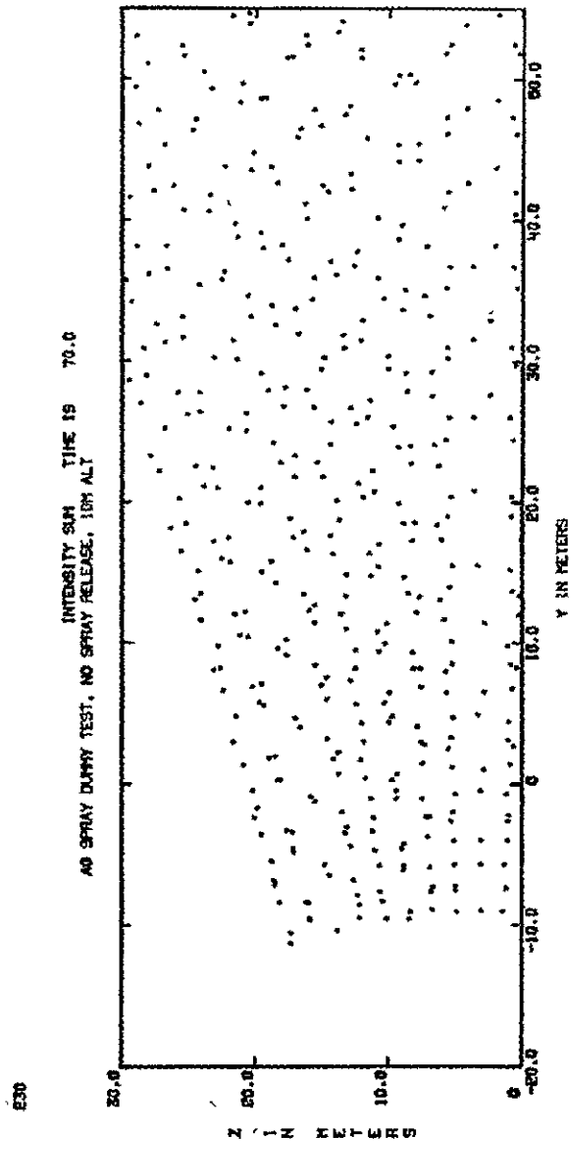

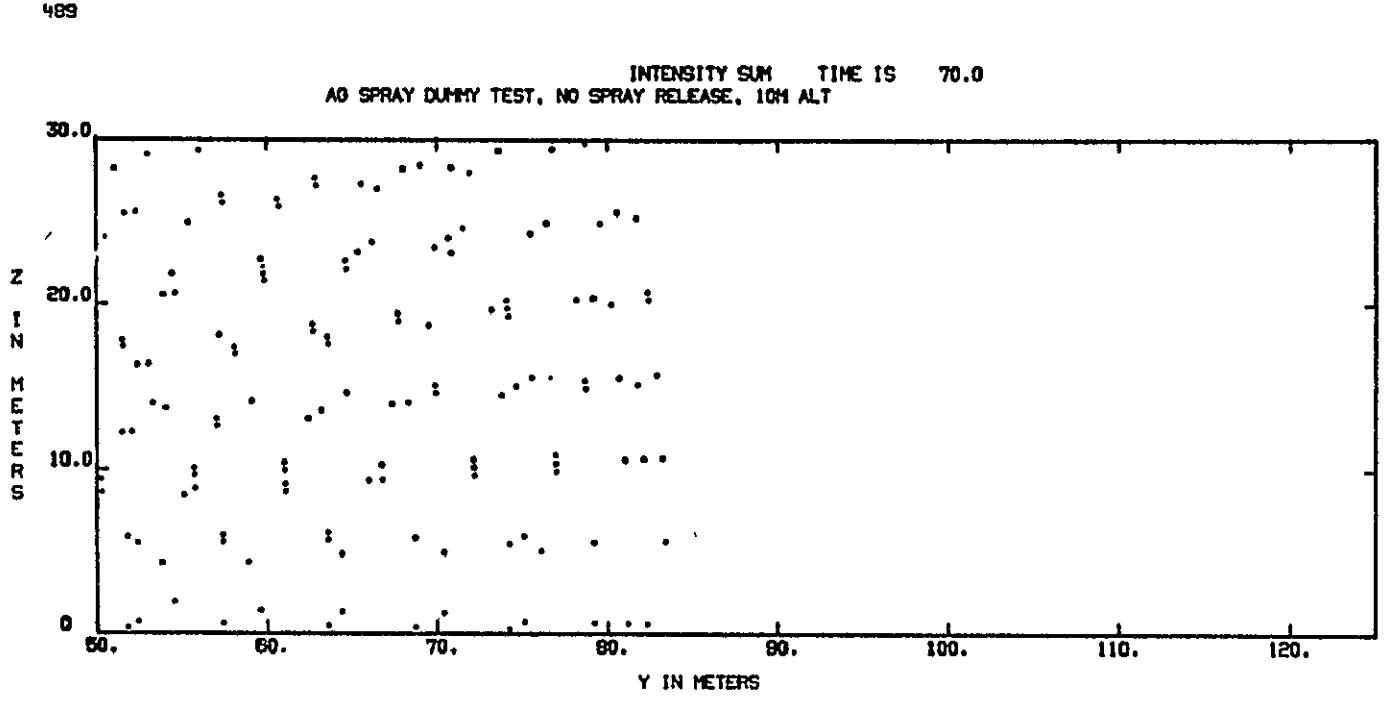
489
INTENSITY SUM TIME IS 70.0
AO SPRAY DUMMY TEST, NO SPRAY RELEASE, 10M ALT
30.0
20.0
10.0
0
Z IN METERS
50.
60.
70.
80.
90.
100.
110.
120.
Y IN METERS

1 Report No	2 Government Accession No	3 Recipient's Catalog No
NASA CR-141433		

4 Title and Subtitle	5 Report Date
LASER DOPPLER VELOCIMETER AERIAL SPRAY MEASUREMENTS	April 1978
	6 Performing Organization Code

7 Author(s)	8 Performing Organization Report No
Andrew D. Zalay, William R. Eberle, Robert E. Howle, Kenneth R. Shrider	
	10 Work Unit No

9 Performing Organization Name and Address	11 Contract or Grant No
Lockheed Missiles & Space Company, Inc. Huntsville Research & Engineering Center Huntsville, Alabama 35807	NAS6-2825
	13 Type of Report and Period Covered

12 Sponsoring Agency Name and Address	14 Sponsoring Agency Code
National Aeronautics and Space Administration Wallops Flight Center Wallops Island, Virginia 23337	

15 Supplementary Notes

Distribution of this report is provided in the interest of information exchange. Responsibility for the contents resides in the author or organization that prepared it. Appendix A "Spray Applications and Conventional Drift Measurements" was authorized by L. F. Bouse, J. B. Carlton and H. R. Crookshank of the U. S. Department of Agriculture.

16 Abstract

An experimental research program for measuring the location, spatial extent, and relative concentration of airborne spray clouds generated by agricultural aircraft is described. The measurements were conducted with a ground-based laser Doppler velocimeter. The remote sensing instrumentation, experimental tests, and the results of the flight tests are discussed. The cross-section of the aerial spray cloud and the observed location, extent, and relative concentration of the airborne particulates are presented.

The report shows that it is feasible to use a mobile laser Doppler velocimeter to track and monitor the transport and dispersion of aerial spray generated by an agricultural aircraft.

17 Key Words (Suggested by Author(s))	18 Distribution Statement
Doppler Velocimeter Aerial Spray Agricultural Aircraft Infrared Laser System	Unclassified - unlimited STAR Category - 35

19 Security Classif (of this report)	20 Security Classif (of this page)	21 No. of Pages	22 Price*
Unclassified	Unclassified	222	

*For sale by the National Technical Information Service, Springfield, Virginia 22151